DISSECTING MT1-MMP INDUCED SIGNALLING PATHWAYS

Dissertation

zur Erlangung des Doktorgrades

der Mathematisch-Naturwissenschaftlichen Fakultät

der Christian-Albrechts-Universität zu Kiel

Vorgelegt von

Patricia Alice Eisenach

Kiel

2009

Referent/in:
Ko-Referent/in:

Tag der mündlichen Prüfung:
Zum Druck genehmigt:

gez. _____

(Dekan)

Abbreviations

18s	....	18s rRNA
AG1296	....	6,7-Dimethoxy-3-phenylquinoxaline
APP	....	*β*-amyloid precursor protein
bp	....	base pairs
BCA	....	bicinchoninic acid
BSA	....	bovine serum albumie
cDNA	....	complementary DNA
CO_2	....	Carbon dioxide
CpE	....	Compound E
C_T	....	threshold cycle
CTGF	....	Connective tissue growth factor
$CuSO_4$	....	Copper(II) sulfate
DAPT	....	*N*-[*N*-(3,5-difluorophenacetyl)-L-alanyl]-(*S*)-
	....	phenylglycine *t*-butyl ester
DCI	....	3,4-Dichloroisocoumarin
DMEM	....	Dulbecco's Modified Eagles Medium
DMSO	....	Dimethyl sulfoxide
DNA	....	Deoxyribonucleic acid
dNTP	....	Deoxyribonucleotide triphosphate
ds	....	double stranded
DTT	....	Dithiothreitol
ECL	....	Enhanced chemiluminescence
ECM	....	Extracellular Matrix
ERK	....	Extracellular signal Regulated Kinase
E. Coli	....	*Escherichia coli*
EDTA	....	ethylenediaminetetraacetic acid
EGTA	....	ethylene glycol tetraacetic acid
ERK	....	Extracellular signal-regulated kinase
et al.	....	and others
FCS	....	Foetal Calf Serum
Fig	....	Figure
FLAG	....	protein tag (seq)
g	....	gram
GAPDH	....	Glyceraldehyde 3-phosphate dehydrogenase
GPI	....	glycosylphosphatidylinositol
HARP	....	Heparin affin regulatory peptide
HCl	....	Hydrochloric acid
HIF	....	Hypoxia-inducible factor
HPX	....	hemopexin domain
HRP	....	Horseradish Peroxidase
ICD	....	Intracellular Domain
IGF	....	Insulin-like growth factor
IgG	....	Immunglobulin G
IKK	....	IκB kinase
IP	....	immunoprecipitation
JNK	....	c-Jun N-terminal kinase
kb	....	kilo base pairs
KCl	....	Kaliumchloride
kDa	....	kilo Dalton
l	....	Liter

LB	....	Growth medium by Luria Bertani
m	....	milli (10^{-3})
M	....	molar
mA	....	milli ampere
MAP Kinase	....	Mitogen activated protein kinase
$MgCl_2$	....	Magnesium Chloride
$MgSO_4$	.....	Magnesium sulphate
min	....	minute
MMP	....	Matrix Metalloproteinase
MOI	....	Multiplicity of Infection
mRNA	....	messenger RNA
MT1-MMP	....	Membrane type 1-Matrix Metalloproteinase
mTOR	....	mammalian target of rapamycin
M2H	....	Mammalian-Two Hybrid
µ	....	micro (10^{-6})
n	....	nano (10^{-9})
1N	....	1 Normal
NaCl	....	Sodium chloride
NaOH	....	Sodium hydroxide
nm	....	nanometer
NP40	....	nonyl phenoxylpolyethoxylethanol
nt	....	Nucleotide
ONPG	....	*o*-nitrophenyl-β-D-galactopyranoside
p	....	pico (10^{-12})
PAGE	....	Polyacrylamide Gel Electrophoresis
PAI-1	....	Plasminogen Activator Inhibitor 1
PBS	....	Phosphate buffered Saline
PCR	....	Polymerase Chain Reaction
p-	....	phosphorylated
PI3K	....	phosphatidylinositol-3 kinase
PMA	....	Phorbol 12-myristate 13-acetate
PP2	....	4-amino-5-(4-chlorophenyl)-7-(*t*-butyl)pyrazol[3,4-*d*]pyrimidine
PVDF	....	Polyvinylidendifluoride
Q	....	Glutamine
qPCR	....	quantitative PCR (Real-Time PCR)
RIP	....	Regulated Intramembrane Proteolysis
RIPA buffer	....	radio-immuneprecipitation buffer
RNA	....	Ribunucleic acid
RNase	....	Ribunuclease
rpm	....	rounds per minute
RT	....	room temperature
RT-PCR	....	Reverse Transcriptase PCR
RUP	....	Regulated ubiquitin/proteasome-dependent processing
SD	....	standard deviation
SDS	....	sodium dodecyl sulfate
sec	....	second
S2P	....	site-2 protease
TAE buffer	....	Tris Acetate buffer
TBS	....	Tris buffered saline
TBS-T	....	TBS containing 0.1% (*v*/*v*) Tween®20
TE buffer	....	Tris-EDTA buffer
TEMED	....	N,N,N',N'-Tetramethylendiamin
TIMP	....	Tissue Inhibitor of MMPS
T_M	....	melting temperature

TMD	....	Transmembrane Domain
Tris	....	Tris (hydroxymethyl) aminomethane
U	....	unit
UV	....	ultravilolet
VEGF	....	Vascular Endothelial Growth Factor
VEGFR	....	VEGF receptor
WT	....	Wild-type

Amino acid nomenclature

A	Ala	Alanine
C	Cys	Cysteine
D	Asp	Aspartic acid
E	Glu	Glutamic acid
F	Phe	Phenylalanine
G	Gly	Glycine
H	His	Histidine
I	Ile	Isoleucine
K	Lys	Lysine
L	Leu	Leucine
M	Met	Methionine
N	Asn	Asparagine
P	Pro	Proline
Q	Gln	Glutamine
R	Arg	Arginine
S	Ser	Serine
T	Thr	Threonine
V	Val	Valine
W	Trp	Tryptophan
Y	Tyr	Tyrosine

Nucleotide nomenclature

A	Adenine
C	Cytosine
G	Guanine
T	Thymidine
R	Guanine or Adenine
W	Adenine or Thymidine

List of figures

List of tables

1 Introduction

Normal cellular homeostasis depends on a balanced regulated interaction between cells and their immediate environment. In response to these interactions, cell surface receptors are activated and induce intracellular signals leading to the maintenance of normal physiological functions and cellular integrity. During tumourigenesis this tissue homeostasis is perturbed and subpopulations of cells acquire the ability to grow, detach from the surrounding tissue, migrate through the extracellular matrix and to invade host tissue eventually leading to metastatic dissemination. These cellular responses are the result of genetic and epigenetic alterations resulting in dysregulation of various genes during tumour initiation, progression and metastasis. One of the hallmarks of cancer progression is the capacity of cells to invade through tissue boundaries. Proteolytic enzymes that degrade the surrounding extracellular matrix play a fundamental role in cancer progression by facilitating cell migration and providing access for tumour cells to the vascular or lymphatic systems (chapters 1.1 and 1.2).

A major line of current oncologic research addresses the molecular changes accumulated in tumour cells to selectively target proteins for the design of novel therapeutics. However, recent findings emphasise the importance of molecular networks and pathways downstream of potential targets, as these proteins are involved in a plethora of cellular functions involved in both, physiological and pathophysiological processes. A better understanding of the mechanistic and molecular level of potential target-proteins is therefore crucial to selectively inhibit specific functions without affecting the roles of the respective proteins in normal physiological processes.

1.1 The role of proteinases in carcinogenesis

Proteinases play a key role in physiological as well as pathophysiological conditions. Their involvement in biological processes exceeds the initial characterisation of proteinases as non-specific degrading enzymes that are involved in protein catabolism. There is an emerging body of data implicating proteinase activity in a plethora of biological processes including the shedding of cell surface proteins, receptors and adhesion proteins, activation or inactivation of proteases, other enzymes, cytokines, chemokines, hormones and growth

factors as well as determining the subcellular localisation of proteins, and thus modulating key cellular responses [1].

Analysis of the human genome revealed currently 662 proteinases annotated in the peptidase database (http://merops.sanger.ac.uk), which are distributed into 5 classes: Metalloproteinases, Serine proteinases, Cysteine proteinases, Threonine proteinases, Aspartic proteinases and proteinases of an unknown class. These proteinases function both intracellularly and extracellularly and are recognised as being important for all stages of tumour progression. Their functional spectrum includes regulation of cell proliferation, adhesion, migration, differentiation, angiogenesis, senescence, autophagy and apoptosis. The role of the intracellular caspases, deubiquitylases (DUBs) and autophagins is generally associated with the removal of damaged or unwanted proteins, whereas the extracellular proteinases are actively involved in tumourigenesis. They are frequently overexpressed in human tumours and are implicated in facilitating cell motility by degrading the extracellular matrix, processing of cell receptors, thus attenuating cell adhesion and inducing intracellular signal transduction pathways [2,3]. In addition to the members of serine, cysteine and aspartic proteinases, the extracellular metalloproteinases (MPs) play an essential role during cell migration and were shown to be most abundantly expressed in malignant cells clustered at the leading edge of migrating cells (chapter 1.2) [4,5].

1.2 Matrix Metalloproteinases

The family of Matrix Metalloproteinases (MMPs) belongs to the metzincin family of zinc-dependent endopeptidases. They are considered to be key proteinases involved in the remodelling and turnover of the extracellular matrix (ECM) and play therefore an essential role in physiological and pathophysiological processes including embryonic development, tissue morphogenesis, inflammation and wound healing as well as tumour growth, tumourigenic angiogenesis and metastasis [6-8]. Their specific but often overlapping substrates comprise a wide range of cell surface proteins, growth factors, growth factor binding proteins, other proteinases, cytokines, chemokines and cell adhesion molecules [6,9-11]. Under normal physiological conditions, the activity of MMPs is tightly regulated on the level of transcription, activation of the zymogen, inhibition by endogenous inhibitors, internalisation and ectodomain shedding. A loss of activity control may lead to the development of various diseases including cancer, atherosclerosis, arthritis and fibrosis [12].

Accordingly, the expression of these proteinases was shown to be increased in malignant tissue and MMPs are especially enriched in areas at the tumour-stroma interface [13]. Their presence often correlates with poor prognosis [14-18]. Several findings have emphasised that MMPs contribute not only to the initiation of tumour-formation but also to tumour growth, angiogenesis and metastasis, making MMPs a particular promising target in oncologic research.

1.2.1 Structure and function of MMPs

The MMP family is highly conserved across different species and includes 24 members in humans. MMPs share a conserved domain structure comprising of a propeptide, a zinc-dependent catalytic domain, a flexible linker/hinge region and a hemopexin-like domain (HPX) (except MMP-7, -23, and -26) followed either by a linker- and transmembrane domain as well as an intracellular domain or by a glycosylphosphatidylinositol (GPI) -anchor (Figure 1.1). The cysteine switch motif (PRCGXPD) within the propeptide, that maintains the latent zymogen form (pro-MMP) as well as the zinc-binding motif (HEXGHXXGXXH) assign proteinases to the MMP family. Only MMP-23 is lacking the cysteine switch motif but exhibits strong homology of its catalytic sequence to MMP-1. The members of the MMP family are divided into two subgroups: the soluble MMPs and the Membrane-type MMPs (MT-MMPs) (Figure 1.1).

The MT-MMP subgroup comprises of 6 members, of which 4 are type-I transmembrane proteinases (MT1- (MMP-14)-, MT2- (MMP-15), MT3- (MMP-16) and MT5-MMP (MMP-24)), whereas MT4- (MMP-17) and MT6-MMP (MMP-25) are anchored to the plasma membrane via a GPI-anchor (Figure 1.1). Based on their substrate specificity and sequence homology the subgroup of soluble MMPs can be subdivided further in: Collagenases (MMP-1, MMP-8, MMP-13, MMP-18 (*Xenopus*)), Gelatinases (MMP-2, MMP-9), Stromelysins (MMP-3, MMP-10), Matrilysins (MMP-7, MMP-26) and other MMPs (MMP-11, MMP-12, MMP-19, MMP-20, MMP-21, MMP-22, MMP-23, MMP-27, MMP-28) [19]. The domain-structure of the MMP family is summarised in Figure 1.1 based on their sequence homology.

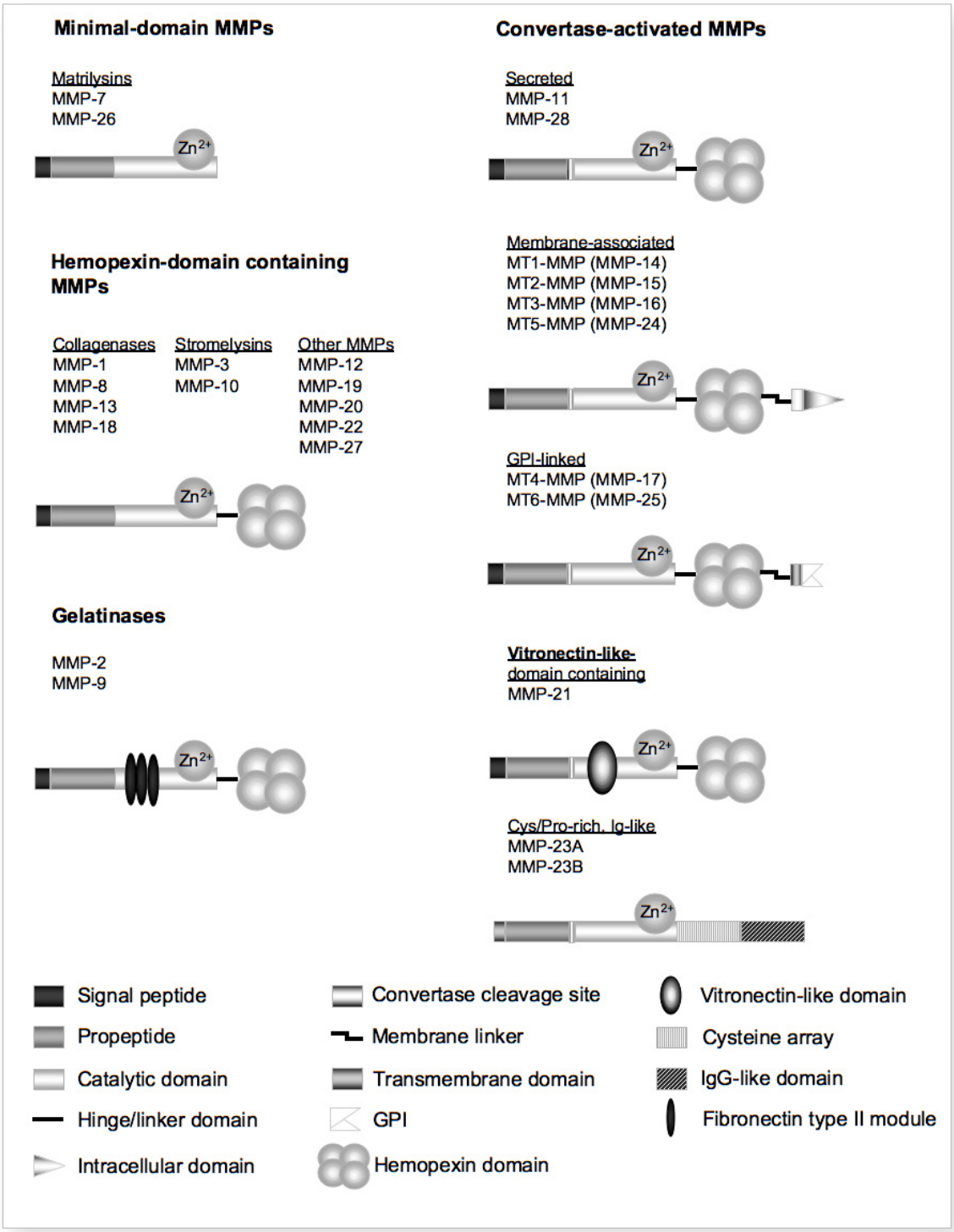

Figure 1.1: The Matrix Metalloproteinase family

Schematic representation of the domain-structure of MMPs, comprising of a signal peptide (directs the MMP to the secretory pathway or to membrane insertions), a prodomain (confers latency of the zymogen), catalytic domain (with indicated active zinc ion), a hemopexin-like domain (determines in addition to catalytic domain the substrate specificity) and a hinge/linker region. The MT-MMP subgroup contains an additional transmembrane and intracellular domain (membrane-associated MMPs) or a GPI anchor (GPI-linked MMPs). MMP-2 and MMP-9 exhibit fibronectin-like type II repeats, which facilitate collagen substrate binding. MMP-7 and MMP-26 lack the hemopexin domain. Adapted from [20].

MMPs are synthesised as inactive zymogens that are activated by cleavage of the prodomain at a conserved amino acid stretch (RXK/RR) by furin, plasmin or related proprotein convertases. The activation of MMPs may occur either intracellularly or extracellularly [21,22]. As an exception, pro-MMP-2 is not activated by one of the previously described proteinases but its activation takes place on the cell surface mediated by MT1-MMP and TIMP-2 (chapter 1.3.4.3).

MMPs are multi-functional enzymes, which main function is the degradation and re-organisation of the extracellular matrix (ECM) by cleaving various ECM components (collagens, laminin, fibronectin, vitronectin, aggrecan, enactin, versican, perlecan, tenascin, elastin and many others). Processing of these components plays a pivotal role in liberating various growth factors and cytokines that are sequestered within the ECM milieu. In addition to the cleavage of ECM components, MMPs have also been shown to process a variety of proteins via their "sheddase" function, including the shedding of bioactive molecules from the cell surface as well as processing transmembrane proteins and cell surface receptors. Surface anchoring of the membrane-bound MMPs has been recognised to be important for the cells to modify their pericellular environment and provides an essential mechanism for the spatial regulation of substrate processing.

1.3 Membrane type-1 Matrix Metalloproteinase (MT1-MMP)

Membrane type 1-Matrix Metalloproteinase (MT1-MMP) was first described in 1994 by Sato *et al.* as a specific activator of MMP-2 activity [23] and is the best characterised MMP to date. MT1-MMP has been implicated in various physiological and pathophysiological processes including wound healing, bone development, angiogenesis, inflammation, rheumatoid arthritis, atherosclerosis, cancer invasion and metastasis [24]. MT1-MMP is highly expressed in different cancers and its expression was shown to promote migration, invasion and metastasis of cancer cells *in vitro* and *in vivo* [25]. Indeed, overexpression of MT1-MMP in cells *in vivo* enhances the growth and size of tumours, and the cells acquire a more invasive and malignant phenotype [26-28]. Subcutaneous inoculation of normally benign MDCK (Madin-Darby canine kidney) cells that are induced to express MT1-MMP was demonstrated to be sufficient to initiate tumour formation *in vivo* [29]. Expression of MT1-MMP as well as MMP-2 correlates with a poor prognosis in patients with advanced neuroblastoma, small cell lung cancer, tongue squamous cell carcinoma, head and neck

carcinoma, bladder cancer and ovarian cancer [30-34]. Interestingly, MT1-MMP expression is not only detected in various malignant cells but also in the adjacent stromal cells of various human tumours [24].

1.3.1 Structure of MT1-MMP

MT1-MMP shares the conserved domain structure with the other MMP family members, including a pre/propeptide (M^{1} – R^{111}), the zinc-dependent catalytic domain (Y^{112} – G^{285}), a flexible hinge region (E^{286} – I^{318}), the hemopexin domain (C^{319} – C^{508}) and a stalk region (P^{509} – S^{538}). In addition MT1-MMP is attached to the plasma membrane with a transmembrane domain (A^{539} – F^{562}) and a short intracellular tail (R^{563} – V^{582}) [23,25,35] (Figure 1.1). Following synthesis, MT1-MMP is matured in the trans-Golgi complex and is transported to the plasma membrane via a Rab8- [36], VAMP7- [37] and by a microtubule-dependent process [38-40]. It has been shown that the enzyme is post-translationally modified by *o*-glycosylation at T^{291}, T^{299}, T^{300}, and/or S^{301} within the hinge region. In the absence of glycosylation, pro-MMP-2 activation was ablated, although the mutants retained the ability to degrade collagen I and to undergo autocatalytic processing [41].

1.3.2 Substrates of MT1-MMP

Initial studies on MT1-MMP revealed its ability to process various components of the extracellular matrix including collagens I, II, and III, fibronectin, gelatin, laminins 1 and 5, vitronectin, fibrin, aggrecan, lumican and proteoglycan [42-46]. More recently new MT1-MMP functions have emerged including the processing of growth factors, cell surface proteins, receptors, cytokines and chemokines, including the activation of latent transforming growth factor *β* (TGF-*β*) [47,48], tumour necrosis factor α (TNF-α) [42] as well as processing of CD44 (chapter 1.4.1) [49], tissue transglutaminase [2], low-density lipoprotein receptor related protein (LRP) [50], Syndecan-1 [51] and the α_v integrin subunit [2,23,49,51-53]. Additionally, angiogenesis was shown to be enhanced by the MT1-MMP mediated release of sequestered $VEGF_{165}$ from extracellular CTGF (connective tissue growth factor)/$VEGF_{165}$ and HARP (heparin affin regulatory peptide)/$VEGF_{165}$ complexes [54]. Cellular proteolytic responses initiated by MT1-MMP function are further increased by MT1-MMP mediated activation of pro-MMP-2 [23] and pro-MMP-13 [52]. These functions

indicate that MT1-MMP surface expression induces a wide proteolytic repertoire, facilitating ***(i)*** cell migration, ***(ii)*** invasion through the extracellular matrix, ***(iii)*** angiogenesis and ***(iv)*** proliferation [55].

MT1-MMP induced functions are summarised in Figure 1.2.

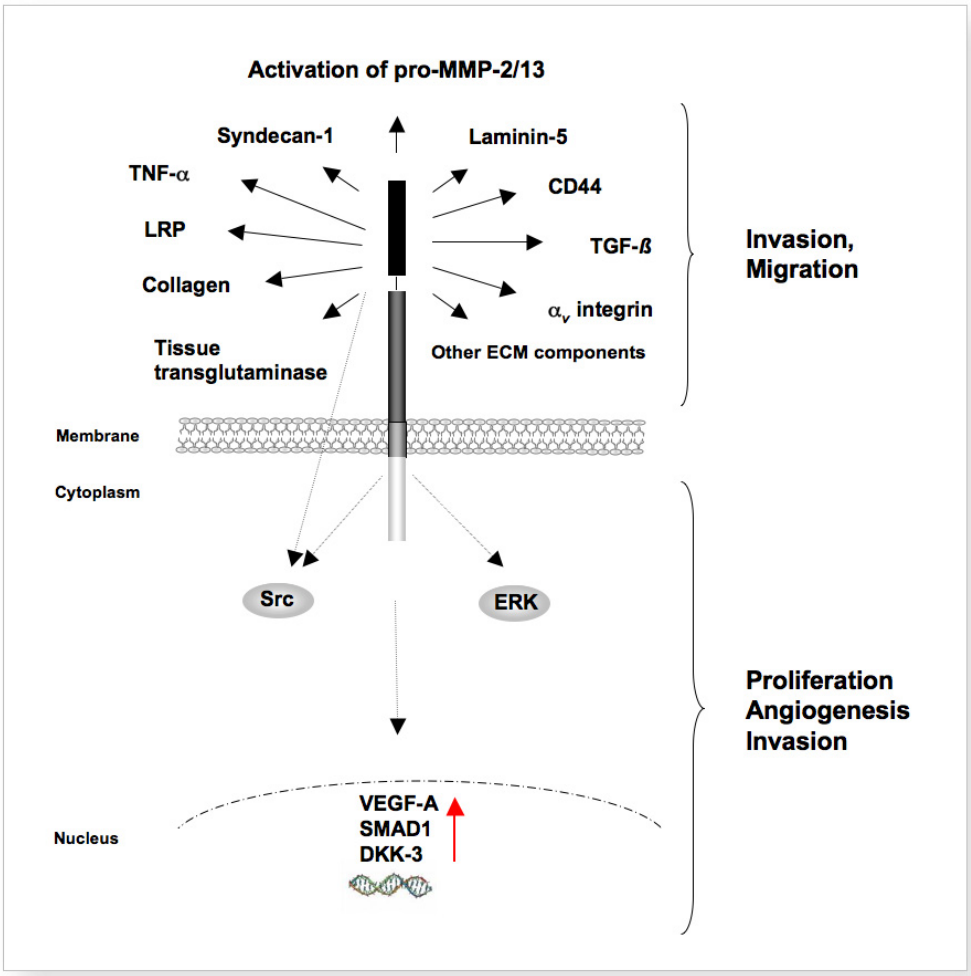

Figure 1.2: Summary of MT1-MMP functions

Schematic representation of MT1-MMP functions. Cellular invasion and cell migration is enhanced through *(i)* the activation of the proteolytic cascade by activating pro-MMP-2 and pro-MMP-13, *(ii)* the cleavage of Collagen, the basement membrane component Laminin-5 and further ECM components as well as *(iii)* the processing of Syndecan-1, CD44, LRP, TGF-β, tissue transglutaminase, α_v integrin and TNF-α. MT1-MMP was also found to induce the ERK intracellular signalling pathway and to modulate gene transcription of VEGF-A (dependent on Src activity), Smad1 and DKK-3, inducing proliferation, angiogenesis and invasion.

1.3.3 Functions of MT1-MMP

Due to the variety of substrates that are processed by MT1-MMP (Figure 1.2), the enzyme is involved in a plethora of cellular functions involved in physiological and pathophysiological processes as listed below.

1.3.3.1 MT1-MMP regulates cell motility

Overexpression of MT1-MMP has been shown to enhance cellular invasiveness in *in vitro* invasion assays using Matrigel [23] and in *in vivo* lung metastasis assays [56], whereas MT1-MMP gene silencing was sufficient to decrease Matrigel invasion of cancer cells [57]. MT1-MMP mediated increase in cell motility was shown to be at least partly driven by CD44 sheddding [49]. CD44 is a ubiquitously expressed hyaluronan receptor that mediates interaction with the cytoskeleton through its intracellular domain [58]. Although the exact mechanism of the MT1-MMP - CD44 mediated cell motility is not exactly known, MT1-MMP may play a role in either modulating adhesion properties of lamellipodia through CD44 shedding or by modulating CD44 dependent signalling after release of the CD44 intracellular domain (chapter 1.4.1) [59]. A similar increase of cell motility was observed following MT1-MMP mediated syndecan-1 shedding [51]. Although the molecular mechanism underlying the MT1-MMP and syndecan-1 induced cell migration has not been identified yet, syndecan-1 is known to associate with and stabilise $\alpha_v\beta_3$ integrin [60], raising the possibility that MT1-MMP induced syndecan-1 shedding affects integrin signalling pathways. Additionally, the extracellular signal-regulated protein kinase (ERK) pathway has been shown to be activated by MT1-MMP expression, a process being implicated in cell migration [61,62] (chapter 1.3.6, Figure 1.2). However, it is not clear whether ERK is directly activated by MT1-MMP or if its activation is a cellular response occurring down-stream of transmembrane protein shedding. Adhesion of cells to the ECM seems to be important for this process since activation of the ERK signalling pathway was observed in cells growing on type I collagen but was ablated in cells growing in suspension or on poly-L-lysine-coated culture vessels [61,62]. Cancer cell invasion through the basement membrane is an important step in metastasis. Type IV collagen as well as laminin 5 are key components of the basement membrane and were shown to be degraded either by MT1-MMP directly or by MMP-2 activity [45,55]. MT1-MMP mediated cleavage of laminin 5 leads to the release of EGF like domains, which further stimulate cell motility through an EGFR induced signalling pathway [63].

1.3.3.2 MT1-MMP dependent collagen degradation

One of the most prominent roles of MT1-MMP is its ability to cleave collagen. Collagen is a key component of the extracellular matrix and consists of 3 α-chains forming triple helical structures, which are assembled into fibrils. These structures are resistant to most proteinases except MT1-MMP and the soluble collagenases MMP-1, MMP-2, MMP-8 and MMP-13 [19]. The importance of MT1-MMP induced collagen degradation is emphasised by the observations that in mice, MT1-MMP deficiency led to craniofacial dysmorphism, arthritis, osteopenia, dwarfism, fibrosis in periskeletal soft tissues, a reduced vascularisation and premature death [64,65]. These knockout mice die around 7-12 weeks of age [64,65], indicating that MT1-MMP expression is required during embryonic and postnatal development and for survival. Interestingly, engineered soluble MT1-MMP lacking the transmembrane domain, failed to induce cell migration through collagen or fibrin gels despite its proteolytic activity [66]. These findings emphasise that proteolytic activity *per se* is not sufficient for ECM invasion and that the proper localisation of active MT1-MMP at the cell surface is required. The importance of the MT1-MMP cell surface localisation was also confirmed by using an MT1-MMP mutant in which the transmembrane domain was replaced with the MT6-MMP GPI anchor. This membrane-bound chimera retained the ability to invade 3D collagen gels and to proliferate within these matrices [67,68]. Interestingly, replacement of the catalytic domain with that of MMP-1 conferred cells with a collagen invading potential indicating that proteolytic activity correlates with the localisation of the protease at the cell membrane and a potential requirement of the other non-proteolytic MT1-MMP domains in cellular functions [67].

1.3.3.3 MT1-MMP functions during angiogenesis

During angiogenesis new blood vessels are established from pre-existing vessels. In this process endothelial cells have to detach from adjacent cells, invade into stromal tissue and establish new tubular structures. Angiogenesis plays an important role in wound healing and has been implicated in pathophysiological processes including tumour growth and rheumatoid progression [69]. MMP expression was demonstrated to be increased in endothelial cells (ECs) during migration as well as in blood vessels *in vivo*, and was shown to be modulated by angiogenic factors [44,70]. Interestingly, angiogenesis takes place in mice lacking MMP-2, MMP-9, their cell surface receptors (CD44 and β_3-integrin) or

plasminogen whereas aortic vessel explants from *MT1-MMP*$^{-/-}$ mice failed to induce endothelial cell invasion and neovessel formation [71]. Sounni *et al.* showed that MT1-MMP overexpression in human melanoma cells, which express pro-MMP-2 endogenously enhances invasion *in vitro* as well as growth, size and vascularity of tumours *in vivo* [27]. MT1-MMP overexpression in MCF-7 breast cancer cells, which are MT1-MMP and pro-MMP-2 deficient, promoted *in vitro* blood vessel sprouting in the rat aortic ring assay and induced highly vascularised tumours when injected into mice [72], most likely by inducing transcription of the pro-angiogenic vascular endothelial growth factor (VEGF) [73]. Furthermore MT1-MMP affects angiogenesis by degradation of the extracellular matrix, thus either unmasking angiogenic sites and/or releasing pro- and antiangiogenic factors, which were sequestered within the ECM.

1.3.4 Regulation of MT1-MMP function

The functions of MT1-MMP previously described and its role in cancer cell proliferation, metastasis and tumour angiogenesis emphasise that regulation of MT1-MMP activity is critical for the maintenance of normal cellular function. Regulatory mechanisms apply at the level of transcription, activation of the zymogen, endocytosis, interaction with ECM components, endogenous inhibitors and by subcellular localisation, as briefly described in the following sections.

1.3.4.1 Regulation by gene transcription

MT1-MMP is constitutively expressed *in vitro* in fibroblasts, endothelial cells, malignant epithelial cells and smooth muscle cells. Its expression may be up-regulated in phases of inflammation and remodelling in response to mechanical stress, cytokines, growth factors and chemical agents [74]. MT1-MMP mRNA levels were shown to be increased in 3D collagen I matrices by hepatocyte growth factor (HGF) treatment [75] and by granulocyte-macrophage colony stimulating factor (GM-CSF) stimulation of endothelial cells via a MEK-dependent pathway [76], whereas its expression is moderately enhanced following treatment with TGF-β or the chemical agents phorbol 12-myristate 13-acetate (PMA) and concanavalin A, which are known to enhance MT1-MMP ectodomain shedding (chapter 1.3.4.4) [77-79]. Treatment of glioma cells with epidermal growth factor (EGF) was further

found to increase MT1-MMP transcription [80], whereas stimulation of cells with TNF-α led to controversial results. TNF-α dependent MT1-MMP transcription was only observed in fibroblasts cultured within a 3D collagen I matrix, but not in 2D, indicating the regulation of MT1-MMP expression by cytoskeleton-ECM interactions [81]. These results were in agreement with studies demonstrating enhanced MT1-MMP mRNA levels in fibroblasts embedded in a 3D collagen matrix following mechanical stretching and treatment of cells with the cytoskeleton disrupting agent Cytochalasin D [82-84]. Promoter analyses revealed that in contrast to most soluble MMPs the MT1-MMP gene lacks the conserved TATA sequence as well as the AP-1 binding site 5'-upstream of the coding region [85]. Further information about the regulatory elements within the promoter region is incomplete but transcription factor binding sites for the transcription factors Sp1 and Egr-1 have been identified [85,86].

1.3.4.2 Regulation by zymogen activation

MT1-MMP is synthesised as a ~64 kDa latent zymogen that requires the removal of the NH_2-terminal propeptide in order to be catalytically active. The conserved furin recognition site ($RRKR^{111}$) in the prodomain is cleaved either intracellularly by the proprotein convertase furin during the MT1-MMP trafficking between the endoplasmic reticulum to the plasma membrane, or extracellularly by plasmin [21,87-90]. The active ~57 kDa MT1-MMP starting at Y^{112} is subsequently inserted into the plasma membrane with the catalytic domain facing the extracellular milieu (Figure 1.2).

1.3.4.3 Regulation by endogenous inhibitors

Inhibition of active MT1-MMP at the cell surface is a crucial step in regulating its activity. Tissue inhibitors of Metalloproteinases (TIMPs) belong to a family of endogenous proteinase inhibitors which are able to bind and inhibit MMPs in tight non-covalent complexes of 1:1 stoichiometry [91]. MT1-MMP is inhibited by TIMP-2, -3, and -4 but not by TIMP-1 [92,93]. MT1-MMP catalytic activity was further inhibited by RECK (reversion-inducing-cysteine rich protein with Kazal motifs) [94], which also inhibits MMP-2 and MMP-9, as well as by TFPI-2 (tissue factor pathway inhibitor 2) and α_2-Macroglobulin[55].

Various other proteins including chondroitin/heperan sulphate proteoglycans as well as testican 1 and 3 have been reported to block MT1-MMP activity, although the mechanism underlying this inhibition remains to be investigated [55]. Amongst the endogenous inhibitors, TIMP-2 plays an ambivalent role in regulating MMP activity. Although being a potent inhibitor of MT1-MMP function it is also involved in the MT1-MMP mediated pro-MMP-2 activation. Thereby, pro-MMP-2 forms a complex with TIMP-2 through their C-terminal domains, enabling the N-terminal inhibitory domain of TIMP-2 in the complex to bind to MT1-MMP at the cell surface. This pro-MMP-2 – TIMP-2 – MT1-MMP ternary complex is presented to an adjacent active MT1-MMP that is not inhibited by TIMP-2 function, which subsequently activates pro-MMP-2 [21,95,96]. Dimerisation or multimerisation of MT1-MMP on the cell surface through its hemopexin domains facilitates pro-MMP-2 activation [97].

1.3.4.4 Processing of MT1-MMP

MT1-MMP has been shown to undergo autocatalytic and non-autocatalytic processing, thus regulating the amount of active MT1-MMP present at the cell surface. Autocatalytic degradation of the ~57 kDa active membrane-bound MT1-MMP results in a membrane-tethered ~44 kDa form [98-100]. During this process a ~18 kDa fragment corresponding to the catalytic domain is released, whereas the remaining inactive enzyme remains attached to the plasma membrane (G^{285} – V^{582}) [101]. Surprisingly, the presence of the ~44 kDa MT1-MMP form correlates with an enhanced level of pro-MMP-2 activation [98,99]. Exposure of cells to concanavalin A or phorbol esters, chemical agents that are known to increase MT1-MMP-dependent pro-MMP-2 activation, was shown to enhance MT1-MMP processing to its ~44 kDa form [98,100,102-104]. Although autocatalytic cleavage terminates MT1-MMP catalytic activity, the ~44 kDa fragment has been shown to exhibit a regulating function of enzymatic activity. It competes with full-length MT1-MMP for collagen binding, thus reducing the collagenolytic activity and cellular invasion through collagen-rich matrices [105] as well as influencing the formation of the MT1-MMP – pro-MMP-2 – TIMP-2 ternary complex. Sequencing data of the released ~18 kDa fragment indicated that it is processed by two sequential cleavage events. The first occurs at the Gly^{284} – Gly^{285} peptide bond within the hinge region, which generates the ~44 kDa membrane-bound fragment. The

second proteolytic cleavage takes place at the Ala^{255} – Ile^{256} peptide bond within the active site of MT1-MMP, generating an inactive soluble fragment [100,106].

Additionally, MT1-MMP undergoes non-autocatalytic processing, leading to the accumulation of soluble MT1-MMP forms in cell culture supernatants of breast carcinoma [100,107,108], lung fibroblasts [107], endothelial cells [70,109] and fibrosarcoma cells [100]. Soluble MT1-MMP fragments have also been identified in the supernatant of cells overexpressing recombinant MT1-MMP [100,110] or in human sputum and branchoalveolar lavage fluids [111]. The major soluble form detected has a molecular mass of ~50 – 52 kDa corresponding to the entire ectodomain being shed from the cell surface [70,100,107,108]. The 50 kDa from was found to activate pro-MMP-2 [100], indicating that this soluble form sustains its catalytic activity. The non-autocatalytic cleavage has been shown to be a two-step process: the initial cleavage mediated by an unknown proteinase occurs within the stalk region of MT1-MMP leading to the generation of the 52 kDa fragment whereas the second cleavage event, which generates the 50 kDa form was found to be ADAM-dependent [112]. Additionally, a minor fraction of ~30 – 32 kDa forms of MT1-MMP was detected in the supernatant of a variety of cells [100,107], although the mechanism underlying the generation of these fragments remains to be investigated.

1.3.4.5 Regulation by cellular trafficking

Protein localisation that is affected by exocytosis, interacting proteins, endocytosis, recycling to the cell surface or degradation, is a further critical step in regulating MT1-MMP activity. During cell migration, cells generate membrane protrusions, including lamellipodia and invadopodia, that facilitate local ECM degradation. Localisation of MT1-MMP in these protrusive membrane structures is a key process for MT1-MMP proinvasive activity in migrating cells [4,36,97,113]. The localisation of the enzyme is partly mediated by binding via its hemopexin domain to the widely expressed hyaluronan receptor CD44, which in turn associates with F-actin [58,114]. This interaction was reported to promote cell motility [4]. Studies using an intracellular domain deletion mutant of CD44 revealed a decreased localisation of MT1-MMP at lamellipodia, potentially due to an attenuated MT1-MMP interaction with F-actin [4]. β1 integrin has also been implicated to regulate MT1-MMP localisation [115,116], although it remains to be investigated whether both proteins are interacting directly.

However, MT1-MMP expression at the cell surface was usually shown to be weak in most tested cell types due to rapid internalisation of the protease to early and late endocytic structures [39,117]. MT1-MMP accumulates in caveolae and in clathrin-coated regions of the membrane, which was shown to be important for endocytosis and recycling of MT1-MMP from the plasma membrane [39,117-120]. Clathrin-dependent internalisation is mediated by the interaction between the MT1-MMP intracellular domain and the μ2 subunit of adaptor protein 2 (AP-2) [121] (chapter 1.3.5). A smaller fraction of total MT1-MMP has been shown to be associated with caveolae. Caveolae-dependent endocytosis was found to be dependent on Src induced phosphorylation of Caveolin-1 [122]. Subsequently, MT1-MMP binds phospho-Caveolin-1 and this interaction regulates MT1-MMP internalisation [119]. The dynamic modulation of MT1-MMP localisation to invasive structures and its endocytosis emphasise the importance of spatiotemporal regulation of MT1-MMP.

1.3.5 The intracellular domain of MT1-MMP

In addition to the essential role of MT1-MMP mediated pericellular proteolysis in tumour cell migration, there is increasing evidence that the MT1-MMP intracellular domain (ICD) exerts important roles in regulating protein internalisation, cell surface localisation as well as inducing intracellular signalling pathways.

The MT1-MMP ICD consists of 20 amino acids ranging from R^{563} to V^{582} (Figure 1.3). It was shown that the intracellular and the transmembrane domains are not only important for MT1-MMP localisation but are also required for the collagenolytic activity of the enzyme [66,123]. A chimera that expressed the extracellular MT1-MMP domain and the transmembrane and intracellular domains of interleukin-2 retained the ability to activate exogenous pro-MMP-2 [124], but exhibited impaired cell surface localisation and degradation of the ECM [125]. Expression of ICD deletion mutants led to a higher expression level of the enzyme at the cell surface, as shown by an increased level of pro-MMP-2 activation [110,117]. These observations were found to be a consequence of decreased internalisation compared to the wild-type enzyme [67,117,121]. In addition, the ICD deletion mutant failed to localise MT1-MMP at the leading edge of migrating cells and was thus found to decrease cell motility [38,110,125].

As described, MT1-MMP endocytosis is mainly mediated by a clathrin-dependent mechanism, although a smaller fraction is associated with caveolae. Uekita *et al.* reported

that the ICD of MT1-MMP mediates its clathrin-dependent internalisation by recruiting the μ2 subunit of the adaptor protein 2 (AP-2) to its LLY^{573} sequence (Figure 1.3) [121]. AP-2 is known to regulate incorporation of membrane proteins in clathrin-coated vesicles [121]. This finding correlates with the observation that the cytoplasmic domain of MT1-MMP is essential for its trafficking, its recruitment to the cell surface and endocytosis [126]. Interestingly, mutation of the LLY^{573} sequence or deletion of the intracellular domain resulted in decreased cell migration and invasion, indicating a link between regulated endocytosis of MT1-MMP and cell locomotion [121]. Following internalisation of MT1-MMP, a sub-fraction is transported to the trans-Golgi network through early endosomes and subsequently recycled back to the cell surface. This MT1-MMP recycling mechanism was shown to be dependent on the DKV^{582} sequence (Figure 1.3) [127]. Interestingly, this carboxy-terminal motif (DKV^{582}) has also been implicated in binding to the PDZ domain of neuronal nitric oxide synthase [128]. PDZ motifs mediate protein-protein interactions [129], thus raising the possibility that this MT1-MMP ICD motif facilitates the assembling of signalling complexes.

Recently, Labrecque *et al.* reported an association of MT1-MMP with phosphorylated caveolin-1 in Src-expressing cells dependent on the Cys^{574} and Val^{582} residues (Figure 1.3) [119]. Following Src-dependent phosphorylation, phospho-caveolin-1 interacts with integrins at focal adhesions [130], raising the possibility that the phospho-caveolin-1 – MT1-MMP complex is implicated in cell adhesion and migration. Furthermore, MT1-MMP undergoes palmitoylation at the C^{574} within the intracellular domain (Figure 1.3) [131]. This lipid post-translational modification was reported to affect cell migration and clathrin-mediated internalisation. Recent findings demonstrate that the Y^{573} is phosphorylated in a Src-dependent manner and plays an important role in endothelial and tumour cell migration [132]. Notably, stable transfection of fibrosarcoma cells with a non-phosphorylable MT1-MMP mutant showed an impaired proliferation level within 3D but not on 2D type I collagen gels [133], emphasising the importance of Src-dependent phosphorylation of the MT1-MMP intracellular domain. This reduction in proliferation has been shown to be independent of MT1-MMP catalytic activity and raises the possibility that signal pathways are induced depending on MT1-MMP phosphorylation. Interestingly, recent work by Moss *et al.* demonstrated that the MT1-MMP ICD is also phosphorylated at its Thr^{567} residue in a protein kinase C (PKC) dependent way, thus regulating collagenolytic activity [134] (Figure 1.3).

Additionally, the MT1-MMP ICD is involved in the activation of the extracellular signal-regulated protein kinase (ERK) signalling pathway, which was shown to depend on the YCQR^{576} sequence [61] (Figure 1.3, chapter 1.3.6). Another protein, MTCBP-1 (MT1-MMP cytoplasmic-binding protein-1), has been recently identified to bind to the MT1-MMP ICD at an unknown intracellular motif, and to co-localise with MT1-MMP at the plasma membrane [135]. MTCBP-1 is a member of the cupin superfamily and was shown to decrease MT1-MMP induced cell migration but not to affect pro-MMP-2 activation levels.

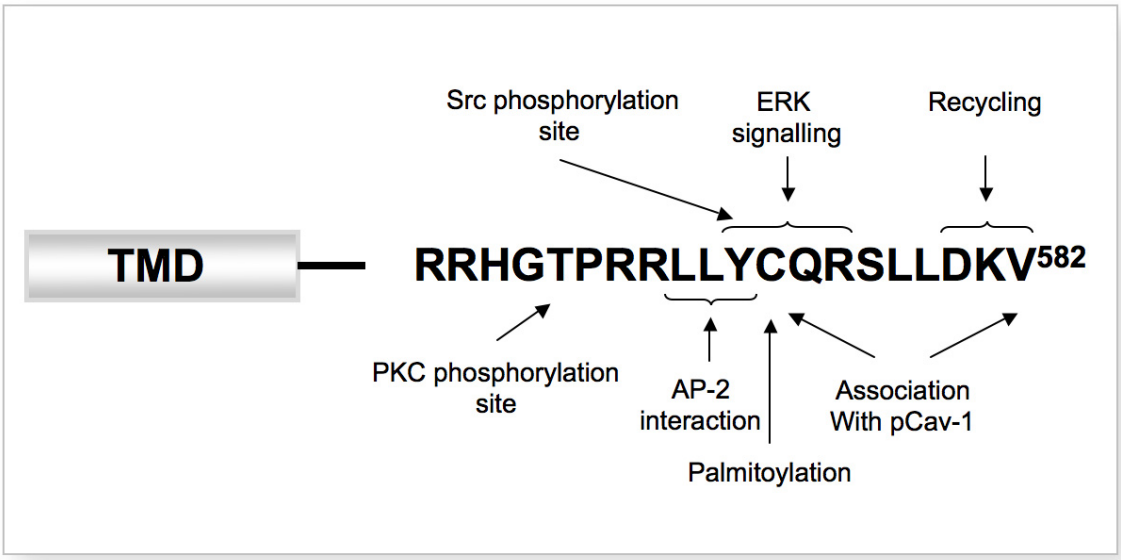

Figure 1.3: The cytoplasmic domain of MT1-MMP

Schematic representation of the 20 amino acid comprising ICD with its reported functions. *TMD*, transmembrane domain. *pCav-1*, phosphorylated Caveolin-1.

1.3.6 Transcriptional regulation by MT1-MMP

The pro-angiogenic effect of MT1-MMP was shown to be at least partly driven by the MT1-MMP dependent up-regulation of VEGF-A expression at both the mRNA and protein level in MCF-7 and U251 cells [26,72,73]. MT1-MMP overexpression in tumours stimulates angiogenesis *in vivo* by increasing VEGF-A synthesis within the tumour cells [26,72]. A correlation between MT1-MMP and VEGF-A expression was confirmed by immunohistochemical staining and RT-PCR of human glioma tissue samples and have been found in early physiological cartilage formation [136,137]. In contrast, the expression of other angiogenic factors including VEGF-B, -C, -D, P1GF, angiopoietin or their receptors

VEGFR-1, -2, neuropilin, Tie-1 and Tie-2 were not affected by MT1-MMP [73]. MT1-MMP induced expression of VEGF-A was further shown to require the functional catalytic and intracellular domain as well as involving the activity of Src kinase [73].

shRNA mediated MT1-MMP gene silencing in various cancer cell lines led to the identification of additional genes that were regulated by the proteinase. For instance, Smad1 expression was found to be decreased in MT1-MMP deficient cells compared to wild-type control, which correlated with reduced tumour growth [138]. MT1-MMP silencing using RNAi in human urothelial cell carcinoma cell lines led to an increased level of the tumour suppressor Dickkopf-3 (DKK-3) [139]. However, the identity of intracellular signalling pathways leading to the regulation of the described gene transcription remains to be investigated.

Gingras *et al.* have shown an activation of the ERK signalling pathway in MT1-MMP expressing COS-7 cells. This ERK activation was found to be dependent on the MT1-MMP ICD and its catalytic activity [61]. Reporter assays performed on MT1-MMP expressing cells showed that activation of ERK correlated with an increase of transcription under the control of serum-response elements (SRE) [61]. By using various MT1-MMP intracellular domain mutants, the $YCQR^{576}$ sequence was found to be required for ERK signalling (Figure 1.3) [140]. Thus, the ERK activation signal overlaps with the described LLY^{573} motif being involved in MT1-MMP internalisation (Figure 1.3). However, the role of the intracellular domain in ERK activation remains unclear, since ICD deletion mutants were found to increase ERK activation in another study [141]. In contrast, adding TIMP-2 to MT1-MMP expressing MCF-7 cells, led to an ICD dependent but catalytically independent activation of the Ras-MEK-ERK signalling cascade [140].

1.4 Membrane-tethered transcriptional regulators

Various transcriptional regulators have been identified as latent transmembrane precursors, which have to be processed in order to translocate to the nucleus and regulate gene transcription. Recently, two different pathways (regulated intramembrane proteolysis and regulated ubiquitin/proteasome dependent proteolysis) have been reported in which transmembrane proteins are proteolytically released and their intracellular domains play a key role in different pathways and transcriptional regulation [142].

1.4.1 Regulated intramembrane proteolysis (RIP)

A number of transmembrane proteins have recently been found to undergo regulated intramembrane proteolysis (RIP). The common characteristics of RIP involve ectodomain shedding of the transmembrane proteins, generating a membrane-bound fragment comprising of a short intracellular domain, which is subsequently cleaved within the transmembrane domain thus releasing the intracellular part. The first transmembrane proteins that were discovered to undergo RIP were Notch-1 [143,144] and the amyloid precursor protein (APP) [145]. Recently, additional surface proteins have been identified including SREBP (SRE-binding protein) [146], CD44 [59], the Notch ligands Jagged and Delta [147], ErbB4 [148], E-cadherin [149], syndecan 3 [150] and LRP1 [151] .

Transmembrane proteolysis occurring during RIP is mainly mediated by four families of proteinases: ***(i)*** the presenilin-type aspartyl proteinases, especially the presenilin-dependent γ-secretase which mediates the Notch-1 and APP shedding, ***(ii)*** the site-2 protease family (S2P) that cleaves SREBP, ***(iii)*** the rhomboid serine proteinases cleaving the EGF ligand Spitz and ***(iv)*** the signal-peptide peptidase (SPP) involved in the processing of MHC (class I major histocompatibility complex) proteins [152-154]. The presenilin-type aspartyl proteinase and S2P dependent RIP require a two-step proteolytic mechanism. Initially, the extracellular domain is cleaved off, typically by a metalloproteinase of the ADAM family (e.g. ADAM-9, -10, -17), enabling the second proteolysis within the transmembrane domain [155-161]. In contrast, rhomboid serine proteinases are able to cleave intramembranous protein domains without prior ectodomain shedding. Cell surface proteins which are processed by presenilins and rhomboids belong to the type-I transmembrane proteins, whereas S2P and SPP cleave type-II transmembrane proteins [154,162-164]. The proteolysis of transmembrane proteins results in the release of the intracellular domain, which acts as a bioactive molecule in different pathways or as transcriptional regulator. The mechanism underlying RIP of several key type-I transmembrane proteins is briefly described.

1.4.1.1 γ-secretase dependent RIP

γ-secretase is a multiprotein complex comprising of presenilin-1, presenilin-2, APH-1 (anterior pharynx-defective phenotype), nicastrin and PEN-2 (presenilin-enhancer 2). It is involved in the cleavage of various type-I transmembrane proteins including the *β*-amyloid

precursor protein [165] (chapter 1.4.1.1.1), Notch receptor [144] (chapter 1.4.1.1.2), E-cadherin, N-cadherin [149], CD44 [166,167], ErbB-4 [148], the Notch ligands Delta and Jagged [147] and the low density lipoprotein (LDL) receptor related protein (LRP) [151,168]. Presenilin depletion led to a decreased γ-secretase activity and reduced APP processing as well as inducing severe defects in embryonic development similar as observed in Notch1-deficient mice [169-171].

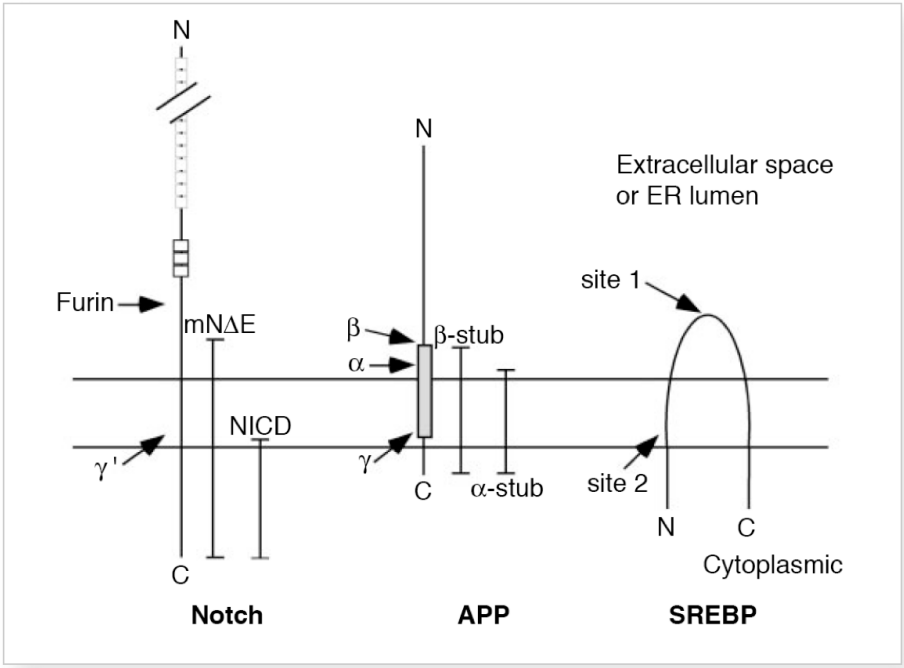

Figure 1.4: Regulated intramembrane proteolysis

Schematic representation of Notch1, APP and SREBP RIP. The proteinases involved (furin, α-, *β*- and γ-secretase, site-1 and site-2 protease) and the proteolytic cleavage fragments (NICD, α- and *β*-stubs) are indicated. Taken from [144].

1.4.1.1.1 RIP of the *β*-amyloid precursor protein (APP)

The *β*-amyloid precursor protein is a large type-I transmembrane glycoprotein, mainly expressed in neurons and vascular cells [172]. It was shown to undergo proteolytic cleavage involving the sequential activity of α-, *β*- and γ-secretase (Figure 1.4) [173]. Generally, an initial α-secretase (e.g. TACE or ADAM-10) dependent cleavage event releases the APP ectodomain [158], although ectodomain shedding mediated by *β*-secretase activity (e.g. BACE-1/2) was also observed [174-177]. Both initial cleavage steps lead to the release of the extracellular domain and the generation of a membrane-bound COOH-terminal fragment.

Subsequent cleavage of the membrane-tethered peptide by γ-secretase leads to the release of the *β*-amyloid protein (A_{β}, following *β*-secretase shedding) or the p3 peptide (following α-secretase shedding) and the APP intracellular domain [178]. The released ICD domain enters the nucleus and modulates gene expression [179,180].

1.4.1.1.2 RIP of Notch-1

Notch-1 is a type-I transmembrane signalling protein, which plays an important role during early stages of embryonic development. It is cleaved by a furin-like proteinase in the Golgi during trafficking to the plasma membrane [181]. Subsequent binding of its ligands, Delta and Jagged, triggers the proteolytic processing of Notch-1 by TACE (ADAM-17) [182] or by ADAM10 (Kuzbanian) [183] followed by a second γ-secretase-mediated cleavage which leads to the release of the Notch intracellular domain (NICD) (Figure 1.4). The released intracellular domain translocates to the nucleus where it regulates transcription of various target genes (e.g. HES-1) [184,185].

1.4.1.2 Rhomboid-dependent RIP

The rhomboid family consists of about 100 members, which are highly conserved from bacteria to humans. However, they are best characterized in the fruitfly *Drosophila melanogaster*. Rhomboids are serine proteinases with seven transmembrane domains which are involved in the regulated intramembrane proteolysis and release of EGF ligands including Spitz, Keren and Gurken [154,162-164]. There are three human rhomboids described so far: RHBDL1 [186], RHBDL2, a presenilin associated rhomboid-like protein (PARL) [187] and RHBDL4 [188]. However, their biological function remains to be investigated. The human rhomboid, RHBDL2, is known to cleave *Drosophila* Spitz when both proteins are co-expressed in mammalian cells. Pascall & Brown suggested B-type ephrins as potential substrates of RHBDL2 [189].

1.4.2 Regulated Ubiquitin/Proteasome-dependent processing (RUP)

Recently, a novel proteolytic cleavage mechanism leading to the maturation of transcription factors was observed in yeast (*Saccharomyces cerevisiae*), which requires the activity of the ubiquitin/proteasome pathway [190]. SPT23 and MGA2 are transcription factors tethered as latent forms to the membrane of the endoplasmatic reticulum (ER). Both play a key role in the OLE pathway (pathway that controls OLE1 desaturase levels) that regulates membrane fluidity and they are known to undergo proteolytic maturation in order to be released from the plasma membrane. The mechanism of SPT23 maturation is briefly summarised (Figure 1.5).

The membrane-bound SPT23 transcription factor interacts with the RSP5 ubiquitin ligase (E3 enzyme) leading to ubiquitination, which induces proteasome-dependent processing (Figure 1.5A, B). Subsequently, the carboxy-terminal and the transmembrane domain are completely degraded by the proteasome whereas only a 90 kDa fragment of the NH_2-terminus is spared (Figure 1.5C). This 90 kDa peptide translocates subsequently to the nucleus to regulate gene transcription (Figure 1.5D).

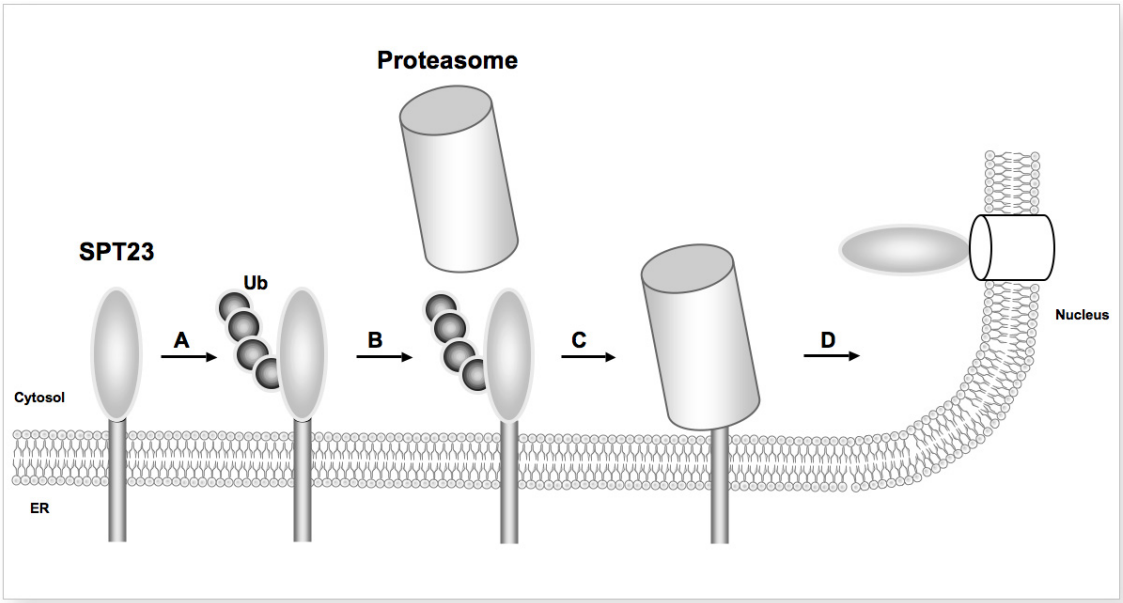

Figure 1.5: Regulated ubiquitin/proteasome-dependent processing

(A) The latent membrane-bound SPT23 is tagged by the RSP5 ubiquitin-ligase, which initiates proteasome-binding ***(B)*** and subsequent degradation of the COOH-terminus ***(C)***. Only a 90 kDa N-terminal fragment is spared from degradation and translocates to the nucleus as a transcription factor ***(D).*** Adapted from [142] .

Hoppe *et al.* suggested that a polypeptide loop of SPT23 enters the proteasome barrel entirely to contact the active site [190]. The N-terminal fragment, by being tightly bound to another protein, is therefore spared from degradation. The following detachment of this protein will release and activate the transcriptional function of SPT23.

The ubiquitination and subsequent processing of proteins by the proteasome is highly conserved. Emerging data reveal that besides degrading proteins that were tagged by ubiquitin, proteasomal function plays a key role in the regulation of various cellular processes, including gene transcription, DNA repair and chromatin remodelling [191]. An example of transcription factor activation in humans and thus regulating gene transcription, is the proteasome-dependent processing of NF-κB. p105, which is a precursor of the p50 subunit of the NF-κB transcription factor, is processed via a ubiquitin/proteasome-dependent mechanism. NF-κB regulates immune and inflammatory responses, is involved in embryogenic development, apoptosis and malignant progression. In this process, the C-terminal part of p105 is rapidly degraded by the proteasome whereas the N-terminal p50 fragment remains stable [192,193], similar to the OLE-pathway in yeast.

1.5 Tumour angiogenesis

Angiogenesis, the generation of new blood supply from existing vessels, depends on the proper regulation of endothelial cell activation, proliferation, adhesion, migration and maturation [194,195]. Following embryonic development, angiogenesis is restricted to processes of wound healing, ovarian and menstrual cycles as well as pregnancy [194]. However, it also plays a key role during pathophysiological conditions including cancer, inflammatory and cardiovascular diseases [196]. The growth of tumours is restricted by its need to provide sufficient nutrients and oxygen to the tumour cells. Under hypoxic conditions tumour cells induce the development of new blood vessels from pre-existing vasculature by secreting pro-angiogenic mitogens, in particular vascular endothelial growth factor.

1.5.1 Vascular endothelial growth factor

Vascular endothelial growth factor (VEGF) is a key pro-angiogenic mitogen that is secreted by endothelial as well as tumour cells to induce endothelial cell differentiation

(vasculogenesis) and sprouting of new capillaries from pre-existing vessels (angiogenesis) [197,198]. VEGF was shown to be a key player during phases of embryogenic development, wound healing and in human pathophysiological conditions including cancer, rheumatoid arthritis as well as cardiovascular disease [199,200]. Expression of VEGF has been correlated with poor prognosis in patients with breast cancer [201]. Recent therapeutic approaches targeting tumour angiogenesis are based on neutralising monoclonal anti-VEGF antibodies or small molecular weight inhibitors against their corresponding receptors. Inhibition of VEGF activity using the monoclonal antibody bevacizumab (Avastin) represents the first successful anti-angiogenic treatment strategy when given in combination with chemotherapy as recently shown in the treatment of lung, colon and breast cancer [202,203]. However, it is crucial to understand the biology of pathologic angiogenesis as well as the development and survival of blood vessels under physiologic conditions when anti-angiogenic therapies are applied in the long-term treatment of cancer. The attempt to develop selective therapeutic agents that are designed to attenuate only specific signalling pathways led to an increased interest in understanding VEGF receptor (VEGFR) induced signalling.

VEGF (VEGF-A) belongs to a family of conserved growth factors including VEGF-B, -C, -D and placenta growth factor (PlGF), which are endogenously expressed in mammals [204,205]. Alternative splicing of human VEGF mRNA from a single gene generates various VEGF isoforms, including 121, 145, 165, 189 and 206 amino acid forms [206]. Amongst these isoforms $VEGF_{165}$ and $VEGF_{121}$ are the most abundant splice variants and were found to be the most biologically active forms in *in vitro* studies. Both isoforms are secreted by various different tumour cells with particularly high mRNA levels being detected in breast cancer cell lines [207]. Human $VEGF_{165}$ is glycosylated at Asn^{75} and forms typically 46 kDa homodimers [208]. The expression of VEGF-A has been shown to be up-regulated through the activation of tyrosine kinase receptors including receptors of the EGF family [209] as well as insulin [210], IGF [211], HGF [212], PDGF [213] and FGF receptors [214]. These receptors were shown to induce two different canonical pathways leading to the activation of Ras – Raf – MEK – ERK as well as the phosphatidylinositol 3-kinase (PI3K) – Akt pathway. The Ras – Raf – MEK – ERK pathway is essential for the up-regulation of VEGF-A in fibroblasts, whereas the PI3K induced pathway is implicated in VEGF-A expression in epithelial cells [215]. The main transcriptional regulation of the VEGF gene is mediated through the proximal region of the promoter, which contains GC-rich regions binding factors of the Sp family as well as AP-2 and Egr-1 transcription factors

(summarised in Figure 1.6). The expression of VEGF-A is furthermore rapidly induced under hypoxic conditions, which enables the binding of the transcriptional regulator hypoxia inducible factor 1 (HIF-1) to the corresponding hypoxia response elements (HRE) in the 5' flanking region of the VEGF-A human promoter region (Figure 1.6) [216-218]. A variety of external factors and stimuli have been shown to induce VEGF-A expression mainly via activation of the Sp proteins, including TNF-α [219], TGF-α [220], basic fibroblast growth factor (bFGF) [200], TGF-*β*1 [221], interferon α [222] and interleukin-1*β* [223] in various cell types.

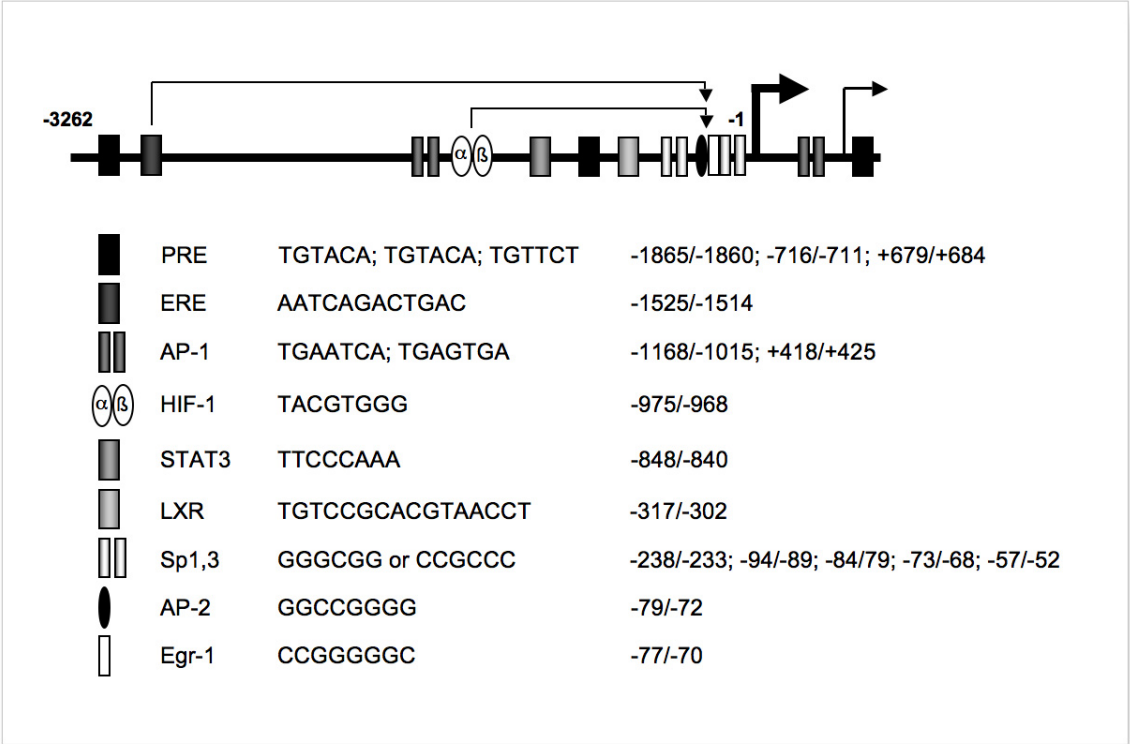

Figure 1.6: VEGF-A promoter region

The entire VEGF-A promoter region is represented. The heavy arrow indicates the classical initiation of transcription, whereas another cryptic promoter was described within the 5' UTR region (light arrow). Long arrows indicate a connection between *cis*-regulatory elements and *trans*-activating factors. Adapted from [224].

1.5.2 VEGF signalling

Members of the VEGF family of growth factors exhibit their biological functions through binding to corresponding receptor tyrosine kinases. Three VEGF receptors (VEGFR) have been identified: VEGFR-1 (flt-1), VEGFR-2 (KDR, flk-1) and VEGFR-3 (flt-4). VEGFR-1 binds to VEGF-A, -B and PlGF, VEGFR-2 binds to VEGF-A and -E and VEGFR-3

interacts with VEGF-C and -D [225]. Proteolytic processing of human VEGF-C and -D facilitates binding to VEGFR-2, however this binding occurs with a lower affinity than binding to VEGFR-3 [226]. In addition to the formation of homodimers, VEGFRs have also been described to form heterodimers, although the signal-transduction capacities of these heterodimers remain to be elucidated. The ligand specificities of the receptors are summarised in Figure 1.7.

The three VEGFRs are structurally related to the PDGF family of receptors, sharing a similar domain structure consisting of an intracellular domain containing a split tyrosine kinase domain that is interrupted by a 70 amino acid kinase insert, a single hydrophobic transmembrane domain and seven immunoglobulin-like domains in the extracellular region. Their conserved structure is summarised for VEGFR-2 in Figure 1.8.

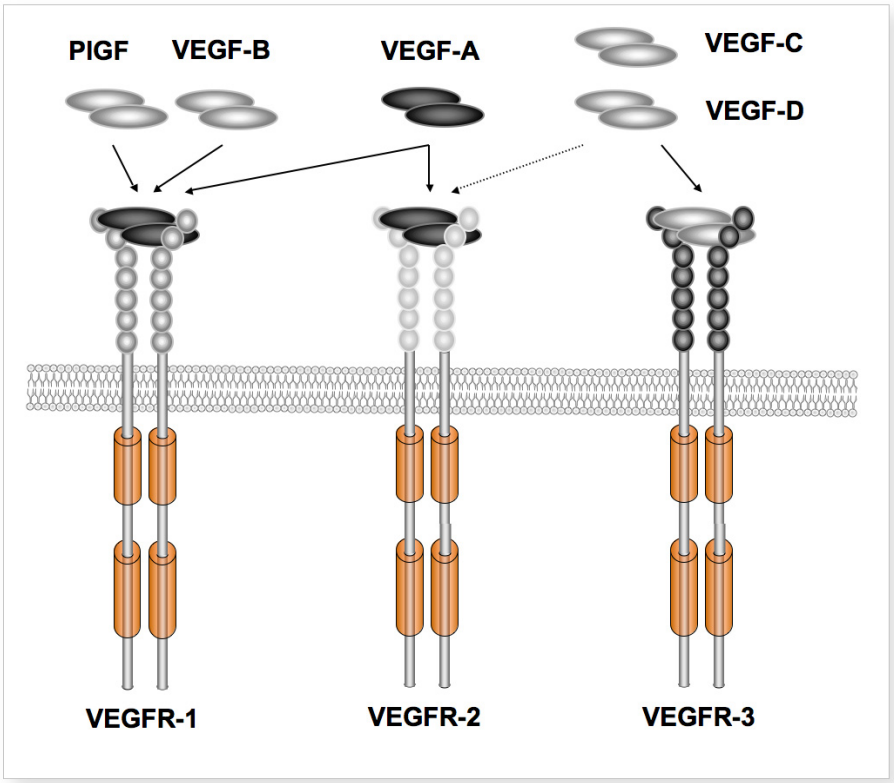

Figure 1.7: The VEGFR family with ligands

Mammalian vascular endothelial growth factors (VEGFs) bind to three VEGF receptor (VEGFR) tyrosine kinases (indicated by arrows), leading to the formation of VEGFR homodimers. Processing of VEGF-C and -D allows for binding to VEGFR-2 (dotted arrow). Adapted from [226].

Neuropilin-1 and -2 constitute another class of non-tyrosine kinase receptors for members of the VEGF family and bind to certain isoforms of VEGF-A, -B, -E and PlGF. Neuropilins are transmembrane glycoproteins that exhibit a short intracellular domain with

no known signalling function, suggesting that they are not functional receptors themselves. Notably, NRP-1 was shown to function as a critical co-receptor for $VEGF_{165}$, resulting in an increased affinity of $VEGF_{165}$ to VEGFR-2 [225]. Furthermore, heparin was found to amplify the signalling of $VEGF_{165}$, but not $VEGF_{121}$, via VEGFR-2 [227]. This NRP-1 and heparin dependent enhanced stimulation of VEGFR-2 is at least partly the reason that $VEGF_{165}$ is the strongest signal transducer among the VEGF subtypes and it is generally accepted that VEGFR-2 is the major mediator of the mitogenic, angiogenic and permeability-enhancing activities of VEGF-A [228].

VEGFR-1 is described as a positive regulator of monocyte and macrophage migration as well as a negative regulator of VEGFR-2 signalling activity. This negative regulatory capacity is at least partly mediated by an alternative soluble VEGFR-1 splice variant that binds to VEGF-A and thus prevents VEGF-A binding to VEGFR-2.

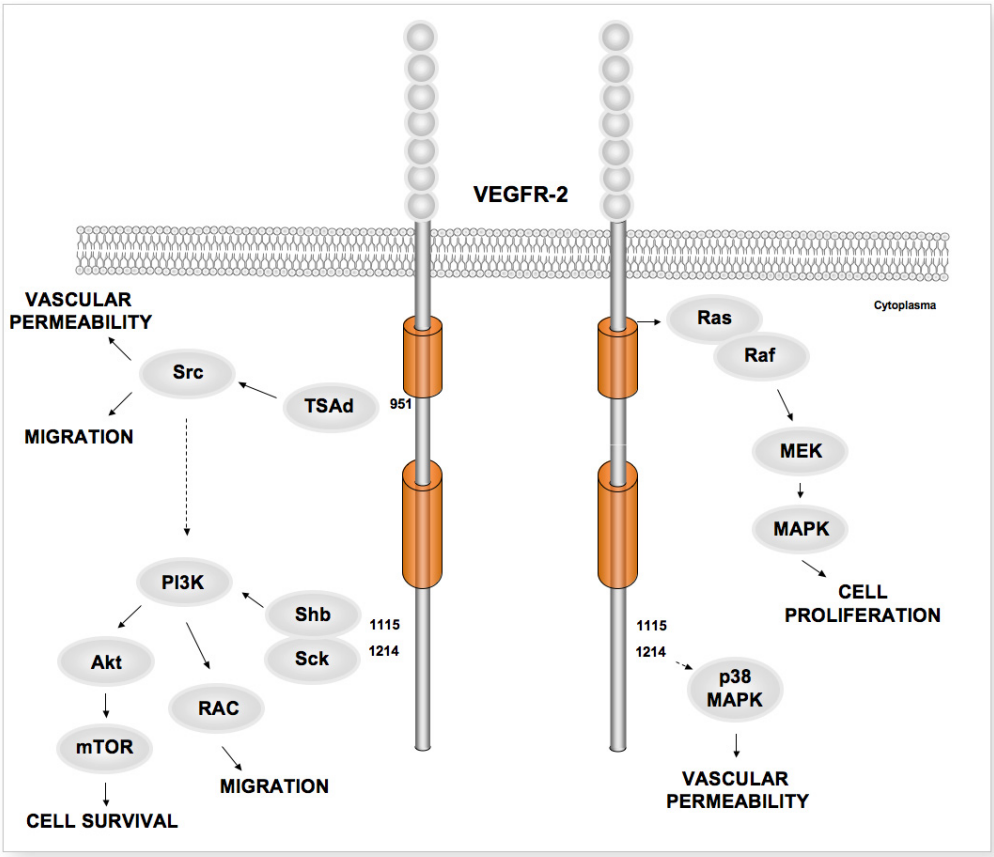

Figure 1.8: VEGFR-2 induced signalling pathways

Schematic representation of VEGFR-2 induced signalling pathways. Upon ligand binding VEGFR-2 forms homo-dimers leading to trans-phosphorylation of the indicated tyrosine residue within its intracellular part. Following binding of adapter proteins, various signalling cascades are activated including the Ras-Raf-MEK-MAPK and the PI3K-Akt-mTOR pathway as well as activation of Src and RAC. VEGFR-2 signalling affects various cellular responses including cell proliferation, cell survival, migration as well as vascular permeability in endothelial cells. Adapted from [226].

VEGFR-2 is implicated in all physiological and pathological aspects of vascular endothelial cell function, whereas VEGFR-3 is selectively expressed on lymphatic endothelium and plays a key role in lymphatic-endothelial-cell development and function [228]. However, there is an increasing body of evidence that VEGFR-1 and particularly VEGFR-2 are also expressed in malignant epithelial cells, providing a mechanism for tumour cells to induce an autocrine VEGF-A signalling loop leading to cell survival and proliferation. Initial evidence for autocrine VEGF signalling has been found in melanoma cells [229], leukaemia cells [230], prostate carcinoma cells [231], colon carcinoma cells [232], bladder tumour [233] and breast carcinoma cells [234-236].

It has been demonstrated that stimulation of the breast cancer cell line T47d induces cell invasion by activating intracellular MAP kinase, PI3K and Akt signalling pathways [235]. Interestingly, suppression of VEGF expression promotes apoptosis of breast cancer cells by inhibition of PI3K activity. This autocrine VEGF loop was further shown to facilitate invasion of breast carcinoma cell lines [236], emphasising the importance of autocrine VEGF stimulation for breast carcinoma cell survival independent of angiogenesis. The molecular mechanisms by which receptor tyrosine kinases are activated have been studied extensively. Briefly, following ligand-stimulated dimerisation of receptor monomers the dimerised receptor undergoes transphosphorylation of tyrosine residues within its intracellular domain, leading to an assembly of signalling proteins to receptor phosphotyrosines. In contrast to VEGFR-1, phosphorylated VEGFR-2 can be readily detected in cells after VEGF-A stimulation and its phosphorylation sites have been mapped (summarised in Figure 1.8).

Among these phosphorylation sites the tyrosine residues Y1054 and Y1059 within the activation loop were shown to be critical for the complete ligand-induced receptor tyrosine kinase activation [237,238]. In recent publications, the PI3K signal transduction pathway has emerged as one of the main signalling pathways downstream of VEGFR-2 activation, leading to cell survival and proliferation. PI3K converts the plasma membrane lipid phosphatidylinositol 4,5-biphosphate (PIP_2) to phosphatidylinositol-3,4,5-triphosphate (PIP_3). Adapter proteins containing a pleckstrin-homology (PH) domain, including Akt, phosophoinositide-dependent kinase-1 (PDK-1) and PDK-2, are able to bind to PIP_3. Akt is subsequently activated and induces cellular responses including cell proliferation, cell cycle progression and cell survival [239,240]. VEGFR-2 phosphorylated at its Y1175 residue has been shown to bind the adapter protein Shb that induces the activation of the PI3K/Akt pathway. Phospholipase Cγ1 (PLCγ1) also binds to phosphorylated Y1175 and induces the

activation of mitogen-activated protein kinase (MAPK)/extracellular-signal-regulated kinase-1/2 (ERK1/2) pathway as well as proliferation of endothelial cells. Furthermore PLCγ hydrolyses phosphoinositides to generate the second messengers inositol-1,4,5-triphosphate (IP_3) and diacylglycerol (DAG). IP_3 increases intracellular calcium levels, whereas DAG activates protein kinase C (PKC) leading to various cellular responses [241]. Furthermore, phosphorylated Y1175 has been shown to bind to the adapter proteins Sck/ShcB, which are required for normal development [242].

Phosphorylated Y951 is known to be a binding site for TSAd (T-cell specific adaptor; VEGF receptor-associated protein (VRAP)). Stimulation of cells with VEGF-A induces the complex formation between TSAd and Src, indicating a potential role of TSAd in Src activation or recruitment of active Src downstream of VEGFR-2. The third phosphorylation site, Y1214, has been implicated in VEGF-mediated actin remodelling through activation of Cdc42 and p38 MAPK [243]. Focal adhesion kinase (FAK) and its substrate paxillin which are involved in the turnover of focal adhesions during cell migration have been shown to be downstream substrates of VEGFR-2 signalling [244,245].

1.6 Aim of the thesis

MT1-MMP has been shown to play a key role in various stages of tumourigenesis, including tumour initiation, progression, tumourigenic angiogenesis and cell migration. In addition to its function as an ectodomain sheddase, recent studies revealed a regulatory effect of MT1-MMP on the transcriptional level of various target genes, including VEGF-A, DKK-3 and Smad1. The MT1-MMP dependent regulation of VEGF-A expression was reported to involve the MT1-MMP intracellular domain, its catalytic function as well as Src kinase activity [73]. Various angiogenesis-related regulator proteins were reported to be synthesised as latent transmembrane precursors that have to be proteolytically processed in order to fulfil their regulatory activity, including transcriptional regulation of target genes. However, the molecular mechanisms underlying this regulation are not understood so far.

The aim of this thesis was ***(i)*** to investigate how MT1-MMP induces signalling pathways, ***(ii)*** to define elements of a potential MT1-MMP induced pathway and in particular to dissect the molecular mechanism underlying the MT1-MMP dependent up-regulation of

VEGF-A and ***(iii)*** to get a better understanding of MT1-MMP mediated transcriptional regulation and its non-catalytic functions, facilitating MT1-MMP dependent signalling.
Therefore, the mechanism of MT1-MMP induced VEGF-A expression, as described previously [73], was further investigated in detail by using the MT1-MMP deficient breast cancer cell line MCF-7 as a model system (chapter 3.1) followed by subsequent testing of various different breast cancer cell lines (chapter 3.2). It was further investigated whether the MT1-MMP intracellular domain, which was shown to be involved in a plethora of cellular responses (chapter 1.3.5), is released following MT1-MMP extracellular domain shedding in a process of regulated intramembrane proteolysis (RIP) or regulated ubiquitin/proteasome dependent processing (RUP) in order to modulate transcription (chapter 3.3).

2 Material and Methods

2.1 Materials

The water used for most applications was deionised, microfiltered through a Milli-Q membrane and autoclaved. The water for PCR was purchased from Sigma-Aldrich. All chemicals were analytical grade unless indicated otherwise and were purchased from Sigma-Aldrich, Fluka or Fisher Scientific.

2.1.1 General materials

2.1.1.1 Equipment

Equipment	Model	Supplier
Incubator	Heraeus HERAcell® 150	Thermo Scientific, Wilmslow, UK
Gel electrophoresis	Mini Protean® II xi (Acrylamide gels)	Bio-Rad, Hemel Hempstead, UK
	Mini-Sub® Cell GT (Agarose gels)	Bio-Rad, Hemel Hempstead, UK
Centrifuges	5810R	Eppendorf, Cambridge, UK
	5415D	Eppendorf, Cambridge, UK
	J6-M1	Beckman Coulter, High Wycombe, UK
	Avanti® J-26 XPI	Beckman Coulter, High Wycombe, UK
Microscopes	Axioplan 2 imaging microscope	Zeiss, Göttingen, GER
	iCys™ laser scanning cytometer	CompuCyte, Westwood, MA
	Tandem SP5 inverted Confocal microscope	Leica Microsystems, Wetzlar, GER
	Eclipse TS100	Nikon Instruments Inc., Düsseldorf, GER
Fridges/Freezers	-80˚C, -20˚C, +4˚C	New Brunswick Scientific, St. Albans, UK; Labcold, Basingstoke, UK
Plate reader	Infinite® M200	Tecan, Reading, UK
Power supply	PowerPac 200	Bio-Rad, Hemel Hempstead, UK
VORTEX	Vortex-Genie 2	Scientific Industries, Bohemia, NY
PCR cycler	DNA Engine Tetrad 2 Peltier Thermal Cycler	Bio-Rad, Hemel Hempstead, UK
	Applied Biosystems 7900HT Fast Real-Time PCR System	Applied Biosystems, Warrington, UK
Serological Pipette	Matrix Cell Mate II	Thermo Scientific, Wilmslow, UK

Spectrophotometer	Nanodrop® ND-1000 UV-Vis	Thermo Scientific, Wilmslow, UK
RNA quality control	2100 Bioanalyzer	Agilent Technologies, Stockport, UK
Cell counter	Vi-CELL™	Beckman Coulter, High Wycombe, UK
Flow cytometry	FACSCalibur™	BD Biosciences, Oxford, UK
Pipettes	2 µl, 10 µl, 20 µl, 100 µl 200 µl, 1000 µl	Gilson, Middleton, WI
Rotator	Stuart SB3	Keison Products, Chelmsford, UK
Rocker	Stuart SSL4	Keison Products, Chelmsford, UK
Heat-stirrer	Stuart CB162	Keison Products, Chelmsford, UK
Heating block	QBD4	Grant Instruments, Shepreth, UK
Roller mixer	Stuart SRT9	Keison Products, Chelmsford, UK
Film processor		Agfa, Düsseldorf, GER
Hood	Bio MAT 2 Class II Mirobiological Safety Cabinet	Medical Air Technology Chadderton, UK
UV	UVP-BioDoc It™ Imaging System	UVP Ltd., Cambridge, UK
Water baths	Universal SUB36	Grant Instruments, Shepreth, UK

2.1.1.2 Consumables

Consumable	Supplier
Bacterial tubes (14 ml)	Sarstedt, Leicester, UK
Syringes	BD Biosciences, Oxford, UK
Cryotubes (1 ml, 1.8 ml)	Nunc, Roskilde, DK
Petri dishes	Sarstedt, Leicester, UK
Pipette tips	Star lab, Milton Keynes, UK
Filter pipette tips	Star lab, Milton Keynes, UK
Amersham Hybond™ ECL™ Nitrocellulose Membrane	GE Healthcare, Bucks, UK
Amersham Hyperfilm ECL™	GE Healthcare, Bucks, UK
Serological pipettes (5 ml, 10 ml, 25 ml, 50 ml)	Sarstedt, Leicester, UK
Sterile filters (0.2 um), Sterile Acrodisc Syringe	BD Biosciences; Millipore
3 MM Whatman paper	Schleicher & Schüll, Relliehausen, GER
Centrifuge tubes (15 ml, 50 ml)	Sarstedt, Leicester, UK
Tissue culture vessels (25 cm^2, 75 cm^2, 175 cm^2)	Sarstedt, Leicester, UK
Microtitre plates (96-well, 24-well, 12-well, 6-well)	Nunc, Roskilde, DK

2.1.1.3 Chemicals

Chemical	Supplier
Acetic acid	Acros, Loughborough, UK
Acetone	Acros, Loughborough, UK
Acrylamide	Fisher Scientific, Loughborough, UK
Agar	Fisher Scientific, Loughborough, UK
Agarose	Fisher Scientific, Loughborough, UK
Ammoniumpersulphate (APS)	Fisher Scientific, Loughborough, UK
Ampicilin	Fisher Scientific, Loughborough, UK
ß-mercaptoethanol	Sigma-Aldrich, Dorset, UK
Bovine serum albumine (BSA)	Sigma-Aldrich, Dorset, UK
Bromphenol blue	Fisher Scientific, Loughborough, UK
Complete Protease Inhibitor Cocktail	Roche Applied Science, Welwyn, UK
Coomassie G250	Fisher Scientific, Loughborough, UK
DNA marker: 1 kB ladder DNA marker VIII	 Invitrogen, Paisley, UK Roche Applied Science, Welwyn, UK
dNTP's	GE Healthcare, Bucks, UK
Dulbecco's modified Eagle's Medium (DMEM)	Invitrogen, Paisley, UK
Dynal® Magnteic Beads	Invitrogen, Paisley, UK
DTT (Dithiothreitol)	Fisher Scientific, Loughborough, UK
EDTA (ethylenediaminetetraacetic)	Fisher Scientific, Loughborough, UK
EGTA (thylene glycol tetraacetic acid)	Fisher Scientific, Loughborough, UK
Ethanol	Acros, Loughborough, UK
Foetal calf serum	Perbio, Thermo Scientific, Wilmslow, UK
Fugene 6	Roche Applied Science, Welwyn, UK
Glycine	Fisher Scientific, Loughborough, UK
Glycerol	Fisher Scientific, Loughborough, UK
HEPES	Fisher Scientific, Loughborough, UK
Kalium chloride (KCl)	Fisher Scientific, Loughborough, UK
Kanamycin	Fisher Scientific, Loughborough, UK
L-alanyl-L-glutamine	Invitrogen, Paisley, UK
Lithium chloride (LiCl)	Fisher Scientific, Loughborough, UK
Magnesium chloride ($MgCl_2$)	Fisher Scientific, Loughborough, UK
Marvel	Fisher Scientific, Loughborough, UK
Methanol	Acros, Loughborough, UK
ONPG (o-Nitrophenyl-β-D-galactopyranoside)	Sigma-Aldrich, Dorset, UK

Nonidet® P40 (NP40)	Sigma-Aldrich, Dorset, UK
Paraformaldehydes (PFA)	Fisher Scientific, Loughborough, UK
Phenol:Chloroform:Isoamyl Alcohol (25:24:1)	Sigma-Aldrich, Dorset, UK
Potassium dihydrogen phosphate (KH_2PO_4)	Fisher Scientific, Loughborough, UK
ProLong® Gold Antifade Reagent	Invitrogen, Paisley, UK
Protein Marker: BenchMark™ Protein Ladder	Invitrogen, Paisley, UK
ReBlot™ Plus Strong Antibody Stripping Solution	Millipore, Watford, UK
Sodiumchloride (NaCl)	Fisher Scientific, Loughborough, UK
Sodium deoxycholate	Fisher Scientific, Loughborough, UK
Sodium dodecyl sulphate (SDS)	Fisher Scientific, Loughborough, UK
Sodium Phosphate (Na_2HPO_4)	Fisher Scientific, Loughborough, UK
Sodium vanadate	Fisher Scientific, Loughborough, UK
SYBR® Safe DNA gel stain	Invitrogen, Paisley, UK
TEMED (N,N,N'N'-Tetraethylmethyldiamine)	Thermo Scientific, Wilmslow, UK
Tris-Base	Fisher Scientific, Loughborough, UK
Tris-HCl	Fisher Scientific, Loughborough, UK
Triton X-100	Fisher Scientific, Loughborough, UK
Trypane blue	Sigma-Aldrich, Dorset, UK
Tryptone	Fisher Scientific, Loughborough, UK
Tween®20	Sigma-Aldrich, Dorset, UK
Yeast extract	Fisher Scientific, Loughborough, UK

2.1.1.4 Kits

Kit	Supplier
BCA™ Protein Assay	Pierce, Thermo Scientific, Wilmslow, UK
Dual Luciferase® Reporter Assay System	Promega, Southampton, UK
Amersham ECL™ Western Blotting Detection Reagents	GE Healthcare, Bucks, UK
Platinum® *Taq* DNA Polymerase	Invitrogen, Paisley, UK
QuickChange® XL Site-Directed Mutagenesis Kit	Stratagene, Cheshire, UK
Qiagen Plasmid Mini Kit	Qiagen, Crawley, UK
Qiagen HiSpeed Plasmid Maxi Kit	Qiagen, Crawley, UK
Qiagen Large-Construct Kit	Qiagen, Crawley, UK
Qiagen RNeasy Plus Kit	Qiagen, Crawley, UK

QIAquick Gel Extraction Kit	Qiagen, Crawley, UK
SigmaSpin™ Post-Reaction Clean-Up Columns	Sigma-Aldrich, Dorset, UK
SuperScript® II Reverse Transcriptase	Invitrogen, Paisley, UK

2.1.1.5 Buffers and solution

Name	Components
2 × Assay Buffer	200 mM Sodium phosphate buffer (pH 7.3), 2 mM $MgCl_2$, 100 mM β-Mercaptoethanol, 1.33 mg/ml ONPG
ChIP dilution buffer	1% (*v*/*v*) Triton X-100, 2 mM EDTA, 150 mM NaCl, 20 mM Tris-HCl, pH 8.1
Coomassie blue stain	0.25% (*w*/*v*) Coomassie G250, 10% (*v*/*v*) acetic acid
Destain solution	10% (*v*/*v*) acetic acid
DNA loading buffer (10 ×)	50% (*v*/*v*) Glycerin, 10 mM EDTA (pH 8.0), 0.1% (*w*/*v*) SDS, 0.025% (*w*/*v*) Bromphenol blue, 0.025% (*w*/*v*) Xylencyanole
HEG buffer	10 mM HEPES (pH 7.5), 1 mM EDTA (pH 8.0), 10% (*v*/*v*) Glycerol
IP lysis buffer	10 mM Tris-HCl (pH 7.4), 150 mM NaCl, 1% (*v*/*v*) Triton X-100, 0.5% (*v*/*v*) Nonidet® P40, 1 mM EDTA, 1 mM EGTA, 1 mM sodium vanadate
Laemmli buffer (5 ×)	0.01% (*w*/*v*) Bromphenol blue, 250 mM DTT, 10% (*w*/*v*) SDS, 200 mM Tris-HCl (pH 8.0), 50% (*v*/*v*) Glycerol
Protein fixation	50% (*v*/*v*) Methanol, 10% (*v*/*v*) acetic acid
TAE	242 g Tris-Base, 57.1 ml acetic acid, 100 ml 0.5 M EDTA (pH 8.0)
TaqMan® Universal PCR Master Mix	Applied Biosystems, Warrington, UK
TBS	136.9 mM NaCl, 2.68 mM KCl, 24.76 mM Tris-Base, pH 7.8
Paraformaldehyde (PFA) 4%	4% (*w*/*v*) PFA, pH 7.5 in PBS
PBS	137 mM NaCl, 4.3 mM Na_2HPO_4, 2.7 mM KCl, 1.47 mM KH_2PO_4, pH 7.4
RIPA buffer	50 mM HEPES (pH 7.6), 1 mM EDTA, 0.7% (*w*/*v*) Sodium deoxycholate, 1% (*v*/*v*) NP-40, 0.5 M LiCl
Sample buffer	1% (*w*/*v*) SDS, 50 mM Tris-HCl (pH 6.8), 8% (*v*/*v*) Glycerol, 4% (*v*/*v*) β-mercaptoethanol
SDS Lysis buffer	1% (*w*/*v*) SDS, 10 mM EDTA, 50 mM Tris-HCl (pH 8.1), Complete Protease Inhibitor Cocktail
SDS-PAGE loading buffer	250 mM Tris-HCl (pH 6.8), 50% (*w*/*v*) Glycerol,

	10% (*w*/*v*) SDS, 0.5% (*w*/*v*) bromphenol blue
SDS-PAGE running buffer	25 mM Tris-HCl, 1.44% (*w*/*v*) Glycine, 1% (*w*/*v*) SDS
SOC	0.5% (*w*/*v*) yeast extract, 2% (*w*/*v*) Tryptone, 10 mM NaCl, 2.5 mM KCl, 10 mM $MgCl_2$, 10 mM $MgSO_4$, 20 mM Glucose
Tris buffer pH 8.8	90.75 g Tris, 2 g SDS, pH 8.8 (500 ml)
Tris buffer pH 6.8	30.25 g Tris, 2 g SDS, pH 6.8 (500 ml)
TM-2 buffer	0.01M Tris-HCl (pH 7.4), 0.002 M $MgCl_2$, Complete Protease Inhibitor Cocktail
Transfer buffer	3.03 g Tris-HCl, 14.4 g Glycine, 200 ml Methanol (1 l)
2 × YT	16 g tryptone, 10 g yeast extract, 5g NaCl (1 l)

2.1.2 Biological material

2.1.2.1 Bacterial strains

For cloning experiments E.cloni EXPRESS *Escherichia coli* (*E.coli*) cells (Lucigen) were used, whereas routine re-preparation of cDNA constructs was performed using Subcloning Efficiency™ DH5α™ Chemically Competent *E.coli* (Invitrogen).

E.cloni Express genotype:	EXPRESS BL21(DE3)pLysS: F- ompT hsdSB (rB- mB-) gal dcm (DE3) pLysS (CmR)
DH5α genotype:	F^- ϕ80*lac*ZΔM15 Δ(*lac*ZYA-*arg*F)U169 *deo*R *rec*A1 *end*A1 *hsd*R17(r_k^-, m_k^+) *pho*A *sup*E44 *thi*-1 *gyr*A96 *rel*A1 λ^-

2.1.2.2 Human cell lines

Breast carcinoma cell lines MCF-7, MDA-MB-231, MDA-MB-468 and MDA-MB-453 as well as HEK293 and HeLa cells were purchased from Cancer Research UK (London, UK). NAUT™ 293 cells were obtained from Microbix. All cell lines were routinely cultured in Dulbecco's Medium with 10% (*v*/*v*) foetal calf serum (FCS) and glutamine (500 µg/ml).

Cell line	Primary tumour	Isolated from	Source
MCF-7	Mammary gland epithelial Adenocarcinoma	Pleural effusion	Cancer Research UK
HeLa	Cervix epithelial Adenocarcinoma		Cancer Research UK
MDA-MB-231	Mammary gland epithelial Adenocarcinoma	Pleural effusion	Cancer Research UK
MDA-MB-468	Mammary gland Adenocarcinoma		Cancer Research UK
MDA-MB-453	Mammary gland Adenocarcinoma	Pericardial effusion	Cancer Research UK
NAUT™ 293	Kidney		Microbix
HEK293	Kidney		Cancer Research UK

Table 2.1: Used cell lines

2.1.2.3 Plasmids

In this study, the following plasmids were used to express various MT1-MMP constructs: pcDNA3.1 Zeo+ (Invitrogen), pEGFP-C1 (Clontech), pMstGV [179] and pEGFP-N1 (Clontech). pAct, pBind and pG5luc were obtained from Promega.

2.1.2.4 Oligonucleotide primers, TaqMan® probes and RNAi

Oligonucleotides were purchased from MWG and Sigma-Genosys. TaqMan® probes were obtained from Applied Biosystems. The sequences of the primers used or the reference numbers for each TaqMan® probe are summarised in Appendix A (Table 8.1 and Table 8.2).

MT1-MMP gene silencing was performed using adenoviral expression of anti-sense RNA (asRNA) (chapter 2.2.2.11), MISSION® small hairpin RNA (shRNA) purchased from Sigma-Aldrich or Dharmacon® Accell™ siRNA obtained from Thermo Scientific. The sequences of the various probes used are summarised in Appendix B.

2.1.2.5 Enzymes, antibodies, peptides and recombinant proteins

Restriction enzymes were purchased from New England Biolabs or Roche and used according to the manufacturer's instruction with the supplied buffers. Platinum® *Taq* DNA Polymerase and SuperScript® II Reverse Transcriptase were obtained from Invitrogen.

Recombinant TIMP-1 and TIMP-2 were prepared as previously described [246]. Purified soluble and catalytic active MT1-MMP ectodomain (AA 21 – 541), MT1-MMP ectodomain E240A and MT1-MMP catalytic domain (AA 21 – 283) were kindly provided by M. Fogarasi (Cancer Research Institute, Cambridge, UK). The recombinant human VEGFR-2/KDR Fc Chimera was purchased from R&D Systems, recombinant VEGF-A was from Autogen Bioclear UK Ltd (Nottingham, UK). Control and MT1-MMP ICD biotinylated penetratin peptides (RQIKIWFQNRRMKWKK-COOH and RQIKIWFQNRRMKWKK- CRRHGTPRRLLYCQRSLLDKV) were obtained from Cancer Research UK.

All primary and secondary antibodies, including the applications they were used for, are summarised in Table 2.2 and Table 2.3.

Antigen	Antibody	Origin	Supplier	Application
ß-Actin		Rabbit	Abcam plc	IB (1:5000)
Akt		Rabbit	Cell Signaling	IB (1:1000)
Akt	5G3	Mouse	Cell Signaling	ICC (1:50)
Phospho-Akt (Ser473)		Rabbit	Cell Signaling	IB (1:1000), ICC (1:25)
Phospho-Akt (Thr308)		Rabbit	Cell Signaling	IB (1:1000)
Biotin	212.26.A2	Mouse	Jackson ImmunoResearch	IB (1.25 μg/ml), ChIP (3 μg)
Caveolin-1		Rabbit	Abcam plc	IB (1 μg/ml)
CTGF		Rabbit	Abcam plc	IB (1:5000)
FLAG	M2	Mouse	Sigma-Aldrich	IB (2.5 μg/ml), ICC (5 μg/ml)
Gal4	8C-1	Mouse	Calbiochem	IB (2 μg/ml)
HA	F-7	Mouse	Santa Cruz	IB (1:5000)
Lamin B1		Rabbit	Abcam plc	IB (0.1 μg/ml)

MT1-MMP		Rabbit	Abcam plc	IB (0.5 μg/ml), IP (3 μg)
MT1-MMP	LEM-2/15.8	Mouse	Chemicon	IB (0.5 μg/ml), IP (3 μg), ELISA (1 μg/ml), FC (10 μg/ml), IHC (2 μg/ml)
MT1-MMP	N175/6	Sheep	Murphy lab	ICC (5 μg/ml), IB (2.5 μg/ml)
Myc	9B11	Mouse	Cell Signaling	IB (1:1000), ICC (5 μg/ml)
Myc	4A6	Mouse	Millipore	IB (1.5 μg/ml)
Pol II	H-224	Rabbit	Santa Cruz	ChIP (3 μg/ml)
RhoB	M-19	Goat	Santa Cruz	ICC (5 μg/ml)
Src	327	Mouse	Abcam plc	IB (2.5 μg/ml), IP (3 μg), ICC (5 μg/ml)
Src (phospho 416)	9A6	Mouse	Upstate	IB (2 μg/ml), ICC (5 μg/ml)
Src (phospho 416)		Mouse	Invitrogen	IHC (1:100)
mTOR		Rabbit	Cell Signaling	IB (1:1000)
pS2448-mTOR		Rabbit	Cell Signaling	IB (1:1000)
Tubulin		Mouse	Sigma-Aldrich	ICC (1:1000)
VEGF-A	26503	Mouse	R&D Systems	IB (2 μg/ml), ELISA (0.5 μg/ml)
VEGFR-2	55B11	Rabbit	Cell Signaling	IB (1:1000), ICC (1:100), IP, FC (1:200), IHC (1:75)
VP16		Rabbit	Abcam plc	IB (1:1000)

Table 2.2: List of primary antibodies

ChIP, chromatin immunoprecipitation; *ELISA*, enzyme-linked immunosorbent assay; *FC*, flow cytometry; *IB*, immunoblot; *ICC*, immunocytochemistry.

Antibody	Origin	Supplier	Appl
Anti-goat HRP conjugated	Donkey	Jackson ImmunoResearch	IB
Anti-mouse HRP conjugated	Sheep	Jackson ImmunoResearch	IB
Anti-rabbit HRP conjugated	Donkey	Jackson ImmunoResearch	IB
Anti-sheep HRP conjugated	Donkey	Jackson ImmunoResearch	IB
AlexaFluor® 488 anti-mouse	Goat	Molecular Probes	ICC
AlexaFluor® 488 anti-rabbit	Goat	Molecular Probes	ICC
AlexaFluor® 488 anti-sheep	Donkey	Molecular Probes	ICC

AlexaFluor® 546 anti-mouse	Goat	Molecular Probes	ICC
AlexaFluor® 546 anti-rabbit	Goat	Molecular Probes	ICC
AlexaFluor® 546 anti-sheep	Donkey	Molecular Probes	ICC
Cy5 anti-mouse	Donkey	Jackson ImmunoResearch	ICC
Cy5 anti-sheep	Donkey	Jackson ImmunoResearch	ICC
APC anti-mouse	Goat	Invitrogen	FC
PE anti-mouse	Donkey	Abcam plc	FC

Table 2.3: List of secondary antibodies.

Appl, Application; *ELISA*, enzyme-linked immunosorbent assay; *FC*, flow cytometry; *IB*, immunoblot; *ICC*, immunocytochemistry.

2.1.3 Other Reagents

Compound - Abbreviation	Compound - Name	Conc.	Supplier
31C	γ-secretase Inhibitor XVII	300 nM	Calbiochem, Nottingham, UK
AG-1296		10 µM	Calbiochem
Akt Inhibitor II	SH-5	20 µM	Calbiochem
ALLN		1 µM	Calbiochem
Clasto-Lactacystin *β*-Lactone		1 µM	Calbiochem
CT1746		various	Calbiochem
Cytochalasin D		1 µg/ml	Calbiochem
DAPT	γ-secretase Inhibitor IX	250 nM	Calbiochem
DCI	3,4- Dichloroisocoumarin	10 µM	Calbiochem
Dimethyl Bisphenol A		50 µM	Marligen Biosciences, Ijamsville, MD
Epoxomicin		1 µM	Calbiochem
Gefitinib		5 µM	Biaffin, Kassel, GER
IGF-1R Inhibitor II	N-(2-Methoxy-5-chlorophenyl)-N' -(-methylquinolin-4-yl)-urea	20 µM	Calbiochem
IGF-1R Inhibitor II	PPP	100 nM	Calbiochem
IKK Inhibitor III	BMS-345541	4 µM	Calbiochem
JNK Inhibitor II	SP006125	1 µM	Calbiochem

Lactacystin		1 µM	Calbiochem
Leptomycin B		10 nM	Calbiochem
LY294002		2 µM	Calbiochem
MG-132	Carbobenzoxy-L-leucyl-L-leucyl-L-leucinal	10 µM	Calbiochem
Nocodazole		0.2 µM	Calbiochem
Proteasome Inh. I		10 µM	Calbiochem
Rapamycin		25 nM	Calbiochem
PD98059		50 µM	Calbiochem
PMA	Phorbol 12-myristate 13-acetate	100 nM	Fluka, Sigma-Aldrich
PP2	4-Amino-5-(4-chlorophenyl)-7-(*t*-butyl)pyrazolo[3,4-*d*]pyrimidine	5 µM	Calbiochem
SB203580	4-(4-Fluorophenyl)-2-(4-methylsulfinylphenyl)-5-(4-pyridyl)-1H-imidazole	20 µM	Calbiochem
SU4312		1.5 nM	Sigma-Aldrich
Tarceva	Erlotinib	5 µM	Genentech, San Francisco, CA
Wortmannin		250 nM	Calbiochem

Table 2.4: Summary of used inhibitors

Conc, concentration.

2.2 Methods

2.2.1 Cell Culture

All cell culture was carried out with autoclaved and 70% ethanol wiped material in a Class II laminar flow hood. Adherent cells were routinely cultured in Dulbecco's modified Eagle's medium (DMEM) supplemented with 10% (*v*/*v*) foetal calf serum (FCS) and L-alanyl-L-glutamine (500 µg/ml) and maintained in a Hera cell incubator with 5.2% CO_2-atmosphere at 37°C. The gradual growth as well as potential contamination of the cells was surveyed daily and medium was changed if required. All cell lines used are summarised in Table 2.1.

2.2.1.1 General mammalian cell culture procedures

All cell culture plastic ware was purchased from BD Biosciences, Falcon or Sarstedt unless indicated otherwise.

2.2.1.2 Cell freezing and thawing

Cell stocks were ordered from Cancer Research UK or Microbix (Table 2.1) and stored in cryotubes in liquid nitrogen. In order to grow cells, the cell suspensions were partly thawed at 37°C and transferred with the ten-fold volume of pre-warmed cell culture medium (DMEM + L-alanyl-L-glutamine and FCS) in 15 ml tubes. Cells were centrifuged at 300 × g for 5 minutes, the DMSO-containing supernatant was discarded and the cell pellets were subsequently resuspended in DMEM and transferred into a T25 flask. Viable cells adhered within 24 hours to the bottom of the plastic vessels.
In order to freeze cell aliquots, the cells were resuspended in 90% FCS (*v*/*v*) and 10% DMSO (*v*/*v*) freezing medium after trypsination. The cell suspension was aliquoted into three 1.8 ml cyotubes (Nunc) per 80% confluent 175 cm^2 flasks. The vials were initially frozen in a pre-cooled Nalgene Cryo 1°C Freezing Container at -80°C for 24 hours and transferred to liquid nitrogen for long-term storage.

2.2.1.3 Cell passage

All cells were passaged at 70 – 80% confluence. The used medium was discarded and the cells were rinsed once with 1 × PBS to remove the remaining medium, dead cells and cell debris. 1 – 2 ml Trypsin/EDTA was added to cover the cells and the flask was incubated at 37°C for 5 – 10 minutes until the cells started to detach. The cells were then washed off the surface with 5 ml pre-warmed culture medium, transferred into a 15 ml tube and centrifuged at 300 × g for 5 minutes. The pellet was resuspended and seeded into a new cell culture vessel containing pre-warmed culture medium.

2.2.1.4 Cell counts and viability test

2.2.1.4.1 Haematocytometer

In order to obtain cell numbers and test for viability, cells were stained with Trypan blue (Sigma-Aldrich) and counted in a haematocytometer (Improved Neubauer, Weber Scientific). Therefore, 70 – 80% confluent cells were trypsinised, resuspended in 1 ml DMEM and 10 µl of this cell suspension was mixed 1:10 with Trypan Blue (0.4%). Only vital colourless cells, which are able to exclude the dye, were counted. All counts were done in duplicate and each count enumerated at least 100 cells to obtain an average value × dilution factor × 10^4/ ml.

2.2.1.4.2 Vi-CELL™

The Vi-CELL™ series cell viability analyser was used to count cells and test for viability in an automated manner. The Vi-CELL™ was primarily used to size cells and to perform quality controls prior flow cytometry and is based on the trypan blue dye exclusion method.

2.2.1.5 Transfection and cell treatments

For treatment with various inhibitors (Table 2.4), cells were seeded in 6-well plates to a density of 5 × 10^5 cells/well and cultured for 24 hours. Cells were then transfected with 1 µg cDNA of various MT1-MMP constructs per well using FuGene6^{TM} (Roche Applied Science) according to manufacturer's instructions. Three hours after transfection, inhibitors were added for 24 hours at concentrations indicated in Table 2.4. rh-TIMP-1 and rh-TIMP-2 were used at 1 µM, rh-MMP-2 was used at indicated concentrations for 24 hours. rh-$VEGF_{165}$ stimulation was performed for 30 minutes at 100 ng/ml. Penetratin peptides were used at 25 µM and cells were incubated for 3 hours.

2.2.2 Molecular biology methods

2.2.2.1 Quantification of DNA

The amount of DNA was quantified using the Nanodrop® ND-1000 UV-Vis spectrophotometer. Following background correction with 1 µl of H_2O, 1 µl of DNA was quantified by measuring the absorbance at OD260 nm.

2.2.2.2 RNA isolation

RNA was isolated with the Qiagen RNeasy Mini Plus Kit according to the manufacturer's protocol. Cells of a 6-well plate were used per RNA isolation and RNA was eluted in 50 µl of RNAse-free water. The concentration of the total RNA was measured using the Nanodrop® ND-1000 UV-Vis spectrophotometer at a wavelength of 260 nm. RNA quality was assessed with the Agilent 2100 Bioanalyzer, according to manufacturer's instructions.

2.2.2.3 Reverse Transcription

First strand cDNA synthesis was performed by using SuperScript® II Reverse Transcriptase. Therefore, 1 µg RNA was diluted in 10 µl RNAse-free H_2O (Invitrogen) and was initially heated and linearised at 70°C for 10 minutes. 10 µl RT-Mastermix (5 × First-Strand Buffer (Invitrogen), 10 mM DTT (Invitrogen), 10 µM dNTPs (10 µM each, Amersham Biosciences), 200 U Superscript (Invitrogen) and 1 µl random hexamers (GE Healthcare)) were added and the mixture was heated at 42°C for 1 hour, followed by a 5 minute incubation at 95°C. The cDNA was diluted in RNAse-free H_2O and stored at -20°C.

2.2.2.4 Polymerase chain reaction

The protocol for standard PCR is based on Saiki *et al.* [247]. 2 µl (10 ng) cDNA were diluted in 28 µl PCR-Mastermix (10 × Buffer (BioLabs), dNTPs (10 µM each, Amersham Biosciences), 200 nM Primer (purchased from MWG Biotech), 2.5 mM $MgCl_2$ (BioLabs) and 1U Platinum® *Taq* DNA Polymerase (Invitrogen)) and initially denatured at 95°C for

2 minutes, followed by 20 – 35 cycles of (i) denaturation for 45 seconds at 95°C, (ii) annealing of oligonucleotides at (T_m - 1-2)°C and (iii) elongation at 72°C for 45 seconds. The samples were separated on a 1% agarose gel after a final elongation step (12 minutes at 72 °C).

2.2.2.4.1 TaqMan® Real-Time PCR

The pre-made TaqMan® probes were obtained from Applied Biosystems, containing pre-mixed primers and a FAM dye labelled TaqMan® probe. All used probes are summarised in Appendix A (Table 8.2).

TaqMan® Real-Time PCR gene expression profiling was done by using the Applied Biosystems 7900HT Fast Real-Time System. All experiments were performed in technical triplicates for each of the three biological replicates in 384 well plates. The used fluorogenic probes were labelled at the 5' end with FAM and at the 3' end with MGB (minor groove binder) nonfluorescent quencher. Reactions were performed in a 12.5 µl final volume containing 6.25 ng cDNA, 100 nM of forward and reverse primers, 200 nM fluorogenic probe (Applied Biosystems) and TaqMan® Universal PCR Master Mix. The fluorescent signal detection used ROX as the internal passive reference dye. The parameters of the PCR reaction were 2 minutes at 50°C, 10 minutes at 95°C followed by 40 cycles of 15 seconds at 95°C and 1 minute at 60°C. During the elongation step the endonuclease activity of the Taq-polymerase causes the cleavage of the probe. This leads to the release of the fluorescent dye from the quencher and to an increase in fluorescence that is proportional to the exponentially amplified amount of cDNA. The C_T (cycle threshold)-value of a sample indicates the number of cycles needed to reach defined fluorescence intensity above background levels.

The relative expression of each sample was calculated using the $2^{-\Delta\Delta CT}$ method:

$$\textbf{Relative Expression} = 2^{-(S\Delta\ CT - C\Delta\ CT)}$$

$\Delta C_T = (GOIC_T - HKGC_T)$

$S\Delta\ C_T - C\Delta\ C_T$ = control value (C) is subtracted from sample value (S)

GOI = gene of interest, HKG = house-keeping gene, S = sample, C = control

2.2.2.4.2 SYBR® Green Real-Time PCR

gDNA samples obtained by chromatin immunoprecipitation (chapter 2.2.4.7) were amplified by SYBR® Green Real-Time PCR using specific primers from the promoter and up-stream region of VEGF-A and XBP-1 (X Box-binding protein 1; primer sequences in Appendix A, Table 8.1). Real-Time PCR gene expression profiling was carried out using the Applied Biosystems 7900HT Fast Real-Time PCR System. All experiments were performed in technical triplicates for each sample in 96 well plates. Reactions were performed in 20 µl final volume containing 5 µl gDNA, 100 nM of forward and reverse primer, and 10 µl SYBR® Green PCR Master Mix (Applied Biosystems). The parameters of the PCR reaction were 10 minutes at 95°C followed by 40 cycles of 15 seconds at 95°C and 1 minute at 60°C. The SYBR® Green dye incorporates into dsDNA strands and therefore increases the amount of fluorescence corresponding to the production of amplificates per cycle. A melting curve was performed at the end of every run to distinguish non-specific double-stranded nucleotides including primer-dimers from the specific product. Unlike longer completely complimentary amplificates, short nucleotide-nucleotide pairings will dissociate with increasing temperature. The relative expression of each sample was calculated using the $2^{-\Delta\Delta CT}$ method (chapter 2.2.2.4.1).

2.2.2.5 Agarose gel electrophoresis

PCR products were separated and analysed by electrophoresis using agarose gels. 1 – 2% (*w*/*v*) agarose was prepared in TAE buffer (chapter 2.1.1.5) with SYBR® Safe DNA gel stain to visualise DNA by using ultraviolet (UV) light. Gels were poured into Mini-Sub® Cell GT electrophoresis chambers and samples mixed with 10 × gel-loading buffer (chapter 2.1.1.5) were loaded. Samples were run next to DNA markers (Marker VIII and 1 kb ladder) for approximate size calculation.

2.2.2.6 DNA ligation

200 ng vector (summarised in chapter 2.1.2.3) were mixed with the insert at a 1:3 molar ratio (vector : insert) in 2 µl 10 × ligation buffer and 1 µl T4 ligase (NEB). The ligation was carried out at room temperature (RT) for 16 hours.

Molar ratios were calculated using the equation:

$$\frac{2 \times 10^6 \ \mu g \text{ dsRNA}}{N_{bp} \times 660 \text{ kDa}} = \text{pmol of ends of dsRNA}$$

with N = total number of nucleotides

2.2.2.7 Transformation of competent bacteria

A vial of 50 µl chemically competent *E.coli* per construct was thawed on ice and 2 µl of the ligation reaction was added. Bacteria were incubated on ice for 30 minutes, heat-shocked for 45 seconds in a 42˚C water-bath to facilitate plasmid uptake into the cells and subsequently put back on ice. Following transformation 800 µl SOC medium was added and transferred to a sterile 15 ml culture tube. *E.coli* were incubated for 1 hour at 37˚C with shaking. The bacteria were briefly centrifuged (30 seconds, 5000 × g), resuspended in 100 µl SOC medium, plated onto agar plates containing the appropriate antibiotic selection and incubated at 37˚C for 16 hours.

2.2.2.8 PCR screen of bacterial colonies

Bacterial colonies were routinely screened for the correct gene insertion into the plasmid backbone. Various single colonies were picked and transferred to 4 ml 2 × TY medium containing the appropriate antibiotic selection. *E.coli* were grown for at least 6 hours at 37˚C with shaking and 2 µl bacteria suspension were used as a template in a 30 µl PCR assay (chapter 2.2.2.4).

2.2.2.9 Preparation of plasmid DNA

Plasmid DNA was prepared with either the Qiagen Plasmid Mini or Maxi kit according to manufacturer's instructions. Purification of the adenoviral backbone vector was performed using the Qiagen Large-scale Plasmid DNA Purification kit.

2.2.2.10 Generation of MT1-MMP constructs

All plasmids used are summarised in Table 2.5 and primer sequences are listed in Appendix A (Table 8.1).

Full-length MT1-MMP (MT1-WT), EGFP tagged MT1-MMP (MT1-ΔECD-EGFP, comprising of MT1-MMP amino acids 508 - 582), L571A/L572A/Y573A MT1-MMP (MT1-^{571}AAA^{573}), the intracellular domain deleted MT1-MMP mutant (MT1-ΔICD, deletion of amino acids 561 – 582), the hemopexin domain deletion mutant (MT1-ΔHPX, deletion of amino acids 318 - 509), the Myc tagged full-length MT1-MMP (MT1-Myc, Myc tag inserted between amino acids 312 and 313) and the catalytic inactive MT1-MMP (MT1-E240A) were described elsewhere [39,73,248,249]. The LRP1 GAL4/VP16 (GVLRP1) construct was kindly provided by P. May, (Department of Molecular Genetics, University of Texas Southwestern Medical Centre, Dallas, TX) [151], the GVAPP construct was provided by T.C. Südhof (University of Texas Southwestern Medical Centre, Dallas, TX) [179]. Ubiquitin and Ubiquitin K11,27,29,48,63A were a gift from K. Fujita (University College London, UK). MT1-MMP point mutations at C^{574} (MT1-C574A), Y^{573} (MT1-Y573A), DKV^{582} (MT1-^{580}AAA^{582}) as well as the double catalytic inactive mutants MT1-E240A-^{571}AAA^{573} and MT1-E240A-ΔICD were kindly provided by C.H. Roghi (Cambridge Research Institute, Cambridge, UK). The MT1-MMP construct containing a GAL4/VP16 fusion domain inserted between the transmembrane and intracellular domain of MT1-MMP (GVMT1) was also generated by C.H. Roghi.

The orientation and sequence of all constructs was verified by DNA sequencing (Cancer Research UK, Cambridge, UK).

Construction of a truncated MYC – FLAG double-tagged MT1-MMP

MT1-MYC (Table 2.5) was amplified by PCR using the CHR521s and BGH2as primer, which insert a PinAI restriction site at position 90 (from the signal sequence) and a FLAG tag at position 96. The PCR fragment was purified using the SigmaSpin™ Post-Reaction Clean-Up Columns. Both, the PCR fragment and MT1-ΔECD-EGFP (Table 2.5) were digested with PinAI and subsequently with PstI (Roche). The PCR fragment and the pEGFP-C1 vector, containing only the MT1-MMP signal sequence were purified from a 1% (*w*/*v*) agarose gel using the QIAquick Gel Extraction Kit. The insert comprising of a C-terminal MYC-tag, the MT1-MMP ICD, TMD, the extracellular stalk-region and the

FLAG tag was fused in the vector with the MT1-MMP signal sequence (MT1MYC-FLAG).

Construction of MT1-MMP Lysine and extracellular domain deletion mutants

The MYC-FLAG double tagged construct containing a point mutation of K^{518} to Alanine (MT1-MYC-FLAG-K581A), the full-length MT1-MMP K^{581} mutant (MT1-K581A) and the FLAG tagged MT1-MMP mutant (MT1-ΔECD-FLAG) were generated by site-directed mutagenesis as previously described [119], using the QuickChange® XL Site-Directed Mutagenesis Kit. Briefly, the QuickChange® XL system is used to generate point mutations as well as to switch or delete amino acids by combining a supercoiled dsRNA vector with an insert of interest and two oligonucleotide primers containing the desired mutation. The primers are complementary to opposite strands of the vector and are extended by pfuTurbo DNA Polymerase during a PCR. The mutation is integrated within the sequence and the parental DNA template is degraded following PCR by Dpn I treatment. DNA isolated from almost all *E.coli* strains is methylated or hemimethylated and thus targeted by Dpn I. The new generated DNA template containing the mutation of interest is transformed as previously described (chapter 2.2.2.7). The thermocycling conditions for mutagenesis were: 1 minute at 95˚C; 18 cycles of 50 seconds at 95˚C, 50 seconds at 60˚C and x minutes at 68˚C following 7 minutes at 68˚C with x = 1 minute/ kb of the plasmid used. The primers used for the K^{581} mutants made from either MT1-WT or MT1-MYC-FLAG constructs were 115.K/As and 115.KAas (Table 8.1). The MT1-ΔECD-FLAG was generated from the MT1-MYC-FLAG template with 115.Stps and 115.Stpas (Table 8.1), inserting a new stop codon downstream of the MT1-MMP ICD (amino acid 583).

Construction of the MT1-MMP APP plasmids

For construction of the MT1-MMP GAL4/VP16 mutant containing an APP ICD or an APP TMD, the MT1-MMP (ECD) - APP (TMD, ICD) – GAL4/VP16 (construct N-MT1-APP, kindly provided by C.H. Roghi) and the GVMT1 construct were used. Both plasmids were cut with BsrGI (Qiagen) and PstI (Roche). Purification was carried out by using the SigmaSpin™ Post-Reaction Clean-Up Columns and the QIAquick Gel Extraction Kit for isolation of fragments from an agarose gel.

The insert of the MT1-MMP GAL4/VP16 vector (GVMT1), containing the MT1-MMP intracellular domain as well as the VP16 domain, was cloned into the pcDNA3.1 Zeo+

vector containing the MT1-MMP extracellular domain, the APP TMD and the GAL4 domain. The insert of the N-MT1-APP, comprising the APP ICD and the VP16 domain was fused in the digested GVMT1 vector (pMstGV) that contains the MT1-MMP extracellular and transmembrane domain as well as the GAL4 domain. For generation of the MT1-TMD-APP consisting of the full-length MT1-MMP containing the APP transmembrane domain, the APP TMD (amino acids 700-723) was subcloned in frame with the full-length MT1-MMP construct (amino acids 542 - 562), thus replacing the MT1-MMP TMD.

pBind-Src

The coding sequence of Src was amplified with the CHR508 and CHR509 primer (Table 8.1) which insert a BamHI cleavage site at the 5'-terminus and a XbaI cleavage site at the 3'-end. The 1.6 kb fragment was extracted and purified from a 1% (*w*/*v*) agarose gel. pAct and pBind vectors and the Src fragment was digested with BamHI (Roche) and XbaI (Roche) followed by purification of vectors and insert. The coding sequence of Src was subsequently cloned in the pAct and pBind vectors.

pBind-MT1-MMP ICD mutants

For the construction of the pBind-MT1-MMP triple mutations (Table 2.5), the mutated ICDs were re-cloned from pAct-MT1-MMP ICD mutants (kindly provided by C.H. Roghi) in the pBind vector. Therefore, pAct-MT1-MMP ICD triple mutants were amplified with pACTs1200 and pACTas1446 primer (Table 8.1) and purified from a 1% (*w*/*v*) agarose gel. Both, inserts and the pBind vector were digested with BamHI (Roche) and XbaI (Roche) and MT1-MMP ICD mutants were cloned in the vector.

Name	Source	Vector	Insert (N => C-terminus)
MT1-WT	CH Roghi	pcDNA3.1 Zeo+	WT MT1-MMP
MT1-E240A	CH Roghi	pcDNA3.1 Zeo+	WT MT1-MMP: E240A point-mutation
MT1-ΔECD-FLAG	CH Roghi	pEGFP-C1	S - FLAG - stalk - TMD - ICD
MT1-ΔECD-EGFP	PA Eisenach	pEGFP-N1	S - EGFP - stalk - TMD - ICD

MT1-ΔHPX	CH Roghi	pcDNA3.1 Zeo+	S - CAT - EGFP - stalk - TMD - ICD
MT1-TMD-APP	PA Eisenach	pcDNA3.1 Zeo+	S - CAT - HPX - stalk - APP TMD - ICD
MT1-C574A	CH Roghi	pcDNA3.1 Zeo+	WT MT1-MMP: C574A point-mutation
MT1-Y573A	CH Roghi	pcDNA3.1 Zeo+	WT MT1-MMP: Y573A point-mutation
MT1-^{571}AAA^{573}	CH Roghi	pcDNA3.1 Zeo+	WT MT1-MMP: LLY^{573} => AAA^{573} mutation
MT1-^{580}AAA^{582}	CH Roghi	pcDNA3.1 Zeo+	WT MT1-MMP: DKV^{582} => AAA^{582} mutation
MT1-ΔICD	PA Eisenach	pcDNA3.1 Zeo+	S - CAT - HPX - stalk - TMD
MT1-K581A	PA Eisenach	pEGFP-C1	WT MT1-MMP: K581A point-mutation
MT1-MYC-FLAG	PA Eisenach	pEGFP-C1	S - FLAG - stalk - TMD - ICD - MYC
MT1-MYC-FLAG K581A	PA Eisenach	pEGFP-C1	S - FLAG - stalk - TMD - ICD - MYC: K581A point Mutation
GVMT1	CH Roghi	pMstGV	S - CAT - HPX - stalk - TMD - GAL4/VP16 - ICD
GVMT1-APP-ICD	PA Eisenach	pMstGV	S - CAT - HPX - stalk - TMD - GAL4/VP16 - APP ICD
GVMT1-APP-TMD	PA Eisenach	pcDNA3.1 Zeo+	S - CAT - HPX - stalk - APP TMD - GAL4/VP16 - ICD
GVAPP	TC Südhof	pMstGV	WT-APP - GAL4/VP16
GVLRP1	P May	pMstGV	WT-LRP1 - GAL4/VP16
pAct	Promega		
pBind	Promega		
pAct-MT1	CH Roghi	pAct	ICD
pAct-Src	PA Eisenach	pAct	Src
pBind-Src	PA Eisenach	pBind	Src
pB-MT1-LLY/AAA	PA Eisenach	pBind	ICD LLY^{573} => AAA^{573}
pB-MT1-CQR/AAA	PA Eisenach	pBind	ICD CQR^{576} => AAA^{576}

pB-MT1-DKV/AAA	PA Eisenach	pBind	ICD DKV^{582} = > AAA^{582}
ß-Gal	Promega	*ß*-Gal	
pG5luc	Promega	pG5luc	
Src	R Béliveau	pcDNA3.1 Zeo+	WT-Src

Table 2.5: DNA constructs

S, signal sequence; *CAT*, catalytic domain; *HPX*, hemopexin domain; *stalk*, stalk region (amino acids 508 – 541); *TMD*, transmembrane domain; *ICD*, intracellular domain, *WT*, wild-type.

2.2.2.11 Generation of adenoviral expression constructs

Recombinant adenovirus (Ad5 ΔE1/E3) expressing MT1-WT was prepared as previously described [76]. MT1-, MT2-, MT3- and MT4-MMP anti-sense (as) RNA expressing constructs were generated as described in the following sections.

2.2.2.11.1 Subcloning of MT1-, MT2-, MT3- and MT4-MMP anti-sense cDNAs into the adenoviral backbone vector

Anti-sense sequences for MT1-, MT2-, MT3- and MT4-MMP (summarised in Appendix B, Table 9.1, kindly provided by C.H. Roghi) were subcloned into the adenoviral shuttle vector pDC516 (Microbix).

2.2.2.11.2 Viral recombination

As shown in Figure 2.1, recombination of the MT1-MMP anti-sense sequences into the adenoviral backbone was performed by co-transfecting Naut™ 293 cells (Microbix) with genomic adenoviral plasmid and MT-MMP containing pDC516 shuttle vector. Naut™ 293 cells express the E1 gene that has been removed from the adenoviral backbone vector to induce viral replication.

For recombination, cells were co-transfected with 50 µg genomic adenoviral backbone vector and 10 µg shuttle vector using 180 µl Fugene, as previously described. For each recombination, one 80% confluent T175 flask of Naut™ 293 cells was trypsinised and cells were resuspendend in 10 ml serum-free medium. The DNA – lipid complex was

added to the cells and incubated in solution for 10 minutes at RT. The cells of each transfectant were split and transferred into ten T25 flasks containing DMEM with 10% (*v*/*v*) FCS. The cells were incubated for 5 days at 37ºC. Subsequently, the medium was exchanged every two days until 30 – 40% of the cell monolayer showed a cytopathic effect. Without changing the medium, the cells were further incubated until all cells died. Cells were collected by centrifugation and freeze-thawed 3 × to free the virus contained in the cells. Lysates were stored at -20ºC.

2.2.2.11.3 Cloning and titration of the adenoviral expression constructs

For titration of each viral construct obtained, a confluent T75 flask of HEK293 cells was trypsinised, resuspended into 20 ml of medium and pipetted into a 96-well plate (100 µl/well). Cells were allowed to adhere by incubation at 37ºC for 16 hours.

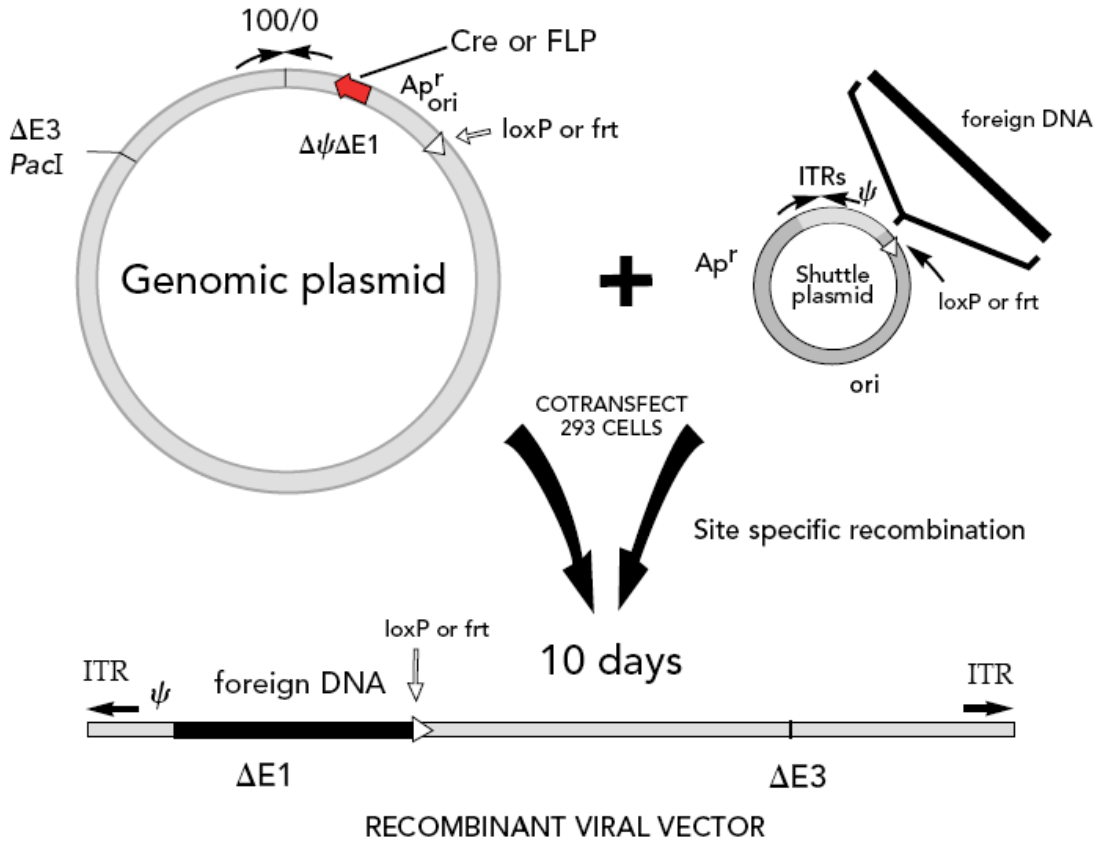

Figure 2.1: AdMax system for adenoviral recombination (Microbix)

NAUT™ 293 cells were co-transfected with the adenoviral genomic plasmid and the shuttle plasmid containing the sequence of interest (MT-MMP anti-sense sequences). The recombinase expressed by the genomic vector induces recombination between the insert and the recombinant viral vector. Taken from AdMax system manual (Microbix).

Viral lysates were centrifuged at 400 × g for 10 minutes at RT and serial dilutions (10^{-2}, 10^{-3}, 10^{-4}, 10^{-5}, 10^{-6}, 10^{-7}, 10^{-8} and 10^{-9}) were prepared in DMEM containing 10% (*v*/*v*) FCS. 100 µl of each dilution was added in 10 wells of a prepared HEK293 containing 96-well plate. DMEM containing 10% (*v*/*v*) FCS was added to control for potential cross-contamination.

The medium was exchanged every other day for 9 days. The same titration was carried out with HeLa cells to screen for replication competent viruses. Since HeLa cells do not express the E1 gene, the virus is not able to replicate in these cells. Thus, no cell death should be observed in HeLa cells. However, low MOI of virus (100 – 200 pfu/cell) as well as overexpression of transgenes have been shown to be toxic for cells. Hence, only death of HeLa cells at dilutions greater than 10^{-3} is regarded as indicating replication competent virus.

To obtain working stocks from plaque purified isolates, cells from three wells of the highest concentration that underwent complete cytopathic effect (cpe) were collected, freeze-thawed as described before and used in a second round of cloning. After titration for 9 days three clones were collected per construct, freeze-thawed and 40 µl were added to a confluent T175 flask of HEK293 cells. When these cells showed 80% cpe, the lysate was used as a seed stock to infect ten 80% confluent T175 flasks of HEK293 cells. The cells were cultured until they reached 80% cpe and they were harvested by centrifugation at 300 × g for 5 minutes at RT. Cells were resuspended in 10 ml of PBS, freeze-thawed 3 × and then centrifuged at 4,000 × g for 10 minutes. The supernatant was subsequently purified using a CsCl gradient.

2.2.2.11.4 Caesium chloride purification of adenoviruses

For each adenoviral expressing construct a 15 ml plastic ultracentrifuge tube (Becton Dickinson) was used, rinsed with 70% (*v*/*v*) ethanol and washed with sterile H_2O. 2 ml of high-density caesium chloride solution (Solution 1, Table 2.6) was added to the tube and was overlayed by the CsCl solution 2 (Table 2.6). 2 ml of 40% glycerol were added as the last layer (Table 2.6). 10 ml of the adenoviral lysate was carefully applied on top of the gradient followed by centrifugation in a Sorval ultracentrifuge for 1.5 hours at 2.5×10^4 rpm (without deceleration).

Solution 1	Solution 2	40% Glycerol
20.5 g CsCl	32g CsCl	40 g Glycerol
2.9 ml 0.5 M Tris pH 7.9	6.8 ml 0.5 M Tris, pH 7.9	2 ml 0.5 M Tris pH 7.9
25.8 ml H_2O	61.2 ml H_2O	0.5 ml 0.2 M EDTA
		ad 100 ml H_20
	sterile filter before use	

Table 2.6: Solutions for adenovirus purification

After centrifugation a distinct white pure virus band was visible in the tube, that was removed with a 2 ml syringe (23 gauge needle) piercing the tube just below the virus layer. The virus solution was dialysed using a Slide-A-Lyzer Dialysis Cassette (Pierce) vs. 5 l PBS for 16 hours at 4ºC. The purified virus was aliquoted and stored at -80ºC.

2.2.2.11.5 Calculation of the viral titre

To determine the titre of the purified virus, a 96-well plate of HEK293 cells was infected with a range of serial dilutions as described before (chapter 2.2.2.11.3). After 9 days, the proportionate distance (PD) was calculated as:

PD = (x - 50%) / (x - y)

with x = dilution where more than 50% of the infected wells died (number of wells in%) and y = dilution where less than 50% of the infected wells died (number of wells in%).

Subsequently, the infectivity dose (ID50) was calculated using:

$ID50 = 10^{(z + (PD \times -1))} \times F_d$

With z = the dilution factor used, where more than 50% of the infected cells showed cpe and F_d = Dilution factor.

100 µl virus lysate were used for the titration. To obtain the infectivity dose per 1 ml, the Fd is 10.

Finally, the titre of the virus solution in plaque forming units (pfu)/ml could be obtained:

$MOI\ (pfu/ml) = 0.7 \times 10^{-ID50}$

2.2.2.11.6 Infection of cells with adenovirus

For transduction of cells with adenoviral expressing MT-MMP constructs, cells were seeded in 6-well plates 16 hours prior to infection. Cells from one well were counted after trypsination allowing the MOI to be calculated in pfu/cell. Different MOI, as indicated in the results section, were added to the cell culture medium for 2 hours followed by exchange of the medium. The cells were cultured for 48 hours and protein or RNA was isolated as previously described.

2.2.2.12 Lentiviral shRNA transduction

For stable knockdown of MT1-MMP expression in MDA-MB-231 and MDA-MB-468 cells as well as VEGFR-1 and VEGFR-2 gene silencing in MCF-7 cells, a lentiviral shRNA approach was used (MISSION® shRNA, Sigma-Aldrich). Prior to lentiviral transduction, a puromycin titration (kill curve) was performed on all cell lines used, using puromycin at concentrations from 0.5 – 10 µg/ml according to manufacturer's instructions. Cells were seeded in a 6-well plate at 2.5×10^5 cells/well (MDA-MB-231 and MDA-MB-468) or 5×10^5 cells/well (MCF-7) and were transduced 24 hours later with 2 pfu/cell of MISSION® shRNA lentiviral particles (5 sequences per target gene), empty pLKO.1-puro control particles or virus expressing a non-targeting control shRNA. The medium was exchanged the following day and puromycin selection with the determined concentration was started 24 hours later. Cells were cultured for 48 hours followed by protein or RNA extraction. Used shRNA sequences are summarised in Appendix B (Table 9.2).

2.2.2.13 MT1-MMP knockdown using siRNA

The expression of MT1-MMP was silenced in MDA-MB-231 cells using Dharmacon® Accell™ siRNA (Thermo Scientific). This approach was shown to reduce off-target effects and cytotoxicity by avoiding the use of transfection reagents.

MDA-MB-231 cells were seeded at 2.5×10^5 cells/well in a 6-well plate and were incubated for 16 hours at 37˚C. The indicated concentrations (0.25 µM or 1 µM) of MT1-MMP targeting or control siRNA, pre-diluted in 1 × siRNA buffer (Thermo Scientific), were prepared in 750 µl Accell™ delivery medium (Thermo Scientific). The growth

medium was removed from the cells and 100 µl of the delivery mix was added to each well. The cells were incubated for 72 hours and MT1-MMP knockdown was verified by TaqMan® Real-Time PCR.

2.2.3 Biochemical methods

2.2.3.1 Western Blot analysis

2.2.3.2 Preparation of protein samples from cell lysates

Cells were seeded in triplicate in 6-well plates and were transfected or stimulated as described previously (chapter 2.2.1.5). 16 hours after treatment the culture medium was removed and the cells were washed 2 × in PBS. 250 µl of sample buffer or SDS lysis buffer was added to the wells and the cells were removed from the wells with a cell scraper. Protein concentration was determined (chapter 2.2.3.5) and equal amounts were loaded by diluting samples in HEG buffer. After adding 5 × reducing Laemmli buffer, samples were heated at 95˚C for 10 minutes, centrifuged at maximum speed in a microfuge for 5 minutes and loaded on a SDS-PAGE gel or stored at -20˚C.

2.2.3.3 Preparation of protein samples from nuclei

To separate MCF-7 nuclei from the cytoplasmic and membrane protein fractions, cells were seeded in 6-well plates and nuclei were obtained by a combination of Triton X-100 mediated detergent lysis and mechanical disruption. 16 hours after cell treatment microtubules and the actin cytoskeleton were disrupted by adding Nocodazole (0.2 µM) and 1 µg/ml Cytochalasin for 1 hour at 37˚C. The medium was removed and cells were washed 2 × in PBS. Cells were scraped in 0.5 ml PBS and three wells were pooled per sample. Following centrifugation at 1200 × rpm at RT for 2 minutes, cells were resuspended in 1 ml TM-2 buffer (chapter 2.1.1.5) and incubated at RT for 1 minute. The tubes were transferred on ice and incubated for 5 minutes. Triton X-100 was added to each sample to a final concentration of 0.5% (*v*/*v*) and cells were incubated for 10 minutes on ice. Subsequently, cells were mechanically disrupted by shearing through a 23-gauge needle. The samples were subjected to another round of incubation on ice for 10 minutes

and shearing by passing through a 23-gauge needle until nuclei were sufficiently separated from the cytoplasm as determined by examination on a phase contrast microscope. To isolate nuclei from the cytosol, the cell lysate was layered on top of a 30% (*w*/*v*) sucrose cushion (4.5 ml in a round 15 ml tube, BD Biosciences) and centrifuged at 800 × rpm at 4˚C for 10 minutes. Samples from the cyoplasmic fraction were taken and nuclei were washed 2 × in TM-2 buffer and subsequently lysed in 300 µl SDS lysis buffer (chapter 2.1.1.5).

2.2.3.4 Concentration of proteins from conditioned medium

MCF-7 cells were seeded at 5 × 10^5 cells/well, the medium was exchanged after 16 hours to serum-free medium and the cells were treated as indicated in the results chapter. Following incubation for 24 hours, the conditioned medium was removed and proteins or RNA was isolated from the corresponding cells. Medium was centrifuged for 5 minutes at 8,000 × g to remove residual dead cells and the remaining soluble protein was concentrated. 2-3 *vol.* of ice-cold acetone was added to the medium, vortexed thoroughly and protein was precipitated at -20˚C for at least 6 – 16 hours. Samples were centrifuged at 16,000 × g for 10 minutes at 4˚C, the supernatant was carefully removed and the pellet was air-dried until residual acetone evaporated. Pellet was resuspended in 20 µl of 2 × Laemmli buffer and subjected to immunoblotting.

2.2.3.5 Measurement of protein concentration by the BCA assay

Protein concentration was measured using the BCA™ Protein Assay, according to the manufacturer's instructions (Pierce, Thermo Scientific). Briefly, aliquots of protein samples were diluted 1:10 and pipetted in duplicate in a 96-well plate. Serial BSA-dilutions were used as a concentration reference. Samples and reference protein were coated with the protein assay reagent. The plate was subsequently incubated for 1 hour at 37˚C. Proteins in the sample wells are reducing Cu^{2+} to Cu^{1+} in the alkaline medium (Biuret reaction), which form a purple complex with bicinchoninic acid (BCA). The BCA/copper complex is water-soluble and exhibits a proportional absorbance at 562 nm with increasing protein concentration. The absorbance obtained using the Infinite® M200

plate reader was converted to protein concentration using BSA standards of known concentration.

2.2.3.6 Sodium dodecyl sulphate polyacrylamide gel electrophoresis (SDS-PAGE), Western Blotting and antibody detection

Protein lysates were loaded with 5 × SDS-PAGE loading buffer on a 10% (*w*/*v*) SDS polyacrylamide gel (SDS-PAGE, Table 2.7). The gel was running in a 135 V electric field for ~1.5 hours in 1 × SDS running buffer in a Mini Protean® II xi chamber. BenchMark™ Protein Ladder was used for estimation of molecular weight of proteins of interest in the sample. The gel was subsequently transferred onto a nitrocellulose membrane at 400 mA for 1 hour using a Trans-Blot cell transfer system. Membranes were blocked for 1 hour in 3% (*w*/*v*) fat free powdered milk (Marvel) in 1 × TBS containing 0.1% (*v*/*v*) Tween®20 (TBS-T) followed by an incubation with the primary antibody at the indicated dilution (Table 2.2) in 3% (*w*/*v*) milk in TBS-T at 4°C for 16 hours. The membranes were washed three times with TBS-T and subsequently incubated with the secondary antibody (Table 2.3) in 3% (*w*/*v*) milk in TBS-T, for 1 hour at RT. The blots were washed three times with 1 × TBS-T. Detection was performed using the Enhanced Chemi-Luminescence kit (Amersham) according to the manufacturer's protocol. Where required, membranes were stripped by incubating for 10 minutes at RT in ReBlot™ Plus Strong Antibody Stripping Solution, blocked for 5 minutes in 3% (*w*/*v*) milk in TBS-T and re-probed with a different primary antibody.

Stacking gel	Separating gel (10%)
0.125 M Tris-HCl, pH 6.8	0.375 M Tris-HCl, pH 8.8
3% (*v*/*v*) Acrylamide	10% (*v*/*v*) Acrylamide
0.1% (*v*/*v*) SDS	0.1% (*v*/*v*) SDS
0.1% (*v*/*v*) APS	0.1% (*v*/*v*) APS

Table 2.7: Preparation of PAGE-gels

2.2.4 Immunological methods

2.2.4.1 Immunostaining of human breast carcinoma cells

For immunostaining cells were seeded onto glass coverslips in 12-well dishes (10^5 cells/well) and transfected as previously described (chapter 2.2.1.5). After 24 hours, cells were washed in pre-warmed PBS and fixed at RT for 20 minutes with 4% (*w*/*v*) PFA in PBS. PFA was quenched using 50 mM Glycine (pH 8.0). Cells were subsequently washed in PBS, permeabilised in PBS containing 0.1% (*v*/*v*) Triton X-100 and incubated with the primary antibody for 1 hour at RT (antibodies used are summarised in Table 2.2). Cells were washed 3 times for 5 minutes with PBS and were incubated with species-specific AlexaFluor® 488, AlexaFluor® 546 or Cy5 conjugated secondary antibodies (summarised in Table 2.3). Slides were mounted in ProLong® Gold Antifade Reagent with DAPI.

2.2.4.2 Immunostaining of human mammary carcinomas

Immunohistochemical analyses were performed in collaboration with Dr. Bence Sipos (Department of Pathology, Universitätsklinikum Schleswig-Hostein, Campus Kiel; current affiliation: Department of Pathology, University of Tübingen). Breast carcinoma sections were obtained from surgical specimens, according to a protocol approved by the ethics committee of the University Hospital, Kiel. Tumour tissues were fixed in formalin and routinely processed for paraffin sectioning. Three-µm-thin paraffin sections were deparaffinized, rehydrated and immunostained according to routine methods. Antigen was demasked by heating the sections under high pressure in Tris-EDTA-citrate buffer (pH 7.8). Antibody were diluted in 2% (*w*/*v*) fat free powdered milk in PBS. The dilutions used are summarised in Table 2.2. After incubation for 16 hours at 4˚C, the reaction was detected with a biotinylated anti-mouse or anti-rabbit antibody (5 µg/ml, Vector Laboratories, Burlingame, CA) and avidin-biotin-peroxidase (ABC-ELITE, Vector Laboratories). Diaminobenzidine served as chromogen.

For negative control the primary antibody was omitted. After staining, sections were counterstained in 50% haemalaun (Merck, Darmstadt, Germany).

2.2.4.3 Microscopy analysis

2.2.4.3.1 Fluorescent microscopy

Images of fluorescently labelled cells were acquired using a Photometrics Coolsnap HQ CCD camera (Roper Scientific, Harlow, UK) attached to a Zeiss Axioplan 2 imaging microscope using a 40 × or 63 × immersion objective as well as by using a differential interference contrast (DIC) prism. Taken images were analysed and processed using the Metamorph software (Universal Imaging Corporation, Downington, PA) as well as by the Photoshop imaging software (Adobe Systems, San Jose, CA).

2.2.4.3.2 Confocal microscopy

Series of optical sections were acquired using a Leica Tandem SP5 Confocal laser microscope (Leica Microsystems, Germany) with a 63 × oil immersion objective at 1024 × 1024 dpi or 2048 × 2048 dpi for co-localisation studies. Various optical sections were imaged every 0.2 µm along the *z*-axis of the cell. Files were transferred to the Volocity 3D imaging and analysis software to generate three-dimensional reconstructions of obtained *z*-stacks or to perform co-localisation analyses.

For co-localisation quantification, a cytofluorogram was generated per optical confocal section of each cell (Figure 2.2A), by plotting the paired fluorescent intensities obtained per voxel (volume pixel) of two different channels in a histogram (Figure 2.2B). As shown in Figure 2.2A, fluorescence is detected for both channels in every voxel of the selected image, leading to double positive voxels as demonstrated in the cytofluorogram (Figure 2.2B). Following background-subtraction performed for every channel, the specific pattern of the antibody-staining remains (Figure 2.2C), while the amount of positive voxels within the selected image decreases (Figure 2.2D). Based on this background-corrected cytofluorogram, the Pearson's linear co-localisation co-efficient (C_L) is calculated, which indicates the degree of overlap between two channels in a microscopy image:

$$C_L = \sum((X_i - X_{avg})(Y_i - Y_{avg}) / \mathrm{sqrt}(\sum X_i - X_{avg})^2 \sum (Y_i - Y_{avg})^2)$$

With X_{avg} and Y_{avg} the averages of the X and Y channel, respectively and the summations with index *i* are over the entire image voxels.

The obtained C_L value lies between -1 and 1. Negative values occur when the majority of values of X above X_{avg} coincide with values of Y below Y_{avg}. A C_L close to 1 indicates an extensive overlap of the two analysed channels. Since the averages are included in the calculation of the Pearson's co-localisation co-efficient, the C_L obtained is generally not affected by the image background. However, the background independence only occurs when a constant value is added to either channel, and introduces a significant bias in the C_L analysis (C_L indicated in Figure 2.2B,D). Therefore, all images analysed were background-corrected prior to calculation of C_L.

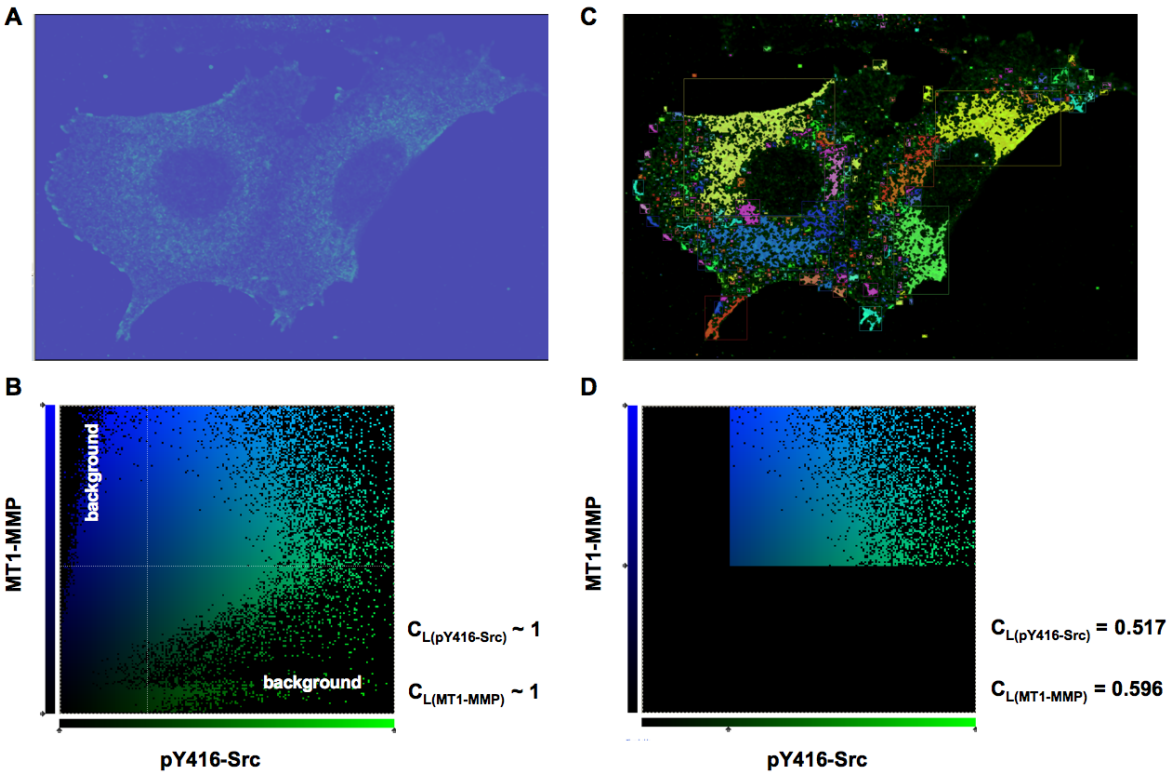

Figure 2.2: Co-localisation analysis using Volocity

(A) Detected pY416-Src staining is indicated without background correction. ***(B)*** Corresponding cytofluorogram shows the co-localisation of MT1-MMP and pY416-Src without background correction. The calculated co-localisation co-efficients are $C_{L(pY416-Src)} \sim 1$ and $C_{L(MT1-MMP)} \sim 1$. ***(C)*** pY416-Src (AlexaFluor® 488 secondary) specific fluorescence as detected after background correction. ***(D)*** To (C) corresponding cytofluorogram of MT1-MMP and pY416-Src co-localisation after correcting for non-specific background for each channel. The calculated co-localisation co-efficients are $C_{L(pY416-Src)} = 0.517$ and $C_{L(MT1-MMP)} = 0.596$.

2.2.4.3.3 iCys™ quantification of MT1-MMP nuclear staining

MT1-MMP nuclear staining intensities were quantified using the iCys™ laser scanning cytometer. Cells were stained as previously described (chapter 2.2.4.1) with either an

antibody directed against the MT1-MMP ICD (ab28209, AlexaFluor® 488 secondary) or an antibody raised against the MT1-MMP ECD (N175/6, AlexaFluor® 488 secondary) and counterstained with DAPI. Figure 2.3B shows a magnification of the scanned area (Figure 2.3A), obtained within the 405 nm channel. The fluorescent intensities of the AlexaFluor® 488 labelled cells within that nuclear contour were detected and normalised to non-specific background noise (Figure 2.3C). Approximately 10,000 cells were scanned per condition, each in biological triplicates (Figure 2.3A).

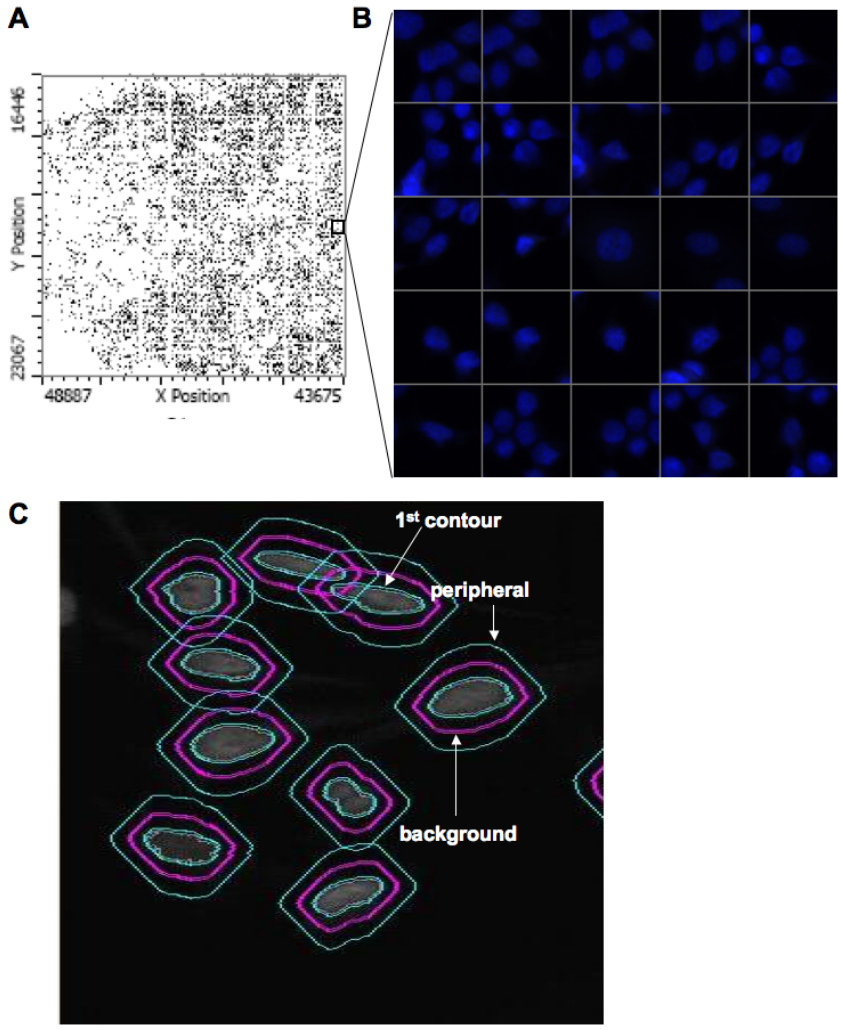

Figure 2.3: iCys quantification of nuclear staining

(A) 5 × 10^5 cells were seeded on a glass coverslip, transfected with MT1-WT and immunostained with an anti-MT1-MMP ICD (ab28209, AlexaFluor® 488 secondary) or an anti-MT1-MMP ECD (N175/6, AlexaFluor® 488 secondary) antibody. Cells of both conditions were counterstained with DAPI. Representation of the scanning area on the glass coverslip obtained with the iCys™ laser scanning cytometer. ***(B)*** Magnification of the scanned area showing DAPI staining as indicated (dashed square). ***(C)*** Automated generation of a 1st contour around the DAPI stained nuclear region of each cell. Detected fluorescent intensities were normalised to background level, which was set by default 8 pixels off the primary contor. One or more peripheral contours could be manually defined to quantify cytoplasmic staining.

2.2.4.4 Flow cytometry

MCF-7 cells were transfected with various cDNAs and/or stimulated with 100 ng/ml rh-$VEGF_{165}$ for 30 minutes where indicated. Cells were then washed, lifted off using 5 mM EDTA/PBS for 5 minutes at 37°C and fixed with PFA (4% (*w*/*v*) in 5 mM EDTA/PBS). Cell surface VEGFR-2 and MT1-MMP were labelled for 1 hour at RT. The cells were washed three times in PBS and incubated for 1 hour at RT with 10 µg/ml PE-conjugated anti-mouse or allophycocyanine (APC) anti-rabbit secondary antibodies (Table 2.3). Cells were washed as previously described, sieved through a 70 µm filter and analysed on a FACSCalibur™ flow cytometer. 10,000 events were acquired per sample and the mean fluorescence intensity of four independent experiments was analysed using FlowJo Flow Cytometry analysis software.

2.2.4.5 ELISA assay

Wells of a microtitre plate were coated either with VEGFR-2-Fc (10 µg/ml) or low-fat milk (10 µg/ml) for 16 hours at 4˚C and blocked with 3% (*w*/*v*) low-fat milk in wash buffer (50 mM Tris, pH 7.4, 150 mM NaCl, 1 mM $CaCl_2$, 0.05% (*v*/*v*) Tween®20) for 1 hour at RT. After three washes in washing buffer, rh-MT1-Ecto, rh-MT1-Ecto-E240A, rh-MT1-Cat (all at 2 µM) or rh-$VEGF_{165}$ (1 µM) were added in wash buffer for 1 hour at RT. Protein complexes were washed 3 × in wash buffer. Bound rh-MT1-MMP domains or rh-$VEGF_{165}$ were detected using the LEM-2/15.8 or VEGF-A antibodies (1 hour at RT), respectively, followed by an HRP-conjugated anti-mouse secondary antibody (1 hour at RT) and incubation with the TMB High Sensitivity Substrate Solution according to the manufacturer's instructions. Reactivity was measured by absorbance at 450 nm using the Infinite® M200 plate reader. OD obtained from wells without rh-MT1-MMP domain or rh-$VEGF_{165}$ incubation was subtracted from OD of each sample well. Samples were assayed in triplicates.

2.2.4.6 Recombinant protein binding assay

Soluble rh-VEGFR-2-Fc – rh-MT1-Ecto or rh-VEGFR-2-Fc – rh-MT1-Cat complexes were generated by incubation of 10 µg VEGFR-2 with MT1-MMP domains at a 1:1 molar

ratio at 37˚C for 30 minutes in 50 mM Tris-HCl, 200 nM NaCl and 5 mM $CaCl_2$ (pH 7.4). Where indicated, 10 µg rh-MT1-Ecto was pre-incubated with 10 µg/ml catalytic activity blocking anti-MT1-MMP antibody LEM-2/15.8 before adding rh-VEGFR-2-Fc. Following complex formation, 15 µl of each sample was taken as Input control. VEGFR-2 antibody (55B11) pre-coated Dynal magnetic beads (Protein G) were added to the remaining sample and the lysates were immunoprecipitated as described in chapter 2.2.4.7. Immunoprecipitates and Input controls were separates by SDS-PAGE followed by coomassie staining of total protein.

2.2.4.7 Immunoprecipitation (IP)

Cells were seeded in 6-well plates and transfected and stimulated as indicated in the results chapter. Following 16 hours incubation, cells were washed 3 × in PBS and lysed in IP lysis buffer (chapter 2.1.1.5). All following steps were conducted at 4˚C. Antibodies (3 µg) were bound to Dynabeads protein G at 4˚C for 16 hours in 5 mg/ml BSA in PBS (chapter 2.2.4.8). Cell lysates were subsequently incubated with antibody-bound Dynabeads for 2 hours at 4˚C under constant rotation. Beads were subsequently washed 4 × 10 minutes with immunoprecipitation buffer and resuspended in 2 × Laemmli buffer. Denatured proteins were separated on 10% SDS- PAGE and electro-transferred onto nitrocellulose membrane as described previously (chapter 2.2.3.6).

2.2.4.8 Chromatin Immunoprecipitation (ChIP)

MCF-7 cells were seeded in a 150 cm^2 dish and 25 µM penetratin peptide was added. 3 hours after treatment, the medium was removed and cells were fixed in 1% (*w*/*v*) formaldehyde in serum-free medium for 10 minutes at 37˚C. The fixation medium was removed, the cells were washed 2 × in cold PBS and scraped in 500 µl ice-cold PBS containing protease inhibitors (Complete Tablets). The cells were collected by centrifugation at 5000 × rpm for 2 minutes and washed 2 × in PBS containing protease inhibitors. After another centrifugation step at 5000 × rpm for 2 minutes, the PBS was removed and cells were resuspended in freshly prepared 300 µl SDS lysis buffer containing protease inhibitors. The samples were sonicated 3 × 10 seconds and centrifuged in a microcentrifuge for 10 minutes at maximum speed at 4˚C. The supernatant containing

total chromatin and protein was collected and 20 µl were taken to use as Input control. The supernatant volume was increased with ChIP dilution buffer (chapter 2.1.1.5) to 2 ml total volume and added to pre-bound magnetic beads. Briefly, for magnetic bead coating 40 µl Protein G coated Dynal magnetic beads were washed 3 × in PBS containing 5 mg/ml BSA. 3 µg of antibody was added in PBS containing 5mg/ml BSA for 16 hours on a mixer at 4˚C. The beads were washed 3 × in PBS containing 5 mg/ml BSA and the chromatin samples were added. Protein – chromatin complexes were immunoprecipitated on a mixer at 4˚C for 2 hours and magnetic beads were collected. Immunocomplexes were washed 6 × in RIPA buffer on a mixer for 20 minutes between every second wash and subsequently washed 2 × in TE buffer (pH 7.6). The immunoprecipitated samples as well as the Input controls were either resuspended in 5 × Laemmli buffer for immunoblotting or subjected to reverse cross-linking to perform Real-Time PCR. Therefore, 100 µl of 1% SDS and 0.1 M $NaHCO_3$ were added to the immunoprecipitates and Input controls. The samples were vortexed every few minutes for 30 minutes at RT. Reverse cross-linking was performed at 65˚C for 16 hours. DNA was extracted by phenol:chloroform:IAA precipitation and used for SYBR® Green Real-Time-PCR (chapter 2.2.2.4.2).

2.2.5 Cell-based functional assays

2.2.5.1 Luciferase assay

The cells were seeded in 6-well plates (1×10^5 HeLa cells/well, 5×10^5 MCF7 cells/well) and were transiently co-transfected 24 hours later with the reporter gene construct pG5luc, *β*-Galactosidase for normalisation and different MT1-MMP constructs (Table 2.5). The cells were inhibited or stimulated 3 hours after transfection (inhibitors used: Table 2.4) and harvested 24 hours later. The culture medium was removed and the cells were rinsed twice in 1 × PBS to remove used medium, dead cells and debris. After addition of 200 µl Reporter Lysis Buffer (Promega), the cells were lysed for 15 minutes and processed according to manufacturer's instructions. The reporter gene expression was detected by using the Luciferase Assay System by Promega. Luciferase activity was normalised by measuring *β*-Galactosidase as an internal control for transfection efficiency. 50 µl 2 × Assay Buffer, containing the substrate ONPG (*o*-nitrophenyl-β-D-galactopyranoside), were added and the samples were incubated for at least 30 minutes at 37°C. During that time *β*-

Galactosidase hydrolyses the colourless substrate to *o*-nitrophenyl, causing a change of colour to yellow. The reaction was terminated by addition of 1 M Tris-base, and the absorbance at 420 nm was measured by spectrophotometry.

Luciferase expression was normalised to *β*-Galactosidase activity by dividing the relative light units values obtained from the Luciferase assay by those from the latter assays. The reporter gene assay was performed in two biological and technical replicates and repeated at least 3 times in independent experiments.

2.2.5.2 Dual Luciferase Assay

For the mammalian two-hybrid assay the Dual Luciferase® Reporter Assay System was used. It allows the simultaneous measurement of two individual reporter enzymes within a single assay, the activities of Firefly (*Photinus pyralis*) and *Renilla* (*Renilla reniformis*) Luciferases. Src and MT1-MMP ICD were both sub-cloned in the pAct and pBind vectors (Table 2.5). The pBind vector contains the GAL4 DNA-binding domain and expresses *Renilla* Luciferase under the control of a SV40 promoter, which allows normalisation of the transfection efficiency. The pAct vector contains the VP16 transactivation domain.

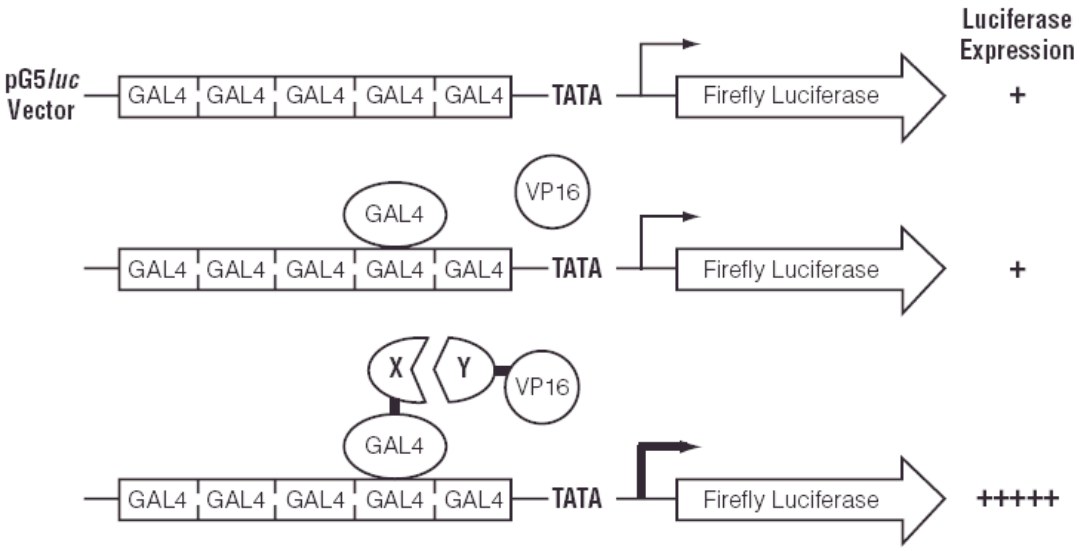

Figure 2.4: Mammalian-two hybrid system

Cells were co-transfected with the pG5luc vector, which contains 5 GAL4 binding sites upstream from the Firefly Luciferase gene, the VP16 domain containing pAct vector and the GAL4 expressing pBind vector. Interaction between the two proteins of interest leads to the assembling of the GAL4 and VP16 domains, which enhances Firefly Luciferase activity. Expression of *Renilla* Luciferase by the pBind vector is detected in order to normalise for transfection efficiency. Taken from: Dual-Luciferase® Reporter Assay System technical manual (Promega).

Src and MT1-MMP ICD were expressed as fusion proteins with the GAL4 and VP16 domains, respectively. MCF-7 and HeLa cells were co-transfected with these constructs and the pG5luc vector. The pG5luc vector contains five GAL4 binding sites followed by a minimal TATA box and the firefly Luciferase gene (Figure 2.4). An interaction between the two genes of interest leads to an interaction between the GAL4 and VP16 domains, which in turn induces the expression of the Luciferase gene. Firefly Luciferase activity is normalised by *Renilla* activity, which is expressed from the pBind vector.

The assay was performed according to the manufacturer's instruction. Briefly, cells were seeded in 12-well plates (1×10^5 MCF-7 cells/well, 5×10^4 HeLa cells/well) and transiently co-transfected with 1 µg pG5luc, 1 µg pAct- and 1 µg pBind-constructs the following day. The cells were stimulated for ~6 hours with 100 nM PMA where indicated and harvested for the gene reporter assay 24 hours after transfection. The culture medium was removed and the cells were rinsed twice in 1 × PBS to remove used medium and dead cells. 200 µl 1 × Passive Lysis Buffer (PLB, Promega) was added per well and cells were lysed for 15 minutes on a rocking platform. Firefly Luciferase activity was detected by adding 20 µl of Luciferase Assay Reagent II (Promega). After quantification of the Firefly Luciferase luminescence, the reaction is quenched while *Renilla* Luciferase reaction is initiated within in the same step. Firefly Luciferase expression was normalised to *Renilla* Luciferase activity by dividing the relative light units values obtained from the Firefly Luciferase assay by those from the latter measurement. Transfection efficiency of the pAct vector was determined by Western Blotting using an anti-VP16 antibody. Each assay was performed in three biological and two technical replicates and repeated at least 2 times in independent experiments.

2.2.6 *In silico* analyses

2.2.6.1 Computer programs

The analysis and presentation of the data showed in this thesis, was performed using the Microsoft® Office 2004 for Mac Version 11.5.3 (Microsoft, Redmond, WI). Image acquisition and analysis were performed with the Leica Application Suite AF version 1.7.0 (Leica), Volocity 3D imaging and analysis software (improvision, Perker Elmer, Coventry, UK), iNovator Application Development Toolkit (CompuCyte, Westwood, MA),

MetaMorph® software (Universal Imaging Corporation, Downigtown, PA) and Adobe® Photoshop® Professional CS3 version 10.0.1 (Adobe, San Jose, CA). Analysis of flow cytometry data were conducted with the FlowJo Flow Cytometry Analysis Software (v.8.8.4, Tree Star Inc., Olten, Switzerland). FinchTV version 1.4.0 (Geospiza Inc., Seattle, WA) and Vector NTI (Invitrogen) have been used for sequence analyses, while the SDS software v2.3 (Applied Biosystems) was used for acquisition and analysis of Real-Time PCR data obtained with the ABI 7900HT Fast Real-Time PCR System. Statistical data analysis was performed using the GraphPad Prism® 5 Software (GraphPad Software, Inc, San Diego, CA) and general data presentation and organisation was carried out using Adobe® InDesign® CS3 version 5.0.4, Adobe® Acrobat 8 Professional CS3 version 8.1.3 and EndNote X2.0.1 (Thomson Reuters, Carlsbad, CA) as well as the Microsoft Office package for Mac v 11.5.3 (Microsoft, Redmond, WA).

2.2.6.2 Statistical analysis

Statistical analysis was performed using the GraphPad Prism® 5 Software. Statistical significance was assessed by one-way ANOVA with the Student Newman-Keuls post-test, unless indicated otherwise. All numerical values shown are the means ± standard error (S.E.M). Statistical significance was defined as $P < 0.05$ (*), $P < 0.001$ (**) and $P < 0.0001$ (***).

3 Results

Although MT1-MMP expression is widely distributed in normal physiology, its expression is frequently increased in malignant or inflamed tissue. MT1-MMP expression has been detected in tumour cells and adjacent stromal cells in a variety of human tumours, including breast, cervical, colon, bladder, gastric, pancreatic, liver, ovarian, prostate and thyroid cancer and MT1-MMP expression has been shown to correlate with a poor prognosis in tumours of various origins (reviewed in [250]). Recently, new non-catalytic roles for MT1-MMP have emerged, which include the induction of intracellular signalling pathways and the regulation of gene expression of various target genes. MT1-MMP has been implicated in regulating the transcription of VEGF-A, Dickkopf-3 (DKK-3) and Smad-1. However, the molecular mechanisms underlying the MT1-MMP induced transcriptional regulation are not understood so far.

MT1-MMP dependent induction of VEGF-A expression has been previously reported to involve MT1-MMP catalytic activity, its intracellular domain as well as Src activity [73] (Figure 3.1A). However, various transcription-regulating proteins were recently reported to be synthesised as transmembrane precursors, which have to be activated by proteolytic processing (chapter 1.4), raising another possibility of MT1-MMP mediated transcriptional regulation (Figure 3.1B). During this process, the ectodomain is shed from the cell surface, whereas the intracellular part is released and translocates to the nucleus to regulate gene expression.

In this study the following questions were addressed: ***(i)*** how does MT1-MMP induce intracellular signalling cascades, ***(ii)*** what are the elements of an MT1-MMP induced signalling pathway and ***(iii)*** what are the target genes regulated by MT1-MMP expression.

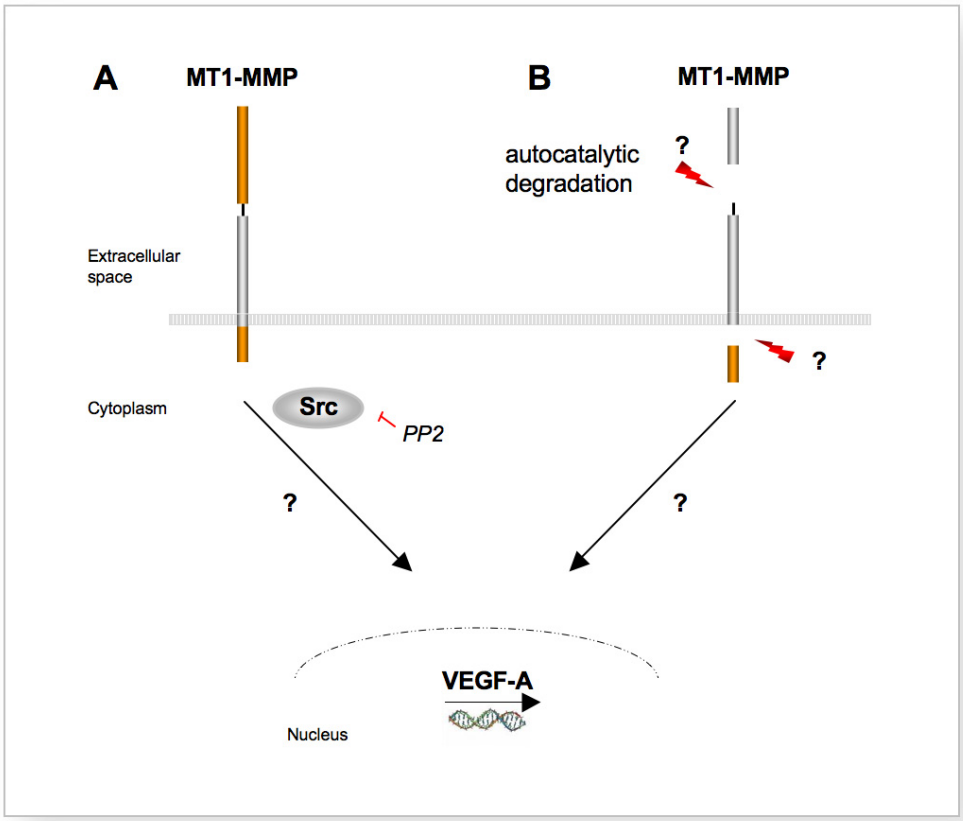

Figure 3.1: Potential MT1-MMP induced signalling pathways

Schematic representation of potential MT1-MMP induced signalling pathways. ***(A)*** MT1-MMP was reported to induce the expression of VEGF-A in a Src dependent way, involving the MT1-MMP catalytic and intracellular domain. ***(B)*** Representation of an alternative mechanism, in which the intracellular domain of MT1-MMP is released from the plasma-membrane and translocates to the nucleus to regulate gene transcription.

3.1 MT1-MMP dependent regulation of VEGF-A expression in MCF-7 cells

MT1-MMP activity has been implicated in various studies to be involved in the formation of new blood vessels in both physiological and pathological conditions (chapter 1.3.3.3). The development of new blood vessels within tumours is an important step in carcinogenesis and is predominantly initiated by secretion of the pro-angiogenic factor VEGF-A (chapter 1.5.1). Many tumour cells have been shown to express and secrete VEGF-A, thus inducing paracrine and/or autocrine signalling leading to angiogenesis as well as cell survival and proliferation in cells expressing VEGF receptors.

MT1-MMP is highly expressed in some tumour cells and MCF-7 and U251 cells, which stably overexpress MT1-MMP, have been shown to enhance the expression of VEGF-A at

the transcriptional level [26,73]. This up-regulation has been shown to be dependent on the catalytic and intracellular domains of MT1-MMP as well as on Src activity [73]. However, the molecular mechanism underlying this transcriptional up-regulation is not understood in detail so far. The aim of the first part of this thesis was to identify the molecular mechanisms linking MT1-MMP expression to VEGF-A transcription and thus refining the role of MT1-MMP in tumourigenic angiogensis.

MCF-7 cells, which are deficient in MT1-MMP expression [251], were used as a model system for breast carcinoma cells in this study to selectively investigate the effect of MT1-MMP in transfected cells as well as to study the role of the different MT1-MMP domains.

3.1.1 Transient transfection or adenoviral transduction of MT1-MMP cDNA increases VEGF-A transcription

In order to confirm the role of MT1-MMP in VEGF-A transcription reported previously [26,73], MT1-MMP was expressed in MCF-7 cells either by transient transfection or by using an adenoviral delivery system. By using these transient transfection techniques, the formation of artefacts resulting from the adaptation to the selection process, which might occur during the generation of stable expressing clones, as described previously [73], may be avoided. Furthermore, the transient expression systems used in this study enabled the observation of early effects following MT1-MMP expression, which might mimic molecular responses in early phases of tumour growth and metastasis.

Thus, MCF-7 cells were either transiently transfected with full-length MT1-MMP (MT1-WT, Figure 3.2A, B) or transduced with multiplicities of infection (MOI) of 150 pfu/cell of MT1-WT expressing adenovirus (Figure 3.2C, D). Total RNA was isolated and the expression levels of MT1-MMP and VEGF-A mRNA were determined by TaqMan® Real-Time PCR. The VEGF-A TaqMan® probe used detected all isoforms derived from alternative splicing (chapter 1.5.1).

As expected, transient expression of MT1-WT in MCF-7 cells led to a significant increase of MT1-MMP mRNA ($P < 0.0001$ compared to pcDNA3.1 control, Student *t*-test, Figure 3.2A) as well as an increase in VEGF-A mRNA expression ($P < 0.001$, Student *t*-test) compared to the empty vector control (pcDNA3.1) transfected cells (Figure 3.2B).

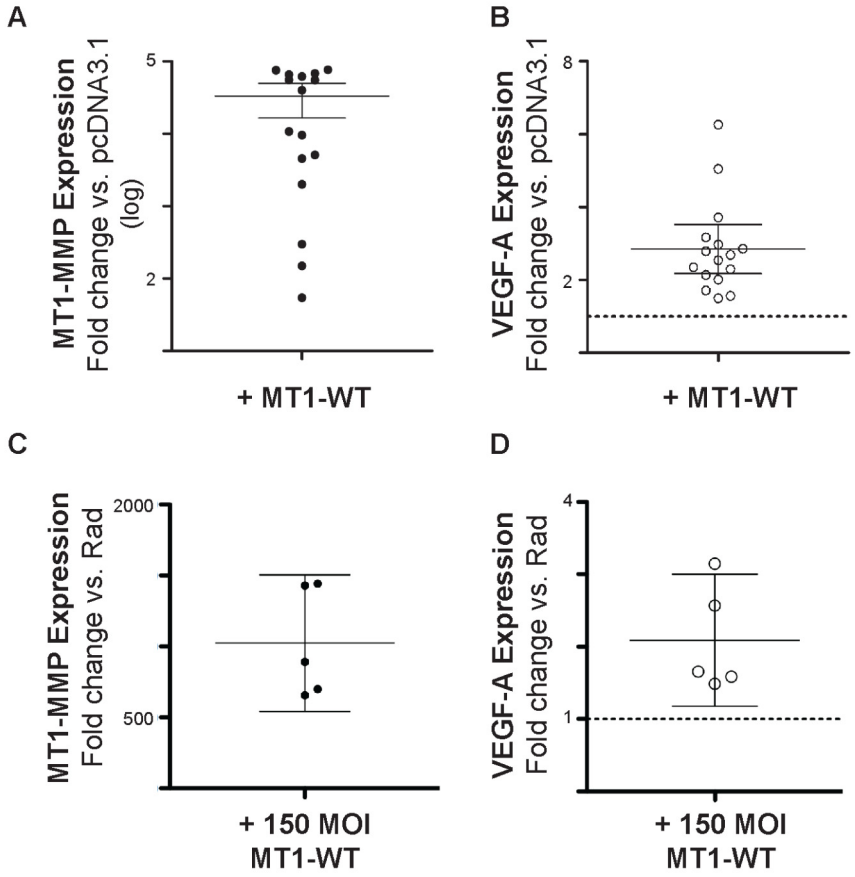

Figure 3.2: MT1-MMP expression increases the VEGF-A mRNA level

(A,B) MCF-7 cells were transfected with either empty pcDNA3.1 control vector or MT1-WT and expression levels of MT1-MMP (A) and VEGF-A (B) were detected by TaqMan® Real-Time PCR. MT1-MMP and VEGF-A relative expression levels were normalised to the mRNA levels of the house-keeping gene GAPDH. Data represent the mean expression in fold change compared to pcDNA3.1 empty vector control (dotted line) of 16 independent experiments ± 95% confidence intervals. ***(C,D)*** MCF-7 cells were transduced with a MOI of 150 pfu/cell of MT1-WT expressing adenovirus or 150 pfu/cell of empty adenoviral vector control (Rad). Expression levels of MT1-MMP and VEGF-A were detected by TaqMan® Real-Time PCR and normalised to the mRNA levels of the house-keeping gene GAPDH. Data correspond to the mean expression in fold change compared to Rad control (dotted line) of 5 independent experiments ± 95% confidence intervals.

Accordingly, the level of VEGF-A expression was found to be increased in cells transduced with MT1-WT expressing adenovirus (Figure 3.2C, D). For both transient and adenoviral expression of MT1-WT in MCF-7 cells, an increase of VEGF-A mRNA could be observed (Figure 3.2B, D), indicating that the MT1-MMP induced expression of VEGF-A is independent of the expression system used.

To test whether VEGF-A expression is directly proportional to the MT1-MMP expression level, MCF-7 cells were transduced with increasing MOI of MT1-WT expressing adenovirus. As shown in Figure 3.3A and B, addition of increasing MOI of MT1-WT expressing adenovirus led to a significant increase of MT1-MMP ($P < 0.0001$; 150 pfu/cell

MT1-WT compared to Rad control) and VEGF-A mRNA levels ($P < 0.05$; 150 pfu/cell MT1-WT compared to Rad control) as compared to empty adenoviral vector control (Rad).

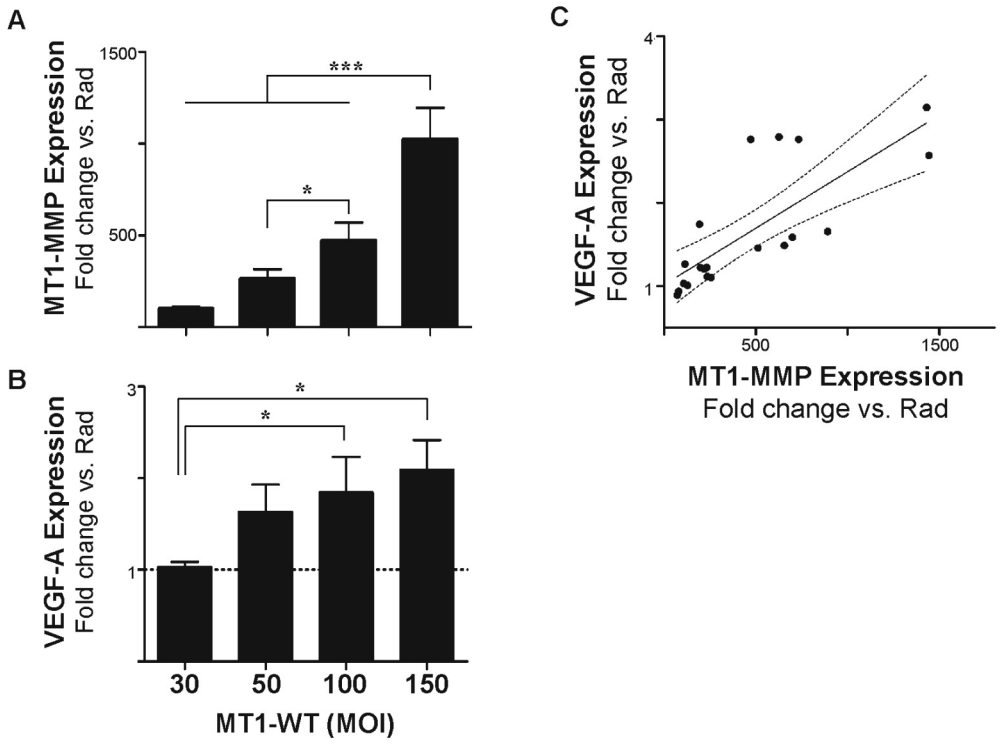

Figure 3.3: VEGF-A mRNA expression is proportional to MT1-MMP mRNA levels

(A,B) MCF-7 cells were transduced with increasing MOI of MT1-WT expressing adenovirus or 150 pfu/cell of Rad empty adenoviral vector control. mRNA levels of MT1-MMP (A) and VEGF-A (B) were detected by TaqMan® Real-Time PCR and the relative expression levels were normalised to the mRNA levels of the house-keeping gene GAPDH. Data represent the mean expression in fold change compared to Rad control (dotted line) of 5 independent experiments ± S.E.M. with $P < 0.05$ (*) and $P < 0.0001$ (***). ***(C)*** MCF-7 cells were transduced with MT1-WT expressing adenovirus as described before. The MT1-MMP mRNA levels in fold change compared to Rad control are plotted against the corresponding VEGF-A mRNA expression levels in fold change compared to Rad control. Data represent the mean expression in fold change compared to Rad of 20 independent experiments ± 95% confidence intervals.

By plotting the relative mRNA expression of MT1-MMP and VEGF-A, both in fold change compared to empty adenoviral vector control (Rad), a direct correlation between VEGF-A and MT1-MMP mRNA expression could be observed (Figure 3.3C; $y = 0.0014x + 1.016$, best-fit values).

These data are consistent with previous observations showing that MT1-MMP expression increases the mRNA level of VEGF-A [73] and further emphasise that this observation is independent of the expression system used (Figure 3.2).

In addition to the MT1-MMP dependent increase in VEGF-A transcription we could also observe a dose-dependent effect on VEGF-A translation. As shown in Figure 3.4A cellular

VEGF-A protein accumulated with increasing MOI of transduced MT1-MMP (up to 150 MOI). To test whether the amount of secreted VEGF-A is also affected by MT1-MMP, proteins of the conditioned medium of cells transduced with MT1-WT expressing adenovirus were concentrated and immunoblotted. With increasing levels of MT1-MMP protein an increasing amount of VEGF-A was found to be secreted into the medium (Figure 3.4.A).

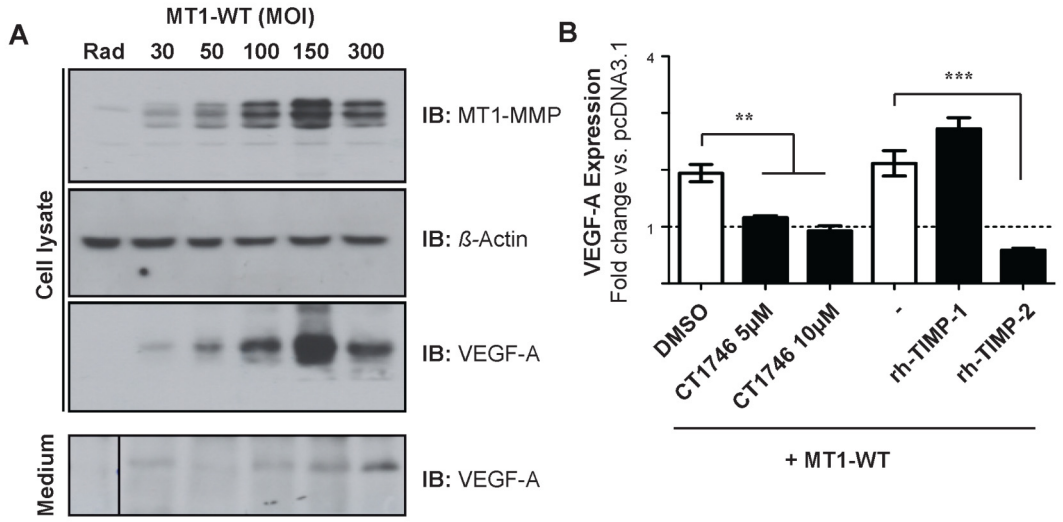

Figure 3.4: Dose-dependent expression of VEGF-A protein and its secretion into the medium with increasing concentrations of MT1-MMP

(A) MCF-7 cells were transduced with the indicated MOI of MT1-WT expressing adenovirus and the protein levels in the cell lysates as well as in the conditioned medium were analysed by immunoblotting with an anti-MT1-MMP (LEM-2/15.8), anti-VEGF-A or an anti-*β*-Actin antibody. ***(B)*** MCF-7 cells were transfected with pcDNA3.1 vector control or MT1-WT and were incubated for 24 hours with 1 µM rh-TIMP-1, 1 µM rh-TIMP-2 or CT1746 at the indicated concentrations. VEGF-A expression levels were determined by TaqMan® Real-Time PCR and normalised to the mRNA levels of the house-keeping gene GAPDH. The data represent the mean expression in fold change compared to pcDNA3.1 (dotted line) of 3 independent experiments ± S.E.M. with $P < 0.001$ (**) and $P < 0.0001$ (***) compared to DMSO treated control (for CT1746 treated samples) or compared to untreated (-) MT1-WT control (for TIMP stimulated samples).

To address whether the up-regulation of VEGF-A transcription is dependent on metalloproteinase (MP) function, as described previously [73], MT1-WT transfected MCF-7 cells were treated with 5 µM or 10 µM of the broad-spectrum MP inhibitor CT1746 or with 1 µM of the physiological recombinant human (rh-) MP inhibitor Tissue Inhibitor of Metalloproteinase -1 (TIMP-1) or rh-TIMP-2. The expression level of VEGF-A in MT1-MMP transfected cells was found to be elevated by ~2 fold compared to pcDNA3.1 control transfected cells, as routinely observed (Figure 3.4B and Figure 3.2B). VEGF-A expression levels were not significantly affected in MT1-MMP expressing cells following

treatment with 5 or 10 μM CT1746 ($P < 0.001$ compared to DMSO control) or rh-TIMP-2 ($P < 0.0001$ compared to untreated (-) control). In contrast, treatment of MT1-WT expressing cells with rh-TIMP-1, which does not inhibit MT1-MMP function [252], increased the level of VEGF-A expression to the level of wild-type control (Figure 3.4B). These findings confirm that a metalloproteinase, possibly MT1-MMP itself, is needed for the transcriptional up-regulation of VEGF-A in MCF-7 cells.

3.1.2 VEGFR-2, PI3 Kinase, mTOR, Src and HIF-1α activities are required for the MT1-MMP induced VEGF-A expression

To obtain a better understanding of the cellular signalling mechanism underlying the MT1-MMP induced up-regulation of VEGF-A, MT1-WT transfected MCF-7 cells were treated with different inhibitors of key signalling pathways (summarised in Table 3.1) and VEGF-A expression levels were assessed by TaqMan® Real-Time PCR. As previously reported inhibition of Src, by using PP2, ablated the MT1-MMP induced up-regulation of VEGF-A mRNA levels (Figure 3.5A) [73]. A similar observation was obtained following inhibition of phosphatidylinositol 3 (PI3) kinase (Wortmannin, LY294002), Akt (SH-5) and mTOR (Rapamycin) (each $P < 0.0001$ compared to DMSO control; Figure 3.5A). Treatment of cells with SU4312 was also found to inhibit MT1-MMP mediated VEGF-A expression in MCF-7 cells. As this compound inhibits both VEGFR and PDGFR activities, the more selective PDGFR inhibitor AG-1296 was used in order to distinguish between these two receptors. As presented in Figure 3.5A, AG-1296 did not affect the MT1-MMP induced VEGF-A mRNA expression compared to DMSO control, thus suggesting that the SU4312 mediated down-regulation of VEGF-A mRNA was due to VEGFR inhibition. To identify candidate members of the Src and VEGFR families a gene-expression profile of the in tumours ubiquitously expressed Src, Fyn, VEGFR-1 and VEGFR-2 was conducted in MCF-7 cells (Figure 3.5B). Src and VEGFR-2 were the only genes to be detected within their respective gene families and were therefore studied further.

Treatment of MT1-WT expressing MCF-7 cells with inhibitors of MEK (PD98059), JNK (SP006125), EGFR (Gefitinib, Tarceva/Erlotinib), IKK (BMS-345541), IGF-1R (PPP, N-(2-Methoxy-5-chlorophenyl)-N'-(-methylquinolin-4-yl)-urea), p38 (SB 203580/4-(4-

Fluorophenyl)-2-(4-methylsulfinylphenyl)-5-(4-pyridyl)1H-imidazole), or the proteasome (Lactacystin) did not affect VEGF-A mRNA levels (summarised in Table 3.1).

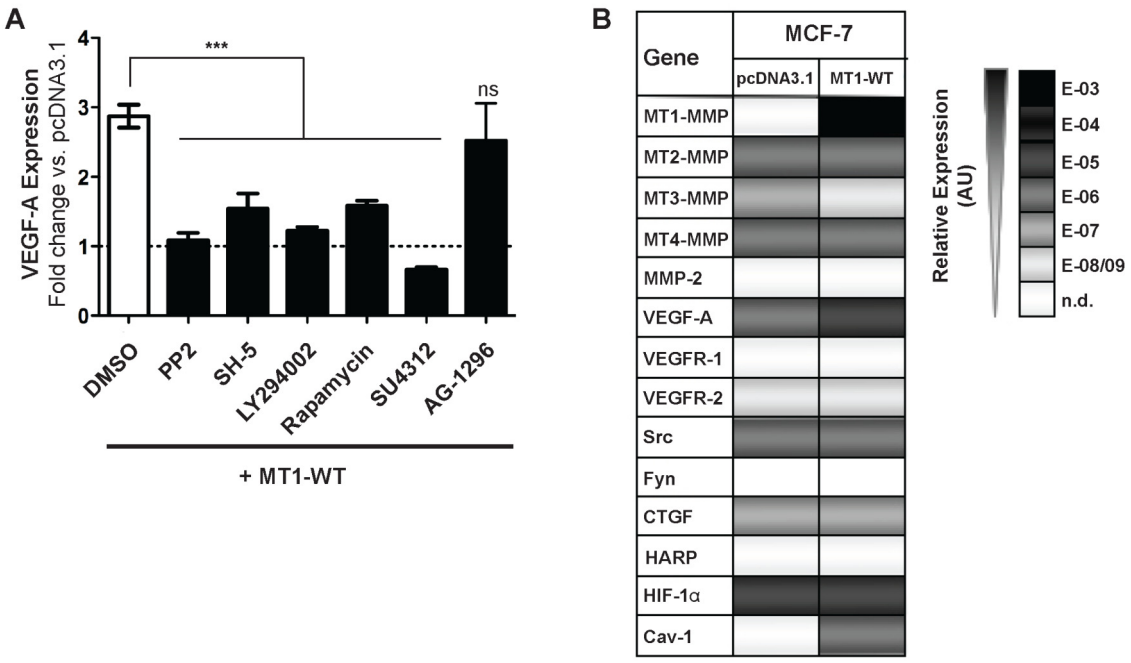

Figure 3.5: The MT1-MMP induced VEGF-A expression depends on Src, VEGFR-2, PI3 Kinase, Akt and mTOR activity

(A) MCF-7 cells were transiently transfected with MT1-WT and treated for 24 hours with DMSO, PP2, SH-5, LY294002, Rapamycin, SU4312 or AG-1296. VEGF-A expression levels were detected by TaqMan® Real-Time PCR and normalised to mRNA levels of the house-keeping gene GAPDH. Data represent the mean VEGF-A expression of three independent experiments in fold change compared to pcDNA3.1 control (dotted line) ± S.E.M. with $P < 0.0001$ (***) compared to DMSO control. *ns*, non-significant. ***(B)*** Gene expression profile of pcDNA3.1 and MT1-WT transfected MCF-7 cells was assessed by TaqMan® Real-Time PCR. Gene expression levels were normalised to mRNA levels of the house-keeping gene GAPDH. Data represent the mean gene expression of three independent experiments in arbitrary units (AU).

To confirm the profiling data, which imply the involvement of VEGFR-2 (VEGFR-1 was expressed at low levels in MCF-7 cells, Figure 3.5B), lentiviral shRNA knock-down was assessed for VEGFR-1 and VEGFR-2 (MISSION® shRNA, Sigma-Aldrich). However, all shRNA sequences tested targeting either VEGFR-1 or VEGFR-2 were found to generate unspecific depletion of either receptor (discussed in chapter 3.2.1.3).

VEGF-A Expression Fold change vs. MT1-WT (DMSO control)	
Decreased ↓	**Unchanged ↔**
Src (PP2)	MEK (PD98059)
PI3 kinase (Wortmannin, LY294002)	JNK (SP006125)
VEGFR / PDGFR (SU4312)	PDGFR (AG-1296)
Akt (SH-5)	EGFR (Tarceva/Erlotinib; Gefitinib)
mTOR (Rapamycin)	IKK (BMS-345541)
HIF-1α (Dimethyl Bisphenol A)	IFG-1R (IGF-1R Inh. II)
	Proteasome (Lactacystin)
	P38 (SB203580)

Table 3.1: Summary of inhibitors tested

MCF-7 cells were transfected with MT1-WT and various inhibitors were added at concentrations indicated in Material and Methods. VEGF-A expression levels were assessed by TaqMan® Real-Time PCR and normalised to the mRNA levels of the house-keeping gene GAPDH. The data representing each inhibitor set have been derived from three independent experiments. VEGF-A mRNA levels have been defined as decreased if $P < 0.05$ compared to MT1-WT transfected control treated with DMSO.

3.1.3 MT1-MMP expression induces activation of Akt and mTOR

The previously described requirement for Akt and mTOR activities in MT1-MMP mediated VEGF-A expression (Figure 3.5A), led to the hypothesis that MT1-MMP expression might affect the phosphorylation state of these kinases. In order to test this hypothesis, cells were transfected either with the pcDNA3.1 empty vector control or MT1-WT and total protein extracts were immunoblotted. As shown in Figure 3.6, the expression of MT1-WT augmented the level of Akt phosphorylation at S^{473} and T^{308}, whereas total levels of Akt were not affected. Accordingly, the phosphorylation of mTOR was also increased in MT1-WT expressing cells compared to the pcDNA3.1 transfected control (Figure 3.6).

In order to further analyse the MT1-MMP induced signalling pathway and to obtain information on the signalling hierarchy, MT1-WT transfected MCF-7 cells were incubated for 24 hours with PP2, SH-5, LY294002, SU4312 or DMSO as control. As shown in Figure 3.6, mTOR phosphorylation at S^{2448} and Akt phosphorylation at S^{473} and T^{308} was ablated with all the inhibitors used, suggesting that the mTOR and Akt phosphorylation events were down-stream of Src, PI3 Kinase and VEGFR-2 activation.

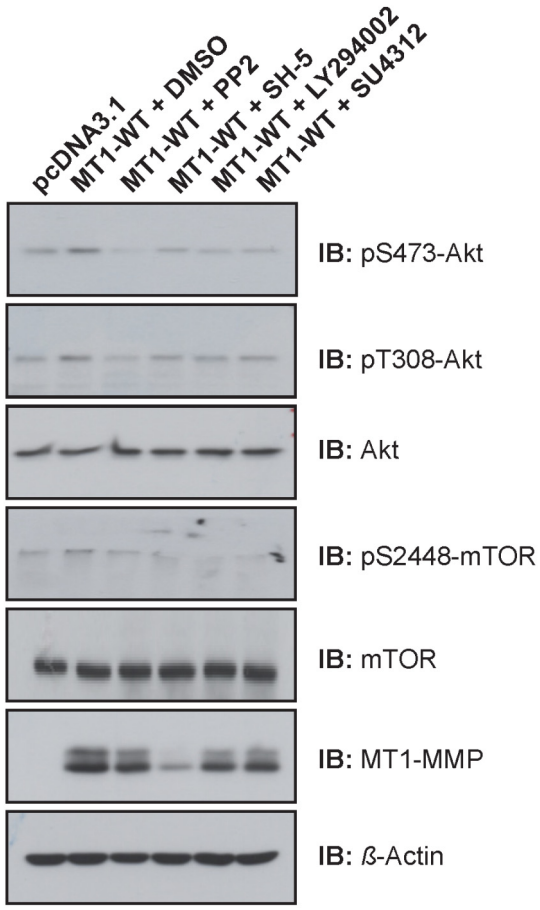

Figure 3.6: MT1-MMP expression increases phosphorylation of Akt and mTOR

MCF-7 cells were transfected with either pcDNA3.1 or MT1-WT, as indicated. DMSO, PP2, SH-5, LY294002 or SU4312 were added for 24 hours. Lysates were immunoblotted with an anti-pS473-Akt, anti-pT308-Akt, anti-Akt, anti-pS2448-mTOR, anti-mTOR, anti-MT1-MMP (LEM2/15.8) or an anti-*ß*-Actin antibody. The increase of Akt and mTOR phosphorylation in the presence of MT1-MMP protein is furthermore shown in Figure 3.7 and Figure 3.8A.

As the treatment of cells with SH-5 showed a reproducible reduction of MT1-MMP protein, which was also observed using Triciribine (API-2), a different Akt inhibitor, the interpretation of the role of Akt inhibition in this system is difficult.

Based on these findings, an MT1-MMP induced signalling pathway is proposed that requires the activity of VEGFR-2, Src, PI3 Kinase, Akt and mTOR (summarised in Figure 3.31).

To test whether Akt phosphorylation is directly dependent on the presence of MT1-MMP, various concentrations of MT1-WT were expressed in MCF-7 cells. As shown in Figure 3.8A, expression of MT1-WT led to a dose-dependent increase of Akt phosphorylation at S^{473} and T^{308}. Accordingly, transduction with various MOI of MT1-WT expressing adenovirus led to an increase in mTOR phosphorylation at S^{2448} (Figure 3.7).

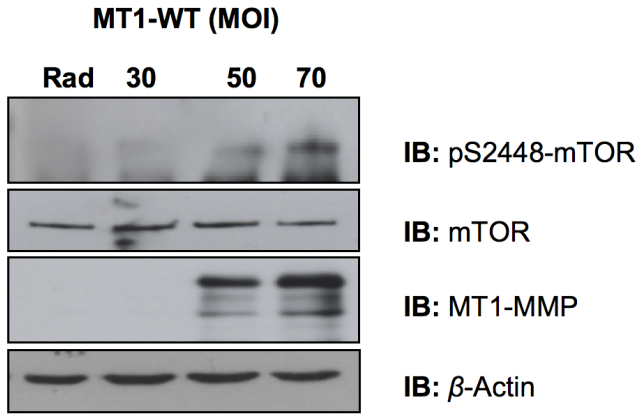

Figure 3.7: MT1-MMP expression increases mTOR phosphorylation

MCF-7 cells were transduced with indicated MOI of MT1-WT expressing adenovirus. Cell lysates were immunoblotted with an anti-pS2448-mTOR, anti-mTOR, anti-MT1-MMP (LEM-2/15.8) or an anti-*β*-Actin antibody. *Rad*, empty adenoviral control vector.

Consistent with the immunoblotting results (Figure 3.8A), immunofluorescence analyses of MT1-WT transfected MCF-7 cells showed an increase in Akt phosphorylation at S^{473} compared to the untransfected control cell (Figure 3.8B, *i*). MT1-MMP and pS473-Akt were routinely found to co-localise in intracellular vesicles and mainly at membrane protrusions of MCF-7 cells, potentially at the leading edge of the cell (Figure 3.8B, *iv*, arrows). Figure 3.8B, *v* shows the strong co-localisation of MT1-MMP, Akt and pS473-Akt within the orthogonal *z*/*x*- section along the *y*-axis of these protrusive membrane structures.

The co-localisation between MT1-MMP and Akt or MT1-MMP and pS473-Akt, respectively, are presented in cytofluorograms using the Volocity 3D imaging and analysis software (Figure 3.8C). Following correction of background fluorescence (as described in chapter 2.2.4.3.2), co-localisation co-efficients were calculated for each of the proteins. Thus, 90% of total MT1-MMP was found to co-localise with pS473-Akt or Akt, respectively, and 53.8% of phosphorylated Akt co-localised with MT1-MMP. Only 12.3% of total Akt was found in the same complex with MT1-MMP, since MT1-MMP was only expressed in one of the two analysed cells (Figure 3.8B). As expected, the antibody against phosphorylated Akt was able to detect an active subpopulation of Akt (with co-localisation co-efficient (C_L): $C_{L(Akt)} = 0.179$ and $C_{L(pS473\text{-}Akt)} = 0.757$).

These data indicate that MT1-MMP expression increases activation of Akt in MCF-7 cells, and therefore suggest a role for MT1-MMP in the Akt signalling pathway.

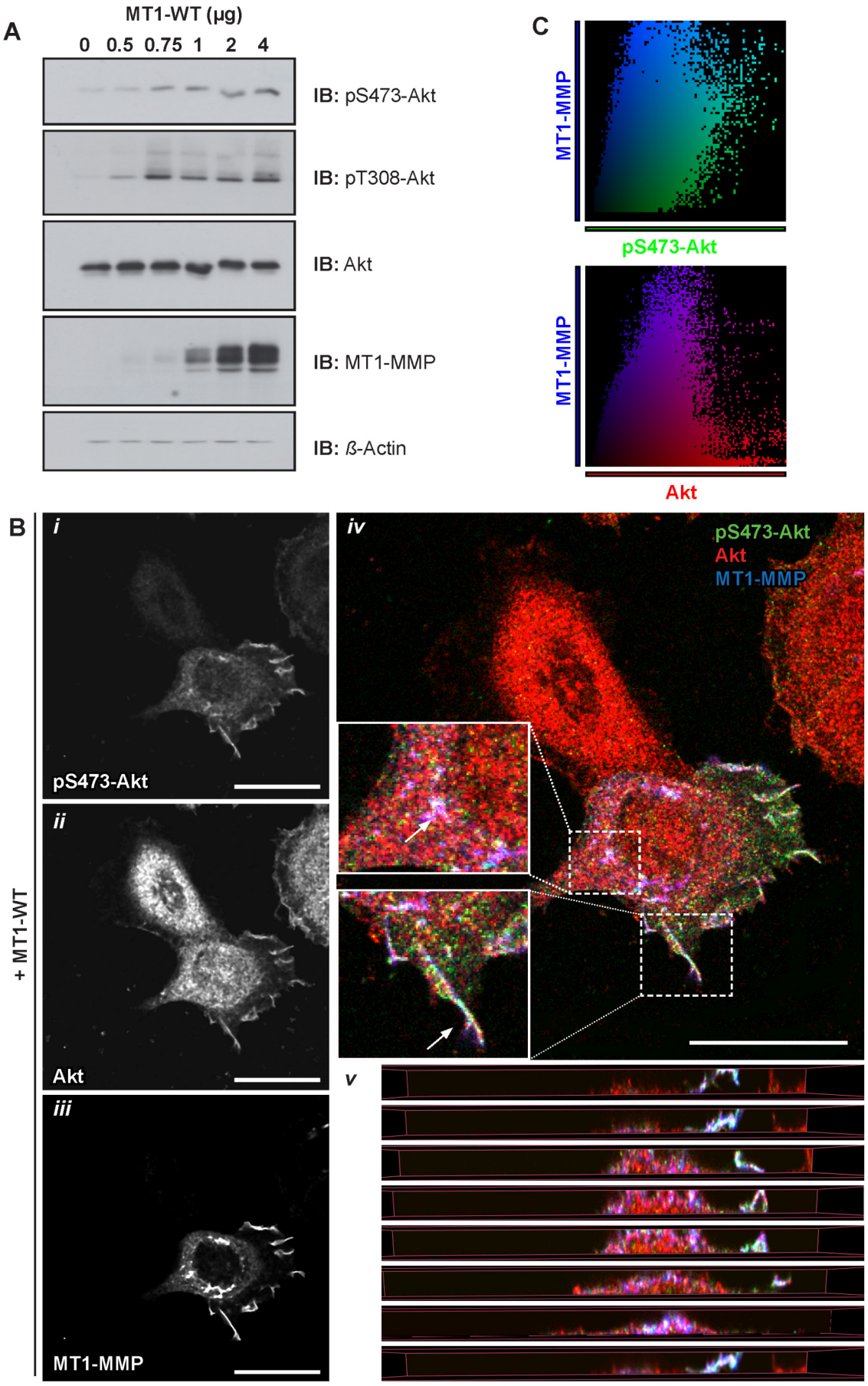
A
MT1-WT (µg)
0 0.5 0.75 1 2 4
IB: pS473-Akt
IB: pT308-Akt
IB: Akt
IB: MT1-MMP
IB: ß-Actin
C
MT1-MMP
pS473-Akt
MT1-MMP
Akt
B
+ MT1-WT
i
pS473-Akt
ii
Akt
iii
MT1-MMP
iv
pS473-Akt
Akt
MT1-MMP
v

Figure 3.8: MT1-MMP expression increases Akt phosphorylation

(A) MCF-7 cells were transfected with increasing concentrations of MT1-WT and cell extracts were immunoblotted with an anti-pS473-Akt, anti-pT308-Akt, anti-Akt, anti-MT1-MMP (LEM-2/15.8) or an anti-*β*-Actin antibody. ***(B)*** MT1-WT transfected MCF-7 cells were immunostained with an anti-pS473-Akt (AlexaFluor® 488 secondary, *i*), anti-Akt (AlexaFluor® 546 secondary, *ii*) and an anti-MT1-MMP antibody (N175/6; Cy5 secondary, *iii*). Arrows in the merged picture indicate co-localisation of Akt, phosphorylated Akt and MT1-MMP within the perinuclear region and at membrane protrusions (*iv*). Inset panels show magnified portions of each merged image, as indicated (dashed squares). Serial images present orthogonal sections along the *y*-axis of the merged confocal laser scanning micrograph (*v*). The white scale bars present a distance of 25 μm. (***C)*** Co-localisation histograms between MT1-MMP and pS473-Akt or Akt. Similar expression and co-localisation is shown by accumulation of pixels along the y = x axis.

3.1.4 MT1-MMP increases phosphorylation of Src

The previously described requirement for Src [73] (Figure 3.5A) in the MT1-MMP mediated VEGF-A expression and the observed MT1-MMP dependent phosphorylation of Akt and mTOR, led to the hypothesis that MT1-MMP expression could affect the phosphorylation level of Src. Src is consistently expressed at low levels in wild-type MCF-7 cells and especially its phosphorylation form (pY416-Src) was difficult to detect using immunological detection methods (Figure 3.9A). In order to increase the level of pY416-Src detection, Src was routinely expressed in MCF-7 cells in a transient manner.

Src expressing MCF-7 cells were transfected with MT1-WT and immunoblotted with an anti-pY416-Src and an anti-Src antibody. As shown in Figure 3.9B MT1-WT expression increased the level of Src phosphorylation at its Y^{416} residue significantly compared to Src only expressing cells, while total Src was expressed at similar levels.

To obtain a better understanding of the signalling hierarchy leading to increased VEGF-A expression, MT1-WT and Src expressing cells were incubated for 24 hours with PP2, SH-5, LY294002, SU4312 or DMSO control to define the position of Src phosphorylation within the proposed pathway (summarised in Figure 3.31). As shown in Figure 3.9B, Src phosphorylation at Y^{416} was effectively inhibited by PP2, SU4312 and SH-5 treatment. As incubation of cells with SH-5 led to a reproducible knockdown of MT1-MMP protein levels, making the interpretation of the role of Akt difficult as described before (chapter 3.1.3), these data indicate that Src is activated down-stream of VEGFR-2.

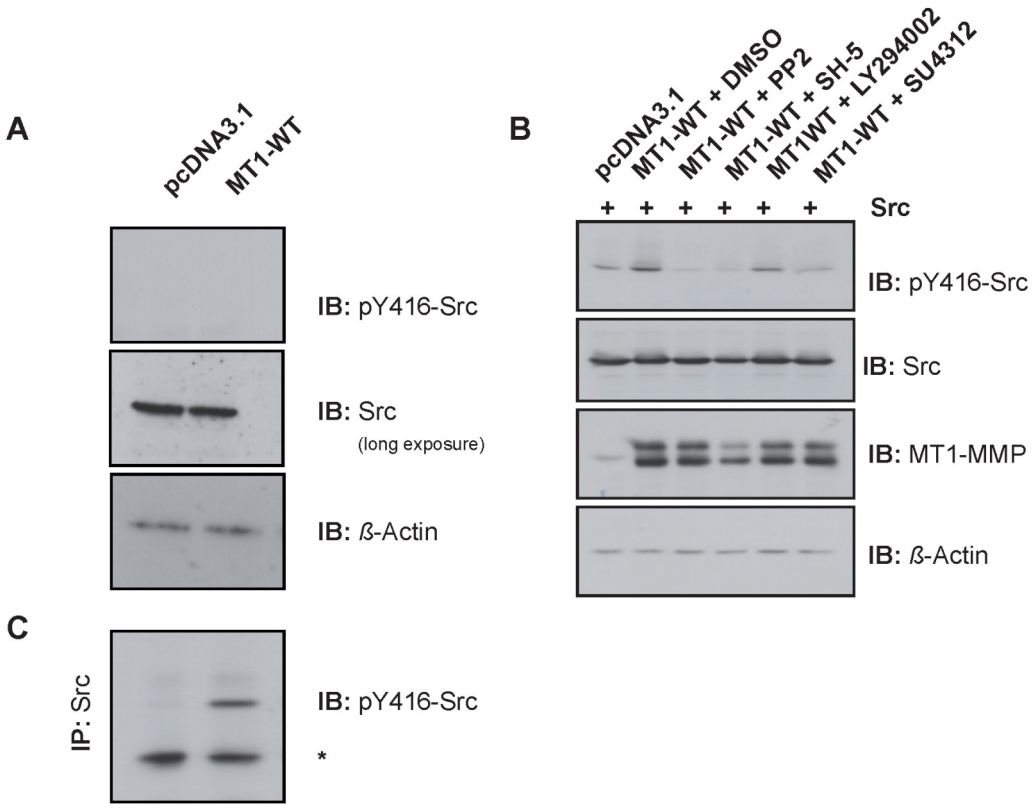

Figure 3.9: MT1-MMP expression increases the phosphorylation of Src at Y^{416}

(A) MCF-7 cells were transfected with either pcDNA3.1 vector control or MT1-WT and cell extracts were immunoblotted with an anti-pY416-Src, anti-Src, anti-MT1-MMP (LEM-2/15.8) or an anti-*ß*-Actin antibody. ***(B)*** Src expressing MCF-7 cells were transfected with either pcDNA3.1 or MT1-WT, as indicated. DMSO, PP2, SH-5, LY294002 or SU4312 were added for 24 hours. Lysates were immunoblotted with an anti-pY416-Src, anti-Src, anti-MT1-MMP (LEM-2/15.8) or an anti-*ß*-Actin antibody. ***(C)*** MCF-7 cells were transfected with either pcDNA3.1 or MT1-WT, as indicated, Total Src was immunoprecipitated with an anti-Src antibody (clone 327) and immunoprecipitates were immunoblotted with an anti-pY416-Src antibody (clone 100F9). Asterisk indicates the size of the IgG heavy chain.

The same increase in Src phosphorylation was also observed in only MT1-WT transfected cells compared to pcDNA3.1 control after immunoprecipitating endogenous Src and subsequently detecting pY416-Src by immunoblot (Figure 3.9C).

These findings indicate, that Src transfection is not necessary to observe the MT1-MMP increase in Src phosphorylation at Y^{416}, and that transfection is used in this system to increase the detection level of pY416-Src. In order to visualise the observed effect of MT1-MMP transfection on Src phosphorylation (Figure 3.9B, C), MCF-7 cells were co-transfected with Src and MT1-WT and the spatial distribution of pY416-Src, total Src and MT1-MMP was assessed by immunofluorescence (Figure 3.10).

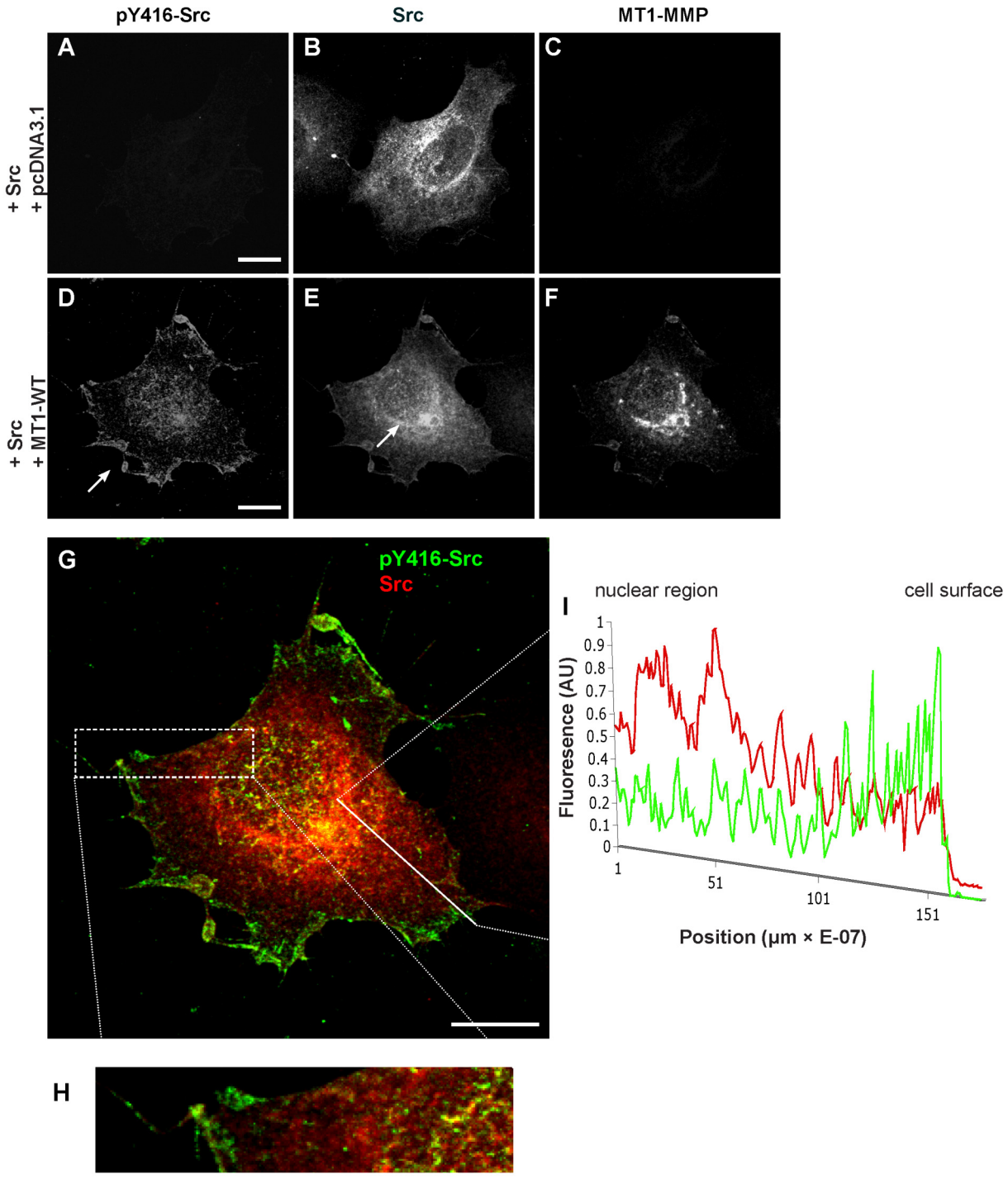

Figure 3.10: MT1-MMP increases Src phosphorylation on Y^{416} and co-localises with pY416-Src

Src expressing MCF-7 cells were either transfected with pcDNA3.1 (A – C) or MT1-WT (D – I). Localisation of active Src was detected using the anti-pY416-Src antibody (AlexaFluor® 488 secondary), total Src using an anti-Src antibody (AlexaFluor® 546 secondary) and MT1-MMP was detected with an antibody raised to the MT1-MMP extracellular domain (N175/6, Cy5 secondary). Arrows indicate pY416-Src at the cell periphery and total Src localising at the perinuclear region of the cell, revealing a Src activation gradient (H). The orthogonal section along the indicated line from the nucleus to the cell surface (G) demonstrates the distribution of both, pY416-Src (green) and total Src (red) (I). The white scale bars present a distance of 10 µm.

In MCF-7 cells expressing only Src, the kinase was detected throughout the cell cytoplasm with a higher intensity of staining observed within the perinuclear region (Figure 3.10B). In these cells, the pY416-Src form was difficult to detect (Figure 3.10A). In contrast, in cells expressing Src and MT1-WT, the pY416-Src form could be clearly detected (Figure 3.10D) and was found to co-localise with MT1-MMP at or close to the plasma membrane (white arrow, Figure 3.10D, F). A clear gradient of pY416-Src staining across the cytoplasm of MCF-7 cells was observed (Figure 3.10H). By cutting an optical orthogonal section along the *x/y*-axis of the cell from the nuclear region towards the cell surface, the relative fluorescence intensity in relation to localisation can be depicted in a histogram (Figure 3.10I). The phosphorylated form of Src was increasingly enriched towards the cell surface, whereas the level of total Src was higher in the perinuclear region of the cell (Figure 3.10I). Since Src and pY416-Src were detected with two antibodies conjugated to different fluorochromes, and being poly- and monoclonal, respectively, the absolute fluorescence intensities could not be compared directly. The co-localisation of pY416-Src and Src was determined with $C_{L(pY416\text{-}Src)} = 0.792$ and $C_{L(Src)} = 0.269$, indicating that ~80% of the pY416-Src antibody co-localised with Src and therefore detected a subset (27%) of total Src protein.

3.1.5 MT1-MMP is found in a complex with Src

Src activity has been implicated in various aspects of MT1-MMP functions. Recently, Labrecque *et al.* reported that Src-dependent phosphorylation of caveolin-1 in bovine aortic endothelial cells (BAEC) induced its association with MT1-MMP [119]. The MT1-MMP – phosphorylated caveolin-1 complex was found to recruit Src and subsequently inhibit its kinase function as a negative feedback loop. It has been further shown that the MT1-MMP intracellular tyrosine residue (Y^{573}) is phosphorylated in a Src-dependent way [249].

In the MCF-7 system, inhibition of Src activity was found to reduce VEGF-A mRNA levels in MT1-MMP transfected cells (Figure 3.5A, Table 3.1). Furthermore, expression of MT1-WT in MCF-7 cells induced phosphorylation of Src at its Y^{416} residue (Figure 3.9B,C and Figure 3.10), and confocal immunofluorescent microscopy revealed the co-localisation of MT1-MMP with Src and especially with pY416-Src (Figure 3.10). In order to test whether MT1-MMP can directly associate with Src, a mammalian-two hybrid assay was

performed. cDNAs of the MT1-MMP intracellular domain (ICD) and full-length Src were sub-cloned into pAct and pBind vectors, containing a GAL4 DNA binding or a VP16 transactivation domain, respectively (Figure 3.11A). Analysis of binding between the two proteins of interest is achieved by co-transfecting cells with the Luciferase reporter gene construct (pG5luc) and both expression vectors followed by detection of luminescence (Figure 3.11B). As shown in Figure 3.11C, expression of the MT1-MMP ICD in the pAct and Src in the pBind vector increased luminescence significantly compared to cells transfected with the empty control vectors ($P < 0.0001$) in both HeLa and MCF-7 cells.

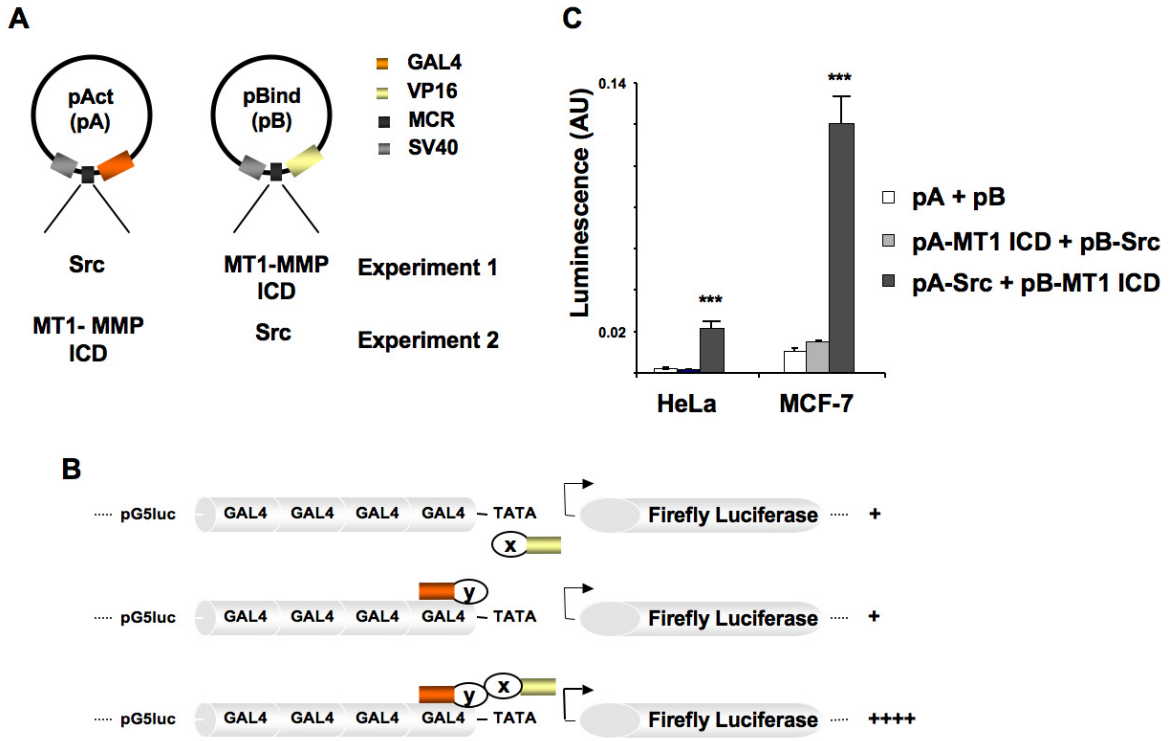

Figure 3.11: The intracellular domain of MT1-MMP interacts with Src

(A) Representation of the GAL4 domain containing pAct and the VP16 domain containing pBind vectors. cDNAs of the MT1-MMP ICD and Src were sub-cloned into each vector. *MCR*, multiple cloning region. ***(B)*** Schematic presentation of the mammalian-two hybrid assay. Cells were co-transfected with 1 µg Luciferase reporter gene construct pG5luc, 1 µg pAct and 1 µg pBind vector, containing the genes of interest (x and y), and the expression of the Luciferase reporter gene was detected by luminescence. ***(C)*** HeLa and MCF-7 cells were co-transfected with pG5luc, pAct and pBind constructs, containing Src and MT1-MMP ICD mutants, as indicated. Data represent the mean luminescence in arbitrary units (AU) ± S.E.M. of 6 independent replicates. *pA*, pAct; *pB*, pBind.

As recommended by the manufacturer, protein-protein interactions were tested in both directions (i.e. exchange the inserts between pAct and pBind), due to the possible inhibitory effect of the fused domains (Promega). These data suggest that the MT1-MMP ICD is directly binding to Src.

To identify the motifs within the MT1-MMP ICD that are involved in the interaction between MT1-MMP and Src, MT1-MMP ICD triple amino acid mutants were generated (Figure 3.12). The MT1-MMP C^{574} residue [73] as well as the LLY^{573} and DKV^{582} motifs have been shown to play a role in MT1-MMP mediated VEGF-A expression (Figure 3.25B) and were therefore tested in the mammalian-two hybrid system. As shown in Figure 3.12, transfection of pAct (pA)-Src expressing MCF-7 cells with pBind (pB)-MT1-ICD or the pB-MT1-DKV^{582} mutant induced a significant increase in reporter gene expression as compared to the empty vector control ($P < 0.001$ and $P < 0.0001$, respectively). In contrast, mutation of the LLY^{573} or CQR^{576} motifs did not affect Luciferase expression compared to the empty vector control, suggesting that the $LLYCQR^{576}$ sequence is involved in the interaction with Src (Figure 3.12).

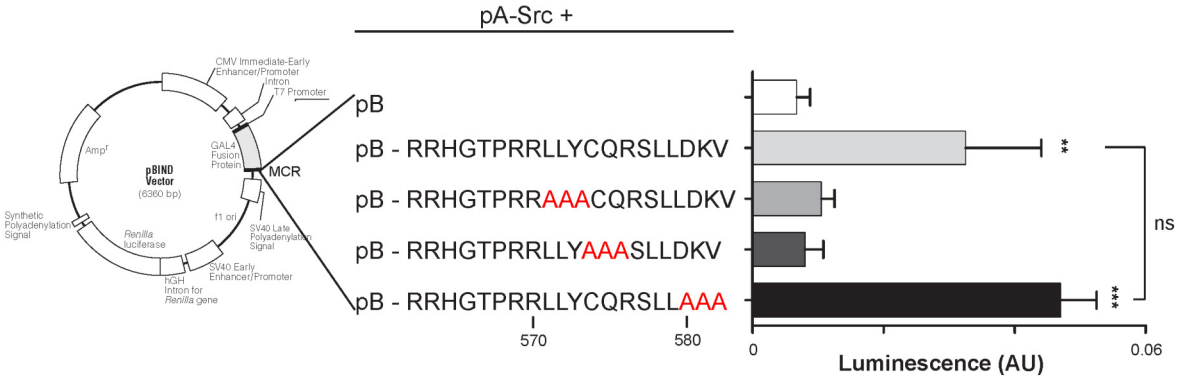

Figure 3.12: The interaction between the MT1-MMP ICD and Src in a mammalian two-hybrid system depends on the LLY^{573} and CQR^{576} sequence

MCF-7 cells were transfected with either empty pAct and pBind vectors as control or with pAct-Src and pBind-MT1-ICD cDNA constructs, and were co-transfected with the reporter gene vector pG5luc. Interaction between MT1-MMP ICD and Src was detected by luminescence of Luciferase expression. Data represent the mean luminescence of 6 independent replicates ± S.E.M with $P < 0.001$ (**) and $P < 0.0001$ (***) compared to empty vector control. *AU*, arbitrary units.

To confirm that the interaction between MT1-MMP and Src observed in the mammalian-two hybrid assay occurs in a cellular system using full-length MT1-MMP, a co-immunoprecipitation assay was performed. Src expressing MCF-7 cells were transfected with or without MT1-WT and Src was immunoprecipitated with an anti-Src antibody (Clone 327). MT1-MMP was immunoprecipitated with an anti-MT1-MMP antibody raised against the ICD as control (Figure 3.13A). Immunoprecipitates were immunoblotted with an anti-MT1-MMP antibody. As shown in Figure 3.13A MT1-MMP was found to co-immunoprecipitate with Src.

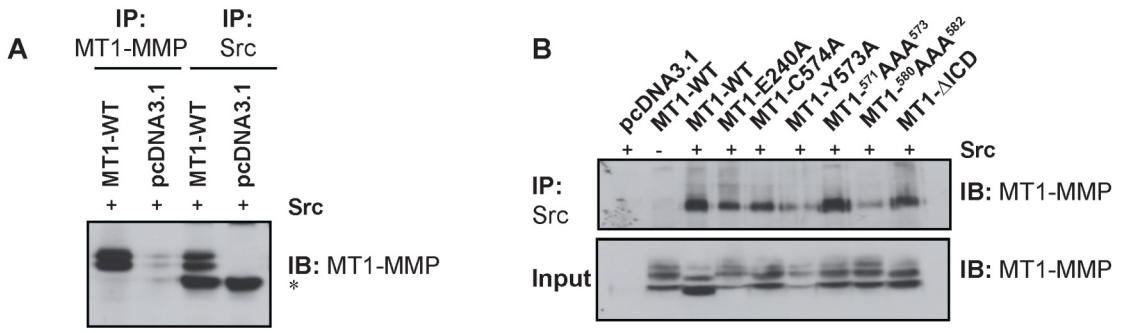

Figure 3.13: MT1-MMP co-immunoprecipitates with Src independent of its intracellular domain

(A) Src expressing MCF-7 cells were transfected with either pcDNA3.1 or MT1-WT and immunoprecipitated with an anti-Src antibody or an anti-MT1-MMP ICD specific antibody (ab28209) as a control. Immunoprecipitates were detected with an anti-MT1-MMP antibody (N175/6). The asterisk indicates the IgG heavy chain. ***(B)*** Src expressing MCF-7 cells were transfected with pcDNA3.1, MT1-WT or different MT1-MMP extra- and intracellular domain mutants and immunoprecipitated with an anti-Src antibody. Immunoblots show MT1-MMP levels (LEM-2/15.8) of the immunoprecipitates and Input control.

To investigate the role of the MT1-MMP intracellular domain in forming a complex with Src, various MT1-MMP intracellular domain mutants were generated (summarised in Figure 3.25A). Src expressing MCF-7 cells were co-transfected with the MT1-MMP catalytic inactive MT1-E240A as well as various MT1-MMP ICD mutants (MT1-C574, MT1-Y573A, MT1-^{571}AAA^{573}, MT1-^{580}AAA^{582}) and cell extracts were co-immunoprecipitated with an anti-Src antibody as previously described. As presented in Figure 3.13B, none of the constructs tested inhibited the formation of the MT1-MMP – Src complex, suggesting that the interaction in this system does not depend on the MT1-MMP ICD and may involve a third party protein. MT1-MMP did not bind unspecifically to the magnetic beads as shown for cells which did not express Src (Figure 3.13B). The total amount of MT1-MMP present in the various complexes was not quantifiable due to the variation of transfection efficiencies observed for the various constructs, as shown in the Input control (Figure 3.13B).

3.1.6 MT1-MMP Y^{573} is required for Src phosphorylation

MT1-MMP expression in MCF-7 cells has been shown previously to induce phosphorylation of Src at its Y^{416} residue (Figure 3.9B, C and Figure 3.10). To determine the MT1-MMP motif involved in the phosphorylation of Src, MCF-7 cells were transfected with the MT1-MMP catalytic inactive MT1-E240A as well as various MT1-MMP ICD

mutants (MT1-C574, MT1-Y573A, MT1-^{571}AAA^{573}, MT1-^{580}AAA^{582}) and the spatial distribution of pY416-Src and MT1-MMP was assessed by immunofluorescent staining (Figure 3.14). As expected, expression of MT1-WT induced an increase in pY416-Src staining throughout the cell and at distinct regions at or close to the plasma membrane. A similar result was observed in cells expressing MT1-MMP with mutations of the E^{240} (MT1-E240A) or C^{574} (MT1-C574A) residue or the DKV^{582} (MT1-^{580}AAA^{582}) motif (Figure 3.14; arrowheads). Interestingly, phosphorylation of Src at Y^{416} was ablated in cells expressing the MT1-ΔICD, MT1-Y573A or MT1-^{571}AAA^{573} mutants (arrows).

The co-localisation between MT1-MMP and pY416-Src was quantified using the Volocity 3D imaging and analysis software. Single optical sections of various MT1-MMP transfectants were obtained by confocal microscopy and analysed for n = 15 cells per transfectant. Each pixel was analysed per confocal laser scanning micrograph for the fluorescence of pY416-Src and MT1-MMP, plotted in a two-dimensional cytofluorogram as described previously and each channel was corrected for background fluorescence (as described in chapter 2.2.4.3.2). The cytofluorograms in Figure 3.14 represent scatter plots of co-localisation prior to background correction. The co-localisation co-efficients were calculated and plotted in Figure 3.15. MT1-MMP was found to co-localise with pY416-Src in MT1-WT and MT1-E240A, MT1-C574A and MT1-^{580}AAA^{582} mutants, whereas mutation of the Y^{573} (MT1-Y573A) residue, the LLY^{573} (MT1-^{571}AAA^{573}) motif or deletion of the intracellular domain (MT1-ΔICD) ablated co-localisation due to the reduced phosphorylation level of Src in cells expressing these constructs (Figure 3.14; Figure 3.15, $P < 0.0001$ compared to MT1-WT transfected cells).

Taken together, these data suggest a role of the intracellular MT1-MMP Y^{573} residue in Src activation.

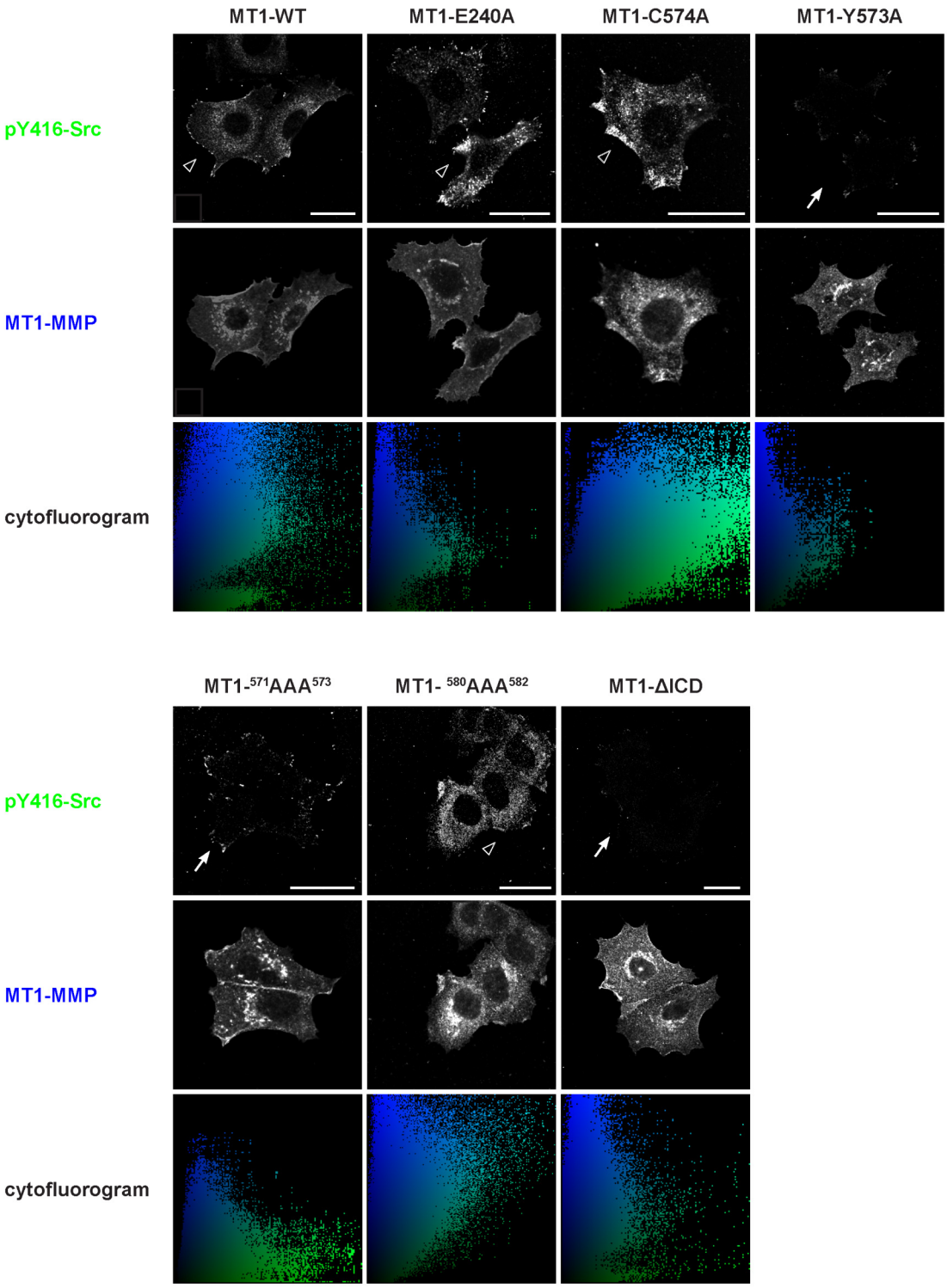

Figure 3.14: MT1-MMP Y^{573} modulates Src phosphorylation in MCF-7 cells

MCF-7 cells were transfected with various MT1-MMP intracellular domain mutants as well as the catalytic inactive MT1-E240A construct. The localisation of active Src (pY416-Src) was detected using the anti-pY416-Src antibody (AlexaFluor® 488 secondary, green) and MT1-MMP was detected with an antibody raised to the MT1-MMP extracellular domain (N175/6, Cy5 secondary, blue). Empty arrowheads indicate pY416-Src at the cell periphery, whereas arrows show the decreased phosphorylation of Src in MT1-MMP Y^{573} mutants. Cytofluorograms of co-localisation were generated with the Volocity 3D imaging and analysis software. Similar expression and co-localisation is shown by accumulation of pixels along the y = x axis. The white scale bars present a distance of 25 μm.

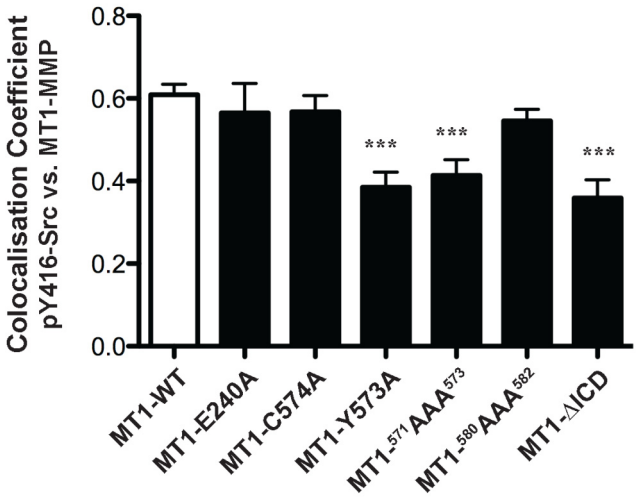

Figure 3.15: Quantification of pY416-Src – MT1-MMP co-localisation

MCF-7 cells were co-transfected with Src and various MT1-MMP mutants. The co-localisation co-efficients of different MT1-MMP transfectants with active Src (pY416-Src) was determined by using the Volocity 3D imaging and analysis software of single optical confocal sections. Data represent the co-localisation co-efficients of 15 cells ± S.E.M. with $P < 0.0001$ (***).

3.1.7 MT1-MMP and Src co-localise in RhoB positive endosomes

Sandilands *et al.* have reported that Src is phosphorylated during transit from the perinuclear region towards the plasma membrane [253]. This activation was shown to take place in RhoB positive cytoplasmic endosomes associated with the perinuclear recycling compartment. The previously described requirement for MT1-MMP, especially its intracellular Y^{573} residue, in Src phosphorylation led to the hypothesis that MT1-MMP dependent Src phosphorylation might occur in RhoB positive endosomes.

To test whether MT1-MMP co-localises with Src in RhoB positive endosomes, Src expressing MCF-7 cells were transfected with MT1-WT and the localisation of MT1-MMP, RhoB and Src was assessed by confocal microscopy. As shown in Figure 3.16E, MT1-MMP was found to co-localise with RhoB in MCF-7 cells and was also detected within the same structure as RhoB and pY416-Src (Figure 3.16F, black arrows). The white arrow confirms the co-localisation between MT1-MMP and pY416-Src, as observed before (Figure 3.16F and Figure 3.14). MT1-MMP has been shown to be redistributed to invasive structures during cell migration in Rab8 positive exocytic endosomes [36]. However, there is no evidence so far that MT1-MMP is present in RhoB containing intracellular vesicles.

These data suggest that MT1-MMP and Src may co-traffic to the plasma membrane in RhoB positive endosomes and that MT1-MMP might play a role in Src phosphorylation during this transit.

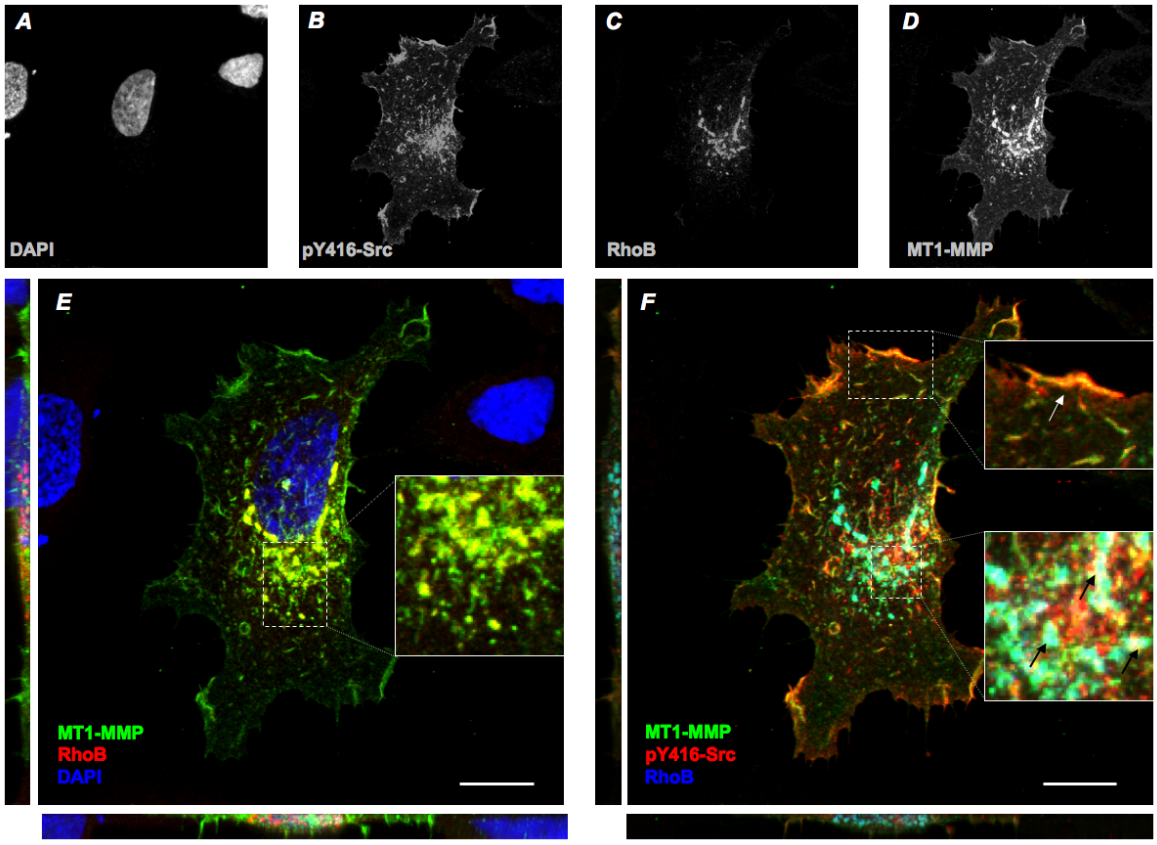

Figure 3.16: MT1-MMP co-localises with the active phosphorylated form of Src (pY416-Src) in RhoB positive endosomes

Src expressing MCF-7 cells were transfected with MT1-WT. The localisation of pY416-Src (AlexaFluor® 488 secondary), RhoB (AlexaFluor® 546 secondary) and MT1-MMP (N175/6, Cy5 secondary) was detected by confocal microscopy. Inset panels show magnified portions of each merged image, as indicated (dashed squares). The white scale bars present a distance of 10 μm.

3.1.8 MT1-MMP is found in a complex with active Src and VEGFR-2

The indirect interaction observed between MT1-MMP and Src in the immunoprecipitation assay (Figure 3.13B) led to the hypothesis that another protein was involved in the formation of a higher order complex. Since VEGFR-2 activity was shown to be required in MT1-MMP induced VEGF-A expression (Figure 3.5A) and it is a key receptor in the VEGF-A signalling pathway, it was tested whether VEGFR-2 can be found in a complex with both MT1-MMP and Src.

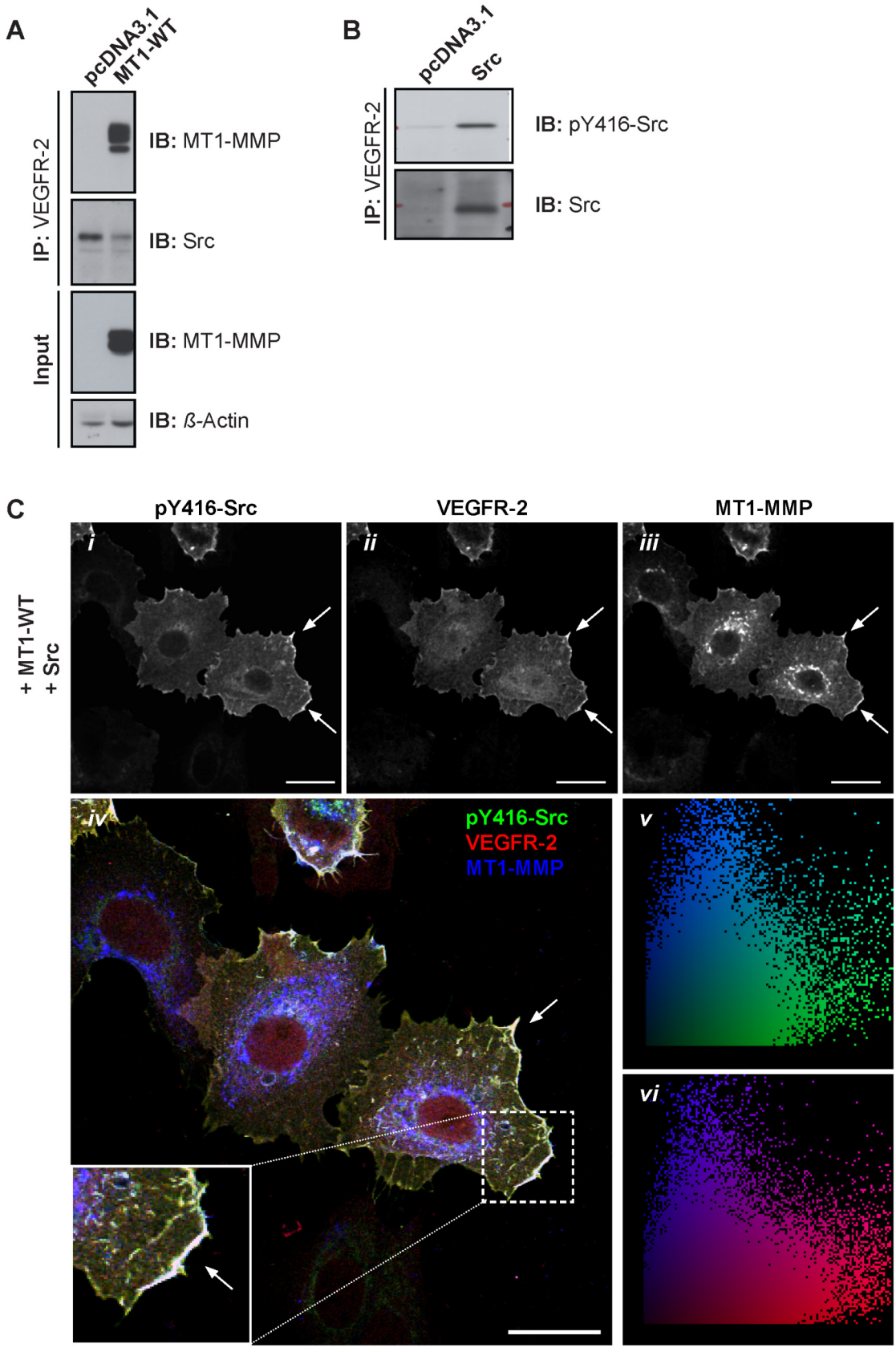
A
pcDNA3.1
MT1-WT
IP: VEGFR-2
IB: MT1-MMP
IB: Src
Input
IB: MT1-MMP
IB: ß-Actin
B
pcDNA3.1
Src
IP: VEGFR-2
IB: pY416-Src
IB: Src
C
pY416-Src
VEGFR-2
MT1-MMP
+ MT1-WT
+ Src
i
ii
iii
iv
v
vi
pY416-Src
VEGFR-2
MT1-MMP

Figure 3.17: MT1-MMP, VEGFR-2 and the phosphorylated form of Src (Y^{416}) are found in a complex

(A) MCF-7 cells were transfected with pcDNA3.1 or MT1-WT and immunoprecipitated with an anti-VEGFR-2 antibody. Immunoprecipitates as well as Input control samples were immunoblotted with an anti-MT1-MMP (LEM-2/15.8), anti-Src or an anti-*β*-Actin antibody. ***(B)*** MCF-7 cells were transfected with pcDNA3.1 or Src and cell lysates were immunoprecipitated with an anti-VEGFR-2 antibody. Immunoprecipitates and Input control samples were immunoblotted with an anti-Src or an anti-pY416-Src antibody. ***(C)*** MCF-7 cells were co-transfected with MT1-WT and Src. The localisation of pY416-Src (AlexaFluor® 488 secondary, *i*), VEGFR-2 (AlexaFluor® 546 secondary, *ii*) and MT1-MMP (Cy5 secondary, *iii*) was detected. Arrows in the merged picture (*iv*) indicate co-localisation of pY416-Src, VEGFR-2 and MT1-MMP at or close to the plasma membrane. Inset panel shows magnified portion of the merged image, as indicated (dashed square). Cytofluorograms show co-localisation of pY416-Src (green) and MT1-MMP (blue) (*v*) or VEGFR-2 (red) and MT1-MMP (blue) (*vi*). Similar expression and co-localisation is shown by accumulation of pixels along the y = x axis. The white scale bars present a distance of 25 μm.

To test this hypothesis, lysates prepared from cells transfected with pcDNA3.1 or MT1-WT (Figure 3.17A) as well as pcDNA3.1 or Src (Figure 3.17B) were immunoprecipitated with an anti-VEGFR-2 antibody. As shown in Figure 3.17A and B, MT1-MMP, Src and in particular the pY416-Src phosphorylation form of Src were found to co-immunoprecipitate with VEGFR-2.

In order to visualise the co-localisation between these proteins, MCF-7 cells expressing MT1-MMP and Src were stained for pY416-Src, VEGFR-2 and MT1-MMP. All proteins co-localised in MCF-7 cells, primarily at or close to the plasma membrane (Figure 3.17C, arrows), as visualised by the cytofluorograms between MT1-MMP and pY416-Src (Figure 3.17C *v*) and between MT1-MMP and VEGFR-2 (Figure 3.17C *vi*). The co-localisation between MT1-MMP – VEGFR-2 – pY416-Src was also routinely observed in membrane protrusions, as seen within three-dimensional reconstructions of *z*-stacks taken every 0.2 μm as confocal images (Figure 3.18A, B). This co-localisation could be visualised by cutting optical sections either along the *z*-axis (Figure 3.18C, D) or by cutting an orthogonal *z*/*x*- section along the *y*-axis through these protrusive structures (Figure 3.18E, F).

Membrane protrusions such as podosomes and invadopodia are found in various tumour cell lines in *in vitro* systems and were shown to play a key role in cell migration, matrix degradation and cell signalling (reviewed in [254]). Both membrane structures were found to exhibit a distinct expression of protein components. However, the data obtained on the MT1-MMP – VEGFR-2 – pY416-Src complex in this study are not sufficient to unambiguously identify these protrusive structures as podosomes or lamellipodia.

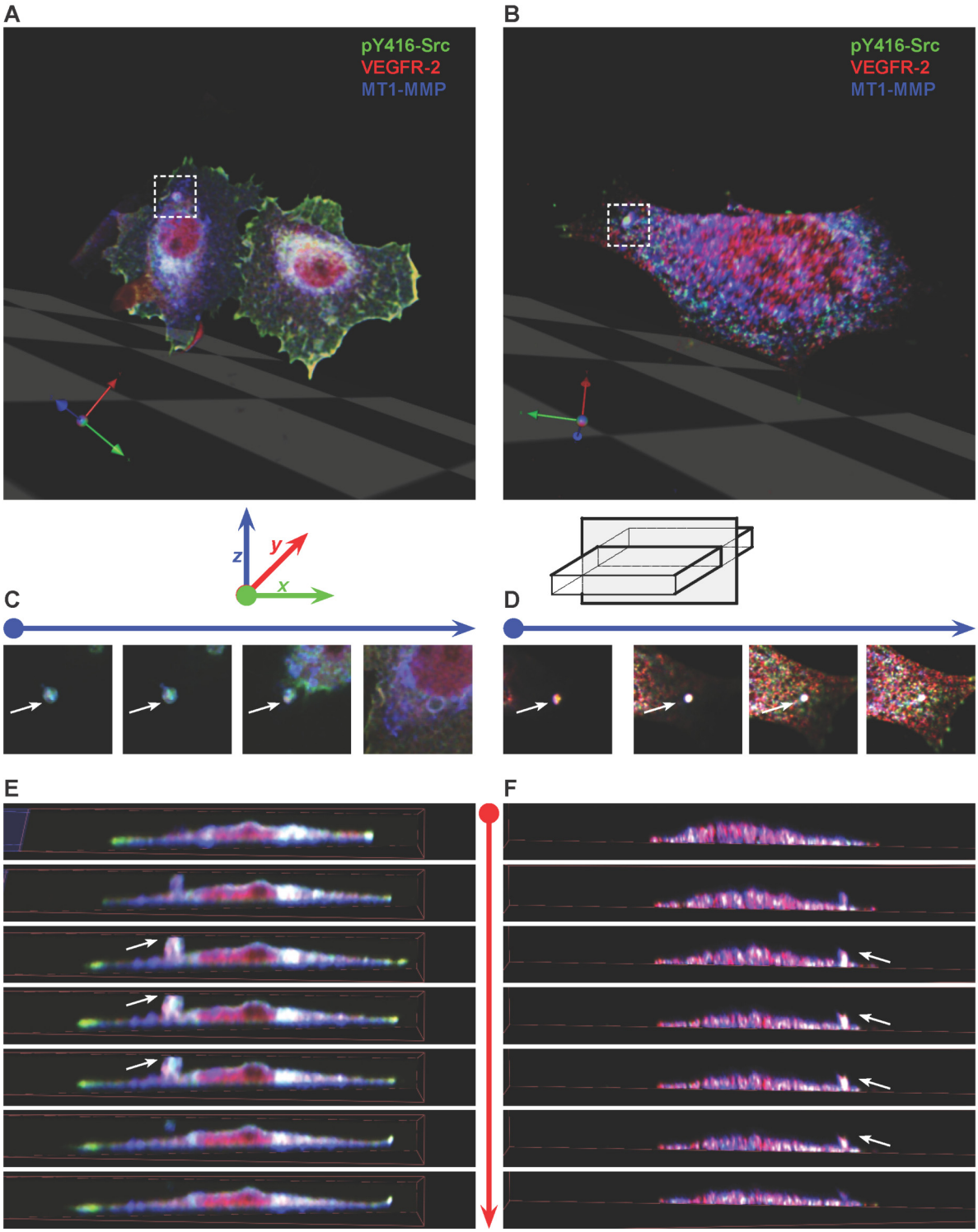

Figure 3.18: The MT1-MMP – VEGFR-2 – pY416-Src complex is expressed in dorsal membrane protrusions

MCF-7 cells were transfected with MT1-WT and Src. The localisation of active Src was detected with an anti-pY416-Src (AlexaFluor® 488 secondary), VEGFR-2 was detected with an anti-VEGFR-2 antibody (AlexaFluor® 546 secondary) and MT1-MMP was detected with an antibody raised to the MT1-MMP extracellular domain (N175/6, Cy5 secondary). ***(A,B)*** Three-dimensional reconstruction of confocal optical images taken every 0.2 µm along the *z*-axis. ***(C,D)*** Series of confocal images taken along the z-axis. ***(E,F)*** Series of confocal images taken from the orthogonal sections along the *x/y*-axis

In order to identify which regions of MT1-MMP were involved in the complex formation with VEGFR-2, MCF-7 cells expressing various MT1-MMP extracellular, intracellular and transmembrane domain mutants were tested by immunoprecipitation (constructs summarised in Figure 3.25A). The MT1-E240A mutant as well as all the ICD mutants tested co-immunoprecipitated with VEGFR-2 (Figure 3.19A). In contrast, replacement of the MT1-MMP transmembrane domain with that of APP (MT1-TMD-APP), which is a type-1 transmembrane protein with a transmembrane domain of 24 amino acids that is functionally unrelated to MT1-MMP, ablated the complex formation between MT1-MMP and VEGFR-2 (Figure 3.19B).

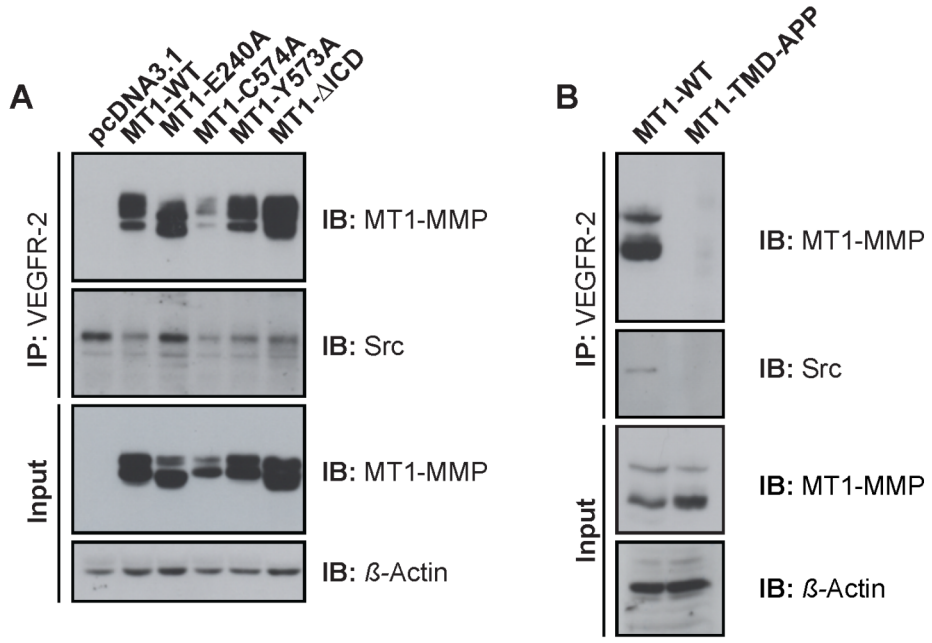

Figure 3.19: The MT1-MMP – VEGFR-2 complex formation depends on the MT1-MMP transmembrane domain, but is independent of its catalytic and intracellular domains

(A) MCF-7 cells were transfected with pcDNA3.1, MT1-WT or MT1-MMP extra- and intracellular domain mutants and cell extracts were immunoprecipitated with an anti-VEGFR-2 antibody. Immunoprecipitates and Input controls were immunoblotted with an anti-MT1-MMP (LEM-2/15.8), anti-Src or an anti-*β*-Actin antibody. ***(B)*** Cells were transfected with either MT1-WT or MT1-TMD-APP. Lysates were immunoprecipitated with an anti-VEGFR-2 antibody and immunoprecipitates and Input samples were immunoblotted with an anti-MT1-MMP antibody (LEM-2/15.8), an anti-Src antibody or an anti-*β*-Actin antibody.

A similar result was observed when most of the MT1-MMP ECD (MT1-ΔECD-FLAG and MT1-ΔECD-EGFP) was deleted or when the MT1-MMP hemopexin domain was replaced by GFP (MT1-ΔHPX) (Figure 3.20A, B). These findings suggest that the MT1-MMP hemopexin and transmembrane domains are required for the MT1-MMP – VEGFR-2 complex formation.

In order to confirm the role of the MT1-MMP extracellular domain (ECD) and in particular the role of the hemopexin domain, in the formation of the MT1-MMP – VEGFR-2 complex, an ELISA assay was performed. Immobilised rh-VEGFR-2-Fc or milk control proteins were incubated with purified recombinant MT1-MMP extracellular domain (rh-MT1-Ecto), recombinant catalytic inactive extracellular domain (rh-MT1-Ecto-E240A) or recombinant catalytic domain (rh-MT1-Cat). rh-$VEGF_{165}$ was used as a positive control for binding to rh-VEGFR-2-Fc (Figure 3.20C). Binding of proteins to rh-VEGFR-2-Fc or control protein was detected using the anti-MT1-MMP catalytic domain (LEM-2/15.8) or the anti-VEGF antibody. The rh-MT1-Ecto and rh-MT1-Ecto-E240A were found to bind to rh-VEGFR-2 significantly over control ($P < 0.0001$; Figure 3.20C), confirming the cell based co-immunoprecipitation data (Figure 3.20A,B and Figure 3.19A). In contrast, no interaction between rh-VEGFR-2 and rh-MT1-Cat was detected in this assay, despite the binding of rh-MT1-Cat to TIMP-2 (data not shown), thus suggesting that the MT1-MMP hemopexin domain/stalk region is required for MT1-MMP binding to VEGFR-2. The difference in binding observed between rh-MT1-Ecto and rh-MT1-Ecto-E240A to rh-VEGFR-2 probably resulted from the partial autocatalytic degradation of rh-MT1-Ecto which occurs during the preparation of the recombinant protein (Figure 3.20D, Input control). Thus, degradation products, which lack the catalytic domain and were not detected by the anti-MT1-MMP catalytic domain antibody, could compete with the full-length MT1-MMP ECD for VEGFR-2 binding.

The role of the MT1-MMP extracellular domain in VEGFR-2 binding could be confirmed by co-immunoprecipitating recombinant VEGFR-2-Fc – MT1-MMP complexes. rh-VEGFR-2-Fc and rh-MT1-MMP domains were mixed at a 1:1 molar ratio and a complex was formed after 30 minutes incubation at 37˚C, as described in chapter 2.2.4.6. These complexes were immunoprecipitated with an anti-VEGFR-2 antibody, subjected in addition to Input control samples to SDS-PAGE and total protein was visualised by coomassie staining. As shown in Figure 3.20D, rh-MT1-Ecto, rh-MT1-Cat and rh-VEGFR-2-Fc could be detected in the Input control, although at varying levels. As expected, VEGFR-2 was found within the immunoprecipitates, indicating the successful immunoprecipitation. Furthermore, the rh-MT1-MMP extracellular domain was found to co-immunoprecipitate with rh-VEGFR-2 whereas the MT1-MMP catalytic domain was not found in a complex with VEGFR-2. The MT1-MMP – VEGFR-2 complex formation was not affected by incubation of rh-MT1-Ecto with the function-blocking anti-MT1-MMP catalytic domain antibody LEM-2/15.8 (Figure 3.20D).

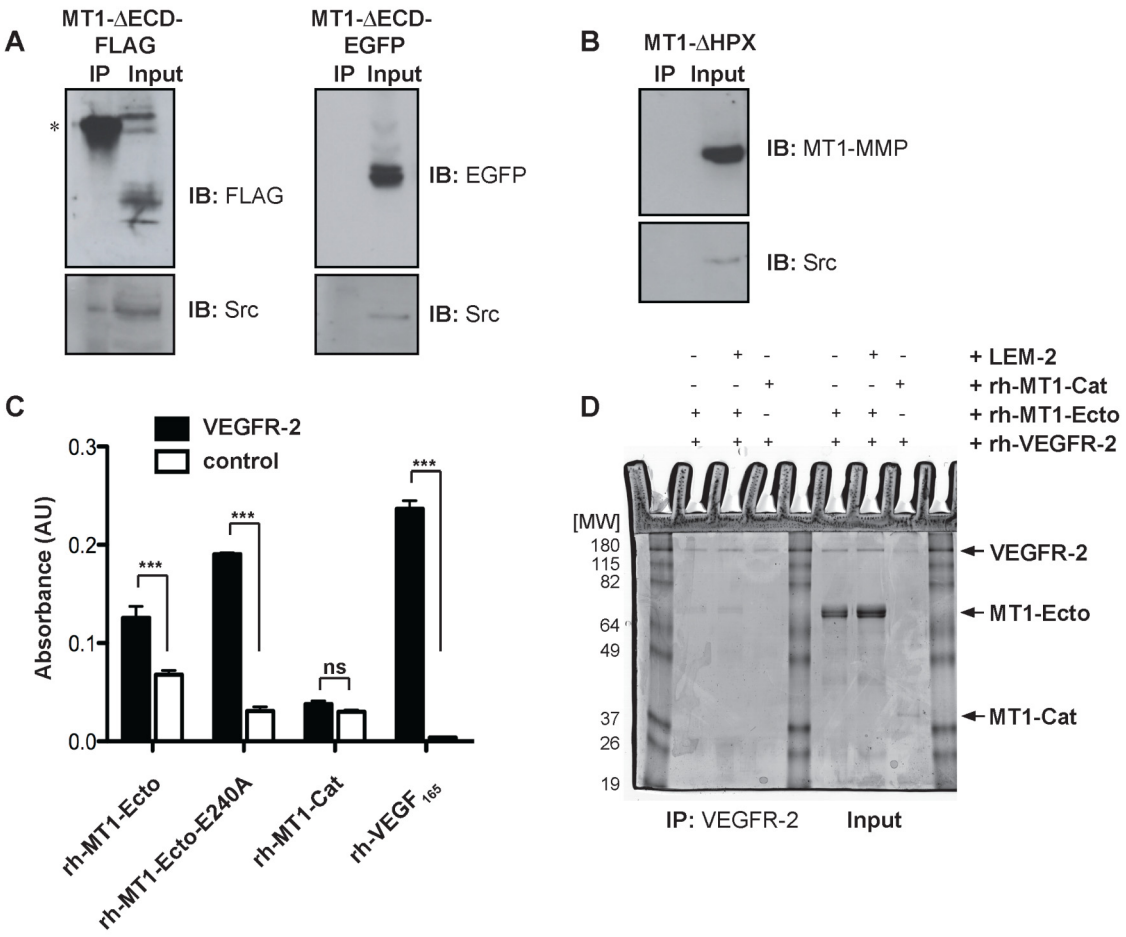

Figure 3.20: MT1-MMP interaction with VEGFR-2 depends on the MT1-MMP extracellular domain, potentially on the hemopexin domain

(A,B) MCF-7 cells were transfected with either MT1-ΔECD-FLAG or MT1-ΔECD-EGFP (A) or MT1-ΔHPX (B). Lysates were immunoprecipitated with an anti-VEGFR-2 antibody and immunoprecipitates and Input samples were immunoblotted with an anti-FLAG, anti-EGFP, anti-Src or an anti-MT1-MMP (LEM-2/15.8) antibody. ***(C)*** A microtiter plate was either coated with 10 µg/ml rh-VEGFR-2-Fc (black bars) or milk control protein (white bars). rh-MT1-Ecto, rh-MT1-Ecto-E240A, rh-MT1-Cat or rh-$VEGF_{165}$ as positive control were added in an ELISA assay. Binding of rh-MT1-MMP domains and rh-$VEGF_{165}$ to rh-VEGFR-2-Fc and control protein is directly proportional to measured absorbance. Data represent mean absorbance ± S.E.M. with $P < 0.0001$ (***). *AU*, arbitrary units; *ns*, non-significant . ***(D)*** Complexes of rh-VEGFR-2-Fc and rh-MT1-Ecto or rh-MT1-Cat with or without pre-incubation with 10 µ/ml LEM-2 antibody were formed in solution for 30 minutes at 37ºC. Complexes were immunoprecipitated with an anti-VEGFR-2 antibody. Total protein of immunoprecipitates and Input control were visualised by Coomassie blue staining.

Src has been reported to associate with VEGFR-2 in human vascular endothelial cells [255]. As expected, Src as well as its pY416-Src phosphorylation form was shown to co-immunoprecipitate with VEGFR-2 in MCF-7 cells (Figure 3.17B). The Src – VEGFR-2 complex formation was impaired in protein extracts from cells transfected with MT1-MMP ECD or transmembrane domain deletion mutants (Figure 3.19 and Figure 3.20).

Accordingly, co-localisation between VEGFR-2 and pY416-Src was also found to be decreased in MT1-MMP Y^{573} mutants (MT1-Y573A, MT1-^{571}AAA^{573} and MT1-ΔICD), which showed little Src phosphorylation, as detected by immunofluorescence of various MT1-MMP mutants expressing MCF-7 cells (Figure 3.21).

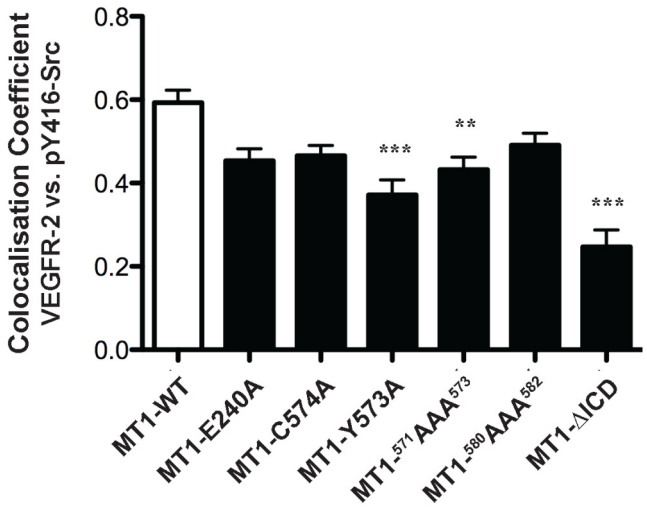

Figure 3.21: Quantification of VEGFR-2 – pY416-Src co-localisation

MCF-7 cells were transfected with Src and various MT1-MMP mutants. The co-localisation co-efficients of VEGFR-2 with active Src (pY416-Src) were determined by using the Volocity 3D imaging and analysis software of single optical confocal sections. Data represent the co-localisation co-efficients of 15 cells ± S.E.M. with $P < 0.001$ (**) and $P < 0.0001$ (***).

3.1.9 MT1-MMP expression induces VEGFR-2 cell surface localisation

The interaction between MT1-MMP and VEGFR-2 led to the hypothesis that MT1-MMP expression in MCF-7 cells could affect the subcellular distribution of VEGFR-2. To test this hypothesis, Src expressing MCF-7 cells were transfected with either MT1-WT, various MT1-MMP extra- and intracellular domain mutants or a vector control and the localisation of VEGFR-2, pY416-Src and MT1-MMP was assessed by immunofluorescence. In Src expressing cells, VEGFR-2 was mainly localised in intracellular vesicles throughout the cell cytoplasm (Figure 3.24A, *ii,* arrow head). In contrast, expression of MT1-WT and Src increased staining of the phosphorylated form of Src at Y^{416}, as previously observed (Figure 3.9, Figure 3.10, Figure 3.22, Figure 3.24A, *iv*). In addition, a clear cellular redistribution of VEGFR-2 was observed in these cells (Figure 3.24A, *v*).

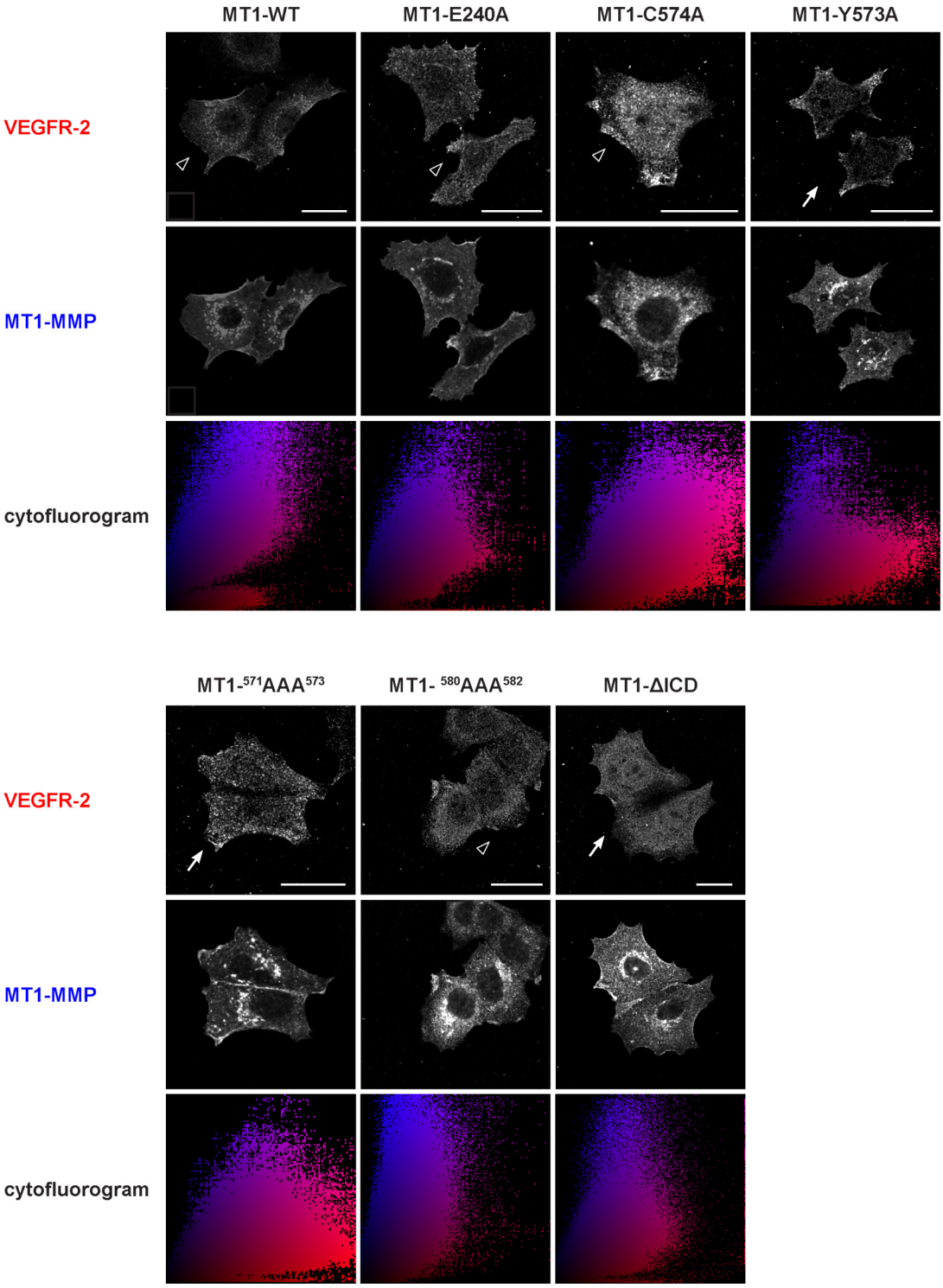

Figure 3.22: Co-localisation between MT1-MMP and VEGFR-2 is not affected by MT1-MMP catalytic or intracellular domain mutations

Src expressing MCF-7 cells were transfected with various MT1-MMP intracellular domain mutants as well as the catalytic inactive MT1-E240A construct. The localisation of VEGFR-2 and MT1-MMP was detected with an anti-VEGFR-2 (AlexaFluor® 546 secondary, red) and an anti-MT1-MMP (N175/6, Cy5 secondary, blue) antibody. Cytofluorograms of co-localisation were generated with the Volocity 3D imaging and analysis software. Similar expression and co-localisation is shown by accumulation of pixels along the y = x axis. The white scale bars present a distance of 25 μm.

VEGFR-2 was found to co-localise with pY416-Src (Figure 3.24A, *iv*, arrows) and MT1-MMP (Figure 3.22, Figure 3.24A, *vi*, arrows). Quantification of the co-localisation revealed similar results for the MT1-E240A and all intracellular domain mutants tested (Figure 3.22, Figure 3.23). Expression of the MT1-ΔICD construct led to a similar VEGFR-2 staining pattern as MT1-WT expressing cells, however the co-localisation co-efficient of VEGFR-2 versus MT1-MMP was slightly decreased (Figure 3.23).

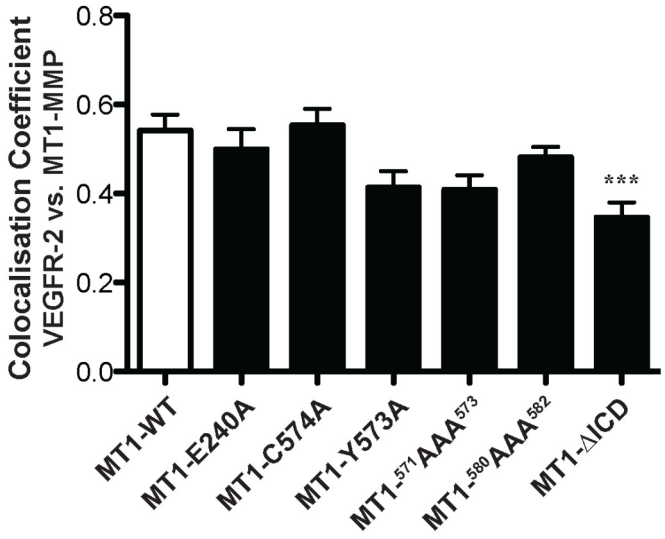

Figure 3.23: Quantification of MT1-MMP co-localisation with VEGFR-2

MCF-7 cells were transfected with Src and various MT1-MMP mutants. The co-localisation co-efficients of different MT1-MMP transfectants with VEGFR-2 were determined by using the Volocity 3D imaging and analysis software of single optical confocal sections. Data represent the co-localisation co-efficients of 15 cells ± S.E.M. with $P < 0.0001$ (***).

Interestingly, expression of the MT1-MMP extracellular domain deletion mutant (MT1-ΔECD-FLAG) did not seem to significantly affect the VEGFR-2 localisation pattern in these cells when compared to vector control transfected cells (Figure 3.24B, *ii*).

The MT1-MMP extracellular domain dependent staining of VEGFR-2 observed at or close to the plasma membrane led us to test whether MT1-MMP regulates localisation of VEGFR-2 at the cell surface. Therefore, MT1-WT, MT1-ΔECD-FLAG, MT1-ΔICD or MT1-TMD-APP constructs were expressed in MCF-7 cells and the cell surface expression of VEGFR-2 was analysed by flow cytometry. As a positive control, VEGFR-2 cell surface expression was analysed in MCF-7 cells transfected with pcDNA3.1 and stimulated for 30 minutes with 100 ng/ml rh-$VEGF_{165}$, as this has been shown to increase VEGFR-2 expression at the cell surface of endothelial cells [256].

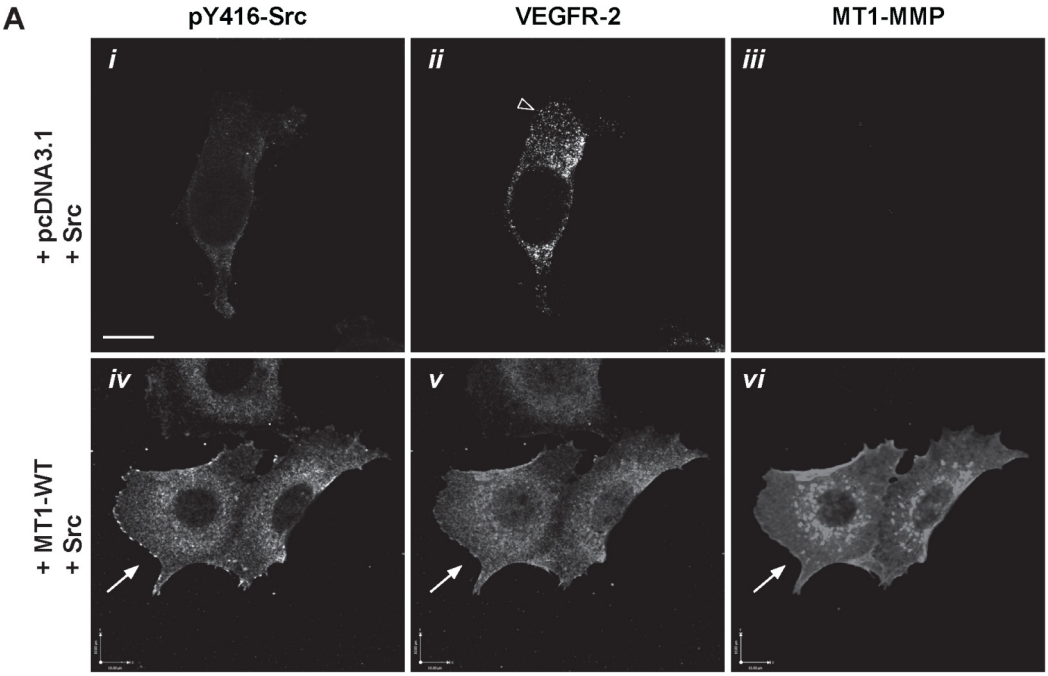
A
pY416-Src
VEGFR-2
MT1-MMP
+ pcDNA3.1
+ Src
+ MT1-WT
+ Src
i
ii
iii
iv
v
vi

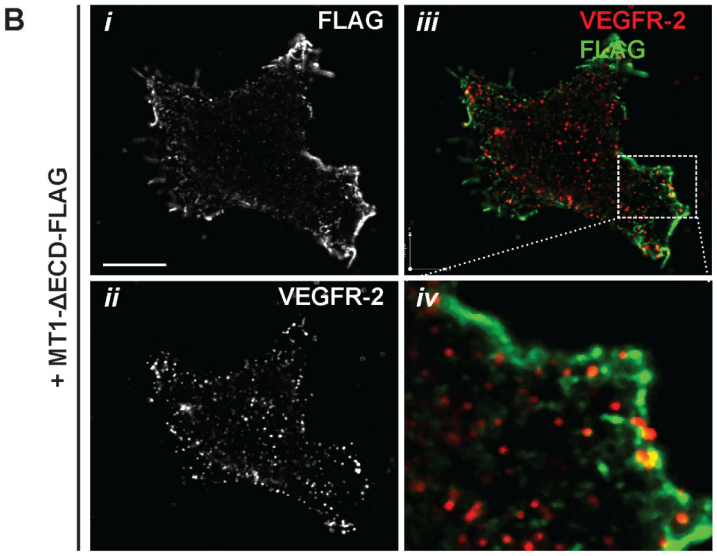
B
+ MT1-ΔECD-FLAG
i
FLAG
iii
VEGFR-2
FLAG
ii
VEGFR-2
iv

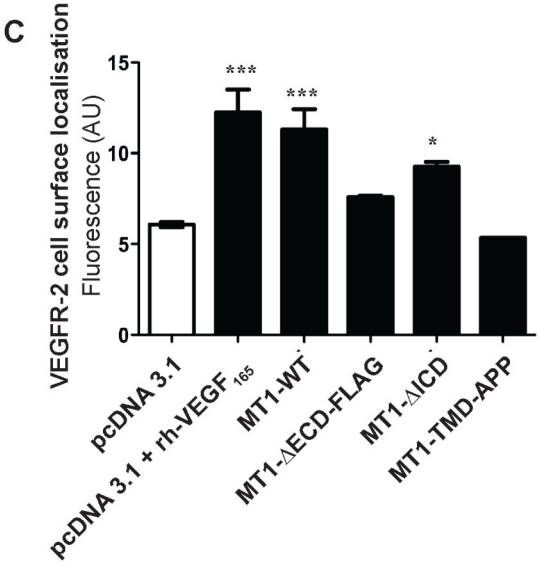
C
VEGFR-2 cell surface localisation
Fluorescence (AU)
15
10
5
0
***
***
*
pcDNA 3.1
pcDNA 3.1 + rh-VEGF 165
MT1-WT
MT1-ΔECD-FLAG
MT1-ΔICD
MT1-TMD-APP

Figure 3.24: **MT1-MMP expression increases the cell surface localisation of VEGFR-2**

(A) Src expressing MCF-7 cells were transiently transfected with either pcDNA3.1 (*i – iii*) or MT1-WT (*iv – vi*) and the localisation of pY416-Src (AlexaFluor® 488 secondary, *i, iv*), VEGFR-2 (AlexaFluor® 546 secondary, *ii, v*) and MT1-MMP (N175/6, Cy5 secondary, *iii, vi*) was detected. Empty arrowhead indicates the vesicular staining pattern of VEGFR-2 in only Src expressing cells, whereas arrows show the common localisation of pY416-Src, MT1-MMP and VEGFR-2 at or close to the cell surface of cells expressing MT1-WT and Src. The white scale bars present a distance of 10 μm. ***(B)*** MCF-7 cells were transfected with MT1-ΔECD-FLAG and the localisation of VEGFR-2 and MT1-MMP was assessed using an anti-FLAG (Cy5 secondary, *i*) and an anti-VEGFR-2 (AlexaFluor® 488, *ii*) antibody. Panel *iv* shows magnified portion of the merged image, as indicated (dashed square). The white scale bars present a distance of 10 μm. ***(C)*** Cells were transfected with pcDNA3.1, MT1-WT, MT1-ΔECD-FLAG, MT1-ΔICD or MT1-TMD-APP and the cell surface localisation of VEGFR-2 was assessed by flow cytometry. As a positive control pcDNA3.1 transfected cells were stimulated for 30 minutes with 100 ng/ml rh-$VEGF_{165}$. Data represent the mean fluorescence of 4 independent biological replicates ± S.E.M. with $P < 0.05$ (*) and $P < 0.0001$ (***) compared to pcDNA3.1 control. 10,000 events were counted per sample. *AU*, arbitrary units.

As observed by others in endothelial cells, treatment with rh-$VEGF_{165}$ significantly increased the localisation of VEGFR-2 at the cell surface by 50.5% (Figure 3.24C, $P < 0.0001$ compared to pcDNA3.1 transfected cells). VEGFR-2 cell surface localisation was also increased in MT1-WT and MT1-ΔICD expressing cells by ~40% ($P < 0.0001$) and 33% ($P < 0.05$), respectively, compared to cells transfected with vector control. In contrast, expression of MT1-ΔECD-FLAG and MT1-TMD-APP did not affect the cell surface expression of VEGFR-2 (Figure 3.24C), suggesting that the increased cell surface expression of VEGFR-2 is dependent on the extracellular and transmembrane domains of the protease.

3.1.10 MT1-MMP induced VEGF-A mRNA expression depends on its extracellular, transmembrane and intracellular domains

MT1-MMP activity as well as the intracellular cysteine residue (C^{574}) has previously been found to be involved in the MT1-MMP-modulated VEGF-A expression [73]. In order to identify if other regions of MT1-MMP were required, deletion and substitution cDNA constructs were generated and tested for their effect on VEGF-A mRNA expression (summarised in Figure 3.25A). The point mutation of the glutamic acid to alanine (E240A) has been previously shown to ablate catalytic activity of MT1-MMP [88]. As expected, MT-E240A was unable to stimulate VEGF-A expression in MCF-7 cells (Figure 3.25B). A similar result was obtained when most of the MT1-MMP extracellular domain was replaced with a Flag (MT1-ΔECD-FLAG) or an EGFP (MT1-ΔECD-EGFP) tag.

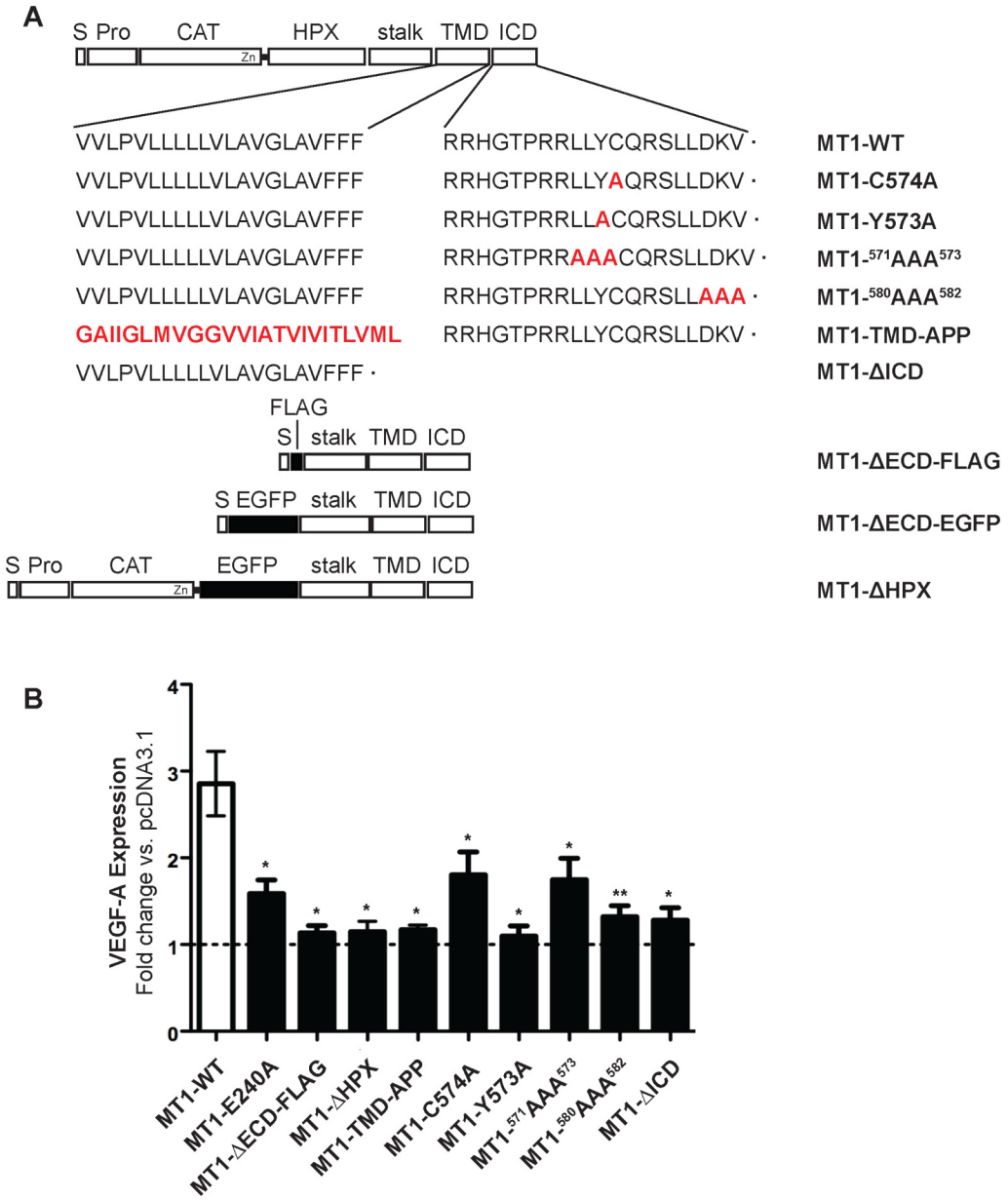

Figure 3.25: Deletion and substitution mutants of MT1-MMP catalytic, hemopexin, transmembrane and intracellular domain ablate MT1-MMP induced VEGF-A expression

(A) Schematic representation of various MT1-MMP extracellular, transmembrane and intracellular domain deletion and substitution mutants. *S*, signal sequence; *Pro*, Propeptide; *CAT*, catalytic domain; *HPX*, hemopexin domain; *stalk*, amino acids P^{509} - S^{538}; *TMD*, transmembrane domain; *ICD*, intracellular domain; *APP*, *ß*-amyloid precursor protein; *FLAG*, FLAG tag (DYKDDDDK); *EGFP*, Enhanced Green Fluorescent Protein. ***(B)*** Various MT1-MMP mutants were transiently expressed in MCF-7 cells and VEGF-A mRNA levels were detected by TaqMan® Real-Time PCR. Relative expression levels of VEGF-A were normalised to mRNA levels of the house-keeping gene GAPDH. Data represent the mean VEGF-A expression in fold-change compared to pcDNA3.1 vector control (dotted line) ± S.E.M. with $P < 0.05$ (*) and $P < 0.001$ (**) compared to MT1-WT transfected control. Data show the mean expression of at least 5 independent experiments (MT1-WT, n = 16; MT1-E240A, n = 11; MT1-ΔECD-FLAG, n = 5; MT1-ΔHPX, n = 6; MT1-TMD-APP, n = 6; MT1-C574A, n= 14; MT1-Y573A, n = 5; MT1-^{571}AAA^{573}, n= 14; MT1-^{580}AAA^{582}, n = 9; MT1-ΔICD, n = 5, MT1-ΔICD + MT1-ΔECD-FLAG, n = 6.

Both constructs still contained the extracellular stalk region. Interestingly, replacement of the MT1-MMP transmembrane domain with that of the *ß*-amyloid precursor protein (APP), also did not increase VEGF-A expression (Figure 3.25B). Deletion of the hemopexin and the intracellular domain as well as mutation of the C^{573} and Y^{574} residues and the LLY^{573} and DKV^{582} motifs led to a similar result (Figure 3.25B). This was also observed with adenoviral transduction of various MT1-MMP mutants (data not shown).
Taken together, these findings are consistent with previous data [73] and furthermore identify Y^{573}, LLY^{573} and DKV^{582} as new intracellular motifs involved in the transcriptional regulation of VEGF-A. The data further show that the MT1-MMP hemopexin and transmembrane domains are also necessary for the MT1-MMP induced VEGF-A expression.

3.1.11 The MT1-MMP catalytic activity is needed to enhance the bioavailability of VEGF-A by cleaving CTGF/$VEGF_{165}$ complexes

The findings so far suggest an MT1-MMP mediated signalling pathway that is induced via VEGFR-2 (summarised in Figure 3.31).
It has been reported previously that both MT1-MMP and MMP-2 are able to cleave CTGF/$VEGF_{165}$ and HARP/$VEGF_{165}$ complexes in an *in vitro* system [54,257]. Both complexes are abundant within the extracellular milieu and HARP as well as CTGF sequesters $VEGF_{165}$ function. It is possible that MP activity is required to release VEGF-A and activate VEGFR-2 feeding into an autocrine signalling loop, which increases VEGF-A mRNA expression. Thus, it was tested whether the previously described requirement for the MT1-MMP catalytic activity [73] (Figure 3.25B, Figure 3.4B) is explained by its ability to cleave CTGF or HARP and thus increase the bioavailability of $VEGF_{165}$.
The MCF-7 cells used in this study are described to be deficient in both MT1-MMP and MMP-2 expression [251]. Similar results were obtained within a gene expression profile of MCF-7 cells transfected with either empty vector control or MT1-WT (Figure 3.26A and Figure 3.5B). HARP mRNA was not detected, whereas CTGF mRNA was readily expressed in MCF-7 cells (Figure 3.26B and Figure 3.5B), suggesting a possible role of the MT1-MMP catalytic activity in cleaving a CTGF/$VEGF_{165}$ complex in the system used.
It was initially tested whether MT1-MMP is able to cleave soluble CTGF in the conditioned medium of MCF-7 cells. Therefore, cells were transduced with increasing

MOI of MT1-WT expressing adenovirus or 150 pfu/cell of empty adenoviral control vector (Rad) and cell lysates as well as conditioned medium was immunoblotted for CTGF and MT1-MMP, respectively. As shown in Figure 3.26C increasing expression of MT1-MMP induced an accumulation of CTGF cleavage products detected within the conditioned medium (arrows).

These results show that MT1-MMP processes CTGF in MCF-7 cells (Figure 3.26C) which is consistent with previous findings showing that MT1-MMP cleaves CTGF/$VEGF_{165}$ complexes *in vitro* [54].

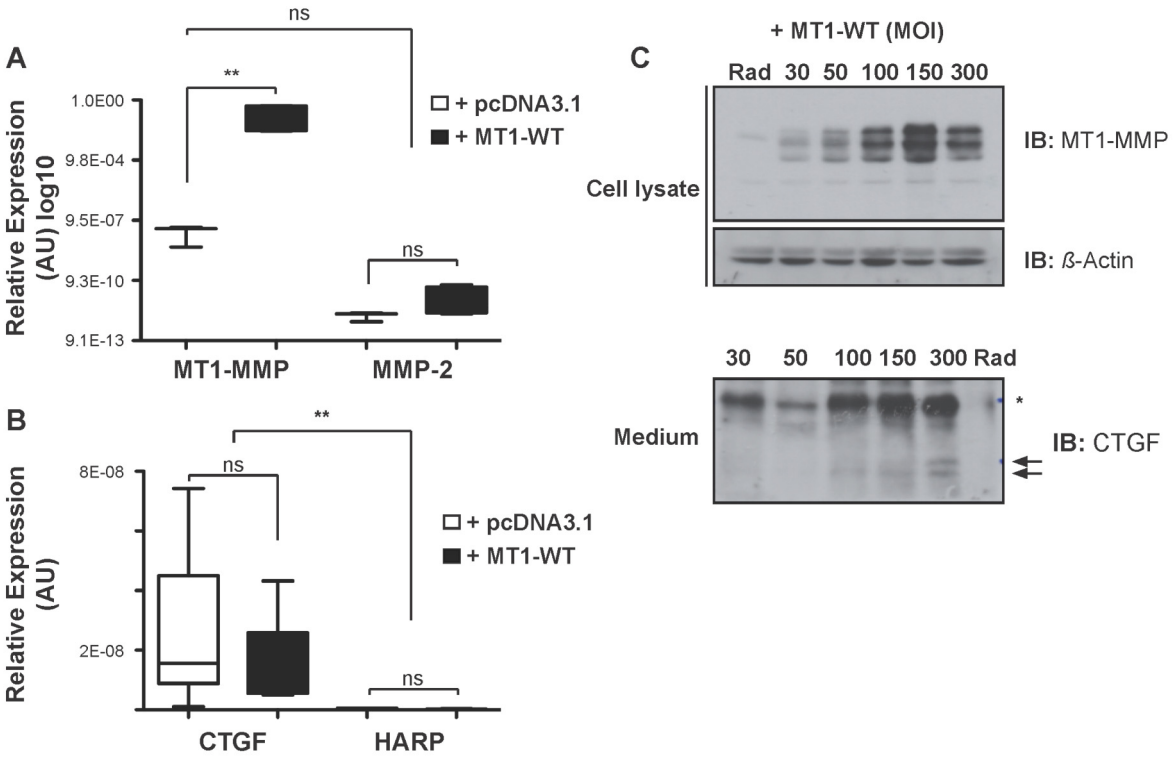

Figure 3.26: MT1-MMP cleaves CTGF and has a potential role in increasing $VEGF_{165}$ bioavailability in MCF-7 cells

(A) MCF-7 cells were either transfected with pcDNA3.1 empty vector control (white bars) or MT1-WT (black bars). Relative mRNA expression levels of MT1-MMP and MMP-2 were detected by TaqMan® Real-Time PCR and normalised to the house-keeping gene GAPDH. Data represent the mean expression in arbitrary units (AU) of 6 independent experiments ± min to max with $P < 0.001$ (**) on a $\log_{10}$ axis. *ns*, non-significant. ***(B)*** MCF-7 cells were either transfected with pcDNA3.1 empty vector control (white bars) or MT1-WT (black bars). Relative mRNA expression levels of CTGF and HARP were detected by TaqMan® Real-Time PCR and normalised to the house-keeping gene GAPDH. Data represent the mean expression in arbitrary units (AU) of 6 independent experiments ± min to max with $P < 0.001$ (**). *ns*, non-significant. ***(C)*** MCF-7 cells were transduced with the indicated MOI of MT1-WT expressing adenovirus and protein levels in the cell lysates as well as in the conditioned medium were analysed by immunoblotting with an anti-MT1-MMP (LEM-2/15.8), an anti-CTGF or an anti-*ß*-Actin antibody. Arrows indicate CTGF cleavage products whereas the asterisk correspond to full-length CTGF. *Rad*, empty adenoviral vector control.

Subsequently, it was tested whether the MT1-MMP catalytic activity is needed to cleave extracellular CTGF/$VEGF_{165}$ complexes and thus possibly increase the bioavailability of $VEGF_{165}$ in order to induce the signalling pathway characterised previously in this thesis. As MMP-2 has also been shown to cleave CTGF/$VEGF_{165}$ complexes, cells were transfected with either MT1-WT or the catalytic inactive MT1-E240A and increasing concentrations of rh-MMP-2 were added. Addition of various concentrations of rh-MMP-2 did not affect VEGF-A transcription in MT1-WT transfected cells as detected by TaqMan® Real-Time PCR (Figure 3.27A). MT1-E240A expression decreased VEGF-A mRNA levels compared to MT1-WT expressing cells, as shown previously (Figure 3.27B and Figure 3.25B). However, adding increasing concentrations of rh-MMP-2 to MT1-E240A expressing cells restored VEGF-A mRNA levels to the level of MT1-WT expressing cells (dotted line, Figure 3.27B).

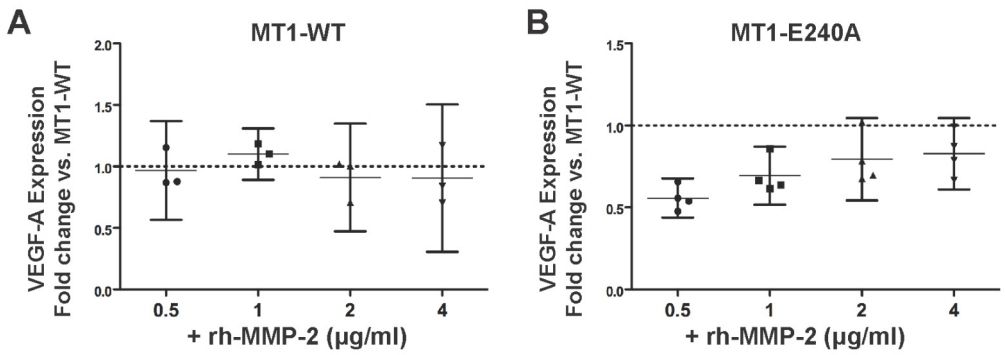

Figure 3.27: MMP-2 is able to substitute for MT1-MMP catalytic activity in increasing VEGF-A mRNA levels

MCF-7 cells were transfected with either MT1-WT ***(A)*** or MT1-E240A ***(B)*** and increasing concentrations of rh-MMP-2 were added for 24 hours, as indicated. VEGF-A relative expression levels were detected by TaqMan® Real-Time PCR and normalised to the mRNA levels of the house-keeping gene GAPDH. Data represent the mean expression of three (A) or four (B) independent experiments in fold change compared to MT1-WT transfected cells without rh-MMP-2 stimulation (dotted line) ± 95% confidence intervals.

It was investigated further whether the MT1-MMP ICD is still required when MT1-E240A expressing cells were treated with rh-MMP-2. Therefore, double MT1-MMP mutants, containing the E240A point mutation as well as either a LLY^{573} => $^{571}AAA^{573}$ mutation (MT1-E240A-$^{571}AAA^{573}$) or the complete deletion of the intracellular domain (MT1-E240A-ΔICD) were generated (Figure 3.28A). Addition of increasing concentrations of rh-MMP-2 to the cells expressing the double mutants did not affect the level of VEGF-A

mRNA (Figure 3.28B, C). Figure 3.28D summarises the effect of exogenous rh-MMP-2 on VEGF-A expression in the different MT1-MMP mutants used.

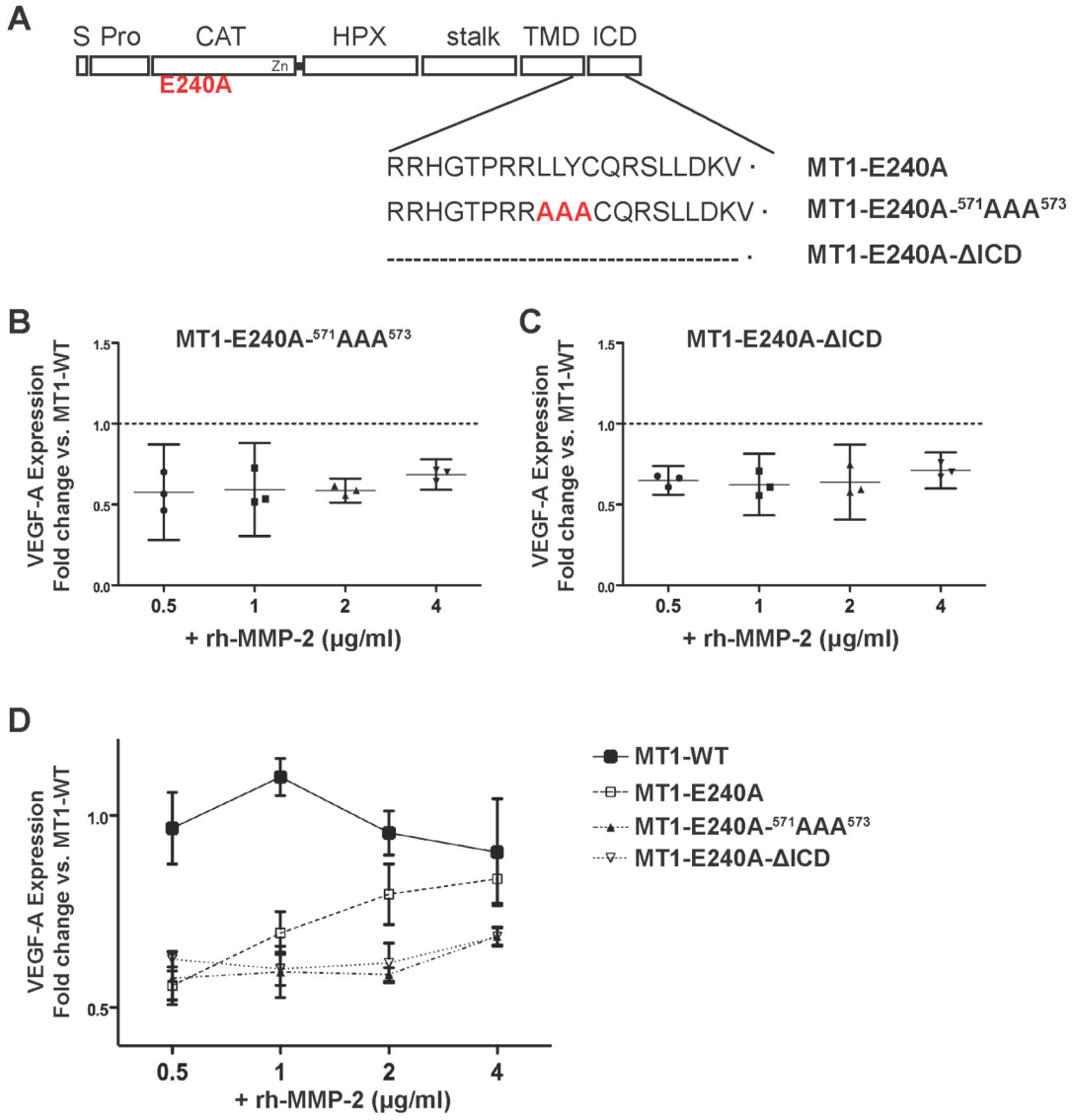

Figure 3.28: MMP-2 mediated increase of VEGF-A mRNA levels is dependent on the MT1-MMP intracellular domain

(A) Schematic representation of the catalytic inactive intracellular domain mutants. *S*, signal sequence; *Pro*, prodomain; *CAT*, catalytic domain; *HPX*, hemopexin domain; *stalk*, amino acids P^{509} - S^{538}; *TMD*, transmembrane domain; *ICD*, intracellular domain. ***(B,C)*** MCF-7 cells were transfected with the catalytic inactive intracellular domain mutants MT1-E240A-^{571}AAA^{573} (B) or MT1-E240A-ΔICD (C) and increasing concentrations of rh-MMP-2 were added for 24 hours, as indicated. VEGF-A relative expression levels were detected by Real-Time PCR and normalised to the mRNA levels of the house-keeping gene GAPDH. Data represent the mean expression of three independent experiments in fold change compared to MT1-WT transfected cells without rh-MMP-2 stimulation ± 95% confidence intervals. ***(D)*** Summary of the VEGF-A mRNA expression levels of MCF-7 cells transfected with either MT1-WT, MT1-E240A, MT1-E240A-^{571}AAA^{573} or MT1-E240A-ΔICD.

Taken together, rh-MMP-2 stimulation increased VEGF-A mRNA levels in MT1-E240A expressing cells but did not affect VEGF-A expression levels in cells transfected with the catalytic inactive intracellular double mutants. Thus, the presence of an intact MT1-MMP intracellular domain is still required for MT1-MMP dependent VEGF-A expression.

These results suggest that $VEGF_{165}$ bioavailability may need to be increased by either MT1-MMP or MMP-2 catalytic activity in order to induce VEGF-A transcription in this system. However, the intact MT1-MMP intracellular domain sequence is still required for signal transduction.

3.1.12 The MT1-MMP domains have different independent functions in the regulation of VEGF-A expression

The data obtained suggest that the different MT1-MMP domains have distinct functions within the MT1-MMP induced signalling pathway (summarised in Figure 3.29A).
MT1-MMP catalytic activity has been previously shown to be involved in the increase in VEGF-A expression (Figure 3.25B, Figure 3.4B) [73]. The findings so far strongly suggest that the catalytic domain is required to cleave CTGF/$VEGF_{165}$ complexes within the extracellular milieu in order to initiate the signalling pathway via VEGFR-2 (Figure 3.26 and Figure 3.27). However, addition of exogenous rh-MMP-2 to MCF-7 cells has been shown to rescue VEGF-A expression in cells expressing inactive MT1-MMP, potentially by substituting for MT1-MMP catalytic function in cleaving CTGF/$VEGF_{165}$ complexes and thus increasing the bioavailability of $VEGF_{165}$. In contrast, the MT1-MMP hemopexin and transmembrane domains have been implicated in the interaction with VEGFR-2 (Figure 3.20) as well as in regulating VEGFR-2 localisation (Figure 3.24), whereas the intracellular domain has been shown to interact with Src (Figure 3.12). However, the interpretation of the specific role of the transmembrane domain in VEGFR-2 interaction is difficult and is discussed in chapter 4.1.1.1.
To test whether the functions identified for different MT1-MMP domains are independent, MCF-7 cells were co-transfected with the extracellular and intracellular deletion mutants (MT1-ΔECD-FLAG and MT1-ΔICD) and VEGF-A mRNA levels were assessed by TaqMan® Real-Time PCR. As previously shown, transfection of MCF-7 cells with either MT1-ΔECD-FLAG or MT1-ΔICD did not affect VEGF-A expression compared to empty

vector control transfected cells (Figure 3.25B and Figure 3.29B, dotted line; $P < 0.05$ compared to MT1-WT transfected cells). However, when cells were co-transfected with both MT1-MMP mutants, VEGF-A expression was found to be increased but the detected mRNA level was not significantly affected compared to MT1-WT transfected cells (Figure 3.29B, $P = 0.29$, Student *t*-test).

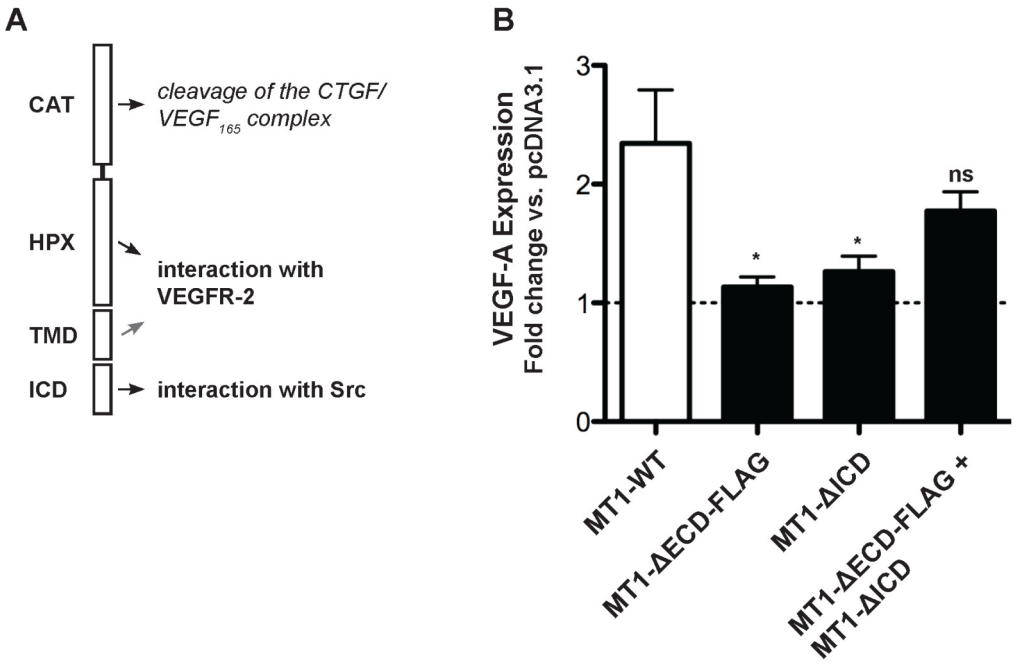

Figure 3.29: The different roles of MT1-MMP domains

(A) Schematic representation of the different roles of MT1-MMP in the regulation of VEGF-A expression. The role of the catalytic domain is shown in italic, since its function can be substituted by MMP-2 activity. The role of the transmembrane domain in the interaction with VEGFR-2 as well as its re-distribution in the cell is difficult to assess using the APP transmembrane domain mutant (shown in grey; discussed in chapter 4.1.1.1). *CAT*, catalytic domain; *HPX*, hemopexin domain; *TMD*, transmembrane domain; *ICD*, intracellular domain. ***(B)*** MCF-7 cells were transfected with the extracellular deletion mutant (MT1-ΔECD-FLAG), the intracellular deletion mutant (MT1-ΔICD) or both (MT1-ΔECD-FLAG + MT1-ΔICD). VEGF-A relative expression levels were detected by TaqMan® Real-Time PCR and normalised to the mRNA levels of the house-keeping gene GAPDH. Data represent the mean expression of six independent experiments in fold change compared to pcDNA3.1 empty vector control transfected cells ± S.E.M. with $P < 0.05$ (*).

These findings suggest that the MT1-MMP extracellular and intracellular domains are involved in different functions and that the presence of both is required for VEGF-A expression in the absence of another MP (e.g. MMP-2). Notably, the expression of both constructs from different cDNAs is sufficient to induce VEGF-A expression.

A slight decrease in VEGF-A expression was observed in the MT1-ΔECD-FLAG and MT1-ΔICD co-transfected cells compared to the MT1-WT expressing control (Figure

3.29B). Both mutants expressed from two different expression vectors were co-transfected with FuGene into MCF-7 cells as described in Material and Methods (chapter 2.2.1.5). The difference in VEGF-A expression may be explained by ***(i)*** the different size and transfection efficiency of both constructs used or by ***(ii)*** the amount of cells that were co-transfected by both, MT1-ΔECD-FLAG and MT1-ΔICD, compared to the proportion of cells that only express one of the deletion constructs.

3.1.13 The role of the microtubular system in MT1-MMP – VEGFR-2 complex formation

In this thesis, MT1-MMP has been shown to co-localise with VEGFR-2 and pY416-Src in MCF-7 cells (Figure 3.17) and furthermore to modulate VEGFR-2 localisation (Figure 3.24) as well as Src activation (Figure 3.9, Figure 3.10, Figure 3.14). VEGFR-2 and MT1-MMP are known to traffic and recycle to the cell surface in a microtubular system-dependent way [39,256], whereas Src activation and its transport to the plasma membrane has been demonstrated to be mediated by Actin filaments [253]. As either the microtubules or the actin cytoskeleton are involved in VEGFR-2, Src and MT1-MMP trafficking, their respective role on the MT1-MMP – VEGFR-2 – pY416-Src complex was assessed.

To test whether MT1-MMP co-localises with VEGFR-2 and the microtubule network, MCF-7 cells were transfected with MT1-WT and the localisation of MT1-MMP, VEGFR-2 and tubulin was assessed by confocal microscopy. As shown in Figure 3.30A, intracellular vesicles containing both VEGFR-2 and MT1-MMP were found close to the microtubular network (arrows). Disruption of the microtubular system or the actin cytoskeleton by treatment of MT1-MMP and Src expressing MCF-7 cells with either Nocodazole or Cytochalasin D was found to reduce the amount of detected MT1-MMP and Src that co-immunoprecipitated with VEGFR-2 (Figure 3.30B).

To test the effect of the actin and microtubular network disruption on MT1-MMP induced up-regulation of VEGF-A, MCF-7 cells were transfected with either pcDNA3.1 vector control or MT1-WT and cells were subsequently treated with Nocodazole, Cytochalasin D or DMSO control. VEGF-A mRNA levels were found to be decreased in cells with a disrupted microtubular system compared to MT1-WT expressing cells, but not in cells treated with Cytochalasin D (Figure 3.30C).

These findings suggest that actin and microtubules could be involved in the complex formation of VEGFR-2, MT1-MMP and Src, potentially by regulating the trafficking of these proteins. In contrast, only disruption of the microtubules but not of the actin cytoskeleton reduced MT1-MMP induced VEGF-A expression.

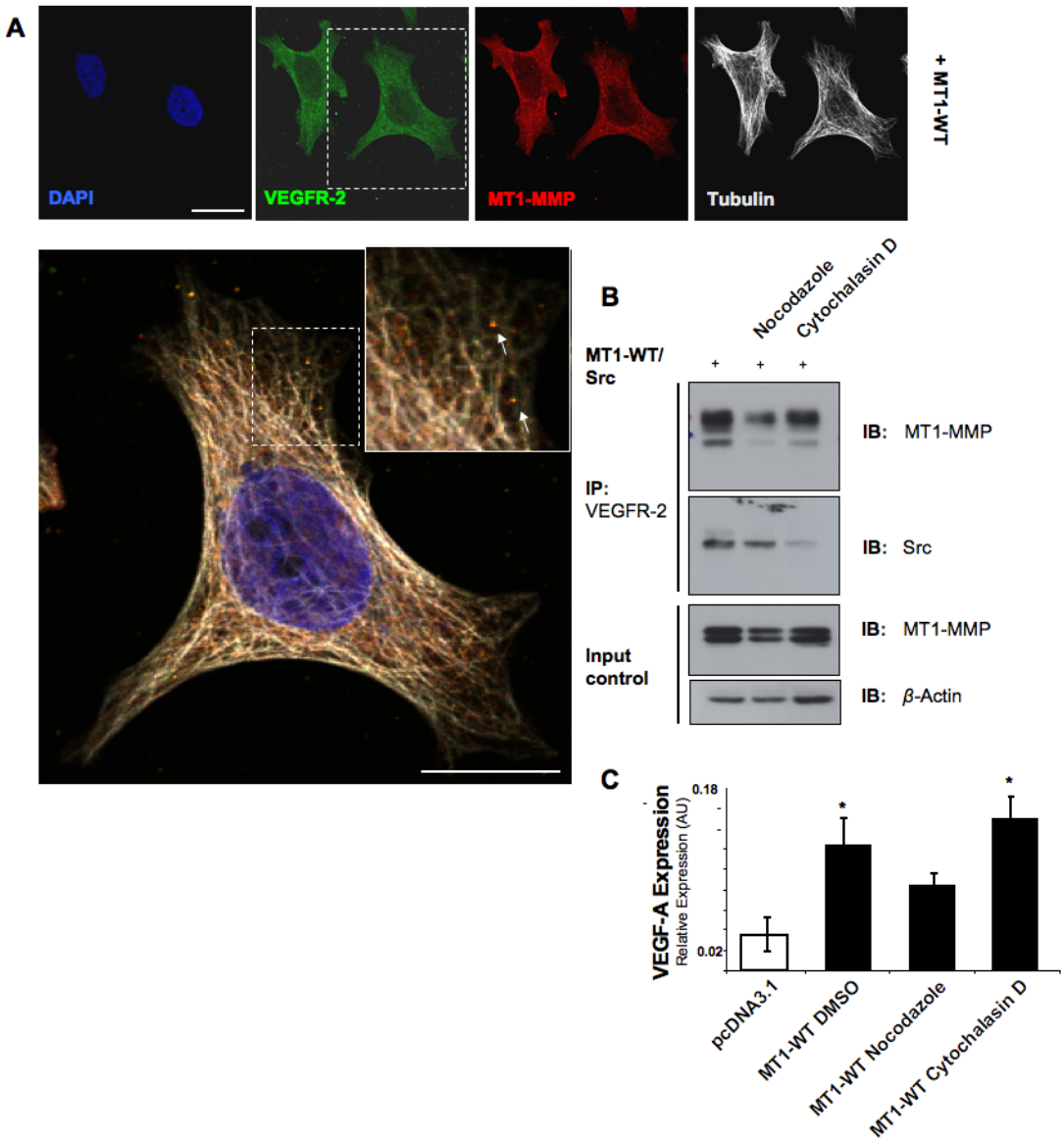

Figure 3.30: MT1-MMP and VEGFR-2 positive vesicles co-localise with the microtubular system

(A) MCF-7 cells were transiently transfected with MT1-WT and immunostained with an anti-VEGFR-2 (AlexaFluor® 488 secondary), anti-tubulin (AlexaFluor® 546 secondary) and an anti-MT1-MMP antibody (N175/6; Cy5 secondary). Inset panel shows magnified portion of the merged image, as indicated (dashed square). The white scale bars present a distance of 25 µm. ***(B)*** MCF-7 cells were transfected with MT1-WT and Src and cell extracts were immunoprecipitated with an anti-VEGFR-2 antibody. Immunoprecipitates and Input controls were immunoblotted with an anti-MT1-MMP (LEM-2/15.8), anti-Src or an anti-*β*-Actin antibody. ***(C)*** MCF-7 cells were transfected with pcDNA3.1 or MT1-WT and treated with Nocodazole or Cytochalasin D for 1 hour as indicated. VEGF-A mRNA levels were detected by TaqMan® Real-Time PCR. Relative expression levels of VEGF-A were normalised to the mRNA level of the house-keeping gene GAPDH. Data represent the mean expression of five independent experiments ± S.E.M. with $P < 0.05$ (*).

3.1.14 Summary: model of MT1-MMP induced increase of VEGF-A expression in MCF-7 cells

Based on the data obtained so far, a model on MT1-MMP induced VEGF-A mRNA expression is proposed (summarised in Figure 3.31).

MT1-MMP was found to form at least a ternary complex with Src and VEGFR-2, presumably at the cell surface of MCF-7 cells (Figure 3.17 - Figure 3.19). The interaction between MT1-MMP and Src was shown to be dependent on the MT1-MMP ICD (Figure 3.11- Figure 3.13), whereas the hemopexin domain/hinge region mediates its interaction to VEGFR-2 (Figure 3.20). This complex was found to be required for the MT1-MMP induced up-regulation of VEGF-A transcription and expression of MT1-MMP furthermore induced the cell surface localisation of VEGFR-2 (Figure 3.24).

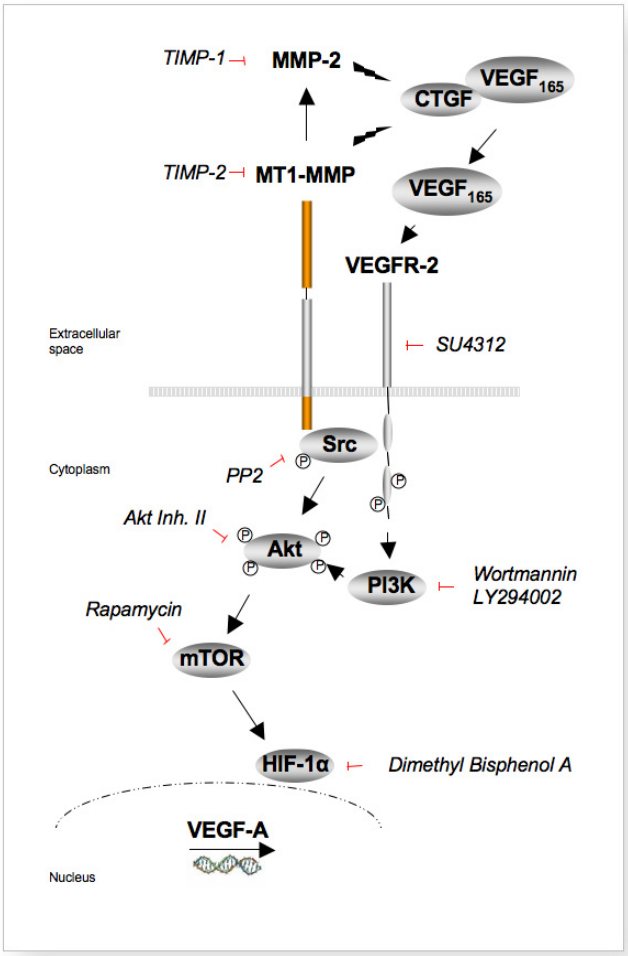

Figure 3.31: Summary of the data obtained so far

MT1-MMP expression in MCF-7 cells induces transcriptional up-regulation of VEGF-A expression. This effect was shown to be dependent on a VEGFR-2, Src, PI3 Kinase, Akt, mTOR and HIF-1α signalling pathway.

The signalling pathway leading to increased expression of VEGF-A mRNA is induced by $VEGF_{165}$, which is potentially released through MP activity from the extracellular CTGF/$VEGF_{165}$ complex (Figure 3.26 - Figure 3.28), and involves the activation of VEGFR-2, Src, PI3 Kinase, Akt, mTOR and HIF-1α (Figure 3.5A).

3.2 The role of MT1-MMP on VEGF-A expression in other human breast carcinoma cell lines

The previous findings suggest an MT1-MMP mediated signalling pathway involving the activities of VEGFR-2, Src, PI3 Kinase, Akt and mTOR as well as the formation of an MT1-MMP – VEGFR-2 – Src complex in MCF-7 cells, leading to the up-regulation of VEGF-A expression (chapter 3.1). To test whether this newly identified autocrine VEGF-A signalling loop is a conserved mechanism for regulating cell proliferation and survival, different breast cancer cell lines were analysed.

The MT1-MMP mRNA and protein expression profile of MCF-7 and MDA-MB-453 cells with and without transfection of full-length MT1-MMP (MT1-WT) as well as MDA-MB-231 and MDA-MB-468 cells is shown in Figure 3.32. As described by others [251], MCF-7 and MDA-MB-453 cells were found to be deficient in MT1-MMP expression at the mRNA (Figure 3.32A) as well as at the protein level (Figure 3.32B), whereas MT1-MMP mRNA was readily detected in MDA-MB-231 and to a lesser extent in MDA-MB-468 cells (Figure 3.32A). Over-expression of MT1-WT in MCF-7 and MDA-MB-453 cells increased the mRNA levels to those in MDA-MB-231 cells, indicating that the amount of transfected MT1-MMP in these cells is comparable to endogenous expression levels in a highly metastatic cell line (Figure 3.32A). Furthermore, MT1-MMP protein was expressed at similar levels in MCF-7 cells transfected with MT1-WT to endogenous levels in MDA-MB-231 cells (Figure 3.32B).

These data indicate, that the observations obtained in MT1-WT expressing MCF-7 cells as described in chapter 3.1 were close to endogenous levels of MT1-MMP expression observed in other cell lines and thus decrease the probability of being an artefact of unphysiological high protein over-expression.

Based on these MT1-MMP expression results, a complementary approach was used where MT1-MMP was either over-expressed in MDA-MB-453 cells by transient expression or MT1-MMP expression was silenced by adenoviral expression of targeted anti-sense RNA, siRNA or lentiviral shRNA in MDA-MB-231 and MDA-MB-468 cells.

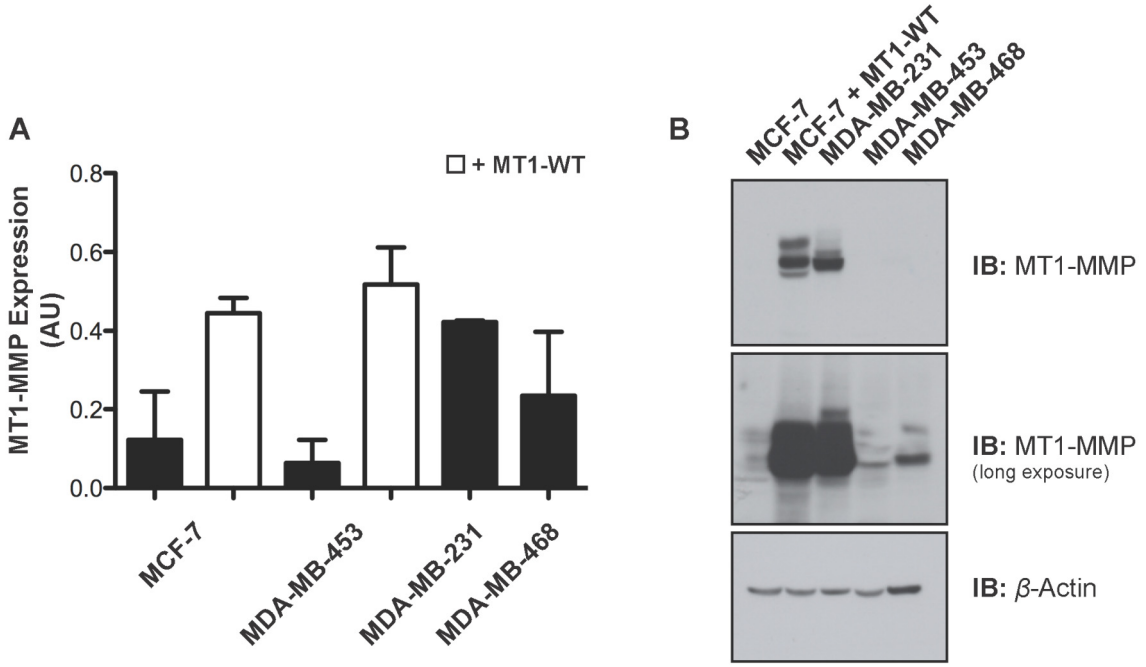

Figure 3.32: MT1-MMP expression in various breast cancer cell lines

(A) The MT1-MMP mRNA expression levels of wild-type MCF-7 and MDA-MB-453 cells, transfected with or without MT1-WT, as well as of MDA-MB-231 and MDA-MB-468 cells was assessed by TaqMan® Real-Time PCR. The relative expression levels of MT1-MMP were normalised to the mRNA levels of the house-keeping gene GAPDH. Data represent the mean MT1-MMP expression in arbitrary units (AU) of six independent experiments ± S.E.M. ***(B)*** Protein lysates of MCF-7 (wild-type and MT1-WT transfected), MDA-MB-231, MDA-MB-453 and MDA-MB-468 cells were immunoblotted with an anti-MT1-MMP (LEM-2/15.8) antibody (at two different exposure times) or an anti-*β*-Actin antibody.

3.2.1 The role of MT1-MMP on VEGF-A expression in MDA-MB-453 cells

The MT1-MMP deficient MDA-MB-453 cells (Figure 3.32) were initially tested for VEGF-A mRNA levels following transient MT1-MMP expression.

Similar to the results obtained in MCF-7 cells, MT1-MMP expressing MDA-MB-453 cells (Figure 3.33A) show an increase in VEGF-A mRNA expression compared to cells transfected with vector control (Figure 3.33B; $P < 0.05$, Student *t*-test), suggesting that the previously described pathway in MCF-7 cells (Figure 3.31) might be a ubiquitous mechanism in breast cancer cell lines to induce an autocrine VEGF-A signalling loop.

The mRNA expression of MT2-MMP, MT3-MMP, MT4-MMP, MMP-2 as well as the key genes involved in the proposed signalling pathway was assessed in MT1-MMP and control vector expressing MDA-MB-453 cells (Figure 3.33C).

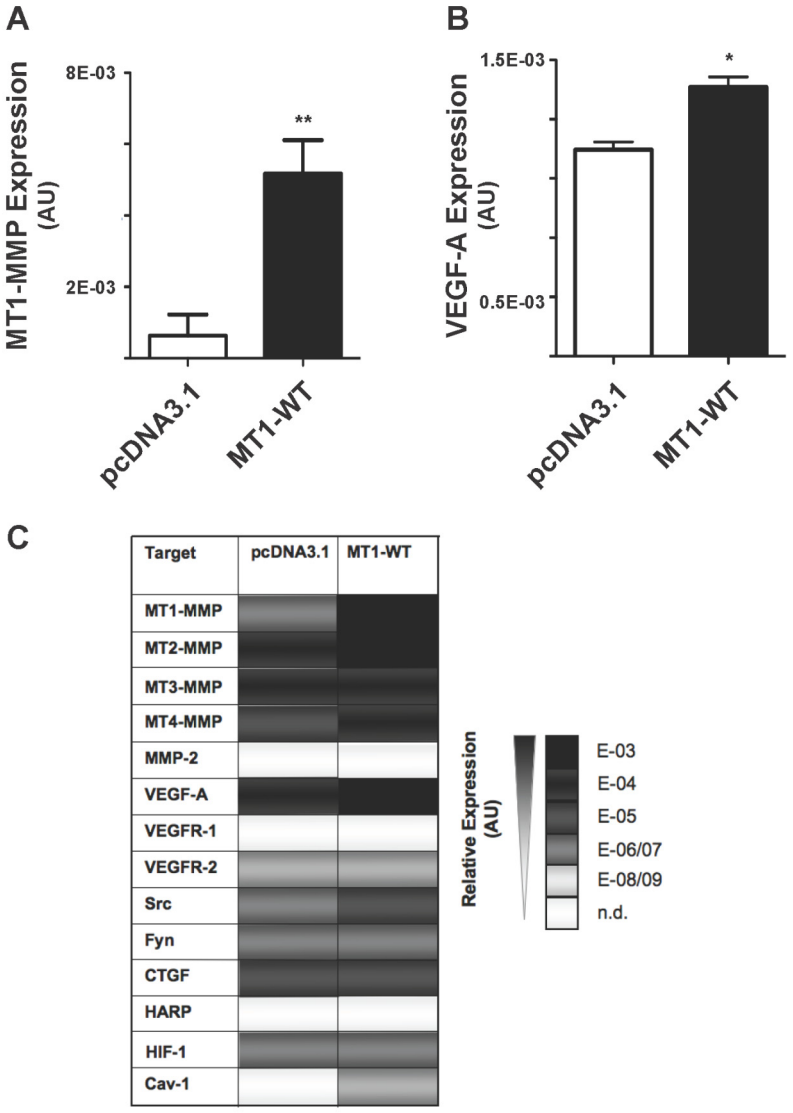

Figure 3.33: Expression profile of vector control and MT1-MMP transfected MDA-MB-453 cells

(A,B) MDA-MB-453 cells were transfected with MT1-WT or empty pcDNA3.1 vector control and the expression levels of MT1-MMP (A) and VEGF-A (B) were detected by TaqMan® Real-Time PCR. MT1-MMP and VEGF-A relative expression levels were normalised to the mRNA levels of the house-keeping gene 18s. The data represent the mean expression in arbitrary units (AU) of three independent experiments ± S.E.M. ***(C)*** Gene expression profile of pcDNA3.1 and MT1-WT transfected MDA-MB-453 cells was assessed by TaqMan® Real-Time PCR. The relative expression levels of various target genes were normalised to the mRNA levels of the house-keeping gene 18s. Data represent the mean relative expression of three independent experiments in arbitrary units (AU).

These data show that ***(i)*** transient expression of MT1-WT cDNA only affected expression levels of MT1-MMP and Caveolin-1 (discussed in chapter 3.2.4) significantly and ***(ii)*** CTGF and Src are both expressed at significantly higher levels than HARP and Fyn, similar to the expression profile obtained in MCF-7 cells (Figure 3.5B).

3.2.1.1 The role of MT1-MMP on VEGF-A expression in MDA-MB-231 and MDA-MB-468 cell lines

To test the role of MT1-MMP on VEGF-A expression in MDA-MB-231 and MDA-MB-468 cells, which endogenously express MT1-MMP (Figure 3.32), MT1-MMP expression was reduced using various approaches as listed in the following sections.

3.2.1.2 Adenoviral anti-sense expression of MT1-, MT2-, MT3- and MT4-MMP

In order to target specifically the effect of MT1-MMP, adenoviruses expressing antisense RNA (asRNA) for MT1-MMP as well as for MT2-, MT3- and MT4-MMP as controls were generated. Adenoviral delivery of these single-stranded asRNAs provides a system to study the function of selective genes based on the high efficiency of adenoviral transduction. Therefore, sequences (Appendix B, Table 9.1) complementary to the mRNA strand of each MT-MMP gene were cloned into the adenoviral backbone as described in Material and Methods (chapter 2.2.2.11). 8 - 10 clones per MT-MMP were selected for subsequent characterisation. After titration and plaque-purification, the different clones were tested for knockdown efficiency and cross-reactivity within the MT-MMP subfamily.

MDA-MB-231 cells were transduced with the different MT-MMP asRNA clones and the mRNA expression of MT1-, MT2-, MT3- and MT4-MMP was assessed by TaqMan® Real-Time PCR. As expected, every clone tested effectively silenced gene expression of the targeted MT-MMP as compared to MDA-MB-231 transduced with empty adenoviral vector control (Rad; Figure 3.34).

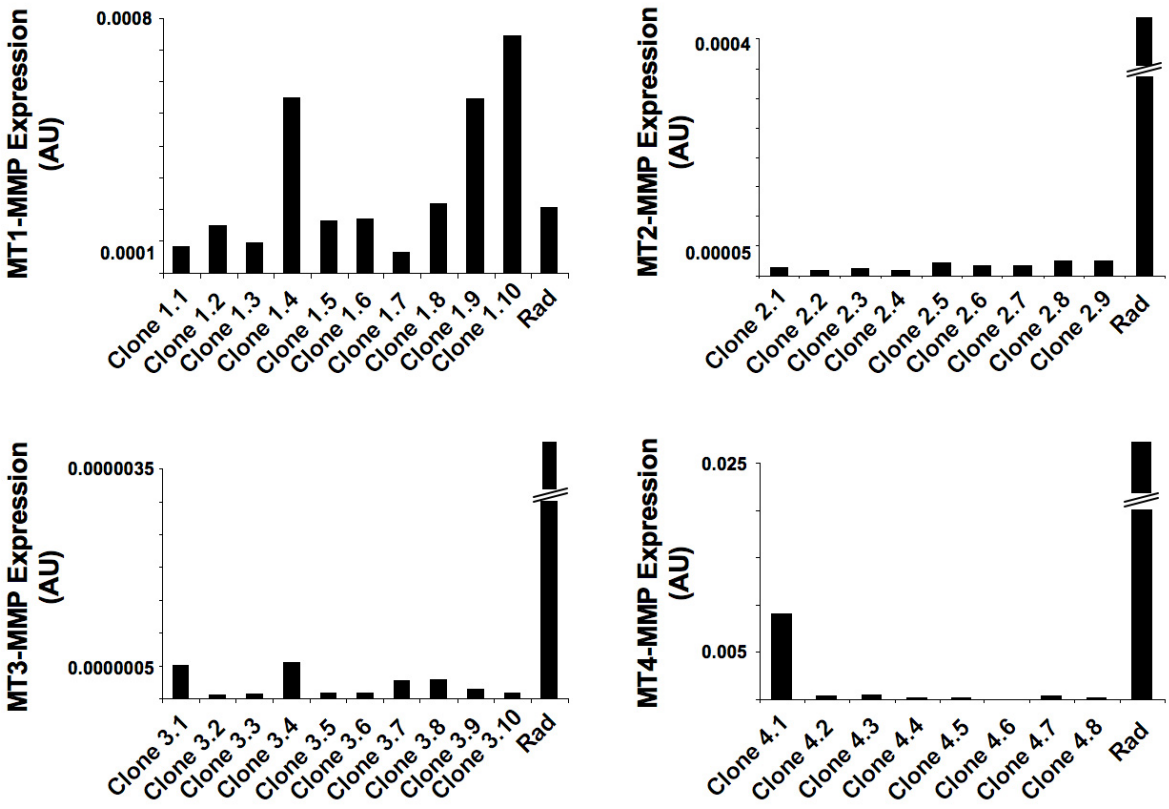

Figure 3.34: Adenoviral asRNA mediated knockdown of MT1-, MT2-, MT3- and MT4-MMP

MDA-MB-231 cells were transduced with 70 pfu/cell of the indicated clones of MT1-, MT2-, MT3- and MT4-MMP asRNA expressing adenovirus. The mRNA expression level of MT1-, MT2-, MT3- and MT4-MMP was assessed for each clone using TaqMan® Real-Time PCR. The expression levels were normalised to the expression level of the house-keeping gene 18s. Data represent the mean expression in arbitrary units (AU) of two independent experiments.

The mRNA expression level of MT1-, MT2-, MT3- and MT4-MMP was next assayed by TaqMan® Real-Time PCR for each clone in order to test for cross-reactivity within the MT-MMP family. Therefore, MDA-MB-231 cells were transduced with 9 different clones expressing MT2-MMP or MT4-MMP asRNA as well as 10 clones expressing MT1-MMP or MT3-MMP asRNA and the mRNA expression level of MT1-, MT2-, MT3- and MT4-MMP was detected for each clone. The relative expression of the MT-MMPs for each clone is normalised to the corresponding adenoviral empty vector control (Rad) and summarised in a heat-map (Figure 3.35).

As shown in Figure 3.35, a broad knockdown of the other members of the MT-MMP subfamily was observed. Similar results were obtained using HeLa cells (data not shown).

Taken together, adenoviral asRNA delivery for MT-MMP silencing was shown to be unsuitable to study the specific role of MT1-MMP function on VEGF-A expression in MDA-MB-231 or MDA-MB-468 cells.

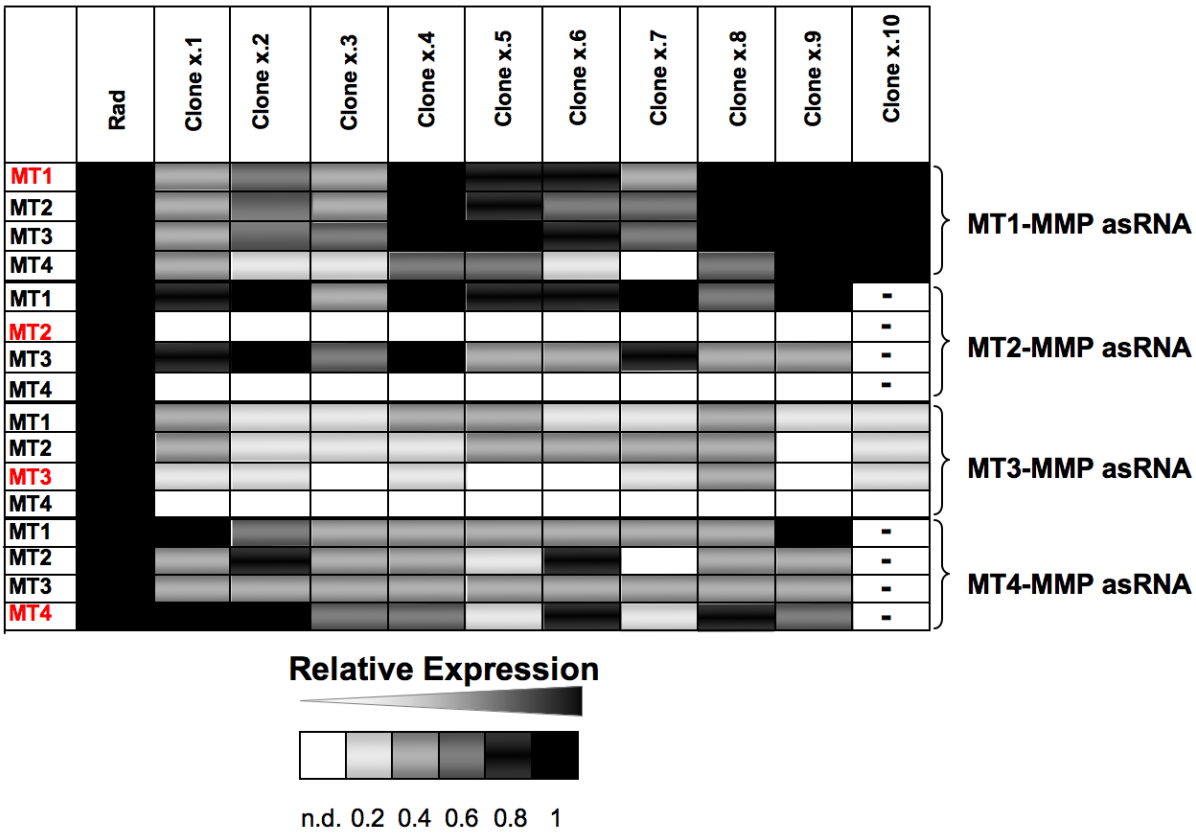

Figure 3.35: Characterisation of adenoviral MT1-MMP asRNA specificity

MDA-MB-231 cells were transduced with 70 pfu/cell of the indicated clones of MT1-, MT2-, MT3- and MT4-MMP asRNA expressing adenovirus (clones x.1 – x.10 with x = MT1 - MT4-MMP specific asRNA). The mRNA expression level of MT1-, MT2-, MT3- and MT4-MMP was assessed for each clone using TaqMan® Real-Time PCR. The expression levels were normalised to the expression level of the house-keeping gene 18s. mRNA levels of each clone were normalised to the expression level of the empty adenoviral vector control (Rad). Data represent the mean expression in arbitrary units of two independent experiments.

3.2.1.3 MT1-MMP knockdown by lentiviral shRNA

As a further approach to effectively reduce MT1-MMP expression, a lentiviral short-hairpin RNA (shRNA) system was used (MISSION® shRNA, Sigma-Aldrich). Lentiviral delivery of shRNA constructs provides long-term, stable gene silencing and clonal selection following puromycin treatment. Several different shRNA lentiviral particles, targeting different regions of the mRNA sequence, were used for each gene of interest (Appendix B, Table 9.2).

Initially, MDA-MB-231 cells were transduced with two different lentiviral MT1-MMP shRNA particles (shRNA3 and shRNA4), since the other shRNAs did not reduce MT1-MMP expression significantly (data not shown), as well as the empty vector control containing the puromycin resistance cassette (pLKO) and a non-targeting shRNA control (nt). As shown in Figure 3.36, MT1-MMP expression was efficiently reduced by shRNA3 and shRNA4 at the RNA (Figure 3.36A, $P < 0.0001$ compared to wild-type cells) as well as at the protein level (Figure 3.36B), albeit shRNA4 transduction did not decrease MT1-MMP protein expression as significantly as shRNA3. MT1-MMP mRNA and protein expression was not affected in the pLKO or non-targeting (nt) control cells (compared to wild-type cells).

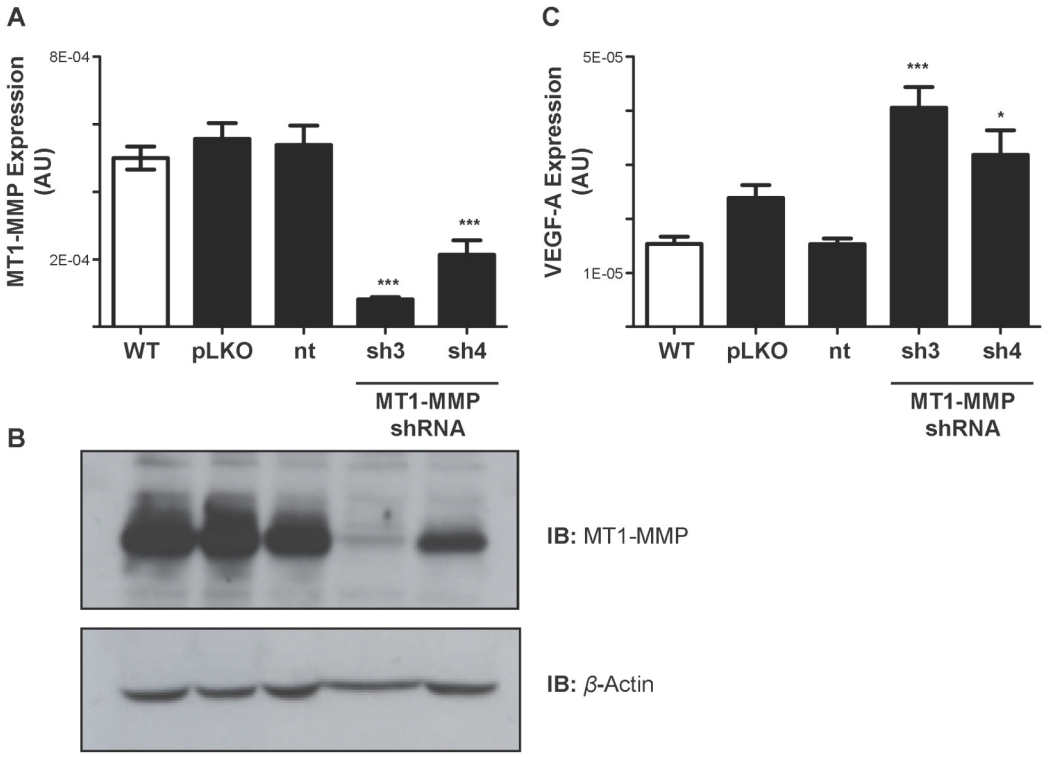

Figure 3.36: MT1-MMP knockdown in MDA-MB-231 cells using lentiviral shRNA

(A) MDA-MB-231 cells were transduced with 1 pfu/cell of Mission TRC lentiviral transduction particles. 48 hours after transduction, RNA was isolated and MT1-MMP RNA expression levels were assessed by TaqMan® Real-Time PCR. Relative MT1-MMP expression levels were normalised to mRNA levels of the house-keeping gene GAPDH. Data represent the mean MT1-MMP expression in arbitrary units (AU) of six independent replicates ± S.E.M. with $P < 0.0001$ (***). *plKO*, empty lentiviral vector containing the puromycin resistance cassette; *nt*, non-targeting shRNA sequence; *sh3*, *sh4*, shRNA sequence 3 and 4 targeting MT1-MMP. ***(B)*** MDA-MB-231 cells were transduced with 1 pfu/cell of Mission TRC lentiviral transduction particles. 48 hours after transduction, cell extracts were immunoblotted using an anti-MT1-MMP (LEM-2/15.8) or an anti-*β*-Actin antibody. ***(C)*** MDA-MB-231 cells were transduced with 1 pfu/cell of Mission TRC lentiviral transduction particles. 48 hours after transduction, RNA was isolated and VEGF-A RNA expression levels were assessed by TaqMan® Real-Time PCR. Relative VEGF-A expression levels were normalised to mRNA levels of the house-keeping gene GAPDH. Data represent the mean VEGF-A expression in arbitrary units (AU) of six independent replicates ± S.E.M. with $P < 0.05$ (*) and $P < 0.0001$ (***).

The mRNA level of VEGF-A was increased in cells expressing MT1-MMP specific shRNA3 (Figure 3.36C, $P < 0.0001$ compared to wild-type cells) or shRNA4 (Figure 3.36C, $P < 0.05$ compared to wild-type cells), showing the opposite effect of MT1-MMP in the regulation of VEGF-A expression in MDA-MB-231 cells compared to MCF-7 (Figure 3.2) and MDA-MB-453 cells (Figure 3.33).

Since MT1-MMP expression led to opposing results in MDA-MB-231 and MCF-7 or MDA-MB-453 cells and to confirm the reliability of the system used, the specificity of the shRNA knockdown was assessed. MT1-MMP targeting shRNA viral particles as well as the corresponding controls were transduced in MDA-MB-231 cells and the mRNA expression of MT1-, MT2-, MT3- and MT4-MMP as well as of key components of the previously described signalling pathway in MCF-7 cells was determined (Figure 3.31). The mRNA levels of 14 genes of interest normalised to the house-keeping gene GAPDH are summarised in a heat-map in Figure 3.37 (single analysis in Appendix C, Figure 10.1).

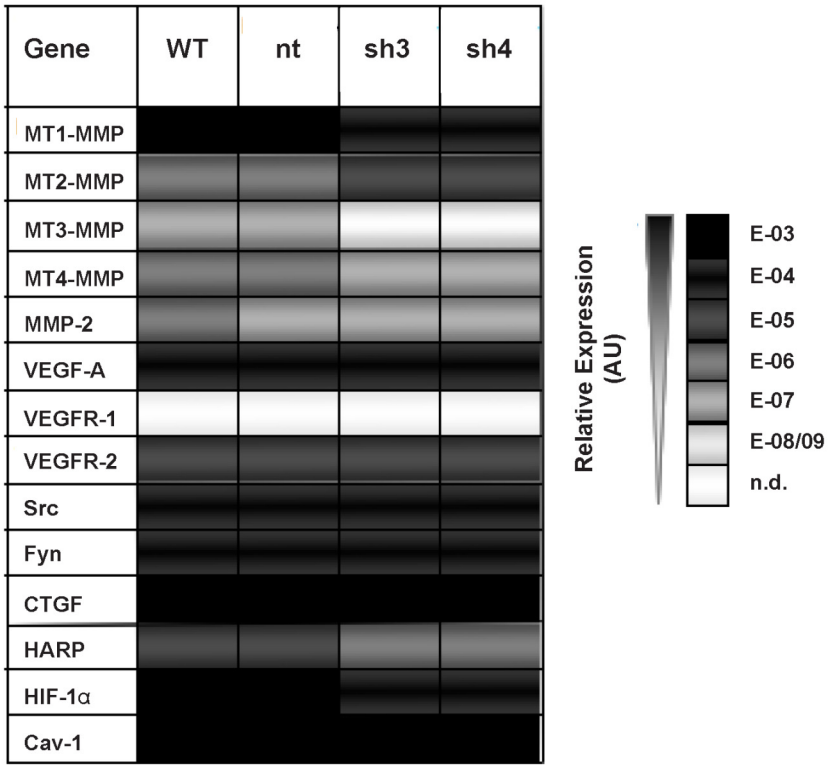

Figure 3.37: Gene expression profile of MDA-MB-231 wild-type and MT1-MMP shRNA transduced cells

MDA-MB-231 cells were transduced with 1 pfu/cell of non-targeting (nt) shRNA control or the MT1-MMP targeting shRNA sequences shRNA3 (sh3) or shRNA4 (sh4). The gene expression profile of wild-type and lentiviral transduced MDA-MB-231 cells was assessed by TaqMan® Real-Time PCR. The relative expression levels of various target genes were normalised to the mRNA levels of the house-keeping gene GAPDH. Data represent the mean expression of three independent experiments in arbitrary units (AU).

As previously shown, transduction of MDA-MB-231 cells with lentiviral MT1-MMP shRNA particles led to a significant reduction of MT1-MMP expression ($P < 0.0001$ compared to MDA-MB-231 wild-type cells, Figure 3.37). However, similar results were obtained for MT3-MMP ($P < 0.001$), MT4-MMP ($P < 0.0001$), MMP-2 ($P < 0.0001$), VEGFR-2 ($P < 0.0001$), HARP ($P < 0.0001$), HIF-1α ($P < 0.0001$) and Caveolin-1 ($P < 0.0001$) expression, while MT2-MMP ($P < 0.0001$) and VEGF-A ($P < 0.0001$) expression levels were found to be increased.
These data indicate that transduction of the MT1-MMP targeting shRNA as well as induction of the non-targeting (nt) shRNA sequence (in 7 genes tested, Figure 10.1) affects the mRNA expression of other genes.

Cells exhibit an innate defence mechanism directed against double-stranded (ds) RNA, such as virus infection. Introduction of short dsRNAs into mammalian cells causes a global, non-specific suppression of gene expression. These effects are known to be mainly mediated by activation of the dsRNA recognition proteins 2',5'-oligoadeylate synthetase-1 (OAS-1) or PKR (dsRNA-dependent protein kinase). Activation of either pathway leads to a general inhibition of protein synthesis and PKR activation induces a signalling pathway leading to the production of interferons (reviewed by [258]). Interferons activate cellular signalling pathways and up-regulate the expression of interferon-stimulated genes, which mediate once again an inhibition of protein synthesis as well as an anti-proliferative and pro-apoptotic activity. These global effects are not apparent unless either global gene expression studies are performed beyond the analysis of the target gene expression, or the expression profile of interferon response genes is assessed.
In order to test whether the shRNA system used is causing an inert non-specific defence response following transduction of dsRNA, the expression of the well-described γ-interferon response genes OAS-1 as well as MX-1 and MX-2 was tested by TaqMan® Real-Time PCR. It is widely accepted that expression of OAS-1 corresponds to an increased risk of inducing off-target effects in the knockout system used [259].

As shown in Figure 3.38, expression of γ-interferon response genes varied between the different cell lines tested. MCF-7 cells were found to be highly responsive to dsRNA transduction and the expression levels of the γ-interferon down-stream targets OAS-1, MX-1 and MX-2 were significantly increased in pLKO, non-targeting (nt) and VEGFR-2

shRNA transduced cells compared to MCF-7 wild-type cells (Figure 3.38C). Similar results, although to a lesser extent, were observed in the MDA-MB-468 cells (data not shown). In contrast, OAS-1 expression was not altered in MDA-MB-231 cells transduced with the pLKO or non-targeted (nt) control, but was slightly increased in these cells infected with the MT1-MMP targeted shRNA sample 4 (Figure 3.38A, B).

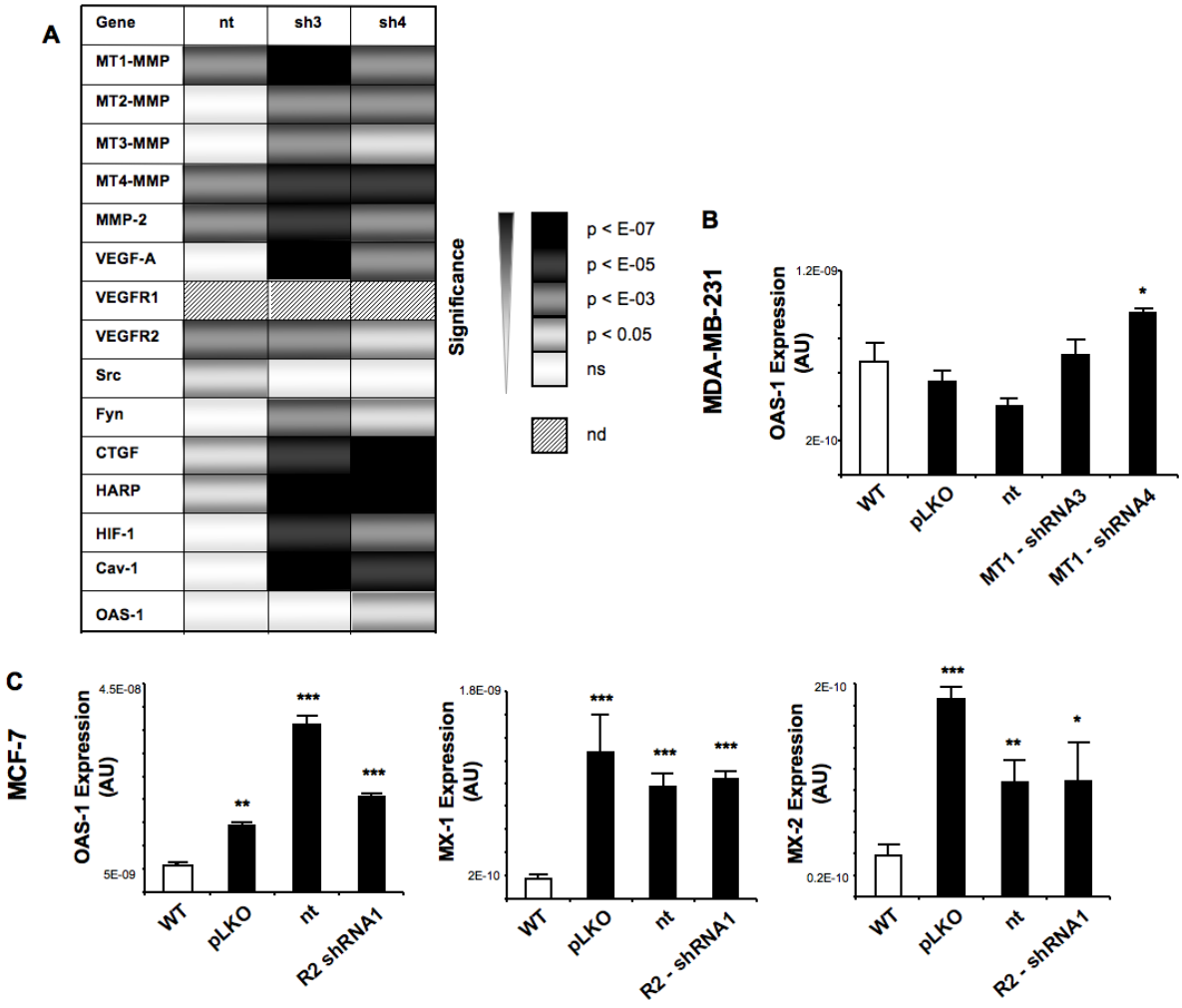

Figure 3.38: Summary of off-target effects and γ-interferon response in MDA-MB-231 and MCF-7 cells

(A) Gene expression profile of MDA-MB-231 cells transduced with non-targeted (nt) shRNA or MT1-MMP specific shRNA3 and shRNA4 probes was assessed by TaqMan® Real-Time PCR. Gene expression-levels were normalised to GAPDH mRNA levels. Data represent the statistical significance of the mean expression of three independent experiments compared to wild-type MDA-MB-231 cells. *ns*, non-significant; *nd*, not detected. ***(B)*** pLKO, non-targeting (nt) shRNA, MT1-MMP specific shRNA3 and shRNA4 sequences were transduced into MDA-MB-231 cells. The relative expression of OAS-1 was detected by TaqMan® Real-Time PCR and normalised to the mRNA levels of the house-keeping gene GAPDH. Data represent the mean expression of three independent experiments in arbitrary units (AU) ± S.E.M. with $P < 0.05$ (*). ***(C)*** pLKO, non-targeting (nt) shRNA and VEGFR-2 specific shRNA1 (R2 – shRNA1) sequences were transduced into MCF-7 cells. The relative expression of OAS-1, MX-1 and MX-2 was detected by TaqMan® Real-Time PCR and normalised to the mRNA levels of the house-keeping gene 18s. Data represent the mean expression of three independent experiments in arbitrary units (AU) ± S.E.M. with $P < 0.05$ (*), $P < 0.001$ (**) and $P < 0.0001$ (***).

These findings demonstrate that the tested cell lines respond differently to infection with short dsRNA molecules. Interestingly, the activation of the inert defence mechanism by inducing γ-interferon pathways was found to correlate with the malignancy of the cell line with the least invasive and malignant MCF-7 cells to show the strongest response. Although MDA-MB-231 cells were not found to increase OAS-1 expression compared to the wild-type control, expression-profiling revealed that several genes were influenced significantly by MT1-MMP knockdown, including members of the MT-MMP sub-family as well as MMP-2 (Figure 3.37 and Figure 10.1). The differential expression of 15 target genes in MDA-MB-231 cells transduced with either non-targeting (nt) control, MT1-MMP shRNA3 or shRNA4 is summarised in Figure 3.38A, representing the statistical significance compared to MDA-MB-231 wild-type cells.
Off-target effects observed, potentially by induction of interferons by dsRNAs, might be explained by the shRNA system used, which expresses shRNA under the control of a Polymerase III dependent U6 promoter. Recent findings suggest that a 5'-triphosphate modification, which is characteristic to all RNAs transcribed by Polymerase III promoters, is required for interferon induction [258,260,261]. This interferon response was shown to be attenuated by removal of the 5'triphosphate. Recent siRNA technology mimics the endogenous miRNA system by transcribing shRNAs by Polymerase II and thus reduce the amount of off-target effects [262].

Taken together, these results emphasise that a thorough characterisation of the gene expression silencing method used is necessary to draw coherent conclusions, especially when knockdown studies are used to determine gene function or the effect on the transcriptional regulation of downstream target genes. To address the role of MT1-MMP on VEGF-A expression in cells which endogenously express MT1-MMP, either a next-generation shRNA system should be used to introduce a stable MT1-MMP knockdown or transient gene silencing by siRNA should be applied.

3.2.1.4 MT1-MMP knockdown by siRNA

In order to circumvent the previously described shRNA introduced off-target effects or interferon responses (Figure 3.37 and Figure 3.38), an siRNA based approach to transiently

silence MT1-MMP expression was next tested using the Dharmacon® Accell^{TM} siRNA system, which is one of the latest generations of RNAi technology.

Therefore, MDA-MB-231 cells were transfected with 0.25 µM or 1 µM of siRNA sequences targeting four different regions of the MT1-MMP mRNA sequence and the MT1-MMP and VEGF-A mRNA expression was detected by TaqMan® Real-Time PCR.

MT1-MMP mRNA levels were effectively reduced by all siRNA sequences used at both concentrations (Figure 3.39A. $P < 0.0001$ compared to wild-type (ctrl)), whereas the level of VEGF-A expression was slightly increased with all siRNAs used (Figure 3.39B, $P < 0.001$ for siRNA 3 compared to wild-type (ctrl) cells).

However, a full RNA and protein expression profile to test the specificity of the siRNA used remains to be assessed.

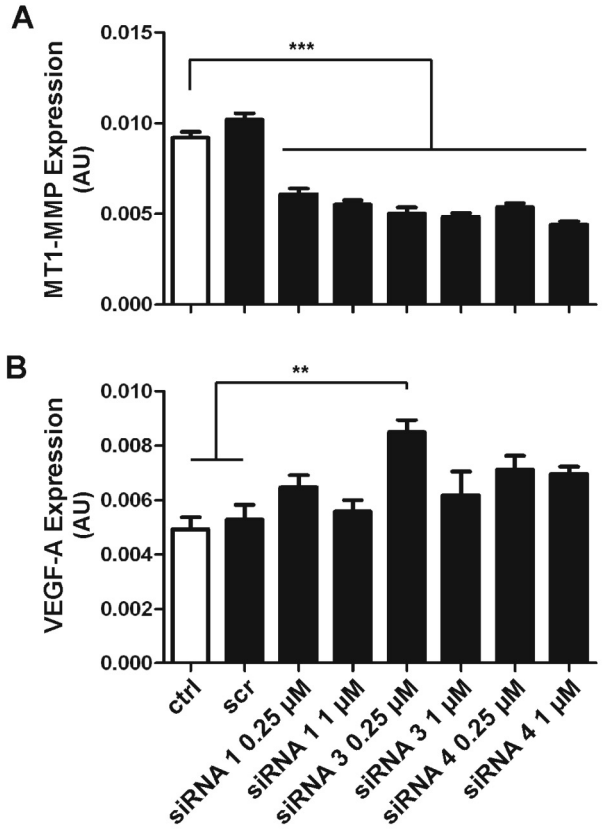

Figure 3.39: VEGF-A expression in MDA-MB-231 cells transfected with MT1-MMP specific siRNA was slightly increased

(A,B) MDA-MB-231 cells were transfected with three different siRNAs targeting different regions of the MT1-MMP mRNA sequence at 0.25 µM or 1 µM as indicated. The relative MT1-MMP (A) and VEGF-A (B) expression levels were analysed by TaqMan® Real-Time PCR and were normalised to the mRNA levels of the house-keeping gene GAPDH. Data represent the mean expression in arbitrary units (AU) of three independent experiments ± S.E.M. with $P < 0.0001$ (***) and $P < 0.001$ (**). *scr*, scrambled control sequence.

Despite the described limitations of the shRNA approach and the lack of a complete characterisation of the siRNA system, both techniques show independently an increase in VEGF-A expression in MT1-MMP silenced MDA-MB-231 cells (Figure 3.36C and Figure 3.39B), suggesting a different mechanism of MT1-MMP dependent regulation of VEGF-A expression in these cells.

3.2.1.5 VEGF-A expression does not depend on the MT1-MMP catalytic activity in MDA-MB-231 cells

Since various knockdown systems in MDA-MB-231 cells made the interpretation of the role of MT1-MMP on VEGF-A expression difficult, an inhibitor-based approach was used in order to test the role of metalloproteinase (MP) function and in particular of MT1-MMP catalytic activity on VEGF-A expression.

Cells were treated for 24 hours with rh-TIMP-1, rh-TIMP-2, the MP broad-spectrum inhibitor CT1746 at indicated concentrations as well as with the MT1-MMP specific catalytic activity-blocking antibody LEM-2/15.8. The mRNA expression of VEGF-A was subsequently determined by TaqMan® Real-Time PCR.

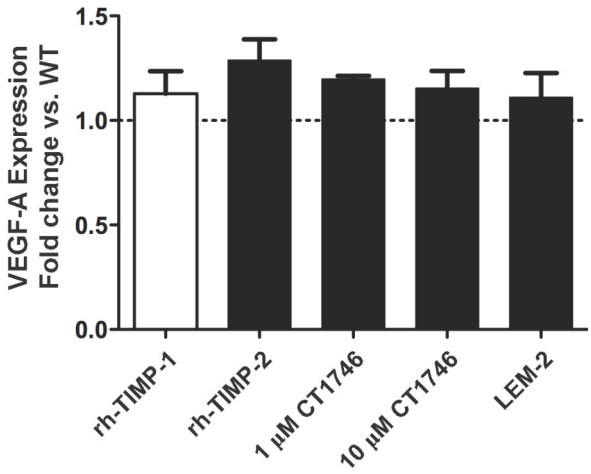

Figure 3.40: MT1-MMP catalytic activity does not affect VEGF-A expression in MDA-MB-231 cells

MDA-MB-231 cells were incubated for 24 hours with 1 µM rh-TIMP-1, 1 µM rh-TIMP-2, the broad-spectrum MP inhibitor CT1746 at the indicated concentrations as well as with 10 µg/ml of the anti-MT1-MMP catalytic activity blocking antibody LEM-2/15.8. VEGF-A expression levels were determined by TaqMan® Real-Time PCR and were normalised to mRNA levels of the house-keeping gene GAPDH. Data represent the mean expression in fold change compared to MDA-MB-231 wild-type cells (dotted line) of three independent experiments ± S.E.M.

In contrast to MCF-7 cells (Figure 3.4B), neither of the inhibitors used were able to alter VEGF-A mRNA expression significantly compared to wild-type control (Figure 3.40, dotted line).

This result suggests that VEGF-A expression is not affected by MT1-MMP catalytic activity in MDA-MB-231 cells. However, as shown in the gene expression profile of these cells (Figure 3.37, wild-type cells), MMP-2 mRNA expression was readily detected. Addition of exogenous rh-MMP-2 to MCF-7 cells expressing a catalytic inactive MT1-MMP mutant has been shown to compensate for the lack of the catalytic activity in these cells (Figure 3.27B, Figure 3.28D). Inhibition of MT1-MMP catalytic activity using the catalytic function blocking antibody LEM-2/15.8 in MDA-MB-231 cells, which endogenously express MT1-MMP and MMP-2, might therefore have led to a MMP-2 dependent rescue for loss of MT1-MMP activity. However, rh-TIMP-1, rh-TIMP-2 and CT1746 inhibit also MMP-2 activity, thus suggesting that VEGF-A expression does not depend on MT1-MMP or MP catalytic activity as observed in MCF-7 cells.

3.2.2 MT1-MMP – VEGFR-2 complex formation in breast cancer cell lines

MT1-MMP was found in a complex with VEGFR-2 and active Src (pY416-Src) in MCF-7 cells and this complex was shown to be required for MT1-MMP induced VEGF-A expression (Figure 3.17 - Figure 3.19, Figure 3.25B). In contrast to MCF-7 and MDA-MB-453 cells, MT1-MMP expression did not increase the level of VEGF-A mRNA in MDA-MB-231 cells, suggesting a different mechanism of VEGF-A regulation depending on the cell line. In order to test whether the MT1-MMP – VEGFR-2 complex is conserved in different breast cancer cell lines, albeit potentially controlling the expression of different target genes, a co-immunoprecipitation assay using an anti-VEGFR-2 antibody was performed as previously described (Figure 3.17A).

In addition to MT1-WT expressing MCF-7 cells, as previously described (Figure 3.17A), MT1-MMP was detected in MDA-MB-231 cells after immunoprecipitation with an anti-VEGFR-2 antibody (Figure 3.41A). The expression levels of MT1-MMP in MDA-MB-468 and especially in MDA-MB-453 were significantly lower than in the MDA-MB-231 cells as demonstrated in the whole cell lysate (Figure 3.41B, Input), making the MT1-

MMP detection after immunoprecipitation difficult. However, MT1-MMP could be detected at low levels in the MDA-MB-468 immunoprecipitates (Figure 3.41A).

These results suggest that formation of the MT1-MMP – VEGFR-2 complex may be a conserved system across different breast cancer cell lines, although the down-stream targets and signalling pathways that are controlled by this complex may vary.

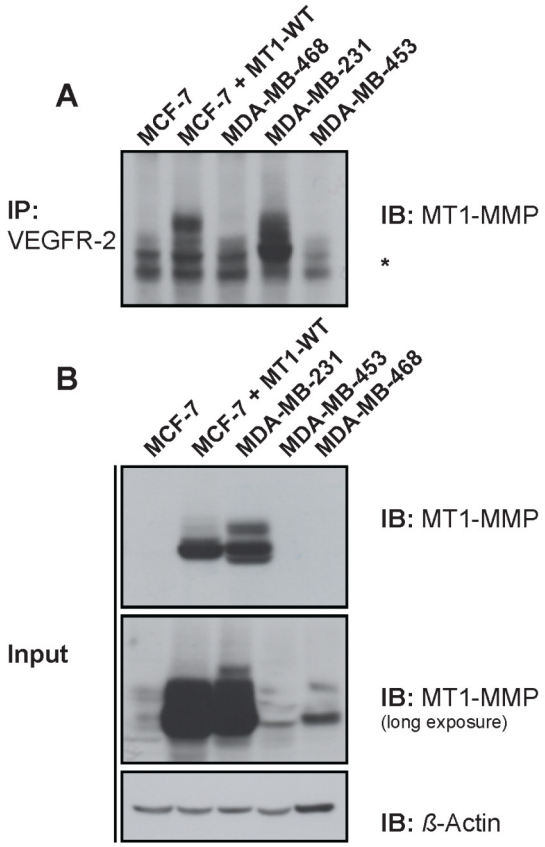

Figure 3.41: MT1-MMP is in a complex with VEGFR-2 in MCF-7, MDA-MB-231 and MDA-MB-468 cells

MCF-7 wild-type cells, MT1-WT transfected MCF-7 cells, MDA-MB-231, MDA-MB-468 and MDA-MB-453 cells were immunoprecipitated with an anti-VEGFR-2 antibody. Immunoprecipitates (A) and Input controls (B) were immunoblotted with an anti-MT1-MMP (LEM-2/15.8) or an anti-*ß*-Actin antibody. Asterisk indicates the IgG heavy chain.

Taken together, the interpretation of the role of MT1-MMP on the regulation of VEGF-A transcription in MDA-MB-231 as well as MDA-MB-468 cells is difficult due to the possible side-effects of MT1-MMP gene silencing (chapters 3.2.1.2 - 3.2.1.4). However, VEGF-A mRNA levels were found to be decreased in two independent systems using MT1-MMP specific shRNA and siRNA in MDA-MB-231 cells (Figure 3.36C and Figure

3.39B), indicating a different mechanism of VEGF-A regulation in MDA-MB-231 as compared to MCF-7 and MDA-MB-453 cells.

Previous findings using a Luciferase reporter gene under the control of a truncated 6 kb region of the VEGF-A promoter containing the hypoxia regulated element (HRE; Figure 1.6) in MCF-7 cells, also led to a decrease in activation following MT1-MMP expression (C.H. Roghi, personal communication), suggesting that MT1-MMP dependent VEGF-A regulation requires additional distant regulatory elements that are not present in the artificial VEGF-A promoter. These could be differentially regulated or modified (e.g. aberrant DNA methylation) in different cell lines leading to an either positive or negative regulation of the VEGF-A promoter.

These data indicate that VEGF-A regulation is dependent on the cell type, potentially due to a difference in regulatory elements distant to the 6 kb promoter region. In contrast, the complex-formation between MT1-MMP and VEGFR-2 was shown to be a more ubiquitous mechanism in various breast cancer cell lines tested.

3.2.3 MT1-MMP, VEGFR-2 and pY416-Src are expressed in tumour cells of human mammary carcinomas

As described before in this thesis, MT1-MMP was found to form a complex with VEGFR-2 and Src, thus modulating the PI3 Kinase/Akt pathway and regulating VEGF-A expression in MCF-7 cells (chapter 3.1; Figure 3.31). The data obtained also revealed the presence of MT1-MMP – VEGFR-2 complexes in other human breast cancer cell lines (Figure 3.41), albeit the genes that are regulated by this complex may vary depending on the cell type.

In order to correlate the data obtained *in vitro* with clinical specimens, sections of human breast carcinomas were obtained, embedded in paraffin and immunostained with an anti-MT1-MMP (LEM-2/15.8) (Figure 3.42A, D), an anti-VEGFR-2 (Figure 3.42B, E) or an anti-pY416-Src antibody (Figure 3.42C, F) (in collaboration with Dr. Bence Sipos, Department of Pathology, Universitätsklinikum Schleswig-Holstein, Campus Kiel; current affiliation: Department of Pathology, University of Tübingen). Figure 3.42 shows a representative sample of human mammary carcinoma sections.

As expected, VEGFR-2 was detected in the endothelial cells lining blood vessels (Figure 3.42B, black arrows), indicating the correct specificity of the antibody used. Expression of

VEGFR-2 was also detected within the cytoplasma and at the plasma membrane of tumour cells (Figure 3.42B,E empty arrowheads) but not in the stromal compartment (black arrowheads). MT1-MMP was highly expressed within the tumour cells, in particular at the plasma membrane (Figure 3.42A,D, empty arrowheads). Consistent with previous data [263] MT1-MMP was also found in the tumour stroma and in endothelial cells lining blood vessels in tumour sections that comprise of a more heterogeneous cell population (data not shown).

A similar staining pattern was obtained following immunostaining with an anti-pY416-Src antibody. A clear pY416-Src signal was detected at the plasma membrane of the tumour cells (Figure 3.42C,F, empty arrowheads), whereas stromal cells remained negative (black arrowhead).

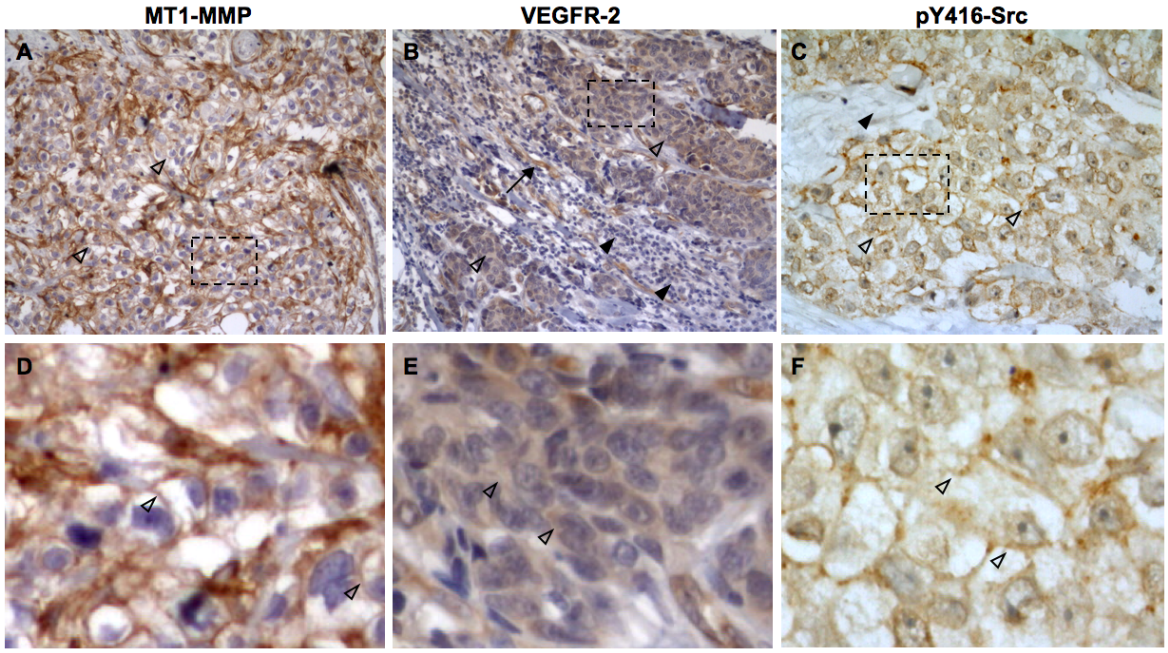

Figure 3.42: MT1-MMP, VEGFR-2 and pY416-Src are expressed in human mammary carcinomas

Representative sample of a paraffin-embedded section of human breast carcinoma was immunostained with an anti-MT1-MMP (LEM-2/15.8), an anti-VEGFR-2 or an anti-pY416-Src (Millipore) antibody. Black arrows indicate the staining of endothelial cells lining blood vessels, empty arrowheads show staining of tumour cells and black arrowheads indicate the stromal compartment. Lower panels (D-F) show magnified portions of each image, as indicated (dashed squares). Tissue specimens were counterstained with 50 % haemalaun. 100 × magnification.

These findings demonstrate that MT1-MMP, VEGFR-2 and pY416-Src are detected in tumour cells, in particular at or close to the plasma membrane, of human mammary carcinomas. To obtain a better understanding of the MT1-MMP – VEGFR-2 – Src complex *in vivo*, a comprehensive study using breast invasive ductal carcinoma tissue

microarrays (US Biomax, Inc., Heidelberg, GER) is currently being performed in collaboration with Dr. Bence Sipos.

3.2.4 The potential role of MT1-MMP in Caveolin-1 regulation

The plasma membrane is organised into various microdomains, including adhesive structures (substrate adhesions and cell-cell junctions), membrane invaginations (clathrin-coated pits and caveolae) as well as lipid rafts, which organise the cellular distribution of cell surface receptors and membrane-associated proteins. Caveolae are organised by clustered transmembrane caveolins and regulate growth factor receptor signalling, raft-dependent endocytosis and focal adhesion dynamics. As reported previously [264-267], wild-type MCF-7 cells do not express detectable levels of caveolin-1 (Figure 3.43A), whereas caveolin-1 expression could be observed on the mRNA and protein level in MDA-MB-231 cells (Figure 3.43B) [268]. Interestingly, expression of MT1-MMP in MCF-7 and MDA-MB-453 cells was consistently found to increase the level of caveolin-1 expression (Figure 3.43A, Figure 3.5B, Figure 3.33C), whereas MT1-MMP gene silencing in MDA-MB-231 cells using MT1-MMP specific shRNA decreased its detection at the mRNA and protein level (Figure 3.43B and Figure 10.1).

Caveolin-1 is a substrate of Src kinase and its phosphorylated form (pY14-Cav-1) has been found to regulate interactions with integrins, the association with various signalling molecules and protein tyrosine phosphatases and was also described to act as a scaffolding complex, which enables intracellular signalling by facilitating the assembly of signalling complexes [269-272].

Interestingly, both MT1-MMP and VEGFR-2 have been identified to localise within caveolae and to interact with caveolin-1 [119,273]. It has been recently shown that stimulation of bovine aortic endothelial cells (BAEC) with VEGF induces the dissociation of the VEGFR-2 – caveolin-1 complex, potentially following VEGF induced phosphorylation of the receptor [273]. Subsequently, caveolin-1 is phosphorylated at its Y^{14} residue in a Src-dependent way, facilitating its interaction with MT1-MMP [119]. This MT1-MMP – pY14-Cav-1 complex recruits Src, thereby inhibiting its activity. Notably, the association of MT1-MMP with pY14-Cav-1 was shown to be dependent on the MT1-MMP ICD, especially on its C^{574} and V^{582} residues.

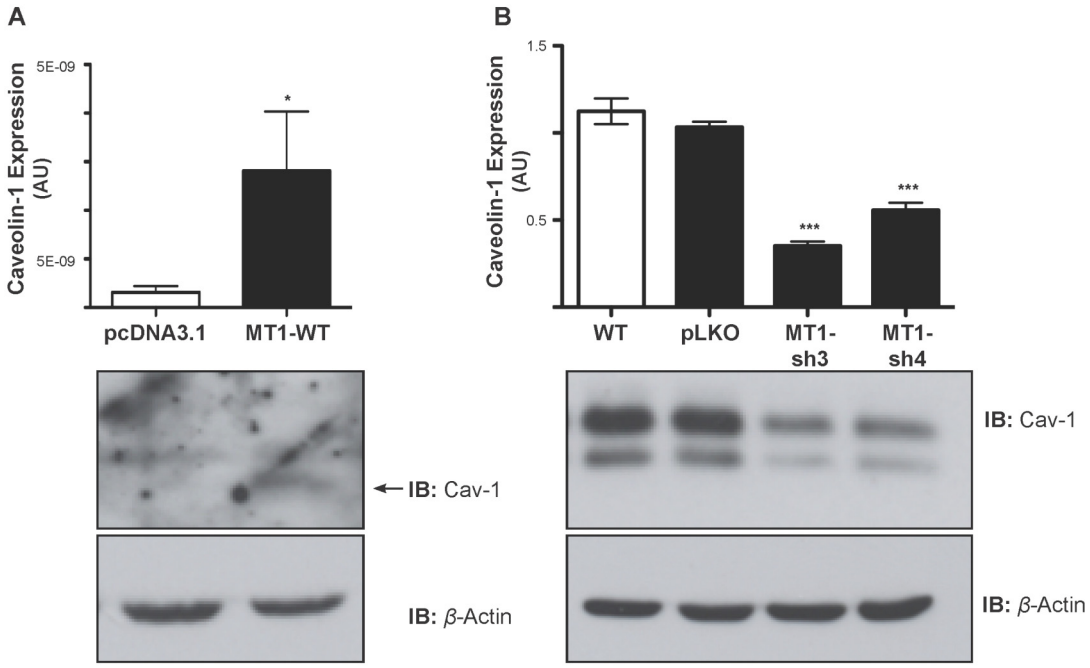

Figure 3.43: Caveolin-1 expression is dependent on MT1-MMP in MCF-7 and MDA-MB-231 cells

(A) MCF-7 cells were transfected with pcDNA3.1 control or MT1-WT. Relative expression levels of caveolin-1 were detected by TaqMan® Real-Time PCR and were normalised to the mRNA levels of the house-keeping gene GAPDH. Data represent the mean expression in arbitrary units (AU) of six independent experiments ± S.E.M. with $P < 0.05$ (*). Lysates from MT1-WT and pcDNA3.1 expressing MCF-7 cells were immunoblotted with an anti-Caveolin-1 (Cav-1) or an anti-*β*-Actin antibody. ***(B)*** MDA-MB-231 cells were transduced with 1 pfu/cell of pLKO empty lentiviral vector control or MT1-MMP targeting shRNA (MT1-sh3, MT1-sh4). Relative expression of caveolin-1 was detected by TaqMan® Real-Time PCR and was normalised to the mRNA levels of the house-keeping gene GAPDH. Data represent the mean expression in arbitrary units (AU) of six independent experiments ± S.E.M. with $P < 0.0001$ (***). Lysates from MDA-MB-231 wild-type (WT) and lentiviral transduced cells were immunoblotted with an anti-Caveolin-1 (Cav-1) or an anti-*β*-Actin antibody.

Combining these findings with the regulation of caveolin-1 expression by MT1-MMP (Figure 3.43) as well as the MT1-MMP – VEGFR-2 – pY416-Src complex-formation that is described in this thesis (Figure 3.17 - Figure 3.19), suggests that caveolin-1 may play a role in the assembly of this signalling complex. However, this remains to be further investigated (discussed in chapter 4.1.3).

3.2.5 Summary: MT1-MMP dependent VEGF-A regulation in other breast carcinoma cell lines and human mammary carcinomas

In addition to the model system MCF-7 (described in chapter 3.1), two other breast cancer cell lines were tested for the MT1-MMP effect on the regulation of VEGF-A expression.

MT1-MMP overexpression in the MT1-MMP deficient MDA-MB-453 cells induced a significant up-regulation of VEGF-A expression, similar to the results obtained in MCF-7 cells.

As a complementary approach, MT1-MMP expression was silenced in MDA-MB-231 cells using adenoviral asRNA, lentiviral shRNA or siRNA technology. The interpretation of the results are difficult due to non-specific off-target effects and a potential induction of γ-interferon responses. However, two independent RNAi approaches, using shRNA and siRNA revealed an increased VEGF-A expression following MT1-MMP gene silencing, suggesting a different MT1-MMP dependent regulatory mechanism in MDA-MB-231 cells compared to MCF-7 and MDA-MB-453 cells. In contrast, the presence of the MT1-MMP – VEGFR-2 complex, as described in MCF-7 cells, was found in all cell lines tested and MT1-MMP, VEGFR-2 and pY416-Src expression was furthermore detected *in vivo* using human mammary carcinomas. These findings indicate that the formation of the MT1-MMP – VEGFR-2 complex might be a conserved mechanism in breast cancer cells, albeit controlling different down-stream target genes.

3.3 MT1-MMP intracellular domain release

Recently a number of transmembrane proteins, including Notch-1, APP, SREBP2, LRP1 and CD44 have been reported to undergo proteolytic processing in order to release their intracellular domains, which subsequently translocate as soluble transcription factors to the nucleus [59,143-146]. Two major pathways have been reported in which transmembrane proteins were cleaved: ***(i)*** regulated intramembrane proteolysis (RIP), which is mainly dependent on the presenilin aspartyl proteinases (e.g. γ-Secretase), the rhomboid serine proteinases, the signal-peptide peptidase (SPP) or the site-2 proteinases (S2P), and ***(ii)*** regulated ubiquitin/proteasome dependent processing (RUP) [190] (chapter 1.4). However, the latter has been only described to take place in *S. cerevisiae* so far.
There is emerging evidence that MT1-MMP undergoes various forms of autocatalytic and non-autocatalytic ectodomain shedding, which has been described to be a potential mechanism for regulating MT1-MMP activity [100,274] (chapter 1.3.4.4). Autocatalytic processing leads to the formation of the membrane-anchored 44 kDa form ($G^{285} – V^{582}$) as well as the soluble released catalytic domain (18 kDa) [101,110], whereas non-autocatalytic processing of MT1-MMP results in a 50 – 52 kDa soluble fragment consistent with the entire extracellular domain [100,107,108,110]. These fragments have been found in the supernatants of various cells, including breast carcinoma, lung fibroblasts, endothelial and fibrosarcoma cells (reviewed in [274]). MT1-MMP shedding of the entire extracellular domain resulting in the secretion of the 50 – 52 kDa fragment into the medium leaves the transmembrane and intracellular domain remaining within the cell membrane. This raises the possibility that MT1-MMP ectodomain shedding is the initial step prior to processing that leads to the proteolytical release of the intracellular domain (chapter 1.4).

The aim of this part of the thesis was to investigate whether the MT1-MMP intracellular domain, which is known to be involved in various cellular responses (chapter 1.3.5), is proteolytically released and has a potential function in regulating gene transcription.

3.3.1 The MT1-MMP intracellular domain is released in a Luciferase reporter gene assay

The intramembrane proteolysis leading to the release of the intracellular domains of Notch-1, APP, SREBP2 and LRP1 in a γ-secretase or S2P dependent way was demonstrated by using a reporter gene assay (summarised in Figure 3.44A) [59,151,179,275,276]. A similar methodical approach was adapted to test whether the MT1-MMP intracellular domain (ICD) is proteolytically released.

Briefly, a construct encoding a full-length MT1-MMP with a GAL4 DNA-binding and a VP16 transactivation fusion domain (GAL4/VP16) inserted between the transmembrane and intracellular domain of MT1-MMP was used (GVMT1, Figure 3.44B). Previous attempts to fuse the GAL4/VP16 domain to the C-terminal end of the MT1-MMP ICD, as done for LRP1 and APP (Figure 3.44B), prevented trafficking of MT1-MMP to the cell surface (CH Roghi, personal communication). Proteolytic release of the carboxy-terminal part of MT1-MMP including the GAL4/VP16 fusion domain was subsequently detected by measuring the expression of a co-transfected Luciferase reporter gene under the control of a minimal GAL4-binding promoter (Figure 3.44B). Thereby, the Luciferase expression measured is proportional to the release of the MT1-MMP ICD. GAL4/VP16 fusion domain containing cDNAs of LRP1 and APP (GVLRP1 and GVAPP, Figure 3.44B), both of which undergo γ-secretase dependent RIP, were used as positive controls in this assay.

Expression of the reporter gene construct pG5luc alone or MT1-MMP wild-type (MT1-WT) was not found to induce Luciferase expression (Figure 3.44C-E). As expected, GVAPP expression in MCF-7 (Figure 3.44C) and HEK293 (Figure 3.44D) cells increased Luciferase activity ($P < 0.0001$ compared to pG5luc transfected control), whereas LRP1 induced Luciferase expression was only detected to be significantly increased in MCF-7 cells (Figure 3.44C, $P < 0.05$).

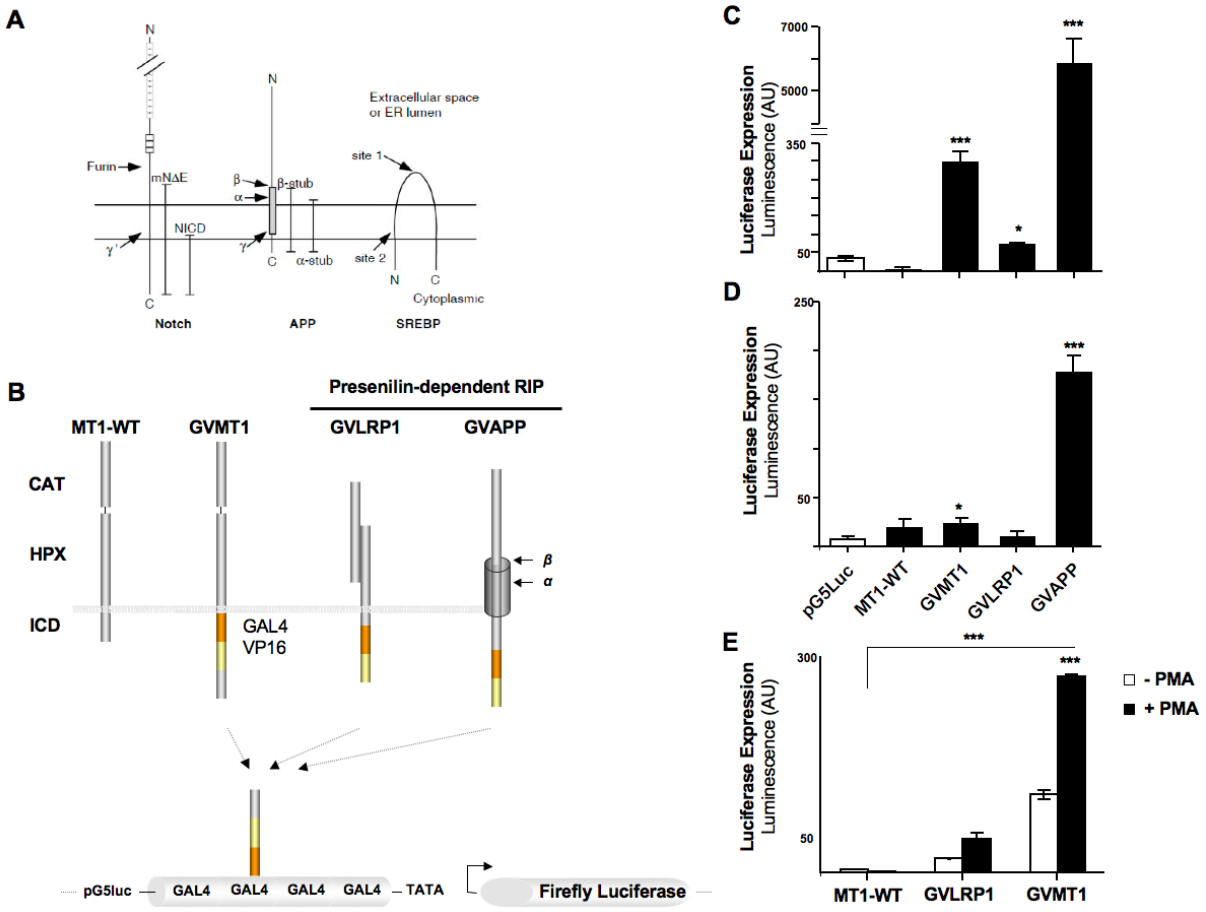

Figure 3.44: The MT1-MMP intracellular domain is proteolytically released as detetcted in a reporter gene assay

(A) Schematic representation of presenilin-or S2P dependent RIP of Notch-1, APP and SREBP. Taken from [144] ***(B)*** Schematic representation of wild-type MT1-MMP (MT1-WT) and MT1-MMP-GAL4/VP16 (GVMT1) constructs as well as the LRP1-GAL4/VP16 (GVLRP1) and APP-GAL4/VP16 (GVAPP) constructs used as positive controls. The GAL4 DNA binding domain (amino acids 1-147) and the VP16 transactivation domain of the Herpes simplex virus protein VP16 were fused between the transmembrane and intracellular domain of full-length MT1-MMP. ICD release was assessed by detection of the transcriptional activation of the co-transfected Luciferase reporter-gene under the control of a GAL4-binding minimal promoter. ***(C)*** MCF-7 cells or ***(D)*** HEK293 cells were co-transfected with the reporter gene plasmid pG5luc, control vector pCMV-*β*-Gal and either MT1-WT, GVMT1, GVLRP1 or GVAPP. The cells were lysed 24 hours after transfection and Luciferase and *β*-galactosidase activities were determined. Luciferase expression was normalised for transfection efficiency by dividing relative light unit values by those obtained for *β*-galactosidase expression. Data represent the mean Luciferase expression of three independent experiments measured in luminescence ± S.E.M. with $P < 0.05$ (*) and $P < 0.0001$ (***), Student *t*-test. ***(E)*** HEK293 cells were transfected with the reporter gene plasmid pG5luc, control vector pCMV-*β*-Gal and either MT1-WT, GVMT1 or GVLRP1 and stimulated in the absence or presence of 100 nM phorbol 12-myristate 13-acetate (PMA) for 24 hours. Luciferase reporter gene expression was corrected as described above. Data represent the mean Luciferase expression of three independent experiments measured in luminescence ± S.E.M. with $P < 0.0001$ (***), Student *t*-test.

The expression level of the Luciferase reporter gene construct was increased in MCF-7 cells overexpressing GVMT1 by ~23 fold compared to pG5luc transfected control ($P < 0.0001$), 5.4 fold more than the positive control LRP1 (Figure 3.44C). A similar result was

obtained in GVMT1 expressing HEK293 cells (Figure 3.44D, $P < 0.05$ compared to pG5luc transfected control). Incubation of the cells with 100 nM phorbol 12-myristate 13-acetate (PMA), which has been shown to induce ectodomain shedding of MT1-MMP [100,108,277] and to increase intracellular domain release of LRP1 [151] (Figure 3.44E), amplified the increase in Luciferase expression by ~147 fold in GVMT1 expressing cells compared to MT1-WT transfected control (Figure 3.44E, $P < 0.0001$).

These findings indicate that the MT1-MMP ICD is released as shown in a reporter gene assay. Since the GAL4 DNA-binding sequence, which is still attached to the released MT1-MMP ICD following cleavage, has a nuclear translocation sequence (NLS) [278], this assay is not sufficient to demonstrate a nuclear translocalisation of the MT1-MMP ICD itself.

3.3.2 Src and proteasome activities are required for the MT1-MMP intracellular domain release

It was subsequently tested whether the activation of Luciferase activity by GVMT1, as previously observed (Figure 3.44, C-E), is dependent on proteinase activity. A comparison of transmembrane domain (TMD) sequences of proteins known to be processed in a presenilin dependent way to the TMD sequence of MT1-MMP, revealed a potential γ-secretase cleavage site at the MT1-MMP AV^{559} motif (Figure 3.45A, empty arrowhead), whereas the intracellular K^{581} residue might provide a target for the proteasome/ubiquitin system involved in RUP.

Various inhibitors of γ-secretase, the proteasome, Src and rhomboid proteinases were tested and the MT1-MMP ICD release was detected using the reporter gene assay as previously described. Inhibitors of site-2 proteinases (S2P) and signal-peptide peptidases (SPP) were disregarded in this initial screen since these proteinases were described to process type-II transmembrane proteins only (chapter 1.4.1).

As observed before, GVMT1 expressing cells increased the expression of the reporter gene significantly compared to the MT1-WT expressing control (Figure 3.45B-D, Figure 3.44C). Inhibition of Src by using PP2 and inhibition of the proteasome (Lactacystin, MG-132, Epoxomicin, *clasto*-Lactacystin β-lactone) led to a decrease in Luciferase expression as compared to the DMSO control (Figure 3.45C, D), whereas inhibition of γ-secretase (γ-secretase inhibitor IX (DAPT), XVII (31C), XXI (Compound E)) and Rhomboid

proteinases (DCI) did not alter the Luciferase activity induced by GVMT1 (Figure 3.45B, D). Luciferase activity was furthermore found to decrease in a dose-dependent way following treatment of GVMT1 expressing cells with increasing concentrations of PP2 or Lactacystin (Figure 3.45E).

These findings indicate that the MT1-MMP ICD is not released in a γ-secretase dependent way but requires Src and proteasome activities as detected in a reporter gene assay.

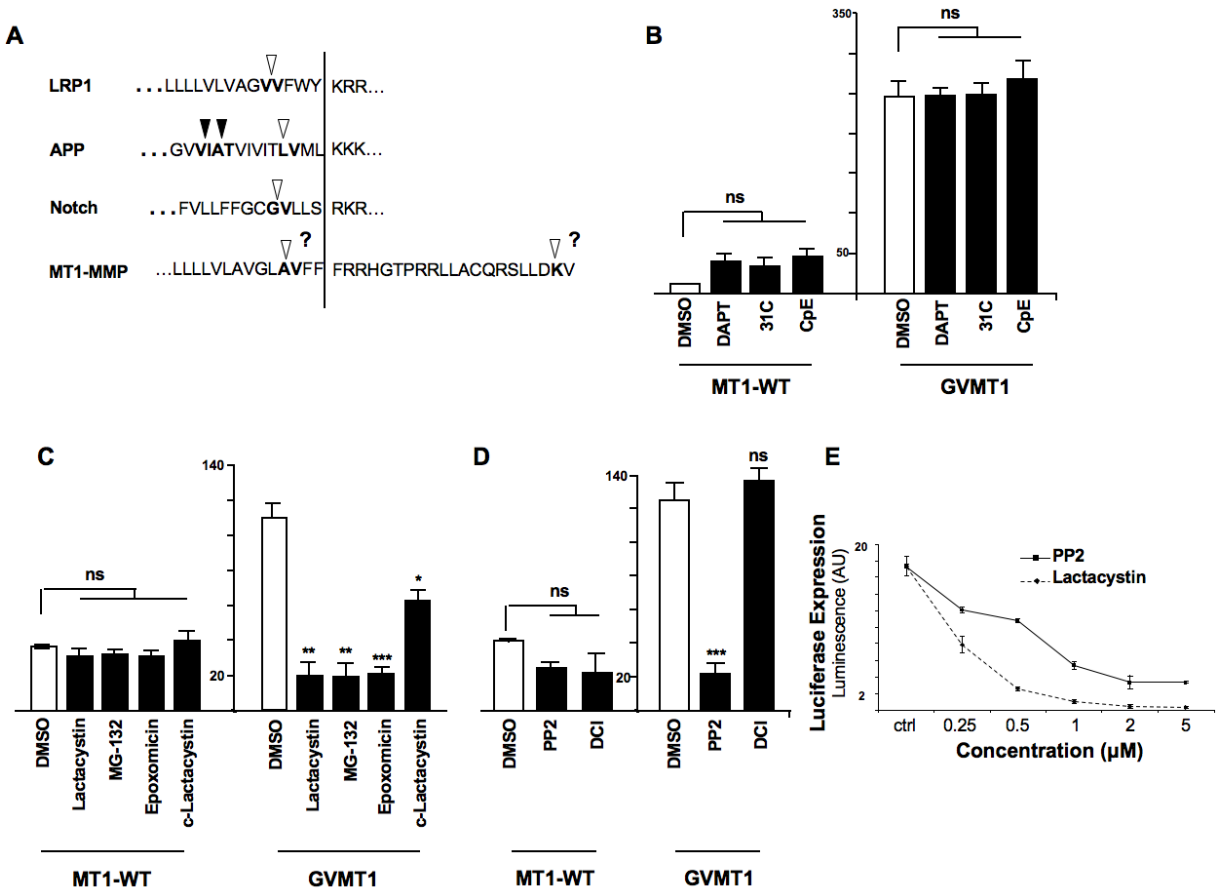

Figure 3.45: The MT1-MMP ICD is released in a Src and proteasome dependent mechanism

(A) Comparison of the amino acid sequences of the presenilin cleavage sites within the LRP1, APP and Notch transmembrane domains with the MT1-MMP TMD sequence. The S3 cleavage site of Notch, the corresponding γ-secretase cleavage site in APP as well as a putative γ-secretase cleavage site in MT1-MMP or an ubiquitination site within the ICD are indicated by open arrowheads. The black arrowheads show the APP γ-secretase cleavage sites that lead to the production of Aβ 40 and Aβ 42. ***(B-E)*** MCF-7 cells were co-transfected with the reporter gene plasmid pG5luc, control vector pCMV-β-Gal and either MT1-WT or GVMT1. Cells were incubated for 24 hours with either DAPT, 31C or Compound E (B), Lactacystin, MG-132, Epoxomicin and *clasto*-Lactacystin β-Lactone (C), DCI and PP2 (D) or various concentrations of PP2 and Lactacystin, as indicated (E). Luciferase expression was normalised for transfection efficiency by dividing relative light unit values by those obtained for β-galactosidase expression. Data represent the mean luminescence of three independent experiments measured in luminescence ± S.E.M. with $P < 0.05$ (*); $P < 0.001$ (**); $P < 0.0001$ (***), Student *t*-test. *ns*, non-significant.

3.3.3 The MT1-MMP transmembrane and intracellular domains are both required for proteolytic cleavage

RIP has been shown to take place within the bilipid layer of the plasma membrane targeting the transmembrane domains of various proteins including APP, Notch-1, SREBP2 and LRP1. In contrast, the release observed of the MT1-MMP ICD was shown to be dependent on the intracellularly active Src and Proteasome function (Figure 3.45C-E) and thus suggests that the MT1-MMP ICD is proteolytically targeted directly during this process.

To investigate the requirement for the MT1-MMP transmembrane and intracellular domains in this proteolytic event independently, both domains were separately exchanged for the corresponding APP domains (Figure 3.46A, B). MCF-7 cells were transfected with MT1-WT, GVMT1 and GVMT1 containing either the APP transmembrane domain (Figure 3.46A, GVMT1-APP-TMD) or an APP intracellular domain (Figure 3.46B, GVMT1-APP-ICD). GVAPP expressing cells were assayed as a positive control.

As previously observed, expression of GVMT1 induced Luciferase reporter gene expression significantly compared to MT1-WT transfected cells ($P < 0.0001$; Figure 3.46C, Figure 3.44C - E, Figure 3.45). This effect was ablated after incubation with PP2 and Lactacystin as shown before (Figure 3.45C – E, Figure 3.46C; $P < 0.0001$ and $P < 0.05$, respectively, compared to DMSO control), but not following treatment with the γ-secretase inhibitor Compound E (Figure 3.46C and Figure 3.45B). In contrast, Luciferase expression in GVAPP expressing cells was effectively reduced by Compound E treatment ($P < 0.0001$ compared to DMSO control) but not after Src and Proteasome inhibition (Figure 3.46C). Compound E treatment ablated reporter gene expression in GVMT1-APP-TMD but not in GVMT1-APP-ICD transfected cells. This observation was expected since γ-secretase inhibition attenuates presenilin dependent intramembrane cleavage of APP. Interestingly, both constructs, GVMT1-APP-TMD and GVMT1-APP-ICD were shown to induce less reporter gene expression following PP2 and Lactacystin treatments as compared to DMSO control (Figure 3.46C, $P < 0.001$ and $P < 0.05$, respectively), suggesting that both domains are necessary for the proteolytic release of the MT1-MMP ICD.

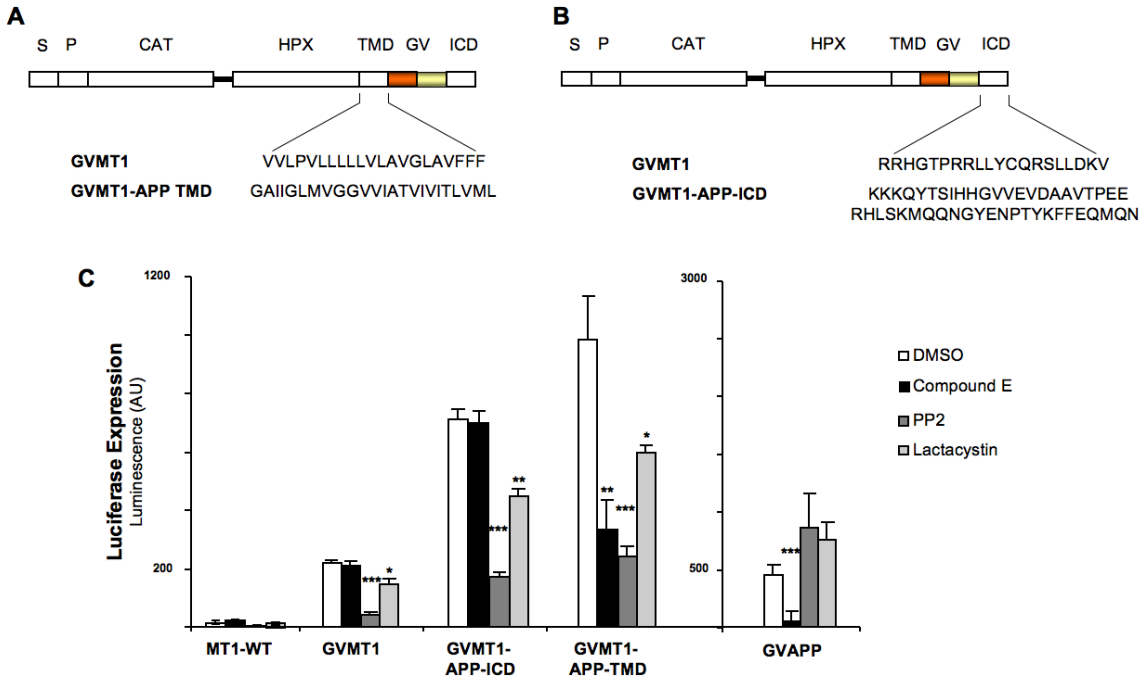

Figure 3.46: The MT1-MMP intracellular and transmembrane domains are both involved in the Src and Proteasome dependent proteolytic cleavage

(A) The transmembrane domain of the GVMT1 construct was exchanged to that of APP (GVMT1-APP-TMD) or ***(B)*** the MT1-MMP intracellular domain was replaced with the APP ICD (GVMT1-APP-ICD). ***(C)*** MCF-7 cells were co-transfected with the reporter gene plasmid pG5luc, the control vector pCMV-*β*-Gal and either MT1-WT, GVMT1, GVMT1-APP-ICD, GVMT1-APP-TMD or GVAPP as control. Cells were incubated with Compound E, PP2, Lactacystin or DMSO as control. Luciferase reporter gene expression was detected and normalised for transfection efficiency by dividing relative light unit values by those obtained for *β*-galactosidase expression. Data represent the mean Luciferase expression of three independent experiments measured in luminescence ± S.E.M. with $P < 0.05$ (*), $P < 0.001$ (**) and $P < 0.0001$ (***), Student *t*-test.

3.3.4 The MT1-MMP intracellular domain is enriched in the nucleus

The induction of reporter gene expression following GVMT1 expression previously described in this thesis (Figure 3.44 - Figure 3.46), raised the possibility that the MT1-MMP ICD might translocte into the nucleus to affect gene expression as either a transcriptional regulator or co-factor. To test this hypothesis, MCF-7 cells were transfected with full-length MT1-MMP (MT1-WT) and the localisation of the MT1-MMP extracellular and intracellular domain was assessed by confocal microscopy using antibodies raised against the MT1-MMP ICD (ab28209) and MT1-MMP extracellular domain (ECD; N175/6).

As shown in Figure 3.47A, antibodies detecting both domains co-localised within the cytoplasm and within the perinuclear region, potentially within the trans-Golgi network where MT1-MMP was previously observed [127]. In contrast, staining was routinely

observed in the nuclear region using the anti-MT1-MMP ICD antibody but not for the ECD specific antibody (Figure 3.47A, *iv*). Staining on empty vector (pcDNA3.1) transfected control cells revealed that the nuclear staining detected by the anti-MT1-MMP ICD antibody was specific for MT1-MMP expression and does not detect non-specific backgound levels (Figure 3.47A, *iii*, arrows).

To confirm these findings using a biochemical approach, cells were transfected with MT1-WT and GVMT1 as control, since the GAL4/VP16 fusion domain is expected to translocate to the nucleus due to its intrinsic NLS, and cell extracts were separated into nuclear and cytoplasmic fractions followed by immunoblotting. Pro-MT1-MMP, active MT1-MMP as well as its ~44 kDa degradation product could be detected within the cytoplasmic fraction. However the ~3 kDa band expected for the MT1-MMP ICD was not found within the nuclear extract in both transfectants, even after blocking the nuclear export by Leptomycin B treatment (Figure 3.47B). Since the intracellular domain of GVMT1 transfected cells was also not found to be enriched in the nucleus, this result is most likely to be a consequence of a lack of sensitivity by either the antibody used or by the detection method itself.

Intramembrane proteolysis has been shown to occur following ectodomain shedding of transmembrane proteins. This first proteolytic step was shown to be mainly mediated by metalloproteinase activity (chapter 1.4). Various publications have shown MT1-MMP to undergo ectodomain shedding, leading to the accumulation of ~15 kDa and ~50 – 52 kDa fragments within the medium [100,274,277]. These fragments have been reported to be released due to an autocatalytic (Figure 3.47C (1)) or non-autocatalytic process (Figure 3.47C (2)). Non-autocatalytic processing has been recently shown to be a two-step mechanism, with an unknown protease involved in the first cleavage and an ADAM to mediate the generation of the 52 kDa fragment [112].

In order to test whether ectodomain shedding is taking place in MCF-7 cells, cells were transfected with MT1-WT or pcDNA3.1 control and were stimulated with PMA for 24 hours, where indicated, to induce the previously described ectodomain shedding of MT1-MMP [100,108,277]. Both, the ~15 kDa and ~50 – 52 kDa fragments were detected in the conditioned medium of MT1-WT expressing MCF-7 cells (Figure 3.47D), indicating that MT1-MMP ectodomain shedding occurs in MCF-7 cells. However, shedding was not found to be altered following PMA stimulation.

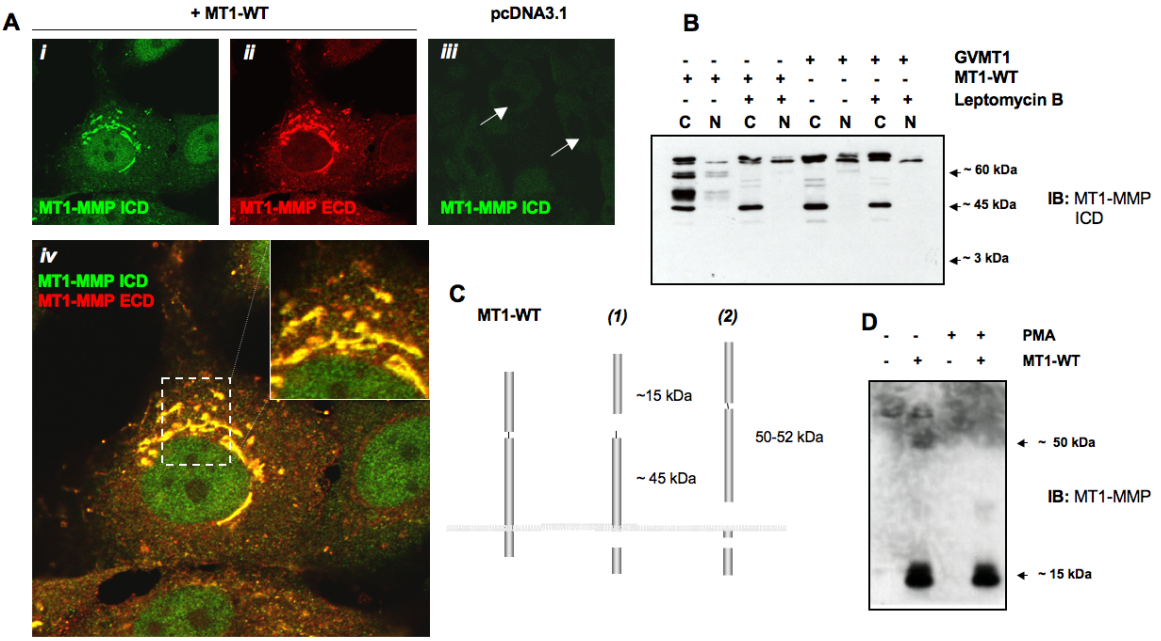

Figure 3.47: The MT1-MMP intracellular domain is released and is detected in the nucleus of MCF-7 cells by immunostaining

(A) MCF-7 cells were transfected with either MT1-WT (*i*, *ii*, *iv*) or pcDNA3.1 empty vector control (*iii*) and the localisation of MT1-MMP was detected with an anti-MT1-MMP ICD specific antibody (ab28209, AlexaFluor® 488 secondary, *i, iii*) and an anti-MT1-MMP antibody raised against the ECD (N175/6, AlexaFluor® 546 secondary, *ii*). Inset panel shows magnified portion of the merged image, as indicated (dashed square). Arrows in *iii* indicate that the nuclear region is not stained unspecifically in pcDNA3.1 transfected cells. ***(B)*** MCF-7 cells were transfected with MT1-WT, GVMT1 or pcDNA3.1 vector control and treated with Leptomycin B, where indicated. Nuclear and cytoplasmic fractions were isolated and immunoblotted with an anti-MT1-MMP ICD antibody (ab28209). ***(C)*** Schematic representation of MT1-MMP ectodomain shedding due to autocatalytic (1) or non-autocatalytic (2) processing (adapted from [274]). ***(D)*** MCF-7 cells were transfected with MT1-WT or pcDNA3.1 control and were treated with 100 nM PMA for 24 hours where indicated. The conditioned medium was collected, total protein was precipitated and immunoblotted with an anti-MT1-MMP ECD antibody (N175/6).

In order to quantify the previously shown nuclear staining of the MT1-MMP ICD (Figure 3.47A) and to test whether the nuclear localisation of the ICD observed correlates with the potential Src and Proteasome dependent ICD release, MT1-WT expressing MCF-7 cells were stained with an anti-MT1-MMP ICD or ECD antibody, as described before. Nuclear staining intensities were subsequently measured using the iCys™ laser scanning cytometer as described in chapter 2.2.4.3.3.

Quantification of the nuclear staining intensities revealed that the fluorescence detected by the MT1-MMP extracellular domain antibody was similar between MT1-WT and pcDNA3.1 control transfected cells indicating that only background levels of fluorescence were detected within the nuclear region (Figure 3.48B). A similar detection level of anti-MT1-MMP ECD antibody mediated fluorescence in the nucleus was obtained after

treatment of MT1-WT expressing cells with PP2, Lactacystin or PMA. In contrast, staining with the anti-MT1-MMP ICD antibody led to a significant increase in nuclear fluorescence in MT1-MMP expressing cells compared to pcDNA3.1 transfected controls (Figure 3.48A).

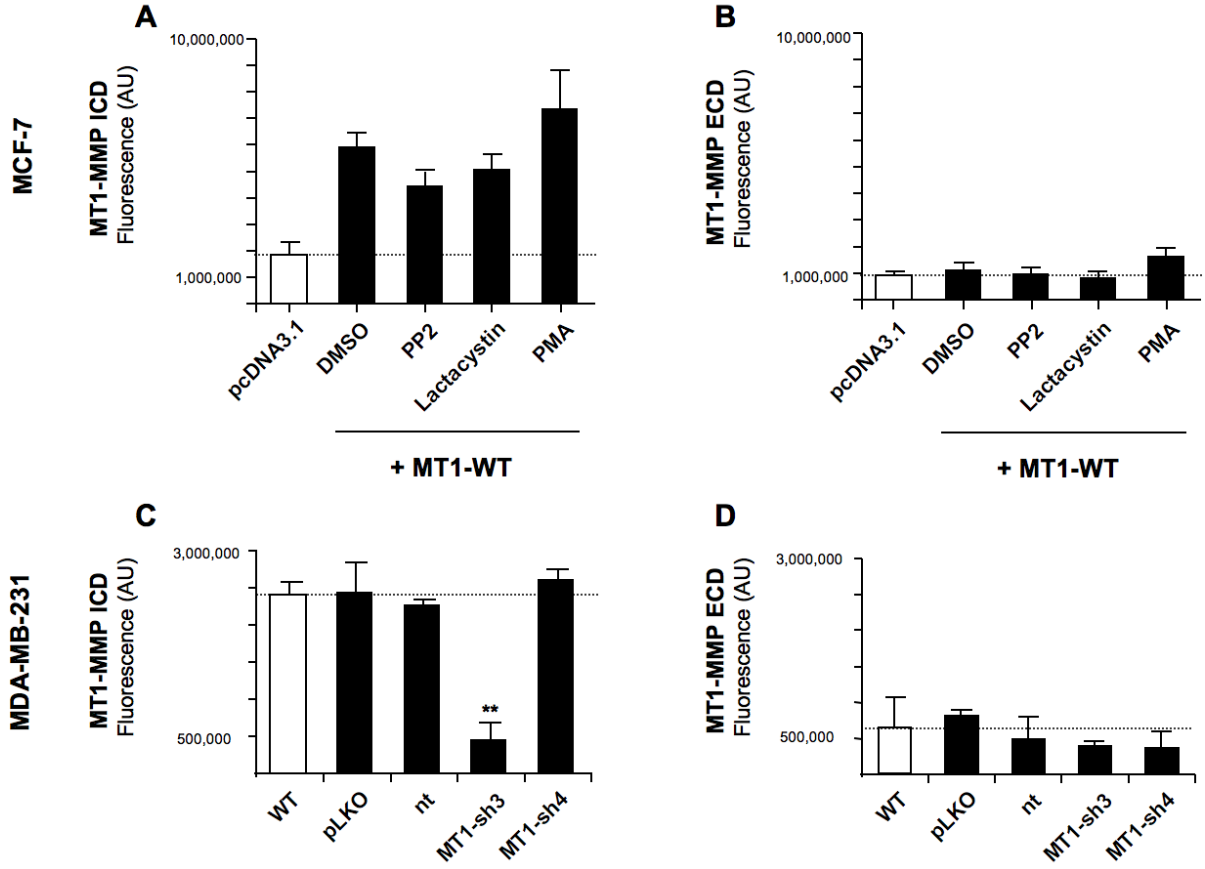

Figure 3.48 Nuclear localisation of the MT1-MMP intracellular domain is reduced by Src- and Proteasome inhibition

(A,B) MCF-7 cells were transfected with either pcDNA3.1 vector control or MT1-WT and treated for 24 hours with PP2, Lactacystin, PMA or DMSO as a control. MT1-MMP was detected with an anti-MT1-MMP intracellular domain antibody (ab28209, AlexaFluor® 488 secondary) or an anti-MT1-MMP extracellular domain specific antibody (N175/6, AlexaFluor® 488 secondary). Bar-graphs represent the quantification of nuclear staining intensities of both antibodies by scanning ~10,000 cells per biological triplicate using the CompuCyte iCys™ laser scanning cytometer ± 95% Confidence Intervals. The nuclear region was defined by counter-staining with DAPI as described in chapter 2.2.4.3.3. Dashed lines indicate the mean fluorescence intensity of pcDNA3.1 transfected cells. ***(C,D)*** MDA-MB-231 cells were transduced with 1 pfu/cell pLKO empty lentiviral vector control, non-targeting shRNA control (nt) or MT1-MMP targeting shRNA (MT1-sh3 and MT1-sh4). MT1-MMP was detected with an anti-MT1-MMP intracellular domain antibody (ab28209, AlexaFluor 488® secondary) or an anti-MT1-MMP extracellular domain specific antibody (N175/6, AlexaFluor 488® secondary). Bar-plots represent the quantification of nuclear staining intensities of both antibodies by scanning ~10,000 cells per biological triplicate using the CompuCyte iCys system ± 95% Confidence Intervals. The nuclear region was defined by counter-staining with DAPI as described in chapter 2.2.4.3.3. Dashed lines indicate the mean fluorescence intensity of MDA-MB-231 wild-type cells.

Inhibition of Src and Proteasome activity using PP2 or Lactacystin respectively reduced the detected nuclear fluorescence significantly compared to the DMSO control (Figure

3.48A). Stimulation of cells with PMA augmented the level of nuclear MT1-MMP ICD detection, albeit not significantly (compared to DMSO treated control). These findings are consistent with the data obtained from the GAL4/VP16 reporter chimera (Figure 3.44 and Figure 3.45) and indicate that the MT1-MMP ICD localisation increases in the nucleus in a Src and proteasome dependent way.

To confirm that the MT1-MMP ICD detection in MCF-7 cells is not a cell specific observation or a potential artefact of MT1-MMP overexpression, the nuclear localisation of the ICD was assessed in MDA-MB-231 cells, which endogenously express MT1-MMP (Figure 3.32). As a control, the expression of MT1-MMP was silenced using shRNA as described previously (chapter 3.2.1.3). Since MT1-MMP silencing is used only as a control for detecting the protease itself rather than investigating MT1-MMP down-stream effects, the previously described limitations of the shRNA approach due to off-target effects and a potential γ-interferon response, were considered negligible (Figure 3.37 and Figure 3.38).

The detection of the MT1-MMP ICD and ECD within the nuclear region led to similar results in MDA-MB-231 cells as in MCF-7 cells. As shown in Figure 3.48C, the MT1-MMP intracellular domain was detected in wild-type cells, pLKO and non-targeting (nt) shRNA controls but its fluorescent detection was significantly reduced in MT1-MMP shRNA3 expressing cells. In contrast, the nuclear MT1-MMP ICD detection level of shRNA4 transduced cells was not affected compared to wild-type MDA-MB-231 cells. These findings are in agreement with the weaker knockdown of MT1-MMP protein expression in shRNA4 expressing cells compared to shRNA3 as determined by immunoblotting (Figure 3.36B). The MT1-MMP extracellular domain staining was detected at low levels within the nuclear region and was not affected by MT1-MMP knockdown (Figure 3.48D).

These data indicate that in two different breast cancer cell lines that are either deficient in MT1-MMP expression or express the protease at high levels, the intracellular domain staining but not the extracellular domain staining was detected within the nuclear region, suggesting that MT1-MMP ICD nuclear accumulation may be a general observation in breast cancer cells.

It has been shown previously that the intracellular domain of MT1-MMP wild-type transfected MCF-7 cells could not be detected in the nucleus by immunoblotting (Figure 3.47B), potentially due to the low amounts of MT1-MMP ICD enriched within the nuclear fraction or due to the lack of sensitivity of the antibody or detection method used. Blocking

the nuclear export by using Leptomycin B and thus enriching proteins within the nuclear region, was not sufficient to detect the MT1-MMP ICD (Figure 3.47B). Therefore, another approach using a soluble biotinylated MT1-MMP ICD penetratin peptide or a biotinylated control penetratin peptide was used in order to detect the MT1-MMP ICD in the nucleus using biochemical detection methods (Figure 3.49A). Thus, the Biotin tag facilitates MT1-MMP ICD detection by using a different antibody.

The penetratin peptide consists of a 16 amino acid sequence (RQIKIWFQNRRMKWKK) taken from the *Drosophila melanogaster* Antennapedia transcription factor which has the ability to penetrate cell membranes [279]. MCF-7 cells were incubated for 3 hours with 25 µM of the MT1-MMP ICD or control penetratin peptide and cells were subsequently trypsinised to remove the residual penetratin peptide from the cell surface, which had not translocated into the cytoplasm. The nuclear and cytoplasmic protein fractions were isolated, and the purity of nuclear protein isolation was confirmed by immunoblotting. The isolated nuclear fraction was found to be positive for the marker of the nuclear envelope Lamin B1 and negative for TGN46, a marker of the trans-Golgi network (TGN) (Figure 3.49B). Both biotinylated peptides could be readily detected in the whole cell lysates (Input), whereas only the MT1-MMP ICD penetratin peptide was found within the cytoplasmic and nuclear fraction (Figure 3.49B).

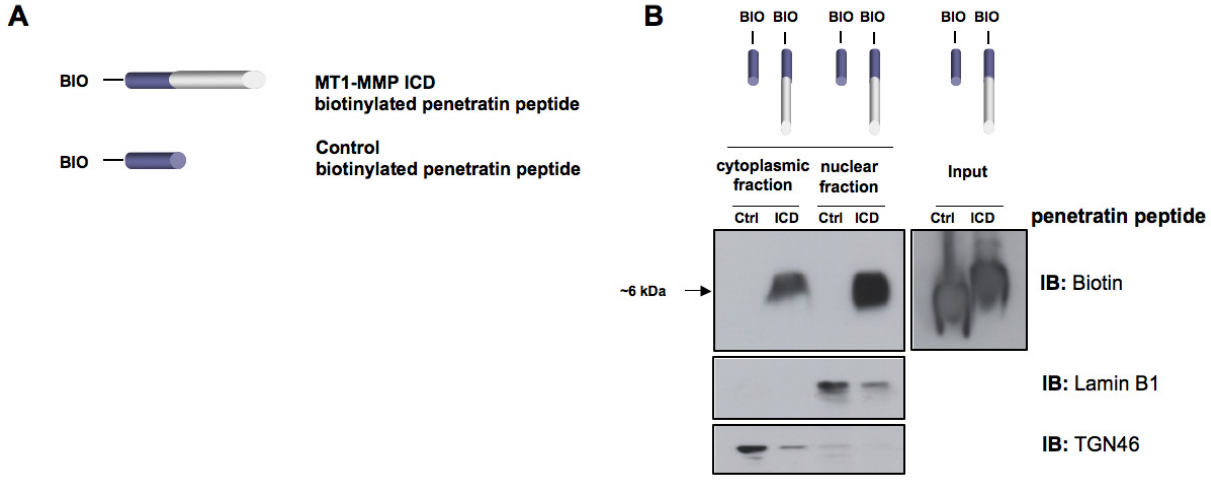

Figure 3.49: The MT1-MMP ICD is found in the nuclear fraction of MCF-7 cells

(A) Schematic representation of the MT1-MMP penetratin peptide constructs used. ***(B)*** MCF-7 cells were incubated with 25 µM MT1-MMP ICD or control biotinylated penetratin peptide for 3 hours. Proteins were isolated in nuclear and cytoplasmic fractions and both fractions as well as Input controls (whole cell lysate) were immunoblotted with an anti-Biotin, an anti-Lamin B1 or an anti-TGN46 antibody.

These findings suggest that the control peptide is most likely membrane associated as it is not detected within the cytoplasmic fraction but is present in the whole cell lysate (Input). In contrast, the MT1-MMP ICD could be detected within the nuclear fraction (Figure 3.49B), indicating that the biotinylated soluble MT1-MMP ICD provides a promising tool to investigate nuclear localisation due to its highly sensitive Biotin-tag detection.

3.3.5 The MT1-MMP intracellular domain is enriched in nuclei *in vivo*

The MT1-MMP ICD was detected in the nucleus of MCF-7 and MDA-MB-231 cells by immunostaining and subsequent quantification (Figure 3.47A, Figure 3.48A, C).

To test whether the MT1-MMP ICD is also enriched in the nuclear region *in vivo*, human mammary carcinoma tissue sections were obtained, embedded in paraffin and immunostained with an anti-MT1-MMP ICD antibody (ab28209) (in collaboration with Dr. Bence Sipos). Representative sections derived from two different mammary tumours are shown in Figure 3.50B and E. Notably, the MT1-MMP ICD was detected in the cytoplasma and nuclei of tumour cells (Figure 3.50C, F; black arrows). Immune cells, which infiltrated the tumour mass, also revealed a membrane-associated and nuclear MT1-MMP ICD staining pattern (Figure 3.50A, D; empty arrowheads). In contrast, detection of MT1-MMP with the extracellular domain specific anti-MT1-MMP antibody revealed the absence of MT1-MMP ECD within the nuclear area (Figure 3.42).

These preliminary immunohistochemical stainings of human mammary carcinoma samples demonstrate that the MT1-MMP ICD is also enriched in the nuclei of tumour cells *in vivo*, emphasising the relevance of the MT1-MMP ICD release in human breast carcinomas. A comprehensive study using breast invasive ductal carcinoma tissue microarrays (US Biomax, Inc., Heidelberg, GER) is currently being performed.

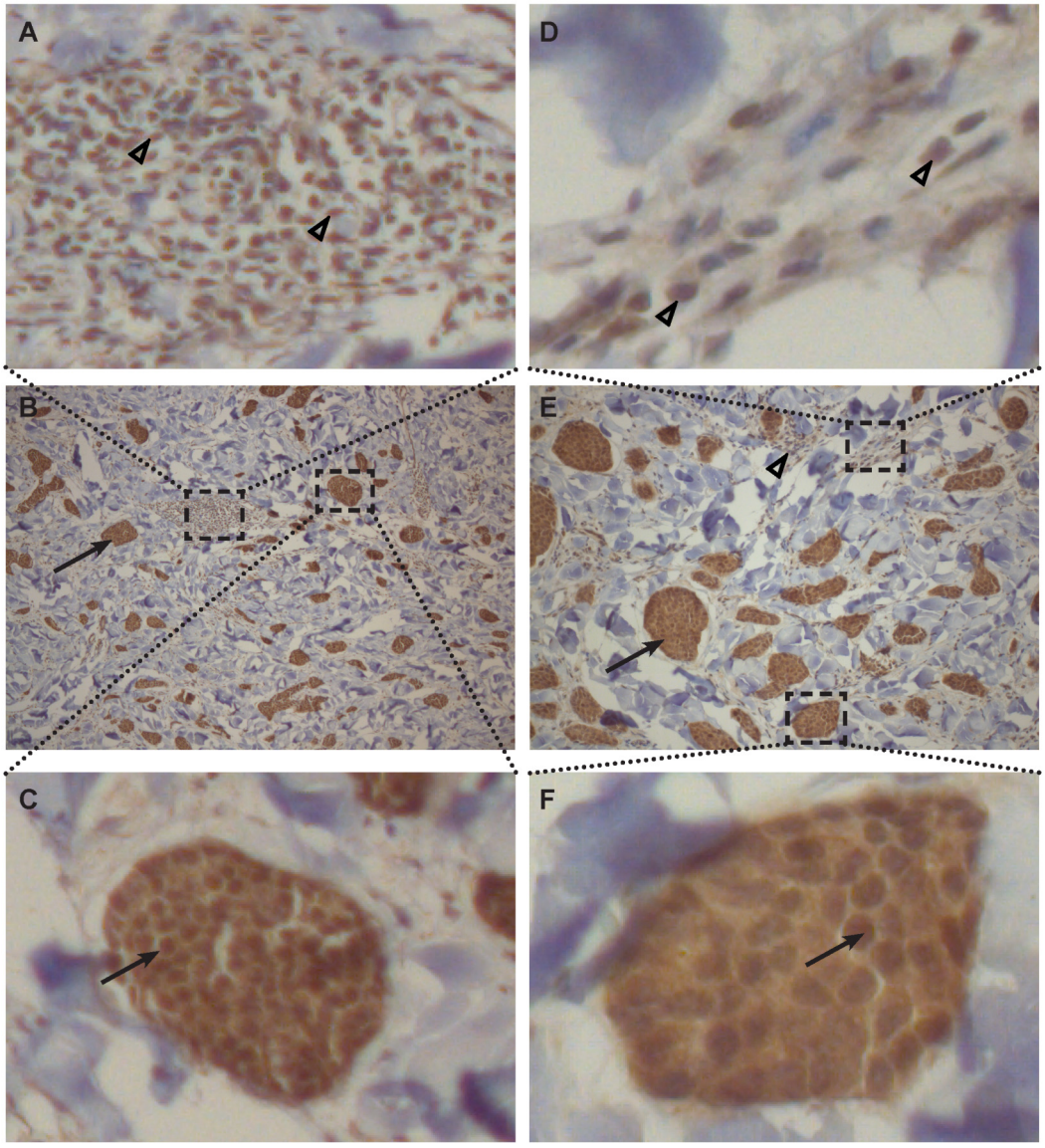

Figure 3.50: The MT1-MMP ICD is detected in the nuclei of human mammary carcinoma tissue sections

Representative samples of paraffin-embedded sections derived from two human breast carcinomas were immunostained with an anti-MT1-MMP ICD (ab28209) antibody. Black arrows indicate the cytoplasmic and nuclear staining of tumour cells, whereas empty arrowheads show membrane-associated and nuclear staining pattern of infiltrating immune cells. Upper and lower panels (A and D, C and F) show magnified portions of each image (B and E), as indicated (dashed squares). Tissue specimens were counterstained with 50 % haemalaun. 100 × magnification.

3.3.6 Identification of MT1-MMP nuclear binding proteins

The previoulsy demonstrated enrichment of the MT1-MMP ICD in MCF-7 cells using immunofluorescence quantification (Figure 3.48A) and the detection of a soluble biotinlylated MT1-MMP ICD within the nuclear fraction by immunoblotting (Figure

3.49B), raised the possibility that the MT1-MMP ICD may associate with nuclear proteins. In order to test whether the MT1-MMP ICD shown to be enriched in the nuclear fraction is interacting with nuclear proteins, MCF-7 cells were transfected with wild-type MT1-MMP (MT1-WT) or pcDNA3.1 control. Protein extracts were isolated from nuclear and cytoplasmic fractions as previously described (chapter 2.2.3.3). Separation of the nuclei from the cytoplasm and membrane fractions was verified by microscopy after each homogenisation step (Figure 3.51A) as well as by immunoblotting with an anti-Lamin B1 or anti-TGN46 antibody, markers of the nuclear or trans-Golgi network, repectively (Figure 3.51B).

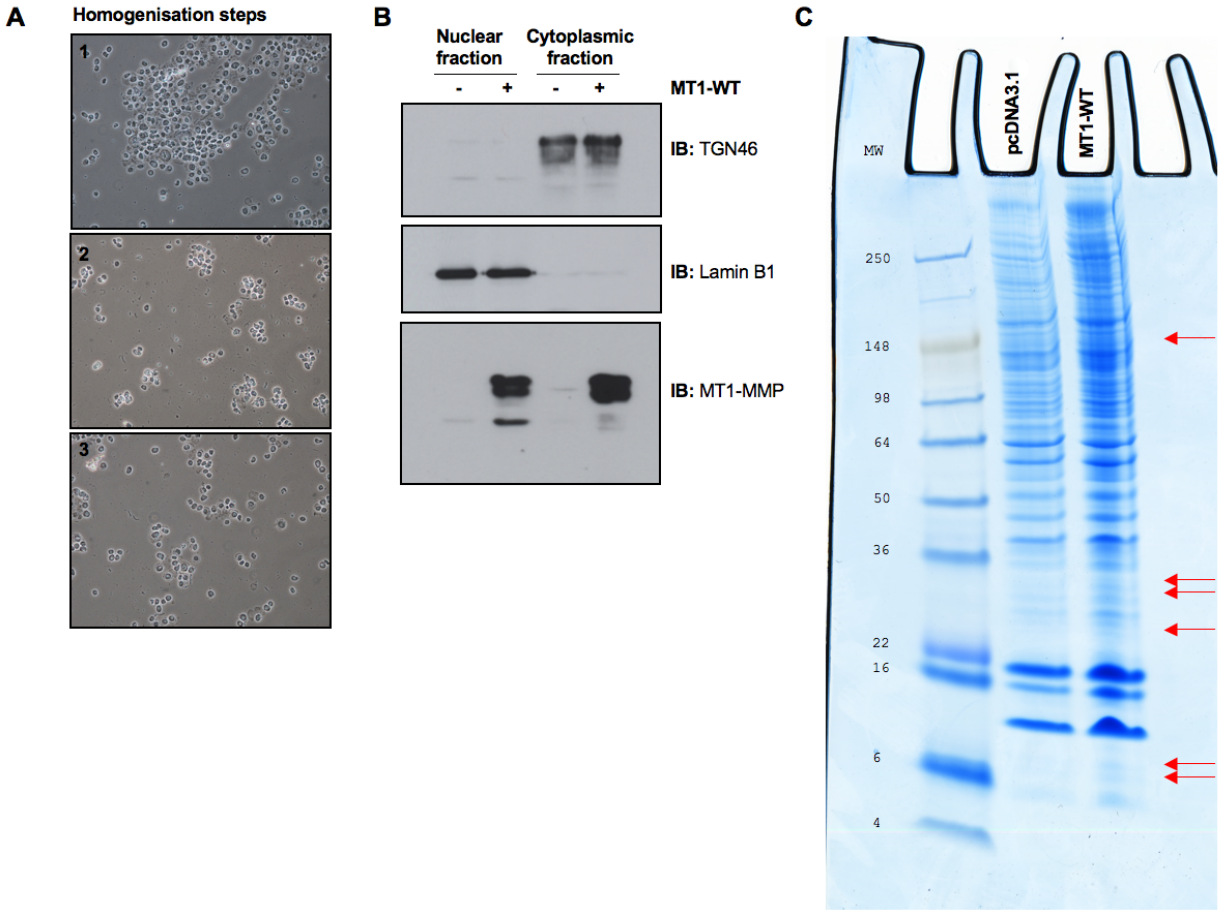

Figure 3.51: Nuclear immunoprecipitation with MT1-MMP intracellular domain specific antibody

(A) Images taken from different steps of mechanical homogenisation. ***(B)*** Western Blot analysis of nuclear and cytoplasmic fractions with an anti-Lamin B1 antibody as nuclear marker, an anti-TGN46 antibody as marker for the trans-Golgi network or an anti-MT1-MMP antibody (LEM-2/15.8). ***(C)*** Proteins of the nuclear fraction, derived from cells transfected with MT1-WT or pcDNA3.1 empty vector control, were immunoprecipitated with an anti-MT1-MMP ICD antibody (ab28209) and total protein was visualised by Coomassie blue staining. Red arrows indicate protein-bands that are present only in the MT1-WT transfected sample.

The nuclear fraction was subsequently immunoprecipitated with an anti-MT1-MMP ICD antibody (ab28209) and immunoprecipitates were run on a 4 – 20% gradient gel (Figure 3.51C). Total protein staining using Coomassie blue revealed proteins in the MT1-MMP expressing sample which were absent in the pcDNA3.1 transfected control, as indicated by red arrows (Figure 3.51C).

These findings indicate that proteins were immunoprecipiated with the anti-MT1-MMP ICD antibody in the nuclear fraction. Mass spectrometry will be performed in order to identify the proteins that were found in a complex with the MT1-MMP ICD.

3.3.7 The MT1-MMP intracellular domain is ubiquitinated

Although the MT1-MMP ICD was found in the nucleus using a tagged penetratin peptide (Figure 3.49B) it was not detected in MT1-WT transfected cells using biochemical detection methods (Figure 3.47B). Therefore, a different approach was applied to test for MT1-MMP ICD enrichment in the nuclear fraction of MCF-7 cells by using a double-tagged MT1-MMP mutant (MT1-MYC-FLAG, Figure 3.52A) in order to ***(i)*** use an alternative method to the penetratin peptide and ***(ii)*** to test whether the lack of sensitivity of the anti-MT1-MMP ICD antibody (ab28209) by immunoblotting is the reason that the MT1-MMP ICD was not detected in the nuclear fraction of wild-type transfected cells (Figure 3.47B).

Cells were transfected with the truncated double-tagged MT1-MMP mutant (MT1-MYC-FLAG), which has a Myc tag fused to its intracellular domain and a Flag tag attached to its extracellular domain (Figure 3.52A), and the nuclear fraction was isolated. Immunoblotting with an anti-Myc antibody directed against the intracellular tag, revealed that in contrast to the expected ~5 – 6 kDa fragment, a higher band at approximately ~16 kDa was observed in the MT1-MYC-FLAG transfected cells compared to pcDNA3.1 transfected control (Figure 3.52B).

The difference in the molecular weight of ~8 - 10 kDa as well as the previous findings indicating that the MT1-MMP ICD release occurs in a proteasome dependent way (Figure 3.45) raised the possibility that the MT1-MMP ICD could be post-translationally modified by ubiquitination. The MT1-MMP intracellular domain has a unique intracellular K^{581} residue, which might be a potential ubiquitination site (Figure 3.45A, arrowhead). In order to test this hypothesis, MCF-7 cells were transfected with MT1-WT, an HA-tagged

Ubiquitin or an HA-tagged K11,27,29,48,63R Ubiquitin mutant, which prevents the formation of poly-ubiquitin chains occurring during ubiquitination. Immunoprecipitation of whole cell lysates with an anti-MT1-MMP ICD antibody and immunoblotting with an anti-HA antibody revealed that MT1-MMP and Ubiquitin interact. A characteristic smear of ubiquitin detection was observed in MT1-WT and Ubiquitin expressing cells, as well as a single band in cells expressing MT1-MMP and the Ubiquitin mutant at a molecular weight corresponding to full-length ubiquitinated MT1-MMP (~70 kDa, Figure 3.52C).

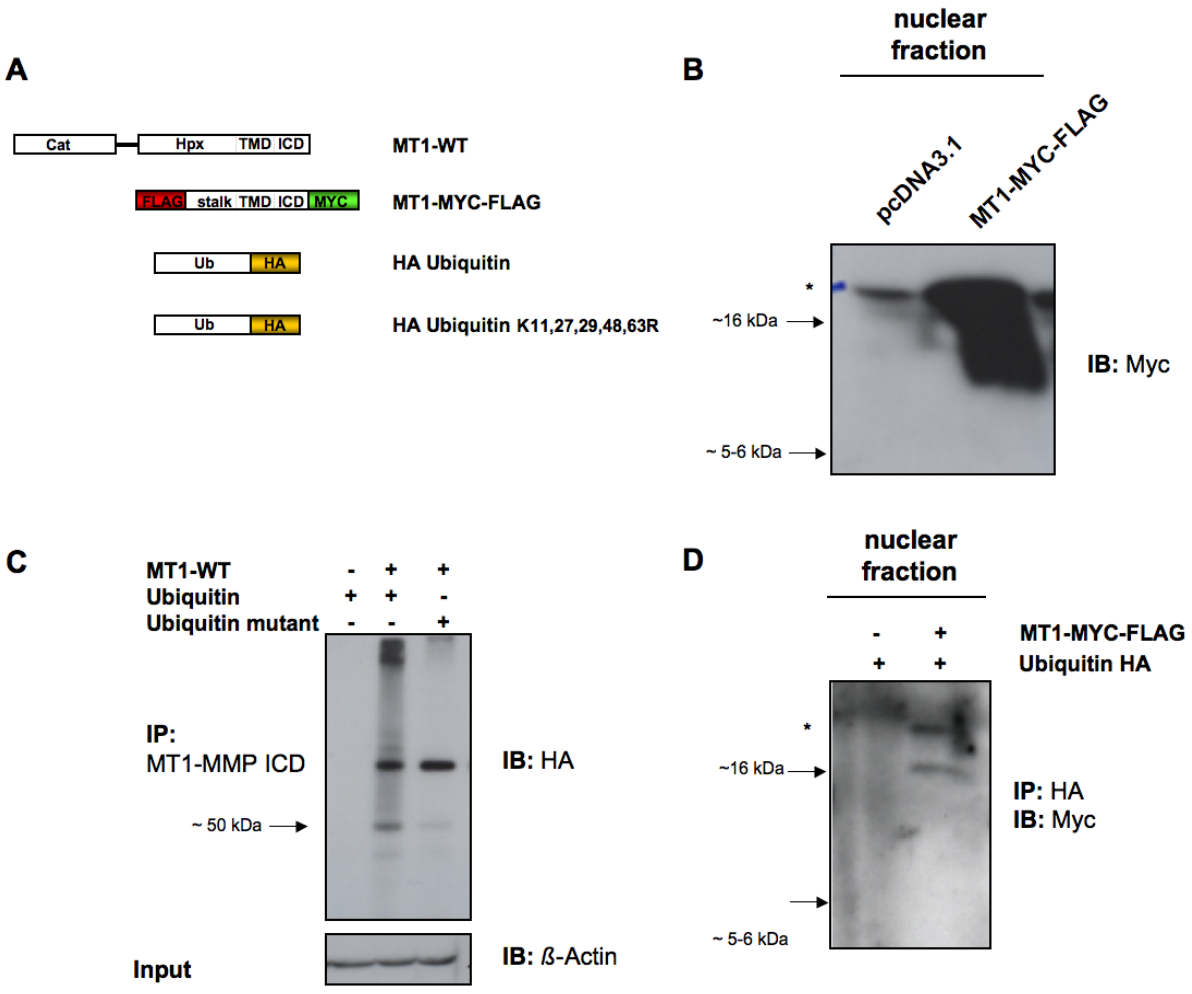

Figure 3.52: The MT1-MMP intracellular domain is ubiquitinated

(A) Schematic representation of the MT1-MMP and Ubiquitin constructs used. *HA*, hemagglutinin epitope (YPYDVPDYA) tag; *Bio*, Biotin tag. ***(B)*** MCF-7 cells were transfected with pcDNA3.1 control or the MT1-MYC-FLAG construct and nuclear proteins were isolated. The nuclear fraction was immunoblotted with an anti-Myc antibody. Asterisk indicates a non-specific signal. ***(C)*** MCF-7 cells were transfected with pcDNA3.1 control, MT1-WT, HA-tagged Ubiquitin, or the HA-tagged Ubiquitin K11,27,29,48,63R mutant, as indicated. Cell extracts were immunoprecipitated with an anti-MT1-MMP ICD specific antibody (ab28209) and immunoblotted with an anti-HA antibody. ***(D)*** MCF-7 cells were co-transfected with pcDNA3.1 control, MT1-MYC-FLAG and HA-tagged Ubiquitin, as indicated. Nuclear proteins were isolated, immunoprecipitated with an anti-HA antibody and immunoblotted using an anti-Myc antibody. Asterisk indicates a non-specific signal.

Another band at ~50 kDa was observed in both samples, raising the possibility of an ubiquitinated ~44 kDa MT1-MMP autocatalytic degradation fragment (Figure 3.52C).

To test whether MT1-MMP ICD ubiquitination is also detected in the nuclear fraction, thus explaining the ~16 kDa fragment detected in the nuclear extract of MCF-7 cells expressing the MT1-MYC-FLAG construct (Figure 3.52B), MCF-7 cells were co-transfected with either pcDNA3.1 control or MT1-MYC-FLAG as well as the HA-tagged Ubiquitin. Cell extracts were immunoprecipitated with an anti-HA antibody and immunoprecipitates were immunoblotted with an anti-Myc antibody. As shown in Figure 3.52D, a ~16 kDa band was detected in cells co-expressing MT1-MYC-FLAG and HA-ubiquitin, thus indicating that the MT1-MMP ICD may be ubiquitinated within the nuclear fraction of MCF-7 cells.

These data show that MT1-MMP may be ubiquitinated, as detected in whole cell lysates and in nuclear extracts. However, the precise mechanism and form of ubiquitination cannot be determined from this experiment. Mono-ubiquitination as well as poly-ubiquitination at K^{63} regulates various processes including endosomal sorting, trafficking, DNA repair, activation of kinases, inflammatory responses as well as regulation of nuclear import [280,281]. Poly-ubiquitination at K^{48} targets proteins for proteasomal degradation only [282,283]. Single lysine mutations within the Ubiquitin sequence need to be generated in order to address the question of MT1-MMP ubiquitination in more detail.

3.3.8 The MT1-MMP intracellular Lysine^{581} is important for nuclear localisation of the MT1-MMP intracellular domain

Ubiquitination was usually associated with targeting proteins for proteasomal degradation. However, in recent publications new functions of protein ubiquitination have emerged, including the regulation of cell cycle progression, stress response, signal transduction, DNA repair, apoptosis and transcriptional regulation (reviewed in [280]). The proteasome does not degrade proteins into their constitutive amino acids, but generates short peptides of approximately 20 amino acids, a similar size to the MT1-MMP ICD. Interestingly, ubiquitination can also play a role in regulating nuclear import by proteasomal processing of transcription factor zymogens or by causing nuclear translocation of proteins lacking a nuclear localisation sequence (NLS) [280,284-286]. As the MT1-MMP ICD may be ubiquitinated at its intracellular lysine K^{581} (Figure 3.52), ubiquitination could provide an

interesting mechanism for nuclear import of the MT1-MMP ICD as it lacks an NLS consensus sequence.

To test whether K^{581} affects nuclear localisation of the MT1-MMP ICD, a double-tagged truncated MT1-MMP lysine mutant (MT1-MYC-FLAG-K581A) was generated (Figure 3.53B). MCF-7 cells were transfected with MT1-MYC-FLAG (Figure 3.53A), MT1-MYC-FLAG-K581A (Figure 3.53B) or MT1-ΔECD-FLAG (Figure 3.53C), permeabilised and the localisation of the external Flag and the internal Myc tag was assessed by confocal microscopy. The nuclei were visualised by counter-staining with DAPI. The external Flag tag could be detected within the cytoplasm for all cDNAs transfected, especially within perinuclear vesicles, possibly the Golgi, and at or close to the plasma membrane (Figure 3.53). The intracellular Myc tag was detected within the nuclear region of MT1-MYC-FLAG expressing MCF-7 cells (Figure 3.53A), consistent with immunofluorescence data obtained from full-length MT1-MMP transfected cells (Figure 3.47A, Figure 3.48A).

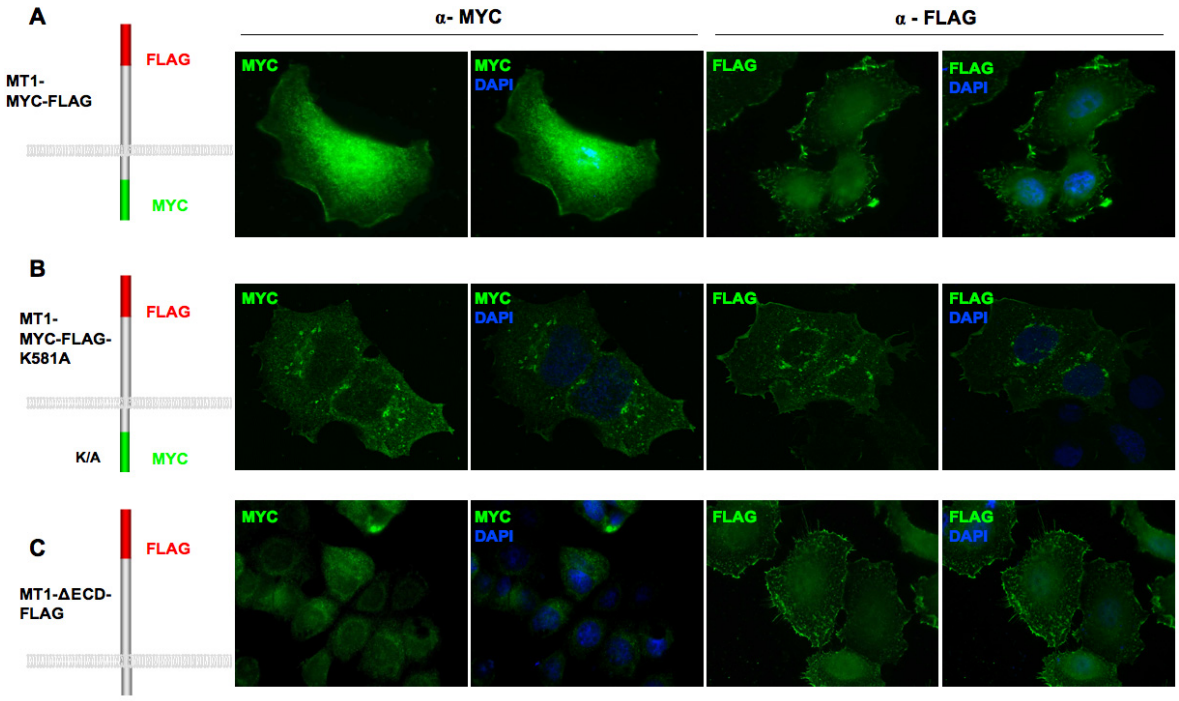

Figure 3.53: Nuclear localisation of MT1-MMP intracellular domain depends on intracellular Lysine^{581}

MCF-7 cells were transfected with the double-tagged MT1-MYC-FLAG ***(A)***, the MT1-MYC-FLAG-K581A ***(B)*** or the MT1-ΔECD-FLAG ***(C)*** construct and the localisation of the internal Myc and the external Flag tag was assessed with an anti-Myc (9B11) or an anti-FLAG (M2) antibody by confocal microscopy. Nuclei were counter-stained with DAPI.

Interestingly, Myc expression in the lysine mutant (MT1-MYC-FLAG-K581A) was redistributed and significantly reduced within the nuclear region (Figure 3.53B). Expression of the non Myc-tagged control (MT1-ΔECD-Flag) led to the non-specific detection of AlexaFluor® 488 induced background staining (Figure 3.53 C).

These findings show that the MT1-MMP K^{581} residue plays a potential role in the MT1-MMP ICD localisation in the nucleus.

In order to confirm this observation and to quantify nuclear localisation of the MT1-MMP ICD, the MT1-MYC-FLAG double tagged construct as well as the corresponding K^{581} mutant were expressed in MCF-7 cells and the nuclear localisation of the internal Myc and the external Flag tag was analysed by iCys™ laser scanning cytometer quantification as previously described using an anti-Myc and an anti-Flag antibody (chapter 2.2.4.3.3).

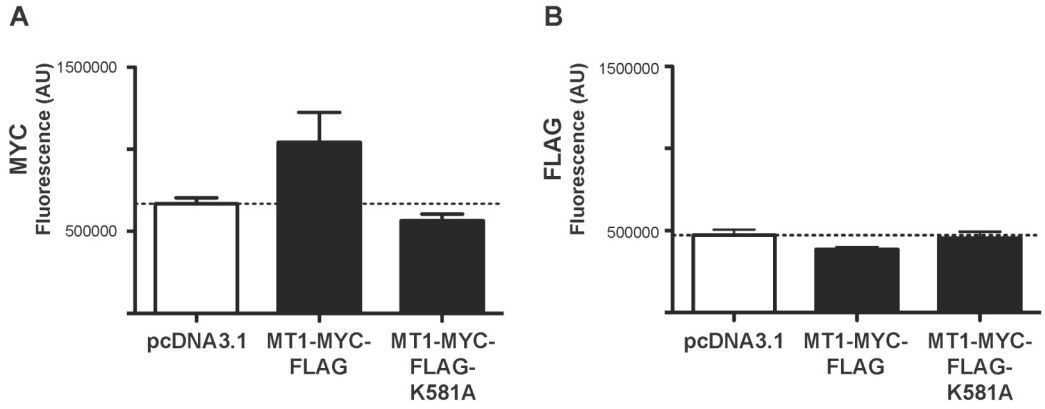

Figure 3.54: Quantification of nuclear staining in MT1-MMP double-tagged cDNA transfected cells

MCF-7 cells were transfected with pcDNA3.1 (detection level presented as dotted lines), the double tagged MT1-MYC-FLAG construct as well as the lysine mutant MT1-MYC-FLAG-K581A. Cells were stained with an anti-Myc antibody (9B11; AlexaFluor® 488 secondary, A) or an anti-FLAG antibody (M2; AlexaFluor® 488 secondary, B) and nuclear staining was assessed using the iCys™ laser scanning cytometer. Data represent the quantification of nuclear staining intensities ± 95% confidence intervals. 10,000 cells were counted per three biological replicates.

As shown in Figure 3.54A, expression of the MT1-MYC-FLAG construct increased the detection of the Myc-tagged MT1-MMP ICD in the nucleus significantly compared to pcDNA3.1 control, similar to full-length MT1-MMP (Figure 3.48A). In contrast, mutation of the K^{581} residue did not affect the Myc detection level compared to pcDNA3.1 control, suggesting that the MT1-MMP intracellular K^{581} plays a role in nuclear localisation. The MT1-MMP extracellular domain antibody staining was detected at similar low levels in the nucleus of pcDNA3.1, MT1-MYC-FLAG and MT1-MYC-FLAG-K581A transfected cells (Figure 3.54B).

Latent forms of transcription factors that are expressed as transmembrane proteins have been described to undergo several steps of processing by either RIP or RUP (chapter 1.4). The common sequence of action includes ectodomain shedding mediated mainly by a metalloproteinase and subsequent proteolysis by either transmembrane proteinases or the intracellular functioning proteasome (chapters 1.4) [148,180,183,287]. It has been shown that MT1-MMP is processed, leading to the release of either a ~16 kDa or a ~50 – 52 kDa fragment into the medium [100,108,277], which might be followed by the MT1-MMP ICD release (Figure 3.47D). Since the MT1-MMP intracellular lysine (K^{581}) has been shown to play a role in nuclear localisation (Figure 3.53, Figure 3.54A), the role of K^{581} on MT1-MMP processing within the transmembrane and intracellular domain was tested. Therefore, MCF-7 cells were transfected with the double-tagged MT1-MYC-FLAG, the corresponding lysine mutant (MT1-MYC-FLAG-K581A) or the pcDNA3.1 vector control. Whole cell extracts were immunoblotted with two different anti-Myc antibodies and an anti-Flag antibody confirming similar expression levels between the mutants used (Figure 3.55).

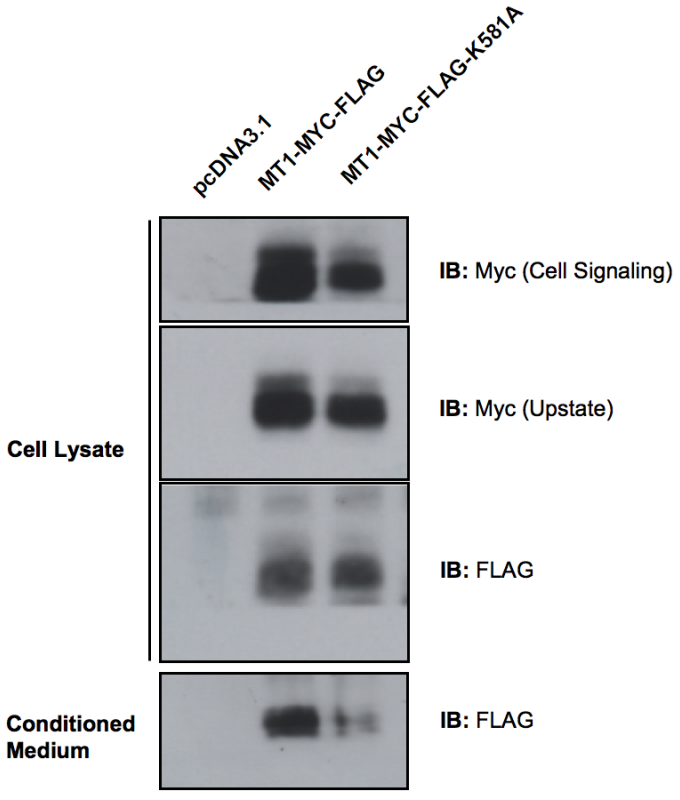

Figure 3.55: MT1-MMP ectodomain shedding is reduced following Lysine^{581} mutation

MCF-7 cells were transfected with pcDNA3.1 vector control, MT1-MYC-FLAG or MT1-MYC-FLAG-K581A and the proteins of the conditioned medium as well as whole cell extracts were analysed by immunoblotting with two different anti-Myc antibodies (9B11, 4A6) and an anti-FLAG antibody (M2).

The corresponding conditioned medium was collected, cleared from remaining cells and the total soluble protein was concentrated as described (chapter 2.2.3.4). Immunoblotting with an anti-Flag antibody revealed that a signal was detected in cells expressing both mutants corresponding to the size of the Flag-tagged extracellular stalk region (Figure 3.55). Interestingly, the amount of MT1-MMP soluble cleavage fragments detected was reduced in cells expressing the lysine mutant (MT1-MYC-FLAG-K581A).

These findings suggest that the MT1-MMP K^{581} residue plays a role in MT1-MMP processing, either within the transmembrane or intracellular domain, leading to the release of the extracellular domain.

3.3.9 The soluble MT1-MMP intracellular domain penetratin peptide co-immunoprecipitates with RNA-Polymerase II in a ChIP assay

The data obtained previously indicate a proteolytic release of the MT1-MMP ICD (Figure 3.44 - Figure 3.46), its enrichment in the nucleus (Figure 3.47 - Figure 3.50) as well as its interaction with nuclear proteins (Figure 3.51). However, these potential binding-partners of the MT1-MMP ICD in the nucleus remain to be identified.

To test whether the MT1-MMP ICD may play a role in regulating gene transcription, a chromatin immunoprecipitation (ChIP) assay was performed. The requirement for a highly sensitive and ChIP grade compatible antibody in this assay led to the usage of a tagged MT1-MMP ICD construct rather than using the MT1-MMP ICD specific antibody in wild-type MT1-MMP transfected cells. Also due to the small size of the MT1-MMP ICD, epitopes could be masked by binding other proteins.

Therefore, MCF-7 cells were incubated with 25 µM control or MT1-MMP ICD penetratin peptide and protein – protein as well as protein – DNA complexes were cross-linked by paraformaldeyde treatment. Following disruption of the chromatin into ~200 – 1000 bp fragments, lysates were immunoprecipitated with an anti-Biotin or an anti-RNA-Polymerase II (Pol II) antibody and genomic DNA (gDNA) was isolated (summarised in Figure 3.56A).

As no potential target gene was known to be regulated by the MT1-MMP ICD directly using the proposed mechanism of ICD release, the previously described regulatory effect of MT1-MMP on VEGF-A transcription (chapter 3.1) [73] was tested. The potential presence of the VEGF-A promoter region in the MT1-MMP immunoprecipitate was assessed by

SYBR® Green based Real-Time PCR, using primer corresponding to the promoter region of VEGF-A (Appendix A, Table 8.1). As a positive control gDNA isolated from Pol II immunoprecipitated samples was amplified with XBP-1 (X Box-binding protein 1) primer, targeting the promoter region of this transcription-factor previsouly described in MCF-7 cells to recruit Pol II [288].

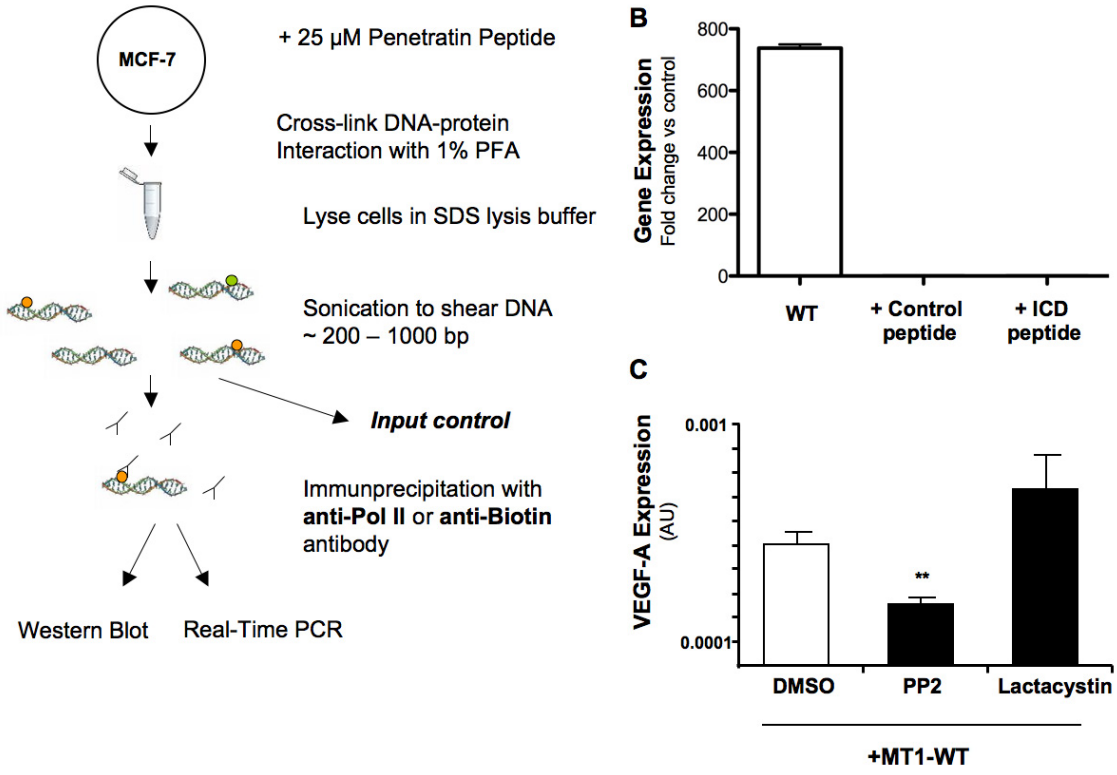

Figure 3.56: The MT1-MMP intracellular domain penetratin peptide does not bind to the VEGF-A promoter sequence

(A) Experimental set-up of the chromatin immunoprecipitation (ChIP) assay. MCF-7 cells were treated with 25 µM biotinylated penetratin peptides for 3 hours, washed and protein-protein as well as DNA-protein interactions were cross-linked with 1% PFA. Cells were lysed and gDNA was sheared into 200 – 1000 bp fragments by sonication. Cell extracts were immunoprecipitated with 3 µg anti-RNA-Polymerase II or anti-Biotin antibody and subjected to either immunoblotting or gDNA isolation with subsequent SYBR® Real-Time PCR analysis. ***(B)*** Wild-type MCF-7 cells as well as cells incubated with 25 µM of either control or MT1-MMP ICD penetratin peptide for 3 hours were chromatin immunoprecipitated as described. Samples were fixed, sonicated and immunoprecipitated with an anti-Biotin antibody (penetratin peptide samples) or with an anti-Polymerase II antibody (wild-type MCF-7) as a control. gDNA of immunoprecipitates was isolated and the VEGF-A (penetratin peptide samples) or XBP-1 promoter region (wild-type MCF-7) was amplified by SYBR® Green Real-Time PCR. As a negative control up-stream regions of VEGF-A and XBP-1 were amplified. Data represent the mean relative expression of the promoter region of two independent experiments ± S.E.M. in fold change compared to the up-stream regions of VEGF-A or XBP-1 respectively. ***(C)*** MCF-7 cells were transfected with MT1-WT and treated for 24 hours with DMSO, PP2 or Lactacystin where indicated. VEGF-A relative expression levels were detected by TaqMan® Real-Time PCR and were normalised to the house-keeping gene GAPDH. Data represent the mean expression of two independent experiments ± S.E.M. with $P < 0.001$ (**).

As expected, the XBP-1 promotor region was found to co-immunoprecipitate with Pol II and was detected by Real-Time PCR (Figure 3.56B, WT sample). Its expression was found to be ~740 fold enhanced over the corresponding XBP-1 up-stream control level, a sequence which is not associated with Pol II due to its distance to the promoter. In contrast, no amplification of the VEGF-A promoter region was observed in the control or MT1-MMP ICD penetratin peptide treated samples (Figure 3.56B), suggesting that VEGF-A is not regulated by the MT1-MMP ICD directly. These findings are consistent with previous results indicating an MT1-MMP induced signalling pathway leading to VEGF-A mRNA expression (chapter 3.1, Figure 3.31).
In addition to Src activity the involvement of proteasome function has been implicated in the MT1-MMP ICD release (Figure 3.45C). To confirm that MT1-MMP ICD is not regulating VEGF-A expression as part of a transcription-initiation complex, the VEGF-A mRNA expression levels of PP2 and Lactacystin treated MT1-WT transfected cells were determined by Real-Time PCR. As previoulsy found, the increase of VEGF-A mRNA level in MT1-MMP expressing cells treated with the Src inhibitor PP2 was significantly less than the increase observed in MT1-WT transfected cells treated with DMSO ($P < 0.001$, Figure 3.5A, Figure 3.56C). However, inhibition of proteasome activity by Lacatcystin did not affect the increase of VEGF-A mRNA expression compared to DMSO treated control, suggesting that MT1-MMP dependent VEGF-A regulation is indeed independent of the MT1-MMP ICD release.

To investigate whether the MT1-MMP ICD could be functionally involved in gene transcription, albeit the lack of known target genes, a potential complex of the MT1-MMP ICD with Pol II was tested by ChIP following immunoblotting. MCF-7 cells were incubated with MT1-MMP ICD or control penetratin peptide as previously described and cell extracts were co-immunoprecipitated with an anti-Pol II antibody. Immunoprecipitates and whole cell lysates (Input) were subsequently analysed by immunoblotting with an anti-Biotin antibody.

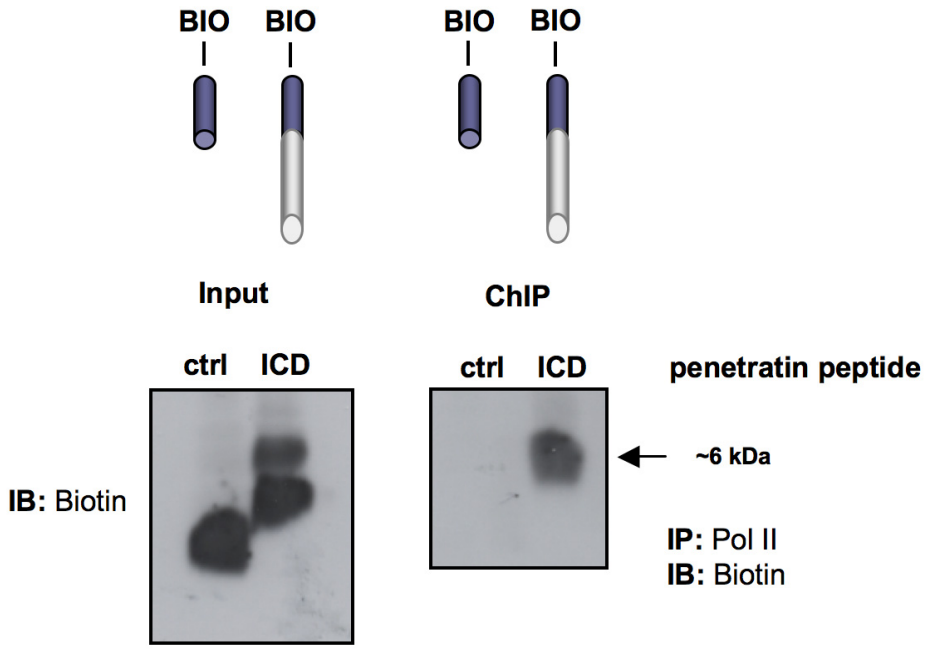

Figure 3.57: The MT1-MMP intracellular domain penetratin peptide co-immunoprecipitates with Polymerase II

MCF-7 cells were incubated with 25 µM of MT1-MMP ICD or control penetratin peptide for 3 hours and protein – protein as well as protein – chromatin complexes were fixed as decribed above (Figure 3.56A). Sonicated chromatin fragments were immunoprecipitated with an anti-Pol II antibody. Input and imunoprecipitates were immunobloted with an anti-Biotin antibody.

Both peptides were found at similar expression levels in the whole cell lysate (Input), indicating comparable biotinylated peptide penetration in both samples prior to ChIP (Figure 3.57). However, in contrast to the control peptide only MT1-MMP ICD containing penetratin peptide could be clearly detected after ChIP with Pol II (Figure 3.57).
These data are ***(i)*** consistent with previous findings showing MT1-MMP ICD to be enriched in the nuclear fraction and ***(ii)*** indicate that MT1-MMP co-immunoprecipitates with RNA-Polymerase II, suggesting a potential role of the MT1-MMP ICD in transcriptional regulation.

The molecular mass detected for the MT1-MMP ICD (~6 kDa) after ChIP with Pol II (Figure 3.57) indicates that it was not ubiquitinated. The current understanding of the MT1-MMP ICD release implies that MT1-MMP ubiquitination at its K^{581} residue is required for a proteaome dependent ICD release and its subsequent translocation to the nucleus. As the MT1-MMP ICD penetratin peptide is a soluble membrane-penetrating peptide, it might enter the nucleus by a different ubiquitin/proteasome independent way.

3.3.10 Summary: MT1-MMP intracellular domain release

The current understanding of the MT1-MMP intracellular domain release is summarised in Figure 3.58.

Data obtained in this thesis indicate that the MT1-MMP ICD is released in a Src and Proteasome-dependent way as detected in a reporter gene assay. The intracellular domain was found to be ubiquitinated at its K^{581} residue, thus potentially inducing the proteolytic release by the proteasome. Ubiquitination also raises an interesting possibility of a mechanism for nuclear translocation of the MT1-MMP ICD, which lacks an intrinsic NLS. The role of Src, which is activated and transported in an MT1-MMP dependent way (chapter 3.1), is not completely understood in this system. Src-dependent phosphorylation, as reported previously [249], might play a role in initiating the MT1-MMP ICD ubiquitination. Immunofluorescence data further supported the notion that ubiquitination is required for nuclear localisation of the MT1-MMP ICD since the MT1-MMP K^{581} mutant showed a decreased nuclear localisation of the ICD. Using tagged MT1-MMP ICD constructs, the intracellular domain was further detected in the nuclei of MCF-7 cells and was found to co-immunoprecipitate with RNA-Polymerase II. These findings indicate a potential role of the MT1-MMP ICD in a transcription-initiation complex.

ChIP-Seq experiments need to be performed in order to identify target genes that are regulated by the MT1-MMP ICD directly.

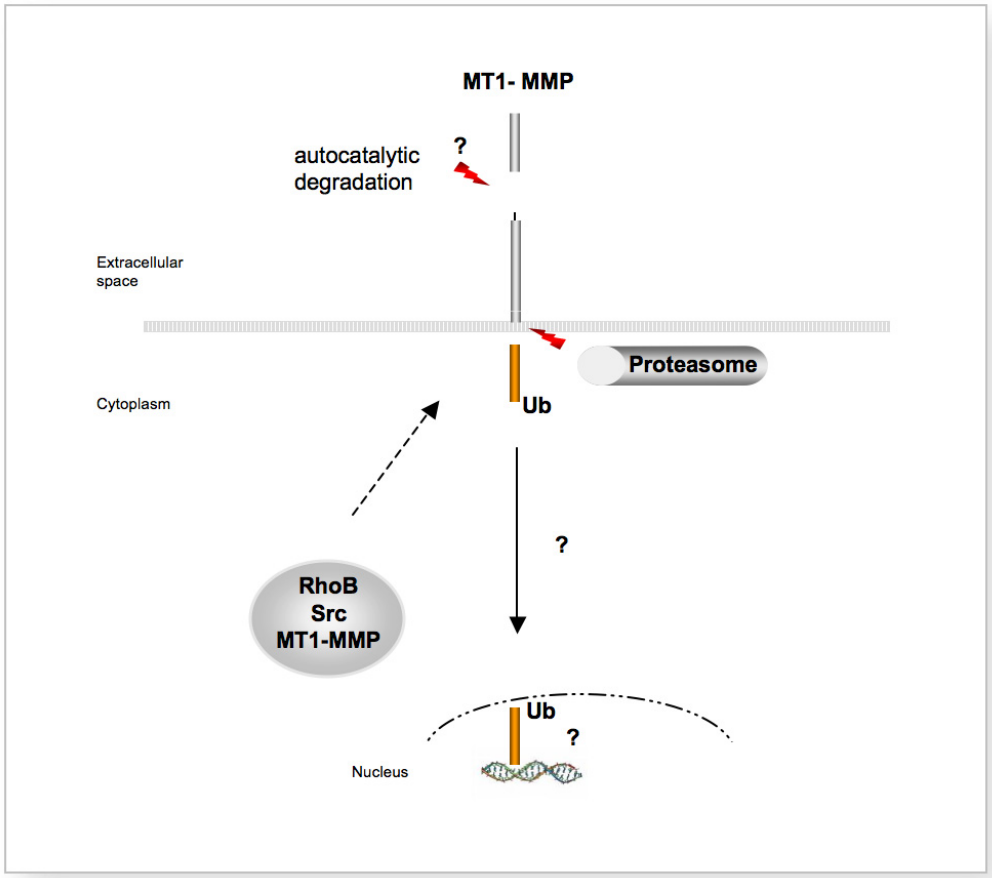

Figure 3.58: Summary and working hypothesis for the MT1-MMP ICD release based on data obtained so far

The data obtained so far indicate that MT1-MMP and Src may co-traffic to the cell surface, thus activating Src activity. The MT1-MMP ICD is subsequently released in a Src- and Proteasome dependent mechanism, potentially induced by ubiquitination of the MT1-MMP K^{581} residue. Ubiquitination may be a consequence of MT1-MMP autocatalytic degradation resulting in the 44 kDa membrane-tethered form. The K^{581} residue was shown to be required for MT1-MMP ICD nuclear localisation, thus raising the possibility that ubiquitination is needed for nuclear translocation. The MT1-MMP ICD was further found to co-immunoprecipitate with RNA-Polymerase II, suggesting a role for the MT1-MMP ICD in transcriptional regulation.

4 Discussion

MT1-MMP has been implicated in the modulation of gene expression including the regulation of VEGF-A [73], DKK-3 [139] and Smad1 [138] (chapter 1.3.6), although the molecular mechanisms remain to be investigated.
Thus, the aim of this thesis was ***(i)*** to investigate how MT1-MMP induces signalling pathways, ***(ii)*** to characterise MT1-MMP induced signalling pathways leading to the transcriptional regulation of target genes and in particular to dissect the molecular mechanism underlying the MT1-MMP induced up-regulation of VEGF-A expression and ***(iii)*** to get a better understanding of MT1-MMP mediated transcriptional regulation and its non-catalytic functions.

In this thesis, two novel and independent MT1-MMP induced signalling pathways have been described in breast carcinoma cell lines that regulate gene transcription either indirectly (discussed in chapter 4.1) or directly (discussed in chapter 4.2). Both signalling pathways are induced by non-proteolytic functions of MT1-MMP, thus broadening the functional spectrum of the proteinase and emphasising the multiple roles of MT1-MMP in tumour initiation, angiogenesis and metastasis (chapter 1.3.3).

4.1 Indirect MT1-MMP induced signalling

In the first sections of this thesis (chapters 3.1 and 3.2) the molecular mechanism of the MT1-MMP induced up-regulation of VEGF-A expression has been dissected and a novel MT1-MMP – VEGFR-2 – Src dependent pathway has been identified in breast carcinoma cell lines.
In MCF-7 cells, which were used as a model system, MT1-MMP was found to ***(i)*** increase the levels of VEGF-A mRNA and protein via a VEGFR-2, Src, PI3K, Akt, mTOR and HIF-1α dependent pathway, ***(ii)*** enhance the phosphorylation of Src, Akt and mTOR, ***(iii)*** form a tri-molecular complex with VEGFR-2 and pY416-Src that is required for VEGF-A transcription, ***(iv)*** regulate VEGFR-2 cell surface localisation and to ***(v)*** play a potential role in the VEGF-A – VEGFR-2 autocrine signalling axis.

Based on these observations an MT1-MMP induced signalling pathway is proposed (Figure 4.2A). The implications of the afore mentioned key findings will be summarised and discussed in the following chapters.

4.1.1 MT1-MMP induces the PI3 Kinase – Akt pathway

Initially, the role of MT1-MMP in up-regulating VEGF-A transcription, as described previously [73], was confirmed in the MCF-7 cells used as a model system (chapter 3.1). MCF-7 cells express neither MT1-MMP nor MMP-2 [251] and are therefore an ideal model to study the effect of these proteinases individually as well as to introduce various mutants in order to study the role of the different MT1-MMP domains. By using transient expression or adenoviral delivery of MT1-MMP cDNAs, VEGF-A expression data were obtained immediately following MT1-MMP expression, resembling molecular changes in the early stages of tumour growth and metastasis. MT1-MMP expression in MCF-7 cells increased VEGF-A mRNA (Figure 3.2 and Figure 3.3) and protein levels, as well as protein secreted into the extracellular milieu (Figure 3.4), independently of the MT1-MMP expression system used.

Although MT1-MMP has been implicated in the regulation of gene transcription, only one MT1-MMP mediated signalling pathway has been described so far. Gingras *et al.* reported previously an MT1-MMP dependent increase in ERK activation followed by subsequent induction of transcription through serum response elements (SRE), which induced cell migration in COS-7 cells [61]. Similar to the requirements for MT1-MMP induced increase in VEGF-A expression [73], the ERK pathway was shown to be dependent on the MT1-MMP catalytic activity, as well as on its intracellular domain, and in particular on the YCQR^{576} motif. By using an inhibitor based screening method targeting a variety of key signalling proteins (summarised in Table 3.1), the MT1-MMP dependent expression of VEGF-A was found to be independent of ERK signalling but required Src, consistent with previous findings [73], as well as PI3 Kinase, Akt, mTOR and HIF-1α activity (Figure 3.5A). Notably, expression of MT1-MMP was routinely observed to increase the phosphorylation level of Src at Y^{416}, mTOR at S^{2448} and Akt at T^{308} and S^{473}, whereas total Src, mTOR and Akt protein expression levels were not affected (Figure 3.6 - Figure 3.10). Akt was found to be phosphorylated downstream of VEGFR-2 and Src activation, as determined by an

inhibitor-based assay followed by immunoblotting (Figure 3.6). Breast carcinoma cell lines have been shown before to exhibit constitutively elevated PI3K activity following VEGF-A stimulation [236], supporting the role of a PI3K/Akt pathway as described in this thesis. Interestingly, inhibition of Akt activity using the Akt inhibitors SH-5 or Tricibine led to the down-regulation of MT1-MMP protein expression, whereas the level of the loading control β-Actin or total Akt was not affected. These findings suggest that Akt activity may be needed in order to maintain MT1-MMP expression, potentially acting as a positive feedback loop.

Nyalendo *et al.* have reported previously that MT1-MMP is phosphorylated in a Src dependent manner at its unique intracellular tyrosine residue Y^{573}, leading to tumour and endothelial cell migration [249]. In this study MT1-MMP expression led to the phosphorylation of Src at Y^{416}, downstream of VEGFR-2 activity (Figure 3.9B). Mutation of the MT1-MMP Y^{573} residue was however found to ablate MT1-MMP induced Src phosphorylation suggesting that this tyrosine residue may play a role in the activation of Src. Accordingly, mutation of Y^{573} was found to ablate the MT1-MMP induced up-regulation of VEGF-A at the mRNA level, potentially due to the lack of Src activation (Figure 3.25B).

The previously described MT1-MMP induced activation of the ERK signalling pathway led to transcription of target genes under the control of serum-response elements [61]. Inhibition of HIF-1α was found in the inhibitor-screening assay to reduce the level of VEGF-A mRNA in MT1-MMP expressing MCF-7 cells. HIF-1α is a well-described transcription factor that translocates to the nucleus following activation of the PI3 Kinase, Akt and mTOR pathway [218]. It is widely acknowledged that this pathway is activated by various growth factors and angiogenic mitogens, including VEGF-A [218]. Structural analyses of the VEGF-A genomic sequence revealed HIF-1 binding motifs within the promoter region (Figure 1.6), thus strongly supporting the notion that MT1-MMP dependent up-regulation of VEGF-A depends on the HIF-1 transcription factor.

By binding to glycosylated proteins, the extracellular matrix stores and masks many latent cytokines. Thus, degradation of components of the extracellular milieu by different proteinases affects various cellular responses. CTGF has been shown to be processed by MT1-MMP, MMP-1, -2, -3, -7 and -13 [54,257], thus releasing biologically active $VEGF_{165}$

from CTGF/$VEGF_{165}$ complexes. MMP dependent cleavage leads to the generation of the NH_2- and COOH-terminal CTGF degradation products, whereas biological activity of $VEGF_{165}$ is restored [257].

Ablation of MT1-MMP activity by mutating the extracellular E^{240} residue or treatment with the synthetic broad-spectrum MP inhibitor CT1746 as well as rh-TIMP-2 reduced the MT1-MMP induced up-regulation of VEGF-A (Figure 3.4B). Interestingly, when cells expressing the catalytically inactive MT1-MMP mutant were treated with increasing concentrations of rh-MMP-2, VEGF-A expression was restored (Figure 3.27B and Figure 3.28D). Furthermore, increasing concentrations of MT1-MMP transfected into MCF-7 cells resulted in an accumulation of CTGF cleavage products (Figure 3.26C). These findings strongly suggest that MMP dependent release of $VEGF_{165}$ from CTGF/$VEGF_{165}$ complexes induces VEGFR-2 signalling via the proposed mechanism shown in Figure 4.2A. However, further evidence for the involvement of this complex remains to be obtained. One way to answer that question could be by using an *in vitro* approach with recombinant CTGF/$VEGF_{165}$ complexes that are processed by MT1-MMP catalytic activity in solution. Following inhibition of MT1-MMP activity (using synthetic or recombinant endogenous MMP inhibitors) the *in vitro* processed CTGF/$VEGF_{165}$ complexes would be added to cells expressing catalytically inactive MT1-MMP and VEGF-A mRNA expression levels would be detected. Although this experiment would address the role of the CTGF/$VEGF_{165}$ complexes, it would generate various questions and biases due to its experimental setup.

It has been reported previously that TIMP-2 expression in murine mammary tumours conferred an anti-angiogenic tumour phenotype by down-regulating VEGF-A expression [289]. Accordingly, synthetic broad-spectrum inhibitors also down-regulated VEGF-A expression *in vivo* using a T cell lymphoma model [290]. These findings were believed to occur due to inhibition of MT1-MMP catalytic activity. However, both synthetic broad-spectrum MP inhibitors and TIMP-2 are inhibiting MT1-MMP as well as MMP-2 function, emphasising the role of MMP function in the transcriptional regulation of VEGF-A, potentially by liberating $VEGF_{165}$ from CTGF.

The role of MT1-MMP in the up-regulation of VEGF-A mRNA expression was also confirmed in another breast carcinoma cell line, MDA-MB-453 (Figure 3.33). MT1-MMP gene silencing in the MT1-MMP expressing MDA-MB-231 cells was performed using adenoviral asRNA, lentiviral shRNA or siRNA. These RNAi-based approaches led to off-

target effects or interferon responses, which have already been described and discussed in more detail in the chapters 3.2.1.2 - 3.2.1.4. Notwithstanding these limitations, MT1-MMP gene silencing using two independent RNAi techniques (lentiviral shRNA and siRNA) led to the up-regulation of VEGF-A expression at the mRNA and protein level (Figure 3.36C and Figure 3.39B). These observations are opposing the results obtained in MDA-MB-453 and MCF-7 cells, which showed an increase of VEGF-A mRNA expression levels in MT1-MMP expressing cells (Figure 3.2B, D, Figure 3.3B,C, Figure 3.33B). Consistent with the findings in MDA-MB-231 cells, expression of a reporter gene construct comprising of a Luciferase gene under the control of a 6 kb VEGF-A promoter in MT1-MMP expressing MCF-7 cells led to a decrease in reporter gene expression (CH Roghi, personal communication). These findings may be explained by the lack of additional regulatory sequences in the artificial promoter. Also, a cell-type specific variation in DNA modification including DNA methylation, might affect the transcriptional activity of the VEGF-A promoter region.

In this study MCF-7 cells were chosen as a model system to ***(i)*** study the role of the different MT1-MMP domains separately and ***(ii)*** to particular mimic early events in tumour growth and metastasis following MT1-MMP expression. Since the highly metastatic MDA-MB-231 cells express MT1-MMP constitutively at high levels, the MT1-MMP effect on VEGF-A expression may be temporarily restricted and/or attenuated by negative feedback loops.

4.1.1.1 Formation of an MT1-MMP – VEGFR-2 – Src tri-molecular complex in breast carcinoma cells

Using immunofluorescence and immunoprecipitation assays, a complex comprising of MT1-MMP, VEGFR-2 and Src was found in MCF-7 cells (Figure 3.17).

The interaction between MT1-MMP and VEGFR-2 was shown to be dependent on the MT1-MMP hemopexin and transmembrane domains (Figure 3.19 and Figure 3.20). The MT1-MMP hemopexin domain is known to confer substrate specificity and to be involved in the binding to substrates or interacting proteins, including its binding to native type I collagen and its role in the activation of pro-MMP-2 (chapter 1.3.4.3) [114,291]. In contrast to the co-immunoprecipitation of various MT1-MMP transfectants with VEGFR-2, the lack of the transmembrane domain using recombinant proteins in an ELISA assay did not affect

the interaction between MT1-MMP ECD and VEGFR-2 (Figure 3.20C). The mutant used to study the function of the transmembrane domain comprised of the full-length MT1-MMP with an APP transmembrane domain (MT1-TMD-APP, Figure 3.25A). The different results obtained from the experiments using the TMD mutant and the recombinant protein lacking the TMD, may be explained by differences in folding of the mutant that interfered with the hemopexin-dependent binding to VEGFR-2 or by different trafficking patterns and subcellular localisation.

VEGFR-2 is a member of the immunoglobulin (Ig) superfamily. Interestingly, MT1-MMP has been shown previously to interact with another Ig family member, ICAM-1, in an *in vitro* binding assay using purified full-length MT1-MMP and to co-localise in HEK293 and human aortic endothelial cells overexpressing ICAM-1 [292]. However, the MT1-MMP domain involved in the interaction with ICAM-1 has not been further characterised. Combining these findings and the identification of the MT1-MMP – VEGFR-2 complex described in this thesis, suggest that binding of MT1-MMP to Ig family members may be a conserved mechanism. Since the Ig family comprises of various cytokine and growth factor receptors, receptor tyrosine kinases/phosphatases, adhesion molecules as well as co-receptors, this potential interaction may provide an interesting mechanism to modulate cellular signalling.

In contrast to MT1-MMP binding to VEGFR-2 via its hemopexin/transmembrane domain, MT1-MMP was shown to interact with Src via its intracellular domain as shown by using a mammalian-two hybrid assay in different cell lines (Figure 3.11C and Figure 3.12). The MT1-MMP – Src interaction was confirmed by co-immunoprecipitation in MCF-7 cell lysates, however the interaction was not ablated by using the MT1-MMP ICD deletion mutant, suggesting the involvement of a third party protein (Figure 3.13B). Src is a known down-stream effector of VEGFR-2 signalling, although mainly described in endothelial cells (reviewed in [226]), and was found to co-immunoprecipitate with VEGFR-2 in MCF-7 cells (Figure 3.17B). These findings suggest that the direct binding of the MT1-MMP intracellular domain to Src as observed using the mammalian-two hybrid model, may be spacio-temporarily restricted or only occur in a sub-fraction of total MT1-MMP protein. Caveolin-1 is another protein that is known to associate with VEGFR-2, Src and MT1-MMP and might provide an additional interesting possibility as a bridging protein (discussed in chapter 4.1.3.).

4.1.2 MT1-MMP regulates VEGFR-2 localisation

In endothelial cells, VEGFR-2 was found to mainly localise in intracellular vesicles, whereas only a small sub-fraction of active receptor is localised at the cell surface [256]. VEGFR-2 cell surface localisation was increased following stimulation with exogenous VEGF-A. Similar results were obtained in wild-type MCF-7 cells (Figure 3.24C). Notably, in cells expressing MT1-MMP, VEGFR-2 cell surface localisation was significantly increased compared to empty vector transfected cells (Figure 3.24A). This MT1-MMP dependent re-distribution of VEGFR-2 was found to be dependent on the MT1-MMP extracellular and transmembrane domain, as detected by flow cytometry (Figure 3.24C). Expression of the extracellular domain deletion mutant led to a similar vesicular staining pattern compared to MCF-7 wild-type cells (Figure 3.24B).
These observations raise the possibility that MT1-MMP may be co-trafficked and co-endocytosed with VEGFR-2 as a mechanism to regulate the signalling capacity of the MT1-MMP – VEGFR-2 – Src complex. Furthermore, MT1-MMP and VEGFR-2 positive intracellular vesicles were found to co-localise with the microtubular network in MCF-7 cells (Figure 3.30), as reported previously for VEGFR-2 in endothelial cells [256]. Consistently, the microtubular cytoskeleton was shown to be important for trafficking and internalisation of MT1-MMP [293].

After reaching the plasma membrane, MT1-MMP was shown to be internalised in Rab4 positive recycling endosomes and Rab11 positive pericentrosomal recycling endosomes (chapter 1.3.4.5). It is believed that the TMD of MT1-MMP is required for the microtubular vesicular trafficking of MT1-MMP, although the TMD is not interacting directly with the microtubuli [40]. On the other hand, deletion of the MT1-MMP hemopexin domain or the ICD did not affect internalisation after membrane association. The potential requirement for the TMD (discussed in chapter 4.1.1.1) in the MT1-MMP induced up-regulation of VEGF-A as well as in MT1-MMP dependent cell surface localisation of VEGFR-2 as described in this thesis, may be explained by the role of the TMD in microtubular trafficking of MT1-MMP. However, the potential intracellular co-trafficking as well as the co-internalisation of MT1-MMP and VEGFR-2 as a mechanism to attenuate intracellular signalling remains to be investigated in more detail.

4.1.3 MT1-MMP: modulator of autocrine VEGF-A signalling

The transcriptional up-regulation of VEGF-A expression by MT1-MMP has many ramifications for tumour growth, angiogenesis and cell migration. VEGF-A expression has been implicated in cell survival and induces breast carcinoma progression mainly via a PI3 kinase pathway as well as inducing angiogenesis as a pro-angiogenic mitogen [236,294,295]. On the other hand MT1-MMP fulfils dual roles: ***(i)*** MT1-MMP expression leads to various cellular responses including cell motility, invasion and proliferation regulated through MT1-MMP catalytic activity (summarised in Figure 1.2) and ***(ii)*** VEGF-A expression is elevated by MT1-MMP in a process independent of its catalytic activity, thus increasing the functional repertoire of MT1-MMP (chapter 1.3.3).

The data obtained in this thesis suggest an MT1-MMP induced pathway dependent on the formation of the tri-molecular MT1-MMP – VEGFR-2 – Src complex that is necessary for VEGF-A expression (Figure 4.2A). However, the precise regulation of complex assembling or the molecular mechanism of the described MT1-MMP dependent phosphorylation of Src as well as the MT1-MMP dependent cell surface localisation of VEGFR-2 require further dissection.

Surprisingly, MT1-MMP expression has been shown to induce caveolin-1 expression in the caveolin-1-deficient MCF-7 and MDA-MB-453 cells, whereas MT1-MMP specific gene silencing reduced the level of caveolin-1 mRNA and protein (Figure 3.43 and Figure 3.33C). Caveolin-1 is known to associate with MT1-MMP, Src and VEGFR-2 and its expression was shown to be modulated by angiogenic factors [296]. Caveolin-1 is a key component of caveolae and acts as a scaffold for the assembling of various signalling proteins, including VEGFR-2, PDGFR and Src family kinases (SFKs) [273,297,298].

Based on the findings obtained in this thesis and consistent with recent publications (as outlined below), a potential multi-step mechanism leading to the assembling of signalling proteins dependent on MT1-MMP is proposed (the various steps are summarised in Figure 4.1):

(i) MT1-MMP potentially co-traffics with Src in RhoB positive endosomes. Src was described to be activated during its transport from the perinuclear region to the cell surface in RhoB positive vesicles [253]. Here, Src and MT1-MMP were found to co-localise in RhoB containing endosomes (Figure 3.16) and MT1-MMP Y^{573} was shown to modulate Src activation, potentially by interacting with Src and modulating its compartmentalisation. MT1-MMP is directed to the leading edge of the cell at distinct microdomains of the

plasma membrane, including lamellipodia, focal adhesions and caveolae (chapter 1.3.4.5).

(ii) VEGFR-2 is enriched in caveolae. VEGFR-2 is predominantly localised to caveolin-enriched membrane microdomains, which have been shown to be important for the induction of downstream signalling events induced by VEGF-A and to interact directly with caveolin-1 [273]. The mRNA and protein expression levels of caveolin-1 were found to be increased by MT1-MMP (Figure 3.43 and Figure 3.33C).

(iii) VEGF-A ligand binding. VEGF-A binding to VEGFR-2 induces dissociation of caveolin-1 from VEGFR-2 [273] and Caveolin-1 is subsequently phosphorylated by Src [273,299].

(iv) phospho-Caveolin-1 (pCav-1) binds to MT1-MMP followed by recruitment of Src [119]. Src activity is subsequently attenuated by Csk (C-terminal Src kinase).

(v) MT1-MMP complex-formation with VEGFR-2. MT1-MMP was shown to interact with VEGFR-2, although the hierarchical and temporal process of sequential protein interaction needs to be further investigated.

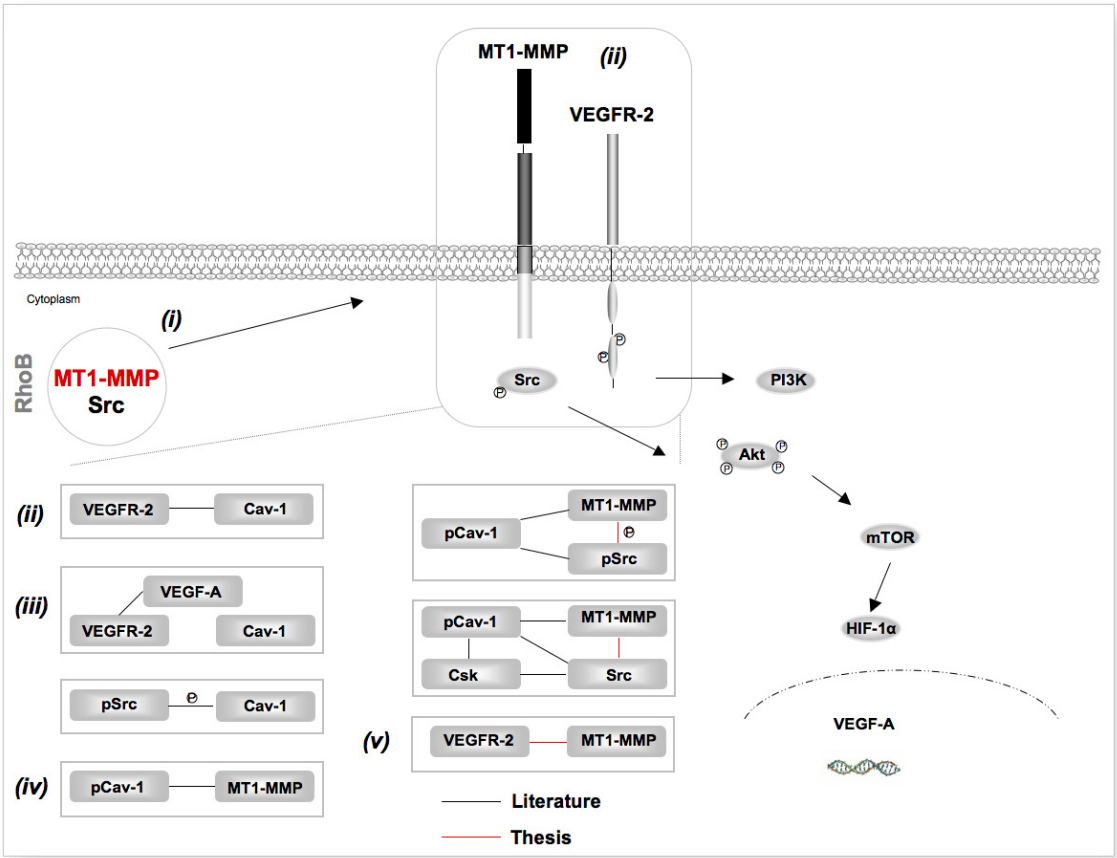

Figure 4.1: Potential mechanism of trafficking, protein activation and interaction leading to the assembling of the MT1-MMP – VEGFR-2 – Src complex.

A mechanism of MT1-MMP – VEGFR-2 – Src assembly is proposed. Details are described in the text.

This proposed pathway could be negatively regulated by Src de-phosphorylation, which was shown to occur after Src recruitment to MT1-MMP – phospho-caveolin-1 complexes, potentially due to phospho-caveolin-1 association with Csk (Figure 4.1 *iv*) [300]. Furthermore, the MT1-MMP – VEGFR-2 complex may be co-internalised as a mechanism to attenuate signalling, potentially in a microtubule dependent mechanism.
The signalling could be enhanced by positive feedback loops including the autocrine VEGF-A expression described (chapter 3.1, Figure 3.31) as well as the reported induction of MT1-MMP expression following VEGF-A stimulation in endothelial cells [301].
Although the involvement of caveolin-1 as a bridging protein raises an interesting hypothesis, the precise mechanism as well as the hierarchical sequence of action remains to be further investigated.

4.1.4 MT1-MMP dependent signalling – implications for tumourigenesis

Recent findings increased the notion that angiogenesis and in particular the signalling capacities of VEGF-A and its receptors play pivotal roles in pathophysiological conditions making them a promising target in cancer therapy. Accordingly various therapeutic approaches targeting VEGF signalling have been tested in clinical trials. Amongst those, the monoclonal anti-VEGF-A antibody bevacizumab (Avastin) given in combination with 5-fluorouracil (FU)-based chemotherapy, showed the most promising results [203]. Although treatment of patients with bevacizumab increased the survival, the disease proceeded eventually. There is emerging evidence that other pro-angiogenic mitogens compensate for the loss of VEGF-A function. In particular, VEGF-C and -D were shown to bind to VEGFR-2 after being processed and induce VEGFR-2 mediated signalling (Figure 1.7).
MMPs and in particular MT1-MMP are well-known proteinases that are highly expressed in malignant tissue and their role in pathophysiological conditions is widely acknowledged. The various functions and induced down-stream effects mediated by MMPs make it difficult to target the proteinases specifically. Indeed, inhibition of MMP function in clinical trials has been disappointing as treatments failed to increase patient survival or to produce adverse effects [302]. These findings were explained by the lack of specificity of the broad-spectrum inhibitors available, their use in late stage disease as well as the use as a single therapy instead of a combinational approach. The new focus in MMP targeting therapy is the design of agents that do not bind to the conserved sequence of the

catalytic pocket, but target substrate binding motifs or selective down-stream effectors. Dissecting the molecular mechanisms of regulation by distinct MMPs in angiogenesis will provide a basis for the design of new MMP inhibitors.

In the first sections of this thesis, a novel signalling pathway dependent on MT1-MMP, VEGFR-2 and Src was described in breast cancer cell lines. This tri-molecular complex mediated signalling was shown to induce VEGF-A expression in MCF-7 and MDA-MB-453 cells, but not in the MT1-MMP endogenously expressing MDA-MB-231 cells. Since the MT1-MMP – VEGFR-2 – Src complex was found in all cell lines tested, it might be a conserved mechanism to induce intracellular signalling pathways in breast cancer cell lines, albeit regulating different target genes depending on the cell type. Additional target genes that are regulated by this complex in different cell lines remain to be identified.
In order to correlate these *in vitro* findings with clinical data, a meta-analysis of existing mRNA gene expression data of breast cancer tissues derived from tumours of either ***(i)*** different stages (stage I-IV dependent on tumour size, lymph node involvement, metastases), ***(ii)*** different grades (grade 1 – 3 dependent on nuclear polymorphism, tubule formation and mitotic count), ***(iii)*** different estrogen receptor (ER) status or ***(iv)*** different histological classification (apocrine, basal and luminal) was performed by using the Oncomine™ database. Studies that revealed a differential expression of MT1-MMP, VEGF-A or VEGFR-2 are summarised in Appendix D. VEGFR-2 was not found to be differentially expressed in either type of analysis, although a slight increase in mRNA expression was observed in ER negative tumours as detected in 3 studies ($P < 0.05$). Differential expression of MT1-MMP was not consistent in tumours of different grading, but was found to be increased in ER negative (2 studies $P < 0.0001$) and to a lesser extent in luminal tumours ($P < 0.05$). The mRNA expression of VEGF-A was significantly enriched in ER negative ($P < 0.0001$) and luminal tumours ($P < 0.0001$). These findings confirm VEGF-A detection to be a prognostic marker in breast carcinomas corresponding to a poor outcome. VEGFR-2 expression levels were not found to be significantly affected by different types of analyses. This observation strengthen the current understanding of the proposed MT1-MMP dependent pathway, that the MT1-MMP – VEGFR-2 – Src signalling complex may be regulated by cellular localisation rather than by transcriptional control. The model cell lines used in this study originate from different breast cancer types. Whereas MCF-7 cells are derived from luminal and ER positive tumours, MDA-MB-231 cells are ER negative and basal. VEGF-A and MT1-MMP expression detected in these cell

lines correspond to the expression data obtained in the meta-analysis of the cell origin. The data furthermore emphasise that the expression of MT1-MMP and VEGF-A correlate in human physiology.

Although mRNA microarray studies provide an important tool for correlating *in vitro* findings with clinical data, it is necessary to acknowledge that the mRNA used is derived from an heterogeneous tumour cell population consisting of tumour cells, stromal and infiltrating immune cells. In order to address this heterogeneity within the tumour mass, a study using human mammary carcinoma tissue sections was performed (in collaboration with Dr. Bence Sipos). Preliminary data revealed that MT1-MMP, VEGFR-2 and pY416-Src are expressed in the cytoplasma and at or close to the plasma membrane of tumour cells (Figure 3.42). To get a deeper understanding of the expression of MT1-MMP, VEGFR-2 and pY416-Src depending on different histological sub-categories (e.g. grading, staging), a comprehensive study using breast invasive ductal carcinoma tissue microarrays is currently performed (in collaboration with Dr. Bence Sipos).

As the MT1-MMP effect on VEGF-A regulation was solely performed on breast cancer cell lines, it will be interesting to test whether this pathway or the MT1-MMP – VEGFR-2 – Src complex is a common mechanism in different carcinoma cell lines or in stromal and endothelial cells. As MT1-MMP plays a key role in angiogenesis and is constitutively expressed in endothelial cells (ECs), this pathway may provide a mechanism to enhance the angiogenic response as well as cell proliferation in ECs.

Taken together, the data obtained in this thesis enhance the understanding of the mechanism underlying the MT1-MMP transcriptional regulation of VEGF-A. These observations strengthen the role of MT1-MMP in tumourigenic angiogenesis and provide a link between MT1-MMP and an autocrine VEGF-A activation loop. It is essential to get a deeper functional understanding of the different roles of MT1-MMP in tumourigenesis, in particular based on clinical samples, in order to target specific signalling pathways for therapeutics.

4.2 Direct MT1-MMP dependent signalling

In the third part of this thesis (chapter 3.3), a novel mechanism of MT1-MMP processing leading to the release of its intracellular domain was described. The results obtained

indicate for the first time that the MT1-MMP intracellular domain (ICD) ***(i)*** is released in a Src-and Proteasome-dependent way, ***(ii)*** is ubiquitinated at its intracellular K^{581} residue, ***(iii)*** is detected in the nucleus using a soluble tagged MT1-MMP ICD penetratin peptide, a MYC-FLAG double-tagged truncated MT1-MMP construct and in human mammary carcinoma sections and ***(iv)*** co-immunoprecipitates with RNA-Polymerase II, suggesting a role in transcriptional activation.

4.2.1 MT1-MMP intracellular domain release

An increasing number of transcriptional regulators have been shown to be synthesised as latent transmembrane precursors that have to undergo proteolytic processing in order to be activated (chapter 1.4). Intramembrane proteolysis is mainly mediated by presenilin-dependent γ-secretase, site-2 proteinases (S2P), signal peptide peptidases (SPP) or rhomboid proteinases. Recently, a novel mechanism of intracellular domain release was observed in *S. cerevisiae* depending on the ubiquitin-proteasome system (chapter 1.4).
The proteins undergoing intramembrane processing share several characteristics. They are mainly type-I transmembrane proteins (except proteins that are processed by S2P or SPP) oriented with their NH_2-termini towards the extracellular milieu and their COOH-termini in the cytosol. Another shared feature is the sequential proteolytic processing at various extracellular and intramembranous sites that eventually leads to the release of their intracellular domains from the plasma membrane [148,179,180,183,287]. In each case, the extracellular domain is removed in a primary cleavage event, resulting in the truncation of the extracellular segment to less than 30 amino acids. This initial cleavage is a prerequisite for intramembrane cleavage and occurs mainly in a metalloproteinase dependent step [161,182] except for the *β*-secretase dependent APP cleavage [173]. Similar to Notch1 and LRP1, MT1-MMP undergoes activation by furin in a late secretory compartment cleaving the Arg-Arg-Lys-Arg motif between the catalytic domain and pro-peptide [21,88-90] as well as undergoing a metalloproteinase (e.g. ADAM) dependent extracellular domain cleavage step, resulting in the release of a soluble ~50 kDa fragment, which corresponds to the entire extracellular domain (chapter 1.3.4.4) [112]. These similarities raised the possibility of MT1-MMP undergoing either regulated intramembrane proteolysis (RIP) or regulated ubiquitin/proteasome dependent processing (RUP).

Adapting the methodology that was used for the identification of Notch1 [144,184], APP [179] and LRP1 [151] RIP, the MT1-MMP intracellular domain was shown to be released and to induce transcription in a reporter gene assay. A variety of inhibitors targeting proteinases known to be involved in RIP or RUP were tested for their capacity to induce MT1-MMP processing (Figure 3.45). Since Site-2 proteinases (S2P) and signal peptide peptidases (SPP) were only shown to be required for cleaving type-II transmembrane proteins, agents inhibiting these proteinases were omitted in this screening. In contrast to other proteins undergoing RIP, MT1-MMP ICD release was not dependent on γ-secretase or rhomboid proteinases but required Src and Proteasome activity (Figure 3.45). This Src and Proteasome mediated MT1-MMP ICD release was found to depend on the MT1-MMP intracellular and transmembrane domains (Figure 3.46). In the reporter gene assay, MT1-MMP mutants were used where the ICD or transmembrane domain (TMD) were exchanged by those of the APP protein. The reduction of reporter gene activity following Src or Proteasome inhibition in cells expressing either mutant suggests that both MT1-MMP domains are required for the proteolytic release of the ICD. These observations are consistent with the direct interaction observed between MT1-MMP ICD and Src (Figure 3.12) and suggest a potential difference in folding of the protein due to the APP TMD, that potentially attenuates the interaction with Src or the activity of the proteasome.

There is limited knowledge about the mechanism of ubiquitin/proteasome dependent release of membrane-bound transcription factor precursors. So far, this processing has only been reported for the yeast homologs of NF-κB, SPT23 and MGA2 (chapter 1.4.2) [190]. During this process, the membrane-bound precursors interact with the RSP5 ubiquitin ligase (an E3 enzyme), are subsequently ubiquitinated and the intracellular part is released via proteasome-dependent proteolysis (Figure 1.5). Notably, only the 90 kDa ubiquitinated intracellular part is spared from proteasomal degradation and released into the cytoplasm [190]. The possibility of an ubiquitin/proteasome dependent release of the MT1-MMP ICD is further discussed in chapter 4.2.2.

As the Gal4/VP16 tagged MT1-MMP construct used for the reporter gene assay contained an intrinsic nuclear localisation sequence (NLS) [278], further independent approaches were used to study the nuclear localisation of MT1-MMP. Immunocytochemical detection methods using MT1-MMP expressing MCF-7 cells revealed the presence of the MT1-MMP ICD in the nucleus (Figure 3.47 and Figure 3.48). However, the intracellular domain could not be detected in the nuclear fraction by immunoblotting (Figure 3.47B). This

observation may be explained either by the small amount of MT1-MMP protein enriched within the nuclear fraction and thus being below the critical threshold of antibody-detection, as observed for the Notch1 ICD [184], or by the insufficient sensitivity of the antibody used. The first analyses of Notch1 ICD release were performed using constructs encoding the transmembrane and the intracellular domain to mimic endogenous transmembrane processing or by using a soluble ICD mutant in order to increase the sensitivity by using biochemical detection methods [144]. These constructs as well as cDNAs used in other RIP studies were C-terminal modified by Myc or EGFP tags in order to facilitate detection [144,148,168,184].

Accordingly, different tagged MT1-MMP constructs were generated and used in further MT1-MMP ICD localisation studies. The intracellular domain of the truncated MYC-FLAG tagged MT1-MMP construct (MT1-MYC-FLAG) as well as the MT1-MMP ICD containing biotinylated soluble penetratin peptide were detected in the nuclei of MCF-7 cells by immunostaining and immunoblotting (Figure 3.49, Figure 3.52 - Figure 3.54). The presence of the MT1-MMP ICD in tumour cell nuclei was further confirmed in human mammary carcinoma tissue sections, indicating that the MT1-MMP ICD is also localised in the nucleus *in vivo* (Figure 3.50). This observation emphasise the role of the MT1-MMP ICD release and its presence in tumour cell nuclei during tumourigenesis.

Earlier studies addressing the subcellular localisation of MT1-MMP in hepatocellular carcinoma led to the detection of mature MT1-MMP at the plasma membrane, the cytoplasm and also within nuclei [303]. Presence of nuclear MT1-MMP was associated with poor survival and larger tumours in patients with hepatocellular carcinoma [303]. Another study described full-length MT1-MMP accumulation in the centrosomal compartment by binding to the integral centrosomal protein pericentrin in the human glioma cell lines U251 as well as MCF-7 cells [304]. In contrast to these two publications, immunostaining using antibodies specifically raised against the ectodomain of MT1-MMP did not show nuclear localisation in either the literature before, nor in human mammary tissue sections (Figure 3.42). In this thesis only the MT1-MMP ICD was found in the nuclear fractions of MCF-7 and MDA-MB-231 cells as well as in human mammary carcinoma tissue sections (Figure 3.48 and Figure 3.50).

Recently, MMP-3 has also been found to localise in the nucleus [305,306]. Interestingly, a nuclear interaction between MMP-3 and either TRENDIC (transcription enhancer dominant in chondrocytes) or heterochromatin protein gamma has been found on the CTGF promoter, enhancing its expression [306].

Co-immunoprecipitation with an anti-MT1-MMP ICD specific antibody in the nuclear fraction of MT1-MMP expressing MCF-7 cells revealed several proteins that were absent in the control sample, suggesting that MT1-MMP interacts with nuclear proteins (Figure 3.51). The MT1-MMP nuclear localisation as well as its interaction with nuclear proteins was confirmed by chromatin immunoprecipitation (ChIP). Due to the lack of known target genes that are directly regulated by the MT1-MMP ICD, protein – chromatin lysates were immunoblotted following ChIP revealing an interaction between the MT1-MMP ICD and RNA-Polymerase II (Figure 3.57). Thus, raising the possibility that the MT1-MMP ICD is involved in transcriptional regulation. However, potential target genes that are regulated by the MT1-MMP ICD directly remain to be identified. A ChIP sequencing approach using Illumina® Solexa® technology is currently being prepared.

It has been established that the initial proteolytic events during RIP are triggered upon ligand binding to the receptors, leading to shedding of the ectodomain. The molecular mechanism regulating MT1-MMP ectodomain shedding as well as the regulation of its intracellular domain release is not completely understood. Preliminary studies revealed that the MT1-MMP ~44 kDa form is ubiquitinated (chapter 4.2.2), thus indicating that MT1-MMP undergoes autocatalytic processing that is required for the subsequent release of its intracellular domain. However, ectodomain shedding was also observed in cells expressing the MYC-FLAG- tagged truncated MT1-MMP construct that lacks the catalytic domain. It has been shown before that incomplete ectodomain shedding leaving ~30 amino acids of the extracellular part of proteins undergoing RIP is sufficient to induce intracellular domain release, suggesting that the initial step of ectodomain shedding may not be required for the ICD release in cells expressing the extracellular truncated MT1-MMP construct.

4.2.2 MT1-MMP ubiquitination: a potential mechanism for nuclear translocation

There is emerging evidence that, in addition to targeting proteins for proteasomal degradation, ubiquitination regulates many cellular aspects. The consequences of this post-translational modification depend on whether the ubiquitin is attached to the protein as a monomer or as polyubiquitin chains. Generally, a protein that has been modified by a chain of ubiquitins (polyubiquitination) is targeted for degradation by the 26S proteasome

[283], while conjugation of a single ubiquitin to one lysine (monoubiquitination) or to several lysines (multiubiquitination) does not lead to degradation but is a key regulatory mechanism for various cellular responses including histone regulation, endocytosis, Golgi reassembly, DNA repair, nuclear/cytosolic transport and gene transcription (reviewed in [280]). It has been recently shown that the nuclear – cytoplasmic transport and therefore the activity of the transcription factors including p53 [284], PTEN [285] and FOXO [286] depends on monoubiquitination. Thus, ubiquitination provides an intriguing route for proteins that are lacking an intrinsic NLS to translocate to the nucleus. In contrast to other transmembrane proteins undergoing RIP including Notch1, LRP1 and SREBP, the MT1-MMP ICD does not exhibit an intrinsic NLS. Amongst the well-characterised proteins processed by RIP the NLS-lacking APP intracellular domain translocates to the nucleus by interacting with the nuclear adaptor protein Fe65 [179].

In this study, MT1-MMP was found to be ubiquitinated as detected by co-immunoprecipitation in total cell lysates of MT1-MMP expressing cells as well as in the nuclear fraction of cells expressing the MYC-FLAG truncated MT1-MMP construct (Figure 3.52). The presence of a ~16 kDa signal in the nuclear fraction corresponded to the molecular weight of a mono-ubiquinitated MT1-MMP ICD. This observation suggest that the post-translational modification is required for nuclear localisation, thus substituting for a conserved NLS. The MT1-MMP ICD contains a single lysine residue as a potential ubiquitination site (K^{581}, Figure 1.3 and Figure 3.45A). Mutation of that residue to alanine led to a decreased nuclear localisation of the MT1-MMP ICD as detected and quantified by immunofluorescence (Figure 3.53 and Figure 3.54) and furthermore decreased the amount of soluble extracellular cleavage fragments that were released into the medium (Figure 3.55).

So far, a proteasomal release of transcriptional activators from transmembrane precursors has been demonstrated only for the NF-κB homologs in yeast. However, activation of human NF-κB was also shown to be dependent on ubiquitination. Latent NF-κB is bound to IκB proteins that are phosphorylated by IκB kinases (IKK) and are subsequently ubiquitinated. Then, E3 ligases bind to the phosphorylated form of IκB through their C-terminal part allowing the conjugation of ubiquitin to N-terminal lysine residues. The ubiquitinated IκB is selectively degraded by the proteasome, whereas NF-κB is spared from degradation and released from the inhibitory binding partner [281]. This activation of

NF-κB provides a mechanism for selective proteasomal degradation and subsequent activation of transcription factors in humans.

Phosphorylation of proteins is believed to be an initial step for ubiquitination in order to regulate protein activity, stability and specific localisation. MT1-MMP has been shown previously to be phosphorylated at its Y^{473} residue in a Src dependent way [249]. It is tempting to hypothesise that this phosphorylation step may induce MT1-MMP ICD ubiquitination and thus explaining the requirement for Src in the MT1-MMP ICD release.

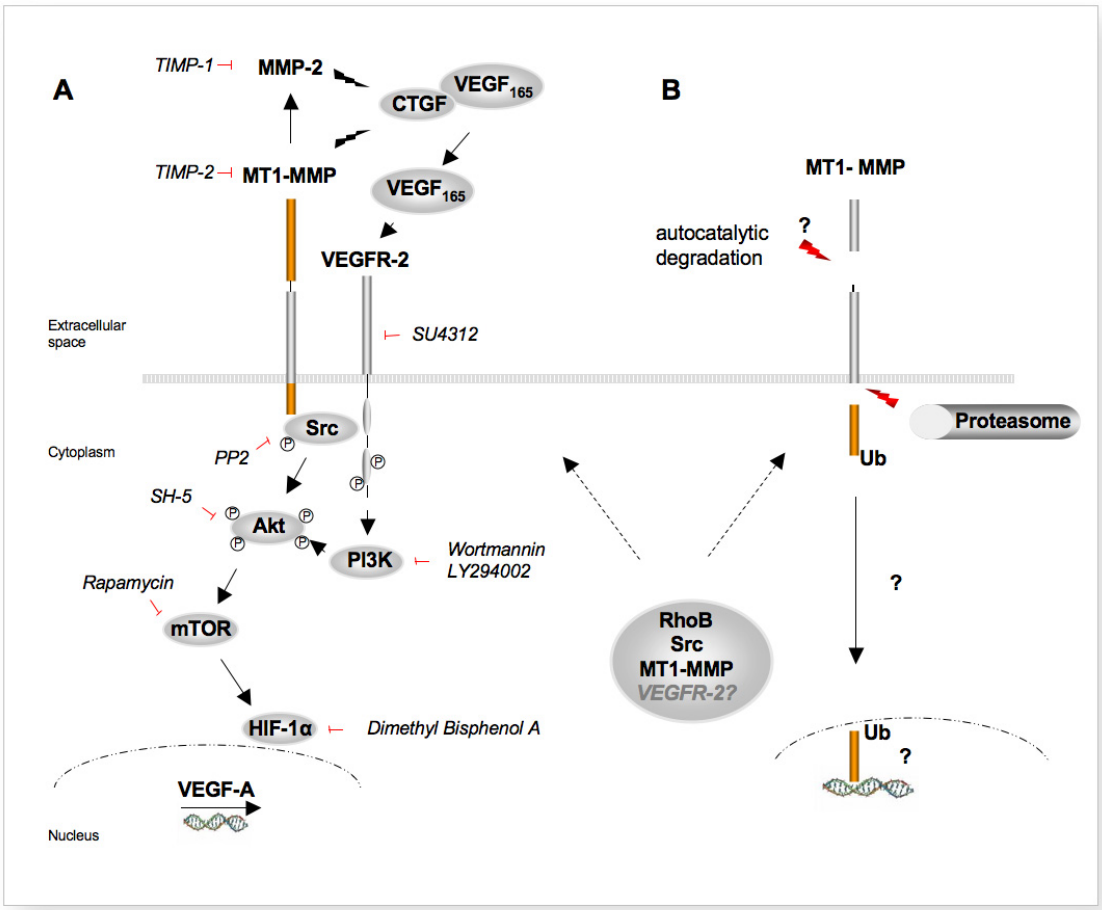

Figure 4.2: MT1-MMP induced signalling pathways in breast cancer cell lines as described in this thesis

MT1-MMP was found to induce at least two independent intracellular signalling pathways leading to transcriptional regulation in beast cancer cell lines. Both signalling pathways are dependent on the MT1-MMP mediated activation of Src, which may occur during the transport of MT1-MMP and Src to the plasma membrane in RhoB positive endosomes. ***(A)*** VEGFR-2 activation leads to transcription of VEGF-A by activating Src, PI3 Kinase, Akt, mTOR and HIF-1α. Initial data suggest that this pathway is presumably initiated by $VEGF_{165}$ following metalloproteinase mediated proteolytic cleavage of CTGF/$VEGF_{165}$ complexes. ***(B)*** The MT1-MMP intracellular domain is released in a Src and Proteasome dependent way. Various methodical approaches confirm the presence of the MT1-MMP ICD in the nucleus of MCF-7 and MDA-MB-231 cells. The nuclear localisation depends on the K^{581} residue, which was shown to be ubiquitinated in whole cell lysates and within the nucleus. The MT1-MMP ICD co-immunoprecipitates with RNA-Polymerase II, suggesting a role of MT1-MMP ICD in a transcription initiation complex. *Ub*, ubiquitin.

5. Summary

Membrane-type-1 matrix metalloproteinase (MT1-MMP, MMP-14) is a zinc-dependent type-I transmembrane proteinase, which is known to play a key role in pericellular proteolysis, cell invasion and angiogenesis. Overexpression or conditional expression of MT1-MMP enhances tumour growth in *in vivo* mouse models and elevated MT1-MMP levels in human cancer cells correlate with a poor prognosis. Tumourigenic angiogenesis and growth has been reported to be at least partly driven by the MT1-MMP-mediated transcriptional activation of the angiogenic factor vascular endothelial growth factor A (VEGF-A), which is dependent on the catalytic and intracellular domain (ICD) of MT1-MMP. There is increasing evidence that in addition to the catalytic activity of MT1-MMP, it is involved in the transcriptional regulation of various target genes. However, the molecular mechanism underlying this regulation has not been investigated in detail so far.

In this thesis two novel and independent MT1-MMP mediated signalling pathways have been identified.

Initially, MT1-MMP dependent regulation of VEGF-A transcription was shown to involve the activity of VEGF receptor 2 (VEGFR-2) as well as key kinases including Src, PI3 kinase, mTOR and Akt. Accordingly, the phosphorylation levels of Src, Akt and mTOR were significantly enhanced by MT1-MMP expression *in vitro* and co-localisation between MT1-MMP and these phospho-forms was observed. Using deletion and substitution mutants of the ICD and catalytic domain, new motifs regulating VEGF-A expression were defined. Co-immunoprecipitation and immunofluorescent analyses revealed a complex of MT1-MMP, VEGFR-2 and active Src, which was primarily located at the cell surface of MCF-7 cells. This expression pattern was also confirmed by immunostaining of human mammary carcinoma sections. The interaction between MT1-MMP and Src was shown to be dependent on the MT1-MMP ICD, whereas its interaction with VEGFR-2 is dependent on the hemopexin and transmembrane domains. VEGFR-2 signalling and its localisation at the cell surface were further shown to be highly dependent on the MT1-MMP hemopexin and transmembrane domains.

These findings suggest the involvement of a VEGFR-2 induced PI3K/Akt pathway in MT1-MMP dependent transcriptional regulation of VEGF-A and further emphasise the non-proteolytic functions of MT1-MMP during tumourigenic angiogenesis.

Another MT1-MMP dependent signalling pathway was identified, which involves the Src- and Proteasome mediated proteolytic cleavage of MT1-MMP. This processing led to the release of the ICD and transcriptional activation in a reporter gene assay. Accordingly, immunostaining and immunoblotting revealed the MT1-MMP ICD within the nucleus of MCF-7 cells transfected with either full-length MT1-MMP or tagged MT1-MMP constructs, in MDA-MB-231 cells and in sections of human mammary carcinomas. A soluble tagged intracellular domain penetratin peptide was found to enrich in nuclear fractions of MCF-7 cells and to co-immunoprecipitate with RNA-Polymerase II in a potential transcription initiation complex. Interestingly, MT1-MMP was found to be ubiquitinated at its intracellular K^{581} and mutation of this residue ablated nuclear detection of the MT1-MMP ICD, suggesting a potential role for MT1-MMP ubiquitination in proteasomal ICD release and nuclear translocalisation.

Taken together, two novel MT1-MMP dependent pathways were identified. These findings ***(i)*** show that MT1-MMP induces a PI3 Kinase/Akt dependent pathway leading to the transcriptional up-regulation of VEGF-A, ***(ii)*** demonstrate an MT1-MMP – VEGFR-2 – Src tri-molecular complex in breast cancer cells, ***(iii)*** reveal the requirement for MT1-MMP, in particular its hemopexin domain, in the sub-cellular localisation of VEGFR-2 and ***(iv)*** demonstrate for the first time that MT1-MMP is ubiquitinated and undergoes proteolytic processing leading to the release of the MT1-MMP ICD, which was found to co-immunoprecipitate with Polymerase II in the nuclei of MCF-7 cells. These observations strengthen the role of MT1-MMP as a key protein in tumour growth, angiogenesis and cell motility and further emphasise the function of its intracellular domain as well as the emerging field of non-catalytic functions of MT1-MMP.

6. Zusammenfassung

Membrane-type-1 matrix metalloproteinase (MT1-MMP, MMP-14) ist ein Zink-abhängiges Typ-I Transmembranprotein, das eine wichtige Rolle in der perizellulären Degradation, der Zellmigration und -invasion sowie der tumorigenen Angiogenese spielt. Endogene Expression bzw. Überexpression von MT1-MMP erhöht die Malignität der Zellen sowie das Wachstum und die Größe von Tumoren. MT1-MMP nimmt eine Schlüsselrolle in der malignen Progression durch die Induktion der Tumorangiogenese ein, die zumindest zum Teil auf die MT1-MMP vermittelte Expression des pro-angiogenetischen Faktors *Vascular Endothelial Growth Factor A* (VEGF-A) zurückzuführen ist. Es konnte gezeigt werden, dass diese MT1-MMP abhängige transkriptionelle Regulation sowohl von der extrazellulären katalytischen Domäne als auch von der intrazellulären Domäne (IZD) des Enzyms abhängt. Neben der Regulation der VEGF-A Expression verstärken sich Hinweise, dass MT1-MMP auch die Transkription von weiteren Zielgenen kontrolliert und dass es in nicht-katalytisch vermittelten zellulären Prozessen involviert ist. Der molekulare Mechanismus der transkriptionellen Regulation durch MT1-MMP wurde bislang jedoch nur unzureichend aufgeklärt.

Im Verlauf dieser Doktorarbeit wurden zwei neue, voneinander unabhängige MT1-MMP vermittelte Signaltransduktionswege identifiziert.
Zunächst wurde gezeigt, dass die beschriebene MT1-MMP abhängige Hochregulierung der VEGF-A Expression von der Aktivität von *VEGF Receptor-2* (VEGFR-2) sowie den Schlüsselkinasen Src, PI3 Kinase, mTOR und Akt abhängig ist. Die in diesem Signalweg beteiligten Kinasen zeigten zudem einen signifikanten Anstieg ihres Phosphorylierungsgrades in Abhängigkeit der MT1-MMP Expression in *in vitro* Zellkultursystemen. Mit Hilfe immunologischer Detektionsverfahren wurde MT1-MMP zudem in einem Komplex mit den aktiven Phosphorylierungsformen von Src und Akt gefunden. Durch den Einsatz von Substitutions- und Deletionsmutationen wurden zusätzlich neue Motive der MT1-MMP Aminosäurensequenz identifiziert, die die transkriptionelle Expression von VEGF-A kontrollieren. Zudem wurde die Formation eines Komplexes bestehend aus MT1-MMP, VEGFR-2 und Src an der Zelloberfläche von MCF-7 Zellen beobachtet, welcher für die Genexpression von VEGF-A notwendig ist. Die IZD von MT1-MMP wurde als MT1-MMP - Src Interaktionsdomäne identifiziert. Die

extrazelluläre Hemopexin- und die Transmembrandomäne hingegen vermitteln bzw. regulieren sowohl die Interaktion zwischen MT1-MMP und VEGFR-2 als auch die Lokalisierung von VEGFR-2. Die nähere Charakterisierung dieses MT1-MMP abhängigen Signalweges, der zur Expression von VEGF-A führt, legt einen VEGFR-2 induzierten Transduktionsweg mit anschließender Aktivierung von PI3 Kinase, Akt und mTOR nahe und unterstreicht die nicht-katalytische Rolle von MT1-MMP im Zuge der Tumorangiogenese.

In dieser Arbeit wurde ein weiterer MT1-MMP abhängiger Signalweg identifiziert und charakterisiert, der durch eine Src- und Proteasom-vermittelte proteolytische Spaltung von MT1-MMP induziert wird. Diese Prozessierung führt zur Abspaltung der IZD und zur transkriptionellen Aktivierung in einem Reportergen System. Dementsprechend wurde die MT1-MMP IZD mittels immunologischer Ansätze in Zellkernen von ***(i)*** MCF-7 Zellen, ***(ii)*** MDA-MB-231 Zellen und ***(iii)*** humanen Mammakarzinomen detektiert. Ein Biotin-markiertes MT1-MMP IZD Peptid wurde in der nukleären Fraktion von MCF-7 Zellen nachgewiesen und ko-immunopräzipitierte mit RNA Polymerase II, was auf einen potentiellen Transkriptions-Initiations Komplex hinweist. Interessanterweise konnte nachgewiesen werden, dass die MT1-MMP IZD ubiquitiniert (K^{581}) wird und dass eine Mutation dieser Aminosäure die nukleäre Lokalisierung der MT1-MMP IZD signifikant reduziert. Die post-translationale Ubiquitinierung bietet eine interessante Erklärung für sowohl die Proteasom-abhängige Abspaltung als auch die nukleäre Translokalisierung der MT1-MMP IZD.

Zusammenfassend wurden im Zuge dieser Arbeit zwei MT1-MMP abhängige Signaltransduktionswege identifiziert. Die hier zusammengefassten Daten zeigen, dass ***(i)*** VEGF-A Expression durch eine MT1-MMP vermittelte Aktivierung des PI3 Kinase/Akt Signalwegs induziert wird, ***(ii)*** MT1-MMP einen trimolekularen Komplex mit VEGFR-2 und Src an der Zelloberfläche bildet, ***(iii)*** MT1-MMP die zelluläre Lokalisierung und Kompartimentalisierung von VEGFR-2 steuert, ***(iv)*** die MT1-MMP IZD post-translational ubiquitiniert wird und dass ***(v)*** die MT1-MMP IZD abgespalten wird und im Nukleus von MCF-7 Zellen mit RNA-Polymerase II ko-immunopräzipitiert. Die hier dargestellten Ergebnisse heben die Rolle von MT1-MMP, insbesondere der intrazellulären Domäne, in der Tumorigenese hervor und fügen dem bereits umfassenden tumorigenen Funktionsspektrum von MT1-MMP neue nicht-katalytische Aktivitäten in der Biologie transformierter Zellen hinzu.

7 References

1. Lopez-Otin C, Overall CM. Protease degradomics: a new challenge for proteomics. Nat Rev Mol Cell Biol. 2002;3:509-519.

2. Belkin AM, Akimov SS, Zaritskaya LS, Ratnikov BI, Deryugina EI, Strongin AY. Matrix-dependent proteolysis of surface transglutaminase by membrane-type metalloproteinase regulates cancer cell adhesion and locomotion. J Biol Chem. 2001;276:18415-18422.

3. Lopez-Otin C, Matrisian LM. Emerging roles of proteases in tumour suppression. Nat Rev Cancer. 2007;7:800-808.

4. Mori H, Tomari T, Koshikawa N, et al. CD44 directs membrane-type 1 matrix metalloproteinase to lamellipodia by associating with its hemopexin-like domain. Embo J. 2002;21:3949-3959.

5. Chen WT, Wang JY. Specialized surface protrusions of invasive cells, invadopodia and lamellipodia, have differential MT1-MMP, MMP-2, and TIMP-2 localization. Ann N Y Acad Sci. 1999;878:361-371.

6. Egeblad M, Werb Z. New functions for the matrix metalloproteinases in cancer progression. Nat Rev Cancer. 2002;2:161-174.

7. Nagase H, Woessner JF, Jr. Matrix metalloproteinases. J Biol Chem. 1999;274:21491-21494.

8. Sternlicht MD, Werb Z. How matrix metalloproteinases regulate cell behavior. Annu Rev Cell Dev Biol. 2001;17:463-516.

9. McCawley LJ, Matrisian LM. Matrix metalloproteinases: they're not just for matrix anymore! Curr Opin Cell Biol. 2001;13:534-540.

10. Overall CM, Lopez-Otin C. Strategies for MMP inhibition in cancer: innovations for the post-trial era. Nat Rev Cancer. 2002;2:657-672.

11. Seiki M. The cell surface: the stage for matrix metalloproteinase regulation of migration. Curr Opin Cell Biol. 2002;14:624-632.

12. Knauper V, Cowell S, Smith B, et al. The role of the C-terminal domain of human collagenase-3 (MMP-13) in the activation of procollagenase-3, substrate specificity, and tissue inhibitor of metalloproteinase interaction. J Biol Chem. 1997;272:7608-7616.

13. Stetler-Stevenson WG, Yu AE. Proteases in invasion: matrix metalloproteinases. Semin Cancer Biol. 2001;11:143-152.

14. MacDougall JR, Bani MR, Lin Y, Rak J, Kerbel RS. The 92-kDa gelatinase B is expressed by advanced stage melanoma cells: suppression by somatic cell hybridization with early stage melanoma cells. Cancer Res. 1995;55:4174-4181.

15. Davies B, Miles DW, Happerfield LC, et al. Activity of type IV collagenases in benign and malignant breast disease. Br J Cancer. 1993;67:1126-1131.

16. Wolf C, Rouyer N, Lutz Y, et al. Stromelysin 3 belongs to a subgroup of proteinases expressed in breast carcinoma fibroblastic cells and possibly implicated in tumor progression. Proc Natl Acad Sci U S A. 1993;90:1843-1847.

17. Murray GI, Duncan ME, O'Neil P, Melvin WT, Fothergill JE. Matrix metalloproteinase-1 is associated with poor prognosis in colorectal cancer. Nat Med. 1996;2:461-462.

18. Chenard MP, O'Siorain L, Shering S, et al. High levels of stromelysin-3 correlate with poor prognosis in patients with breast carcinoma. Int J Cancer. 1996;69:448-451.

19. Visse R, Nagase H. Matrix metalloproteinases and tissue inhibitors of metalloproteinases: structure, function, and biochemistry. Circ Res. 2003;92:827-839.

20. Strongin AY. Proteolytic and non-proteolytic roles of membrane type-1 matrix metalloproteinase in malignancy. Biochim Biophys Acta. 2009.

21. Murphy G, Stanton H, Cowell S, et al. Mechanisms for pro matrix metalloproteinase activation. APMIS. 1999;107:38-44.

22. Pei D, Weiss SJ. Furin-dependent intracellular activation of the human stromelysin-3 zymogen. Nature. 1995;375:244-247.

23. Sato H, Takino T, Okada Y, et al. A matrix metalloproteinase expressed on the surface of invasive tumour cells. Nature. 1994;370:61-65.

24. Zucker S, Pei D, Cao J, Lopez-Otin C. Membrane type-matrix metalloproteinases (MT-MMP). Curr Top Dev Biol. 2003;54:1-74.

25. Seiki M, Yana I. Roles of pericellular proteolysis by membrane type-1 matrix metalloproteinase in cancer invasion and angiogenesis. Cancer Sci. 2003;94:569-574.

26. Deryugina EI, Soroceanu L, Strongin AY. Up-regulation of vascular endothelial growth factor by membrane-type 1 matrix metalloproteinase stimulates human glioma xenograft growth and angiogenesis. Cancer Res. 2002;62:580-588.

27. Sounni NE, Baramova EN, Munaut C, et al. Expression of membrane type 1 matrix metalloproteinase (MT1-MMP) in A2058 melanoma cells is associated with MMP-2 activation and increased tumor growth and vascularization. Int J Cancer. 2002;98:23-28.

28. Hotary KB, Allen ED, Brooks PC, Datta NS, Long MW, Weiss SJ. Membrane type I matrix metalloproteinase usurps tumor growth control imposed by the three-dimensional extracellular matrix. Cell. 2003;114:33-45.

29. Soulie P, Carrozzino F, Pepper MS, Strongin AY, Poupon MF, Montesano R. Membrane-type-1 matrix metalloproteinase confers tumorigenicity on nonmalignant epithelial cells. Oncogene. 2005;24:1689-1697.

30. Sakakibara M, Koizumi S, Saikawa Y, et al. Membrane-type matrix metalloproteinase-1 expression and activation of gelatinase A as prognostic markers in advanced pediatric neuroblastoma. Cancer. 1999;85:231-239.

31. Michael M, Babic B, Khokha R, et al. Expression and prognostic significance of metalloproteinases and their tissue inhibitors in patients with small-cell lung cancer. J Clin Oncol. 1999;17:1802-1808.

32. Yoshizaki T, Maruyama Y, Sato H, Furukawa M. Expression of tissue inhibitor of matrix metalloproteinase-2 correlates with activation of matrix metalloproteinase-2 and predicts poor prognosis in tongue squamous cell carcinoma. Int J Cancer. 2001;95:44-50.

33. Kanayama H, Yokota K, Kurokawa Y, Murakami Y, Nishitani M, Kagawa S. Prognostic values of matrix metalloproteinase-2 and tissue inhibitor of metalloproteinase-2 expression in bladder cancer. Cancer. 1998;82:1359-1366.

34. Davidson B, Goldberg I, Gotlieb WH, et al. The prognostic value of metalloproteinases and angiogenic factors in ovarian carcinoma. Mol Cell Endocrinol. 2002;187:39-45.

35. Itoh Y, Nagase H. Matrix metalloproteinases in cancer. Essays Biochem. 2002;38:21-36.

36. Bravo-Cordero JJ, Marrero-Diaz R, Megias D, et al. MT1-MMP proinvasive activity is regulated by a novel Rab8-dependent exocytic pathway. Embo J. 2007;26:1499-1510.

37. Steffen A, Le Dez G, Poincloux R, et al. MT1-MMP-dependent invasion is regulated by TI-VAMP/VAMP7. Curr Biol. 2008;18:926-931.

38. Ouyang M, Lu S, Li XY, et al. Visualization of polarized membrane type 1 matrix metalloproteinase activity in live cells by fluorescence resonance energy transfer imaging. J Biol Chem. 2008;283:17740-17748.

39. Remacle A, Murphy G, Roghi C. Membrane type I-matrix metalloproteinase (MT1-MMP) is internalised by two different pathways and is recycled to the cell surface. J Cell Sci. 2003;116:3905-3916.

40. Remacle AG, Rozanov DV, Baciu PC, Chekanov AV, Golubkov VS, Strongin AY. The transmembrane domain is essential for the microtubular trafficking of membrane type-1 matrix metalloproteinase (MT1-MMP). J Cell Sci. 2005;118:4975-4984.

41. Wu YI, Munshi HG, Sen R, et al. Glycosylation broadens the substrate profile of membrane type 1 matrix metalloproteinase. J Biol Chem. 2004;279:8278-8289.

42. d'Ortho MP, Will H, Atkinson S, et al. Membrane-type matrix metalloproteinases 1 and 2 exhibit broad-spectrum proteolytic capacities comparable to many matrix metalloproteinases. Eur J Biochem. 1997;250:751-757.

43. Ohuchi E, Imai K, Fujii Y, Sato H, Seiki M, Okada Y. Membrane type 1 matrix metalloproteinase digests interstitial collagens and other extracellular matrix macromolecules. J Biol Chem. 1997;272:2446-2451.

44. Hiraoka N, Allen E, Apel IJ, Gyetko MR, Weiss SJ. Matrix metalloproteinases regulate neovascularization by acting as pericellular fibrinolysins. Cell. 1998;95:365-377.

45. Koshikawa N, Giannelli G, Cirulli V, Miyazaki K, Quaranta V. Role of cell surface metalloprotease MT1-MMP in epithelial cell migration over laminin-5. J Cell Biol. 2000;148:615-624.

46. Li Y, Aoki T, Mori Y, et al. Cleavage of lumican by membrane-type matrix metalloproteinase-1 abrogates this proteoglycan-mediated suppression of tumor cell colony formation in soft agar. Cancer Res. 2004;64:7058-7064.

47. Karsdal MA, Larsen L, Engsig MT, et al. Matrix metalloproteinase-dependent activation of latent transforming growth factor-beta controls the conversion of osteoblasts into osteocytes by blocking osteoblast apoptosis. J Biol Chem. 2002;277:44061-44067.

48. Mu D, Cambier S, Fjellbirkeland L, et al. The integrin alpha(v)beta8 mediates epithelial homeostasis through MT1-MMP-dependent activation of TGF-beta1. J Cell Biol. 2002;157:493-507.

49. Kajita M, Itoh Y, Chiba T, et al. Membrane-type 1 matrix metalloproteinase cleaves CD44 and promotes cell migration. J Cell Biol. 2001;153:893-904.

50. Rozanov DV, Hahn-Dantona E, Strickland DK, Strongin AY. The low density lipoprotein receptor-related protein LRP is regulated by membrane type-1 matrix metalloproteinase (MT1-MMP) proteolysis in malignant cells. J Biol Chem. 2004;279:4260-4268.

51. Endo K, Takino T, Miyamori H, et al. Cleavage of syndecan-1 by membrane type matrix metalloproteinase-1 stimulates cell migration. J Biol Chem. 2003;278:40764-40770.

52. Knauper V, Will H, Lopez-Otin C, et al. Cellular mechanisms for human procollagenase-3 (MMP-13) activation. Evidence that MT1-MMP (MMP-14) and gelatinase a (MMP-2) are able to generate active enzyme. J Biol Chem. 1996;271:17124-17131.

53. Deryugina EI, Ratnikov BI, Postnova TI, Rozanov DV, Strongin AY. Processing of integrin alpha(v) subunit by membrane type 1 matrix metalloproteinase stimulates migration of breast carcinoma cells on vitronectin and enhances tyrosine phosphorylation of focal adhesion kinase. J Biol Chem. 2002;277:9749-9756.

54. Dean RA, Butler GS, Hamma-Kourbali Y, et al. Identification of candidate angiogenic inhibitors processed by matrix metalloproteinase 2 (MMP-2) in cell-based proteomic screens: disruption of vascular endothelial growth factor (VEGF)/heparin affin regulatory peptide (pleiotrophin) and VEGF/Connective tissue growth factor angiogenic inhibitory complexes by MMP-2 proteolysis. Mol Cell Biol. 2007;27:8454-8465.

55. Itoh Y, Seiki M. MT1-MMP: a potent modifier of pericellular microenvironment. J Cell Physiol. 2006;206:1-8.

56. Tsunezuka Y, Kinoh H, Takino T, et al. Expression of membrane-type matrix metalloproteinase 1 (MT1-MMP) in tumor cells enhances pulmonary metastasis in an experimental metastasis assay. Cancer Res. 1996;56:5678-5683.

57. Ueda J, Kajita M, Suenaga N, Fujii K, Seiki M. Sequence-specific silencing of MT1-MMP expression suppresses tumor cell migration and invasion: importance of MT1-MMP as a therapeutic target for invasive tumors. Oncogene. 2003;22:8716-8722.

58. Naor D, Sionov RV, Ish-Shalom D. CD44: structure, function, and association with the malignant process. Adv Cancer Res. 1997;71:241-319.

59. Okamoto I, Kawano Y, Murakami D, et al. Proteolytic release of CD44 intracellular domain and its role in the CD44 signaling pathway. J Cell Biol. 2001;155:755-762.

60. Beauvais DM, Burbach BJ, Rapraeger AC. The syndecan-1 ectodomain regulates alphavbeta3 integrin activity in human mammary carcinoma cells. J Cell Biol. 2004;167:171-181.

61. Gingras D, Bousquet-Gagnon N, Langlois S, Lachambre MP, Annabi B, Beliveau R. Activation of the extracellular signal-regulated protein kinase (ERK) cascade by membrane-type-1 matrix metalloproteinase (MT1-MMP). FEBS Lett. 2001;507:231-236.

62. Takino T, Miyamori H, Watanabe Y, Yoshioka K, Seiki M, Sato H. Membrane type 1 matrix metalloproteinase regulates collagen-dependent mitogen-activated protein/extracellular signal-related kinase activation and cell migration. Cancer Res. 2004;64:1044-1049.

63. Schenk S, Hintermann E, Bilban M, et al. Binding to EGF receptor of a laminin-5 EGF-like fragment liberated during MMP-dependent mammary gland involution. J Cell Biol. 2003;161:197-209.

64. Holmbeck K, Bianco P, Caterina J, et al. MT1-MMP-deficient mice develop dwarfism, osteopenia, arthritis, and connective tissue disease due to inadequate collagen turnover. Cell. 1999;99:81-92.

65. Zhou Z, Apte SS, Soininen R, et al. Impaired endochondral ossification and angiogenesis in mice deficient in membrane-type matrix metalloproteinase I. Proc Natl Acad Sci U S A. 2000;97:4052-4057.

66. Hotary K, Allen E, Punturieri A, Yana I, Weiss SJ. Regulation of cell invasion and morphogenesis in a three-dimensional type I collagen matrix by membrane-type matrix metalloproteinases 1, 2, and 3. J Cell Biol. 2000;149:1309-1323.

67. Li XY, Ota I, Yana I, Sabeh F, Weiss SJ. Molecular dissection of the structural machinery underlying the tissue-invasive activity of membrane type-1 matrix metalloproteinase. Mol Biol Cell. 2008;19:3221-3233.

68. Nie J, Pei J, Blumenthal M, Pei D. Complete restoration of cell surface activity of transmembrane-truncated MT1-MMP by a glycosylphosphatidylinositol anchor. Implications for MT1-MMP-mediated prommp2 activation and collagenolysis in three-dimensions. J Biol Chem. 2007;282:6438-6443.

69. Seiki M, Mori H, Kajita M, Uekita T, Itoh Y. Membrane-type 1 matrix metalloproteinase and cell migration. Biochem Soc Symp. 2003:253-262.

70. Galvez BG, Matias-Roman S, Albar JP, Sanchez-Madrid F, Arroyo AG. Membrane type 1-matrix metalloproteinase is activated during migration of human endothelial cells and modulates endothelial motility and matrix remodeling. J Biol Chem. 2001;276:37491-37500.

71. Chun TH, Sabeh F, Ota I, et al. MT1-MMP-dependent neovessel formation within the confines of the three-dimensional extracellular matrix. J Cell Biol. 2004;167:757-767.

72. Sounni NE, Devy L, Hajitou A, et al. MT1-MMP expression promotes tumor growth and angiogenesis through an up-regulation of vascular endothelial growth factor expression. Faseb J. 2002;16:555-564.

73. Sounni NE, Roghi C, Chabottaux V, et al. Up-regulation of vascular endothelial growth factor-A by active membrane-type 1 matrix metalloproteinase through activation of Src-tyrosine kinases. J Biol Chem. 2004;279:13564-13574.

74. Folgueras AR, Pendas AM, Sanchez LM, Lopez-Otin C. Matrix metalloproteinases in cancer: from new functions to improved inhibition strategies. Int J Dev Biol. 2004;48:411-424.

75. Kadono Y, Shibahara K, Namiki M, Watanabe Y, Seiki M, Sato H. Membrane type 1-matrix metalloproteinase is involved in the formation of hepatocyte growth factor/scatter factor-induced branching tubules in madin-darby canine kidney epithelial cells. Biochem Biophys Res Commun. 1998;251:681-687.

76. Krubasik D, Eisenach PA, Kunz-Schughart LA, Murphy G, English WR. Granulocyte-macrophage colony stimulating factor induces endothelial capillary formation through induction of membrane-type 1 matrix metalloproteinase expression in vitro. Int J Cancer. 2008;122:1261-1272.

77. Ottaviano AJ, Sun L, Ananthanarayanan V, Munshi HG. Extracellular matrix-mediated membrane-type 1 matrix metalloproteinase expression in pancreatic ductal cells is regulated by transforming growth factor-beta1. Cancer Res. 2006;66:7032-7040.

78. Lohi J, Lehti K, Westermarck J, Kahari VM, Keski-Oja J. Regulation of membrane-type matrix metalloproteinase-1 expression by growth factors and phorbol 12-myristate 13-acetate. Eur J Biochem. 1996;239:239-247.

79. Lohi J, Keski-Oja J. Calcium ionophores decrease pericellular gelatinolytic activity via inhibition of 92-kDa gelatinase expression and decrease of 72-kDa gelatinase activation. J Biol Chem. 1995;270:17602-17609.

80. Van Meter TE, Broaddus WC, Rooprai HK, Pilkington GJ, Fillmore HL. Induction of membrane-type-1 matrix metalloproteinase by epidermal growth factor-mediated signaling in gliomas. Neuro Oncol. 2004;6:188-199.

81. Han YP, Tuan TL, Wu H, Hughes M, Garner WL. TNF-alpha stimulates activation of pro-MMP2 in human skin through NF-(kappa)B mediated induction of MT1-MMP. J Cell Sci. 2001;114:131-139.

82. Gilles C, Polette M, Seiki M, Birembaut P, Thompson EW. Implication of collagen type I-induced membrane-type 1-matrix metalloproteinase expression and matrix metalloproteinase-2 activation in the metastatic progression of breast carcinoma. Lab Invest. 1997;76:651-660.

83. Tyagi SC, Lewis K, Pikes D, et al. Stretch-induced membrane type matrix metalloproteinase and tissue plasminogen activator in cardiac fibroblast cells. J Cell Physiol. 1998;176:374-382.

84. Ailenberg M, Silverman M. Cellular activation of mesangial gelatinase A by cytochalasin D is accompanied by enhanced mRNA expression of both gelatinase A and its membrane-associated gelatinase A activator (MT-MMP). Biochem J. 1996;313 (Pt 3):879-884.

85. Lohi J, Lehti K, Valtanen H, Parks WC, Keski-Oja J. Structural analysis and promoter characterization of the human membrane-type matrix metalloproteinase-1 (MT1-MMP) gene. Gene. 2000;242:75-86.

86. Haas TL, Stitelman D, Davis SJ, Apte SS, Madri JA. Egr-1 mediates extracellular matrix-driven transcription of membrane type 1 matrix metalloproteinase in endothelium. J Biol Chem. 1999;274:22679-22685.

87. Pei D, Weiss SJ. Transmembrane-deletion mutants of the membrane-type matrix metalloproteinase-1 process progelatinase A and express intrinsic matrix-degrading activity. J Biol Chem. 1996;271:9135-9140.

88. Rozanov DV, Deryugina EI, Ratnikov BI, et al. Mutation analysis of membrane type-1 matrix metalloproteinase (MT1-MMP). The role of the cytoplasmic tail Cys(574), the active site Glu(240), and furin cleavage motifs in oligomerization, processing, and self-proteolysis of MT1-MMP expressed in breast carcinoma cells. J Biol Chem. 2001;276:25705-25714.

89. Okumura Y, Sato H, Seiki M, Kido H. Proteolytic activation of the precursor of membrane type 1 matrix metalloproteinase by human plasmin. A possible cell surface activator. FEBS Lett. 1997;402:181-184.

90. Sato H, Kinoshita T, Takino T, Nakayama K, Seiki M. Activation of a recombinant membrane type 1-matrix metalloproteinase (MT1-MMP) by furin and its interaction with tissue inhibitor of metalloproteinases (TIMP)-2. FEBS Lett. 1996;393:101-104.

91. Brew K, Dinakarpandian D, Nagase H. Tissue inhibitors of metalloproteinases: evolution, structure and function. Biochim Biophys Acta. 2000;1477:267-283.

92. Will H, Atkinson SJ, Butler GS, Smith B, Murphy G. The soluble catalytic domain of membrane type 1 matrix metalloproteinase cleaves the propeptide of progelatinase A and initiates autoproteolytic activation. Regulation by TIMP-2 and TIMP-3. J Biol Chem. 1996;271:17119-17123.

93. Bigg HF, Morrison CJ, Butler GS, et al. Tissue inhibitor of metalloproteinases-4 inhibits but does not support the activation of gelatinase A via efficient inhibition of membrane type 1-matrix metalloproteinase. Cancer Res. 2001;61:3610-3618.

94. Oh J, Takahashi R, Kondo S, et al. The membrane-anchored MMP inhibitor RECK is a key regulator of extracellular matrix integrity and angiogenesis. Cell. 2001;107:789-800.

95. Strongin AY, Collier I, Bannikov G, Marmer BL, Grant GA, Goldberg GI. Mechanism of cell surface activation of 72-kDa type IV collagenase. Isolation of the activated form of the membrane metalloprotease. J Biol Chem. 1995;270:5331-5338.

96. Atkinson SJ, Crabbe T, Cowell S, et al. Intermolecular autolytic cleavage can contribute to the activation of progelatinase A by cell membranes. J Biol Chem. 1995;270:30479-30485.

97. Itoh Y, Takamura A, Ito N, et al. Homophilic complex formation of MT1-MMP facilitates proMMP-2 activation on the cell surface and promotes tumor cell invasion. Embo J. 2001;20:4782-4793.

98. Lehti K, Lohi J, Valtanen H, Keski-Oja J. Proteolytic processing of membrane-type-1 matrix metalloproteinase is associated with gelatinase A activation at the cell surface. Biochem J. 1998;334 (Pt 2):345-353.

99. Stanton H, Gavrilovic J, Atkinson SJ, et al. The activation of ProMMP-2 (gelatinase A) by HT1080 fibrosarcoma cells is promoted by culture on a fibronectin substrate and is concomitant with an increase in processing of MT1-MMP (MMP-14) to a 45 kDa form. J Cell Sci. 1998;111 (Pt 18):2789-2798.

100. Toth M, Hernandez-Barrantes S, Osenkowski P, et al. Complex pattern of membrane type 1 matrix metalloproteinase shedding. Regulation by autocatalytic cells surface inactivation of active enzyme. J Biol Chem. 2002;277:26340-26350.

101. Hernandez-Barrantes S, Toth M, Bernardo MM, et al. Binding of active (57 kDa) membrane type 1-matrix metalloproteinase (MT1-MMP) to tissue inhibitor of metalloproteinase (TIMP)-2 regulates MT1-MMP processing and pro-MMP-2 activation. J Biol Chem. 2000;275:12080-12089.

102. Yu M, Sato H, Seiki M, Spiegel S, Thompson EW. Calcium influx inhibits MT1-MMP processing and blocks MMP-2 activation. FEBS Lett. 1997;412:568-572.

103. Gingras D, Page M, Annabi B, Beliveau R. Rapid activation of matrix metalloproteinase-2 by glioma cells occurs through a posttranslational MT1-MMP-dependent mechanism. Biochim Biophys Acta. 2000;1497:341-350.

104. Annabi B, Pilorget A, Bousquet-Gagnon N, Gingras D, Beliveau R. Calmodulin inhibitors trigger the proteolytic processing of membrane type-1 matrix metalloproteinase, but not its shedding in glioblastoma cells. Biochem J. 2001;359:325-333.

105. Tam EM, Wu YI, Butler GS, Stack MS, Overall CM. Collagen binding properties of the membrane type-1 matrix metalloproteinase (MT1-MMP) hemopexin C domain. The ectodomain of the 44-kDa autocatalytic product of MT1-MMP inhibits cell invasion by disrupting native type I collagen cleavage. J Biol Chem. 2002;277:39005-39014.

106. Machein MR, Plate KH. VEGF in brain tumors. J Neurooncol. 2000;50:109-120.

107. Li H, Bauzon DE, Xu X, Tschesche H, Cao J, Sang QA. Immunological characterization of cell-surface and soluble forms of membrane type 1 matrix metalloproteinase in human breast cancer cells and in fibroblasts. Mol Carcinog. 1998;22:84-94.

108. Harayama T, Ohuchi E, Aoki T, Sato H, Seiki M, Okada Y. Shedding of membrane type 1 matrix metalloproteinase in a human breast carcinoma cell line. Jpn J Cancer Res. 1999;90:942-950.

109. Zucker S, Drews M, Conner C, et al. Tissue inhibitor of metalloproteinase-2 (TIMP-2) binds to the catalytic domain of the cell surface receptor, membrane type 1-matrix metalloproteinase 1 (MT1-MMP). J Biol Chem. 1998;273:1216-1222.

110. Lehti K, Valtanen H, Wickstrom SA, Lohi J, Keski-Oja J. Regulation of membrane-type-1 matrix metalloproteinase activity by its cytoplasmic domain. J Biol Chem. 2000;275:15006-15013.

111. Maisi P, Prikk K, Sepper R, et al. Soluble membrane-type 1 matrix metalloproteinase (MT1-MMP) and gelatinase A (MMP-2) in induced sputum and bronchoalveolar lavage fluid of human bronchial asthma and bronchiectasis. APMIS. 2002;110:771-782.

112. Toth M, Sohail A, Mobashery S, Fridman R. MT1-MMP shedding involves an ADAM and is independent of its localization in lipid rafts. Biochem Biophys Res Commun. 2006;350:377-384.

113. Sato T, del Carmen Ovejero M, Hou P, et al. Identification of the membrane-type matrix metalloproteinase MT1-MMP in osteoclasts. J Cell Sci. 1997;110 (Pt 5):589-596.

114. Suenaga N, Mori H, Itoh Y, Seiki M. CD44 binding through the hemopexin-like domain is critical for its shedding by membrane-type 1 matrix metalloproteinase. Oncogene. 2005;24:859-868.

115. Ellerbroek SM, Wu YI, Overall CM, Stack MS. Functional interplay between type I collagen and cell surface matrix metalloproteinase activity. J Biol Chem. 2001;276:24833-24842.

116. Wolf K, Mazo I, Leung H, et al. Compensation mechanism in tumor cell migration: mesenchymal-amoeboid transition after blocking of pericellular proteolysis. J Cell Biol. 2003;160:267-277.

117. Jiang A, Lehti K, Wang X, Weiss SJ, Keski-Oja J, Pei D. Regulation of membrane-type matrix metalloproteinase 1 activity by dynamin-mediated endocytosis. Proc Natl Acad Sci U S A. 2001;98:13693-13698.

118. Galvez BG, Matias-Roman S, Yanez-Mo M, Vicente-Manzanares M, Sanchez-Madrid F, Arroyo AG. Caveolae are a novel pathway for membrane-type 1 matrix metalloproteinase traffic in human endothelial cells. Mol Biol Cell. 2004;15:678-687.

119. Labrecque L, Nyalendo C, Langlois S, et al. Src-mediated tyrosine phosphorylation of caveolin-1 induces its association with membrane type 1 matrix metalloproteinase. J Biol Chem. 2004;279:52132-52140.

120. Annabi B, Lachambre M, Bousquet-Gagnon N, Page M, Gingras D, Beliveau R. Localization of membrane-type 1 matrix metalloproteinase in caveolae membrane domains. Biochem J. 2001;353:547-553.

121. Uekita T, Itoh Y, Yana I, Ohno H, Seiki M. Cytoplasmic tail-dependent internalization of membrane-type 1 matrix metalloproteinase is important for its invasion-promoting activity. J Cell Biol. 2001;155:1345-1356.

122. Sverdlov M, Shajahan AN, Minshall RD. Tyrosine phosphorylation-dependence of caveolae-mediated endocytosis. J Cell Mol Med. 2007;11:1239-1250.

123. Sabeh F, Ota I, Holmbeck K, et al. Tumor cell traffic through the extracellular matrix is controlled by the membrane-anchored collagenase MT1-MMP. J Cell Biol. 2004;167:769-781.

124. Cao J, Sato H, Takino T, Seiki M. The C-terminal region of membrane type matrix metalloproteinase is a functional transmembrane domain required for pro-gelatinase A activation. J Biol Chem. 1995;270:801-805.

125. Nakahara H, Howard L, Thompson EW, et al. Transmembrane/cytoplasmic domain-mediated membrane type 1-matrix metalloprotease docking to invadopodia is required for cell invasion. Proc Natl Acad Sci U S A. 1997;94:7959-7964.

126. Rozanov DV, Ghebrehiwet B, Ratnikov B, Monosov EZ, Deryugina EI, Strongin AY. The cytoplasmic tail peptide sequence of membrane type-1 matrix metalloproteinase (MT1-MMP) directly binds to gC1qR, a compartment-specific chaperone-like regulatory protein. FEBS Lett. 2002;527:51-57.

127. Wang X, Ma D, Keski-Oja J, Pei D. Co-recycling of MT1-MMP and MT3-MMP through the trans-Golgi network. Identification of DKV582 as a recycling signal. J Biol Chem. 2004;279:9331-9336.

128. Stricker NL, Christopherson KS, Yi BA, et al. PDZ domain of neuronal nitric oxide synthase recognizes novel C-terminal peptide sequences. Nat Biotechnol. 1997;15:336-342.

129. Harris BZ, Lim WA. Mechanism and role of PDZ domains in signaling complex assembly. J Cell Sci. 2001;114:3219-3231.

130. del Pozo MA, Balasubramanian N, Alderson NB, et al. Phospho-caveolin-1 mediates integrin-regulated membrane domain internalization. Nat Cell Biol. 2005;7:901-908.

131. Anilkumar N, Uekita T, Couchman JR, Nagase H, Seiki M, Itoh Y. Palmitoylation at Cys574 is essential for MT1-MMP to promote cell migration. Faseb J. 2005;19:1326-1328.

132. Nyalendo C, Michaud M, Beaulieu E, et al. Src-dependent phosphorylation of membrane-type 1 matrix metalloproteinase on cytoplasmic tyrosine 573: Role in endothelial and tumor cell migration. J Biol Chem. 2007.

133. Nyalendo C, Beaulieu E, Sartelet H, et al. Impaired tyrosine phosphorylation of membrane type 1-matrix metalloproteinase reduces tumor cell proliferation in three-dimensional matrices and abrogates tumor growth in mice. Carcinogenesis. 2008;29:1655-1664.

134. Moss NM, Wu YI, Liu Y, Munshi HG, Stack MS. Modulation of the membrane type 1 matrix metalloproteinase cytoplasmic tail enhances tumor cell invasion and proliferation in three-dimensional collagen matrices. J Biol Chem. 2009;284:19791-19799.

135. Uekita T, Gotoh I, Kinoshita T, et al. Membrane-type 1 matrix metalloproteinase cytoplasmic tail-binding protein-1 is a new member of the Cupin superfamily. A possible multifunctional protein acting as an invasion suppressor down-regulated in tumors. J Biol Chem. 2004;279:12734-12743.

136. Sekiya I, Vuoristo JT, Larson BL, Prockop DJ. In vitro cartilage formation by human adult stem cells from bone marrow stroma defines the sequence of cellular and molecular events during chondrogenesis. Proc Natl Acad Sci U S A. 2002;99:4397-4402.

137. Munaut C, Boniver J, Foidart JM, Deprez M. Macrophage migration inhibitory factor (MIF) expression in human glioblastomas correlates with vascular endothelial growth factor (VEGF) expression. Neuropathol Appl Neurobiol. 2002;28:452-460.

138. Freudenberg JA, Chen WT. Induction of Smad1 by MT1-MMP contributes to tumor growth. Int J Cancer. 2007;121:966-977.

139. Saeb-Parsy K, Veerakumarasivam A, Wallard MJ, et al. MT1-MMP regulates urothelial cell invasion via transcriptional regulation of Dickkopf-3. Br J Cancer. 2008;99:663-669.

140. D'Alessio S, Ferrari G, Cinnante K, et al. Tissue inhibitor of metalloproteinases-2 binding to membrane-type 1 matrix metalloproteinase induces MAPK activation and cell growth by a non-proteolytic mechanism. J Biol Chem. 2008;283:87-99.

141. Lehti K, Allen E, Birkedal-Hansen H, et al. An MT1-MMP-PDGF receptor-beta axis regulates mural cell investment of the microvasculature. Genes Dev. 2005;19:979-991.

142. Hoppe T, Rape M, Jentsch S. Membrane-bound transcription factors: regulated release by RIP or RUP. Curr Opin Cell Biol. 2001;13:344-348.

143. Mumm JS, Kopan R. Notch signaling: from the outside in. Dev Biol. 2000;228:151-165.

144. De Strooper B, Annaert W, Cupers P, et al. A presenilin-1-dependent gamma-secretase-like protease mediates release of Notch intracellular domain. Nature. 1999;398:518-522.

145. Gao Y, Pimplikar SW. The gamma -secretase-cleaved C-terminal fragment of amyloid precursor protein mediates signaling to the nucleus. Proc Natl Acad Sci U S A. 2001;98:14979-14984.

146. Wang X, Sato R, Brown MS, Hua X, Goldstein JL. SREBP-1, a membrane-bound transcription factor released by sterol-regulated proteolysis. Cell. 1994;77:53-62.

147. LaVoie MJ, Selkoe DJ. The Notch ligands, Jagged and Delta, are sequentially processed by alpha-secretase and presenilin/gamma-secretase and release signaling fragments. J Biol Chem. 2003;278:34427-34437.

148. Ni CY, Murphy MP, Golde TE, Carpenter G. gamma -Secretase cleavage and nuclear localization of ErbB-4 receptor tyrosine kinase. Science. 2001;294:2179-2181.

149. Marambaud P, Shioi J, Serban G, et al. A presenilin-1/gamma-secretase cleavage releases the E-cadherin intracellular domain and regulates disassembly of adherens junctions. Embo J. 2002;21:1948-1956.

150. Schulz JG, Annaert W, Vandekerckhove J, Zimmermann P, De Strooper B, David G. Syndecan 3 intramembrane proteolysis is presenilin/gamma-secretase-dependent and modulates cytosolic signaling. J Biol Chem. 2003;278:48651-48657.

151. May P, Reddy YK, Herz J. Proteolytic processing of low density lipoprotein receptor-related protein mediates regulated release of its intracellular domain. J Biol Chem. 2002;277:18736-18743.

152. Wolfe MS, Xia W, Ostaszewski BL, Diehl TS, Kimberly WT, Selkoe DJ. Two transmembrane aspartates in presenilin-1 required for presenilin endoproteolysis and gamma-secretase activity. Nature. 1999;398:513-517.

153. Wolfe MS, De Los Angeles J, Miller DD, Xia W, Selkoe DJ. Are presenilins intramembrane-cleaving proteases? Implications for the molecular mechanism of Alzheimer's disease. Biochemistry. 1999;38:11223-11230.

154. Urban S, Lee JR, Freeman M. Drosophila rhomboid-1 defines a family of putative intramembrane serine proteases. Cell. 2001;107:173-182.

155. Hooper NM, Turner AJ. The search for alpha-secretase and its potential as a therapeutic approach to Alzheimer s disease. Curr Med Chem. 2002;9:1107-1119.

156. Allinson TM, Parkin ET, Turner AJ, Hooper NM. ADAMs family members as amyloid precursor protein alpha-secretases. J Neurosci Res. 2003;74:342-352.

157. Asai M, Hattori C, Szabo B, et al. Putative function of ADAM9, ADAM10, and ADAM17 as APP alpha-secretase. Biochem Biophys Res Commun. 2003;301:231-235.

158. Lammich S, Kojro E, Postina R, et al. Constitutive and regulated alpha-secretase cleavage of Alzheimer's amyloid precursor protein by a disintegrin metalloprotease. Proc Natl Acad Sci U S A. 1999;96:3922-3927.

159. Buxbaum JD, Liu KN, Luo Y, et al. Evidence that tumor necrosis factor alpha converting enzyme is involved in regulated alpha-secretase cleavage of the Alzheimer amyloid protein precursor. J Biol Chem. 1998;273:27765-27767.

160. Hotoda N, Koike H, Sasagawa N, Ishiura S. A secreted form of human ADAM9 has an alpha-secretase activity for APP. Biochem Biophys Res Commun. 2002;293:800-805.

161. Rio C, Buxbaum JD, Peschon JJ, Corfas G. Tumor necrosis factor-alpha-converting enzyme is required for cleavage of erbB4/HER4. J Biol Chem. 2000;275:10379-10387.

162. Lee JR, Urban S, Garvey CF, Freeman M. Regulated intracellular ligand transport and proteolysis control EGF signal activation in Drosophila. Cell. 2001;107:161-171.

163. Ghiglione C, Bach EA, Paraiso Y, Carraway KL, 3rd, Noselli S, Perrimon N. Mechanism of activation of the Drosophila EGF Receptor by the TGFalpha ligand Gurken during oogenesis. Development. 2002;129:175-186.

164. Tsruya R, Schlesinger A, Reich A, Gabay L, Sapir A, Shilo BZ. Intracellular trafficking by Star regulates cleavage of the Drosophila EGF receptor ligand Spitz. Genes Dev. 2002;16:222-234.

165. Ikezu T, Trapp BD, Song KS, Schlegel A, Lisanti MP, Okamoto T. Caveolae, plasma membrane microdomains for alpha-secretase-mediated processing of the amyloid precursor protein. J Biol Chem. 1998;273:10485-10495.

166. Murakami D, Okamoto I, Nagano O, et al. Presenilin-dependent gamma-secretase activity mediates the intramembranous cleavage of CD44. Oncogene. 2003;22:1511-1516.

167. Lammich S, Okochi M, Takeda M, et al. Presenilin-dependent intramembrane proteolysis of CD44 leads to the liberation of its intracellular domain and the secretion of an Abeta-like peptide. J Biol Chem. 2002;277:44754-44759.

168. Liu CX, Ranganathan S, Robinson S, Strickland DK. gamma-Secretase-mediated release of the low density lipoprotein receptor-related protein 1B intracellular domain suppresses anchorage-independent growth of neuroglioma cells. J Biol Chem. 2007;282:7504-7511.

169. Wong PC, Zheng H, Chen H, et al. Presenilin 1 is required for Notch1 and DII1 expression in the paraxial mesoderm. Nature. 1997;387:288-292.

170. Shen J, Bronson RT, Chen DF, Xia W, Selkoe DJ, Tonegawa S. Skeletal and CNS defects in Presenilin-1-deficient mice. Cell. 1997;89:629-639.

171. De Strooper B, Saftig P, Craessaerts K, et al. Deficiency of presenilin-1 inhibits the normal cleavage of amyloid precursor protein. Nature. 1998;391:387-390.

172. Forloni G, Demicheli F, Giorgi S, Bendotti C, Angeretti N. Expression of amyloid precursor protein mRNAs in endothelial, neuronal and glial cells: modulation by interleukin-1. Brain Res Mol Brain Res. 1992;16:128-134.

173. Esler WP, Wolfe MS. A portrait of Alzheimer secretases--new features and familiar faces. Science. 2001;293:1449-1454.

174. Vassar R, Bennett BD, Babu-Khan S, et al. Beta-secretase cleavage of Alzheimer's amyloid precursor protein by the transmembrane aspartic protease BACE. Science. 1999;286:735-741.

175. Li Q, Sudhof TC. Cleavage of amyloid-beta precursor protein and amyloid-beta precursor-like protein by BACE 1. J Biol Chem. 2004;279:10542-10550.

176. Farzan M, Schnitzler CE, Vasilieva N, Leung D, Choe H. BACE2, a beta -secretase homolog, cleaves at the beta site and within the amyloid-beta region of the amyloid-beta precursor protein. Proc Natl Acad Sci U S A. 2000;97:9712-9717.

177. Yan R, Munzner JB, Shuck ME, Bienkowski MJ. BACE2 functions as an alternative alpha-secretase in cells. J Biol Chem. 2001;276:34019-34027.

178. Sinha S, Lieberburg I. Cellular mechanisms of beta-amyloid production and secretion. Proc Natl Acad Sci U S A. 1999;96:11049-11053.

179. Cao X, Sudhof TC. A transcriptionally [correction of transcriptively] active complex of APP with Fe65 and histone acetyltransferase Tip60. Science. 2001;293:115-120.

180. Cupers P, Orlans I, Craessaerts K, Annaert W, De Strooper B. The amyloid precursor protein (APP)-cytoplasmic fragment generated by gamma-secretase is rapidly degraded but distributes partially in a nuclear fraction of neurones in culture. J Neurochem. 2001;78:1168-1178.

181. Logeat F, Bessia C, Brou C, et al. The Notch1 receptor is cleaved constitutively by a furin-like convertase. Proc Natl Acad Sci U S A. 1998;95:8108-8112.

182. Brou C, Logeat F, Gupta N, et al. A novel proteolytic cleavage involved in Notch signaling: the role of the disintegrin-metalloprotease TACE. Mol Cell. 2000;5:207-216.

183. Mumm JS, Schroeter EH, Saxena MT, et al. A ligand-induced extracellular cleavage regulates gamma-secretase-like proteolytic activation of Notch1. Mol Cell. 2000;5:197-206.

184. Schroeter EH, Kisslinger JA, Kopan R. Notch-1 signalling requires ligand-induced proteolytic release of intracellular domain. Nature. 1998;393:382-386.

185. Struhl G, Adachi A. Requirements for presenilin-dependent cleavage of notch and other transmembrane proteins. Mol Cell. 2000;6:625-636.

186. Pascall JC, Brown KD. Characterization of a mammalian cDNA encoding a protein with high sequence similarity to the Drosophila regulatory protein Rhomboid. FEBS Lett. 1998;429:337-340.

187. Pellegrini L, Passer BJ, Canelles M, et al. PAMP and PARL, two novel putative metalloproteases interacting with the COOH-terminus of Presenilin-1 and -2. J Alzheimers Dis. 2001;3:181-190.

188. Jaszai J, Brand M. Cloning and expression of Ventrhoid, a novel vertebrate homologue of the Drosophila EGF pathway gene rhomboid. Mech Dev. 2002;113:73-77.

189. Pascall JC, Brown KD. Intramembrane cleavage of ephrinB3 by the human rhomboid family protease, RHBDL2. Biochem Biophys Res Commun. 2004;317:244-252.

190. Hoppe T, Matuschewski K, Rape M, Schlenker S, Ulrich HD, Jentsch S. Activation of a membrane-bound transcription factor by regulated ubiquitin/proteasome-dependent processing. Cell. 2000;102:577-586.

191. Demartino GN, Gillette TG. Proteasomes: machines for all reasons. Cell. 2007;129:659-662.

192. Fan CM, Maniatis T. Generation of p50 subunit of NF-kappa B by processing of p105 through an ATP-dependent pathway. Nature. 1991;354:395-398.

193. Palombella VJ, Rando OJ, Goldberg AL, Maniatis T. The ubiquitin-proteasome pathway is required for processing the NF-kappa B1 precursor protein and the activation of NF-kappa B. Cell. 1994;78:773-785.

194. Tomanek RJ, Schatteman GC. Angiogenesis: new insights and therapeutic potential. Anat Rec. 2000;261:126-135.

195. Ellis LM, Liu W, Ahmad SA, et al. Overview of angiogenesis: Biologic implications for antiangiogenic therapy. Semin Oncol. 2001;28:94-104.

196. Bauvois B. Transmembrane proteases in cell growth and invasion: new contributors to angiogenesis? Oncogene. 2004;23:317-329.

197. Ferrara N. Molecular and biological properties of vascular endothelial growth factor. J Mol Med. 1999;77:527-543.

198. Risau W. Mechanisms of angiogenesis. Nature. 1997;386:671-674.

199. Folkman J. Angiogenesis in cancer, vascular, rheumatoid and other disease. Nat Med. 1995;1:27-31.

200. Zachary I, Gliki G. Signaling transduction mechanisms mediating biological actions of the vascular endothelial growth factor family. Cardiovasc Res. 2001;49:568-581.

201. Linderholm BK, Lindh B, Beckman L, et al. Prognostic correlation of basic fibroblast growth factor and vascular endothelial growth factor in 1307 primary breast cancers. Clin Breast Cancer. 2003;4:340-347.

202. Willett CG, Boucher Y, di Tomaso E, et al. Direct evidence that the VEGF-specific antibody bevacizumab has antivascular effects in human rectal cancer. Nat Med. 2004;10:145-147.

203. Ferrara N, Hillan KJ, Gerber HP, Novotny W. Discovery and development of bevacizumab, an anti-VEGF antibody for treating cancer. Nat Rev Drug Discov. 2004;3:391-400.

204. Zachary I. VEGF signalling: integration and multi-tasking in endothelial cell biology. Biochem Soc Trans. 2003;31:1171-1177.

205. Petrova TV, Makinen T, Alitalo K. Signaling via vascular endothelial growth factor receptors. Exp Cell Res. 1999;253:117-130.

206. Poltorak Z, Cohen T, Sivan R, et al. VEGF145, a secreted vascular endothelial growth factor isoform that binds to extracellular matrix. J Biol Chem. 1997;272:7151-7158.

207. Stimpfl M, Tong D, Fasching B, et al. Vascular endothelial growth factor splice variants and their prognostic value in breast and ovarian cancer. Clin Cancer Res. 2002;8:2253-2259.

208. Neufeld G, Cohen T, Gitay-Goren H, et al. Similarities and differences between the vascular endothelial growth factor (VEGF) splice variants. Cancer Metastasis Rev. 1996;15:153-158.

209. Yen L, Benlimame N, Nie ZR, et al. Differential regulation of tumor angiogenesis by distinct ErbB homo- and heterodimers. Mol Biol Cell. 2002;13:4029-4044.

210. Lu M, Amano S, Miyamoto K, et al. Insulin-induced vascular endothelial growth factor expression in retina. Invest Ophthalmol Vis Sci. 1999;40:3281-3286.

211. Warren RS, Yuan H, Matli MR, Ferrara N, Donner DB. Induction of vascular endothelial growth factor by insulin-like growth factor 1 in colorectal carcinoma. J Biol Chem. 1996;271:29483-29488.

212. Zhang YW, Su Y, Volpert OV, Vande Woude GF. Hepatocyte growth factor/scatter factor mediates angiogenesis through positive VEGF and negative thrombospondin 1 regulation. Proc Natl Acad Sci U S A. 2003;100:12718-12723.

213. Finkenzeller G, Marme D, Weich HA, Hug H. Platelet-derived growth factor-induced transcription of the vascular endothelial growth factor gene is mediated by protein kinase C. Cancer Res. 1992;52:4821-4823.

214. Deroanne CF, Hajitou A, Calberg-Bacq CM, Nusgens BV, Lapiere CM. Angiogenesis by fibroblast growth factor 4 is mediated through an autocrine up-regulation of vascular endothelial growth factor expression. Cancer Res. 1997;57:5590-5597.

215. Rak J, Mitsuhashi Y, Sheehan C, et al. Oncogenes and tumor angiogenesis: differential modes of vascular endothelial growth factor up-regulation in ras-transformed epithelial cells and fibroblasts. Cancer Res. 2000;60:490-498.

216. Jiang BH, Rue E, Wang GL, Roe R, Semenza GL. Dimerization, DNA binding, and transactivation properties of hypoxia-inducible factor 1. J Biol Chem. 1996;271:17771-17778.

217. Carmeliet P, Dor Y, Herbert JM, et al. Role of HIF-1alpha in hypoxia-mediated apoptosis, cell proliferation and tumour angiogenesis. Nature. 1998;394:485-490.

218. Jiang BH, Liu LZ. PI3K/PTEN signaling in angiogenesis and tumorigenesis. Adv Cancer Res. 2009;102:19-65.

219. Ryuto M, Ono M, Izumi H, et al. Induction of vascular endothelial growth factor by tumor necrosis factor alpha in human glioma cells. Possible roles of SP-1. J Biol Chem. 1996;271:28220-28228.

220. Gille J, Swerlick RA, Caughman SW. Transforming growth factor-alpha-induced transcriptional activation of the vascular permeability factor (VPF/VEGF) gene requires AP-2-dependent DNA binding and transactivation. Embo J. 1997;16:750-759.

221. Benckert C, Jonas S, Cramer T, et al. Transforming growth factor beta 1 stimulates vascular endothelial growth factor gene transcription in human cholangiocellular carcinoma cells. Cancer Res. 2003;63:1083-1092.

222. von Marschall Z, Scholz A, Cramer T, et al. Effects of interferon alpha on vascular endothelial growth factor gene transcription and tumor angiogenesis. J Natl Cancer Inst. 2003;95:437-448.

223. Tanaka T, Kanai H, Sekiguchi K, et al. Induction of VEGF gene transcription by IL-1 beta is mediated through stress-activated MAP kinases and Sp1 sites in cardiac myocytes. J Mol Cell Cardiol. 2000;32:1955-1967.

224. Pages G, Pouyssegur J. Transcriptional regulation of the Vascular Endothelial Growth Factor gene--a concert of activating factors. Cardiovasc Res. 2005;65:564-573.

225. Soker S, Takashima S, Miao HQ, Neufeld G, Klagsbrun M. Neuropilin-1 is expressed by endothelial and tumor cells as an isoform-specific receptor for vascular endothelial growth factor. Cell. 1998;92:735-745.

226. Olsson AK, Dimberg A, Kreuger J, Claesson-Welsh L. VEGF receptor signalling - in control of vascular function. Nat Rev Mol Cell Biol. 2006;7:359-371.

227. Ashikari-Hada S, Habuchi H, Kariya Y, Kimata K. Heparin regulates vascular endothelial growth factor165-dependent mitogenic activity, tube formation, and its receptor phosphorylation of human endothelial cells. Comparison of the effects of heparin and modified heparins. J Biol Chem. 2005;280:31508-31515.

228. Xie K, Wei D, Shi Q, Huang S. Constitutive and inducible expression and regulation of vascular endothelial growth factor. Cytokine Growth Factor Rev. 2004;15:297-324.

229. Liu B, Earl HM, Baban D, et al. Melanoma cell lines express VEGF receptor KDR and respond to exogenously added VEGF. Biochem Biophys Res Commun. 1995;217:721-727.

230. Dias S, Hattori K, Zhu Z, et al. Autocrine stimulation of VEGFR-2 activates human leukemic cell growth and migration. J Clin Invest. 2000;106:511-521.

231. Qi L, Robinson WA, Brady BM, Glode LM. Migration and invasion of human prostate cancer cells is related to expression of VEGF and its receptors. Anticancer Res. 2003;23:3917-3922.

232. Bates RC, Goldsmith JD, Bachelder RE, et al. Flt-1-dependent survival characterizes the epithelial-mesenchymal transition of colonic organoids. Curr Biol. 2003;13:1721-1727.

233. Wu W, Shu X, Hovsepyan H, Mosteller RD, Broek D. VEGF receptor expression and signaling in human bladder tumors. Oncogene. 2003;22:3361-3370.

234. Kranz A, Mattfeldt T, Waltenberger J. Molecular mediators of tumor angiogenesis: enhanced expression and activation of vascular endothelial growth factor receptor KDR in primary breast cancer. Int J Cancer. 1999;84:293-298.

235. Price DJ, Miralem T, Jiang S, Steinberg R, Avraham H. Role of vascular endothelial growth factor in the stimulation of cellular invasion and signaling of breast cancer cells. Cell Growth Differ. 2001;12:129-135.

236. Bachelder RE, Crago A, Chung J, et al. Vascular endothelial growth factor is an autocrine survival factor for neuropilin-expressing breast carcinoma cells. Cancer Res. 2001;61:5736-5740.

237. McTigue MA, Wickersham JA, Pinko C, et al. Crystal structure of the kinase domain of human vascular endothelial growth factor receptor 2: a key enzyme in angiogenesis. Structure. 1999;7:319-330.

238. Dougher M, Terman BI. Autophosphorylation of KDR in the kinase domain is required for maximal VEGF-stimulated kinase activity and receptor internalization. Oncogene. 1999;18:1619-1627.

239. Rameh LE, Cantley LC. The role of phosphoinositide 3-kinase lipid products in cell function. J Biol Chem. 1999;274:8347-8350.

240. Cantley LC. The phosphoinositide 3-kinase pathway. Science. 2002;296:1655-1657.

241. Sekiya F, Bae YS, Rhee SG. Regulation of phospholipase C isozymes: activation of phospholipase C-gamma in the absence of tyrosine-phosphorylation. Chem Phys Lipids. 1999;98:3-11.

242. Warner AJ, Lopez-Dee J, Knight EL, Feramisco JR, Prigent SA. The Shc-related adaptor protein, Sck, forms a complex with the vascular-endothelial-growth-factor receptor KDR in transfected cells. Biochem J. 2000;347:501-509.

243. Lamalice L, Houle F, Jourdan G, Huot J. Phosphorylation of tyrosine 1214 on VEGFR2 is required for VEGF-induced activation of Cdc42 upstream of SAPK2/p38. Oncogene. 2004;23:434-445.

244. Abedi H, Zachary I. Vascular endothelial growth factor stimulates tyrosine phosphorylation and recruitment to new focal adhesions of focal adhesion kinase and paxillin in endothelial cells. J Biol Chem. 1997;272:15442-15451.

245. Le Boeuf F, Houle F, Huot J. Regulation of vascular endothelial growth factor receptor 2-mediated phosphorylation of focal adhesion kinase by heat shock protein 90 and Src kinase activities. J Biol Chem. 2004;279:39175-39185.

246. Atkinson SJ, English JL, Holway N, Murphy G. Cellular cholesterol regulates MT1 MMP dependent activation of MMP 2 via MEK-1 in HT1080 fibrosarcoma cells. FEBS Lett. 2004;566:65-70.

247. Saiki RK, Scharf S, Faloona F, et al. Enzymatic amplification of beta-globin genomic sequences and restriction site analysis for diagnosis of sickle cell anemia. Science. 1985;230:1350-1354.

248. Atkinson SJ, Roghi C, Murphy G. MT1-MMP hemopexin domain exchange with MT4-MMP blocks enzyme maturation and trafficking to the plasma membrane in MCF7 cells. Biochem J. 2006;398:15-22.

249. Nyalendo C, Michaud M, Beaulieu E, et al. Src-dependent phosphorylation of membrane type I matrix metalloproteinase on cytoplasmic tyrosine 573: role in endothelial and tumor cell migration. J Biol Chem. 2007;282:15690-15699.

250. Stamenkovic I. Extracellular matrix remodelling: the role of matrix metalloproteinases. J Pathol. 2003;200:448-464.

251. Pulyaeva H, Bueno J, Polette M, et al. MT1-MMP correlates with MMP-2 activation potential seen after epithelial to mesenchymal transition in human breast carcinoma cells. Clin Exp Metastasis. 1997;15:111-120.

252. Baker AH, Edwards DR, Murphy G. Metalloproteinase inhibitors: biological actions and therapeutic opportunities. J Cell Sci. 2002;115:3719-3727.

253. Sandilands E, Cans C, Fincham VJ, et al. RhoB and actin polymerization coordinate Src activation with endosome-mediated delivery to the membrane. Dev Cell. 2004;7:855-869.

254. Linder S. The matrix corroded: podosomes and invadopodia in extracellular matrix degradation. Trends Cell Biol. 2007;17:107-117.

255. Chou MT, Wang J, Fujita DJ. Src kinase becomes preferentially associated with the VEGFR, KDR/Flk-1, following VEGF stimulation of vascular endothelial cells. BMC Biochem. 2002;3:32.

256. Gampel A, Moss L, Jones MC, Brunton V, Norman JC, Mellor H. VEGF regulates the mobilization of VEGFR2/KDR from an intracellular endothelial storage compartment. Blood. 2006;108:2624-2631.

257. Hashimoto G, Inoki I, Fujii Y, Aoki T, Ikeda E, Okada Y. Matrix metalloproteinases cleave connective tissue growth factor and reactivate angiogenic activity of vascular endothelial growth factor 165. J Biol Chem. 2002;277:36288-36295.

258. Sledz CA, Holko M, de Veer MJ, Silverman RH, Williams BR. Activation of the interferon system by short-interfering RNAs. Nat Cell Biol. 2003;5:834-839.

259. Bridge AJ, Pebernard S, Ducraux A, Nicoulaz AL, Iggo R. Induction of an interferon response by RNAi vectors in mammalian cells. Nat Genet. 2003;34:263-264.

260. Kim DH, Longo M, Han Y, Lundberg P, Cantin E, Rossi JJ. Interferon induction by siRNAs and ssRNAs synthesized by phage polymerase. Nat Biotechnol. 2004;22:321-325.

261. Bauer M, Kinkl N, Meixner A, et al. Prevention of interferon-stimulated gene expression using microRNA-designed hairpins. Gene Ther. 2009;16:142-147.

262. Chang K, Elledge SJ, Hannon GJ. Lessons from Nature: microRNA-based shRNA libraries. Nat Methods. 2006;3:707-714.

263. Genis L, Galvez BG, Gonzalo P, Arroyo AG. MT1-MMP: universal or particular player in angiogenesis? Cancer Metastasis Rev. 2006;25:77-86.

264. Lavie Y, Fiucci G, Liscovitch M. Up-regulation of caveolae and caveolar constituents in multidrug-resistant cancer cells. J Biol Chem. 1998;273:32380-32383.

265. Lee SW, Reimer CL, Oh P, Campbell DB, Schnitzer JE. Tumor cell growth inhibition by caveolin re-expression in human breast cancer cells. Oncogene. 1998;16:1391-1397.

266. Engelman JA, Zhang XL, Razani B, Pestell RG, Lisanti MP. p42/44 MAP kinase-dependent and -independent signaling pathways regulate caveolin-1 gene expression. Activation of Ras-MAP kinase and protein kinase a signaling cascades transcriptionally down-regulates caveolin-1 promoter activity. J Biol Chem. 1999;274:32333-32341.

267. Hurlstone AF, Reid G, Reeves JR, et al. Analysis of the CAVEOLIN-1 gene at human chromosome 7q31.1 in primary tumours and tumour-derived cell lines. Oncogene. 1999;18:1881-1890.

268. Hino M, Doihara H, Kobayashi K, Aoe M, Shimizu N. Caveolin-1 as tumor suppressor gene in breast cancer. Surg Today. 2003;33:486-490.

269. Goetz JG, Joshi B, Lajoie P, et al. Concerted regulation of focal adhesion dynamics by galectin-3 and tyrosine-phosphorylated caveolin-1. J Cell Biol. 2008;180:1261-1275.

270. Goetz JG, Lajoie P, Wiseman SM, Nabi IR. Caveolin-1 in tumor progression: the good, the bad and the ugly. Cancer Metastasis Rev. 2008;27:715-735.

271. Gaus K, Le Lay S, Balasubramanian N, Schwartz MA. Integrin-mediated adhesion regulates membrane order. J Cell Biol. 2006;174:725-734.

272. Joshi B, Strugnell SS, Goetz JG, et al. Phosphorylated caveolin-1 regulates Rho/ROCK-dependent focal adhesion dynamics and tumor cell migration and invasion. Cancer Res. 2008;68:8210-8220.

273. Labrecque L, Royal I, Surprenant DS, Patterson C, Gingras D, Beliveau R. Regulation of vascular endothelial growth factor receptor-2 activity by caveolin-1 and plasma membrane cholesterol. Mol Biol Cell. 2003;14:334-347.

274. Osenkowski P, Toth M, Fridman R. Processing, shedding, and endocytosis of membrane type 1-matrix metalloproteinase (MT1-MMP). J Cell Physiol. 2004;200:2-10.

275. Lecourtois M, Schweisguth F. Indirect evidence for Delta-dependent intracellular processing of notch in Drosophila embryos. Curr Biol. 1998;8:771-774.

276. Struhl G, Adachi A. Nuclear access and action of notch in vivo. Cell. 1998;93:649-660.

277. Toth M, Osenkowski P, Hesek D, et al. Cleavage at the stem region releases an active ectodomain of the membrane type 1 matrix metalloproteinase. Biochem J. 2005;387:497-506.

278. Chan CK, Hubner S, Hu W, Jans DA. Mutual exclusivity of DNA binding and nuclear localization signal recognition by the yeast transcription factor GAL4: implications for nonviral DNA delivery. Gene Ther. 1998;5:1204-1212.

279. Derossi D, Joliot AH, Chassaing G, Prochiantz A. The third helix of the Antennapedia homeodomain translocates through biological membranes. J Biol Chem. 1994;269:10444-10450.

280. Salmena L, Pandolfi PP. Changing venues for tumour suppression: balancing destruction and localization by monoubiquitylation. Nat Rev Cancer. 2007;7:409-413.

281. Terzic J, Marinovic-Terzic I, Ikeda F, Dikic I. Ubiquitin signals in the NF-kappaB pathway. Biochem Soc Trans. 2007;35:942-945.

282. Hoeller D, Hecker CM, Dikic I. Ubiquitin and ubiquitin-like proteins in cancer pathogenesis. Nat Rev Cancer. 2006;6:776-788.

283. Hershko A, Ciechanover A. The ubiquitin system. Annu Rev Biochem. 1998;67:425-479.

284. Li M, Brooks CL, Wu-Baer F, Chen D, Baer R, Gu W. Mono- versus polyubiquitination: differential control of p53 fate by Mdm2. Science. 2003;302:1972-1975.

285. Trotman LC, Wang X, Alimonti A, et al. Ubiquitination regulates PTEN nuclear import and tumor suppression. Cell. 2007;128:141-156.

286. van der Horst A, de Vries-Smits AM, Brenkman AB, et al. FOXO4 transcriptional activity is regulated by monoubiquitination and USP7/HAUSP. Nat Cell Biol. 2006;8:1064-1073.

287. Lin SY, Makino K, Xia W, et al. Nuclear localization of EGF receptor and its potential new role as a transcription factor. Nat Cell Biol. 2001;3:802-808.

288. Carroll JS, Liu XS, Brodsky AS, et al. Chromosome-wide mapping of estrogen receptor binding reveals long-range regulation requiring the forkhead protein FoxA1. Cell. 2005;122:33-43.

289. Hajitou A, Sounni NE, Devy L, et al. Down-regulation of vascular endothelial growth factor by tissue inhibitor of metalloproteinase-2: effect on in vivo mammary tumor growth and angiogenesis. Cancer Res. 2001;61:3450-3457.

290. Arlt M, Kopitz C, Pennington C, et al. Increase in gelatinase-specificity of matrix metalloproteinase inhibitors correlates with antimetastatic efficacy in a T-cell lymphoma model. Cancer Res. 2002;62:5543-5550.

291. Yanez-Mo M, Barreiro O, Gonzalo P, et al. MT1-MMP collagenolytic activity is regulated through association with tetraspanin CD151 in primary endothelial cells. Blood. 2008;112:3217-3226.

292. Sithu SD, English WR, Olson P, et al. Membrane-type 1-matrix metalloproteinase regulates intracellular adhesion molecule-1 (ICAM-1)-mediated monocyte transmigration. J Biol Chem. 2007;282:25010-25019.

293. Golubkov VS, Boyd S, Savinov AY, et al. Membrane type-1 matrix metalloproteinase (MT1-MMP) exhibits an important intracellular cleavage function and causes chromosome instability. J Biol Chem. 2005;280:25079-25086.

294. Brown LF, Guidi AJ, Schnitt SJ, et al. Vascular stroma formation in carcinoma in situ, invasive carcinoma, and metastatic carcinoma of the breast. Clin Cancer Res. 1999;5:1041-1056.

295. Dvorak HF, Nagy JA, Feng D, Brown LF, Dvorak AM. Vascular permeability factor/vascular endothelial growth factor and the significance of microvascular hyperpermeability in angiogenesis. Curr Top Microbiol Immunol. 1999;237:97-132.

296. Liu J, Razani B, Tang S, Terman BI, Ware JA, Lisanti MP. Angiogenesis activators and inhibitors differentially regulate caveolin-1 expression and caveolae formation in vascular endothelial cells. Angiogenesis inhibitors block vascular endothelial growth factor-induced down-regulation of caveolin-1. J Biol Chem. 1999;274:15781-15785.

297. Li S, Couet J, Lisanti MP. Src tyrosine kinases, Galpha subunits, and H-Ras share a common membrane-anchored scaffolding protein, caveolin. Caveolin binding negatively regulates the auto-activation of Src tyrosine kinases. J Biol Chem. 1996;271:29182-29190.

298. Yamamoto M, Toya Y, Jensen RA, Ishikawa Y. Caveolin is an inhibitor of platelet-derived growth factor receptor signaling. Exp Cell Res. 1999;247:380-388.

299. Li S, Seitz R, Lisanti MP. Phosphorylation of caveolin by src tyrosine kinases. The alpha-isoform of caveolin is selectively phosphorylated by v-Src in vivo. J Biol Chem. 1996;271:3863-3868.

300. Cao H, Courchesne WE, Mastick CC. A phosphotyrosine-dependent protein interaction screen reveals a role for phosphorylation of caveolin-1 on tyrosine 14: recruitment of C-terminal Src kinase. J Biol Chem. 2002;277:8771-8774.

301. Ispanovic E, Haas TL. JNK and PI3K differentially regulate MMP-2 and MT1-MMP mRNA and protein in response to actin cytoskeleton reorganization in endothelial cells. Am J Physiol Cell Physiol. 2006;291:C579-588.

302. Zucker S, Cao J, Chen WT. Critical appraisal of the use of matrix metalloproteinase inhibitors in cancer treatment. Oncogene. 2000;19:6642-6650.

303. Ip YC, Cheung ST, Fan ST. Atypical localization of membrane type 1-matrix metalloproteinase in the nucleus is associated with aggressive features of hepatocellular carcinoma. Mol Carcinog. 2007;46:225-230.

304. Golubkov VS, Chekanov AV, Doxsey SJ, Strongin AY. Centrosomal pericentrin is a direct cleavage target of membrane type-1 matrix metalloproteinase in humans but not in mice: potential implications for tumorigenesis. J Biol Chem. 2005;280:42237-42241.

305. Si-Tayeb K, Monvoisin A, Mazzocco C, et al. Matrix metalloproteinase 3 is present in the cell nucleus and is involved in apoptosis. Am J Pathol. 2006;169:1390-1401.

306. Eguchi T, Kubota S, Kawata K, et al. Novel transcription-factor-like function of human matrix metalloproteinase 3 regulating the CTGF/CCN2 gene. Mol Cell Biol. 2008;28:2391-2413.

8 Appendix A

Primer sequences and TaqMan® probes

Name	Sequence (5' => 3')
VEGFpromotors	CCTCAGTTCCCTGGCAACATCTG
VEGFpromoteras	GAAGAATTTGGCACCAAGTTTGT
GAPDHpromoters	TACTAGCGGTTTTACGGGCG
GAPDHpromoteras	TCGAACAGGAGGAGCAGAGAGCGA
XBP-1s	ATACTTGGCAGCCTGTGACC
XBP-1as	GGTCCACAAAGCAGGAAAAA
CHR521s	CGGCTCGGCCCAATCACCGGTCATGGACTACAAGGACGACG ATGACAAGGCCCCATCGGGAGGCCGGCCGGAT
BGHas	TCCTCATTTTATTAGGAAAG
115.K/As	CGTTCCCTGCTGGACGCGGTCGAGCAAAAGCTAATA
115.K/Aas	TATTAGCTTTTGCTCGACCGCGTCCAGCAGGGAACG
115.Stps	TCCCTGCTGGACAAGGTCTAGCAAAAGCTAATATCA
115.Stpas	TGATATTAGCTTTTGCTAGACCTTGTCCAGCAGGGA
CHR508	CCAGTGTGGTGGGATCCCCATGGGCAGCAACAAGAGCAAG
CHR509	TACCTGCGGCCGCTCTAGACTATAGGTTCTCCCCGGGCTGG
pACTs1200	GACGATTTCGATCTGGACATGTTGGGGGAC
pACTas1446	TGTATCTTATCATGTCTGCTC
VEGF-As	CCTGGTGGACATCTTCCAGGAGTA
VEGF-Aas	CTCACCGCCTCGGCTTGTCACA
MT1-MMPs1335	ATCAACACTGCCTACGAGAG
MT1-MMPas1744	CCCTCAGGGCTGACTTGG

Table 8.1: Oligonucleotides

Name	Assay number
MT1-MMP	Hs_00237119_m1
MT2-MMP	Hs00233997_m1
MT3-MMP	Hs01095537_m1
MT4-MMP	Hs01108847_m1
VEGF-A	Hs_00173626_m1

18s	Hs_9999901_s1
Src	Hs_00178494_m1
Fyn	Hs_00176628_m1
Caveolin-1	Hs_00971716_m1
VEGFR-1	Hs_01052936_m1
VEGFR-2	Hs_00176676_m1
CTGF	Hs_00170014_m1
HARP	Hs_00383235_m1
MMP-2	Hs_00234422_m1
GAPDH	Hs_99999905_m1

Table 8.2: TaqMan® probes

9 Appendix B

List of asRNA and shRNA sequences used in this thesis.

Target gene	Sequence
MT1-MMP	TGGCCGAGGGGTCACTGGAATGCTCGAGCCCCAGGGCATGGCCCAGC TCGTGCACAGCCACCAGGAAGATGTCATTTCCATTCAGATCCTCATTC CTGACAGTCCAAGGCTCGGCAGAGTCAAAGTGGGTGTCTCCTCCAAT GTTGGGGCCTGGGAAGTAGGCATGGGCCAGGAAGCCGCCCTCACCAT CGAAGGGCGTGCTGTCGCCATGGAAGCCCTCGGCAAAGAAGATCAT GATGTCGGCCTGCTTCTCATGGCCCTCACGGATGTAGGCATAGGGCA CACCTCGCGGAAGCGCAGTGGTGTGGCACTCTCCCACACGCGGAACG CCTTGCGAATGGCCTCGTATGTGGCATACTCGCCCACCTTGGGGGTGT AATTCTGGATGCAGAAAGTGATTTCATTATGTTGCCATTTGAGACCCT GGATGGCGTAGCGCTTCCTTCGAACATTGGCCTTGATCTCAGCCCCA AACTTGTCTGGAACACCACATCGGGGGCGCCT
MT2-MMP	ATTGGGGTTGCTGGAGTGCTCCAGCCCCAGCGCGTGGCCCAGCTCAT GCACTGCCACCAGGAAGAGGTTGTTTCCATGCAGGTCAGTGCTGGAG AAGGTCCAGGGCTCATCTGCGTCAAAATGGGTGTCCCCGCCTAGGCC GGGGCCAGGGAAATAGGCGTGGGCCAGAAAGCCACCGGTGCCATCA AACGGCGAGCTGTCGCCGTGGAAGCCAGAGGCAAAGAGTACCATGA TGTCGGCCTCCTTCTGTCGCCGCAGCCGGATGTCCTCATAGGGCACCT CCTGGAAGACCAGGGGCGTGGCCTGCTCCCACACGCGGAAGGCCCTG CGCACCGCCTCCATCGAGTGGTACCAGCCCAACTTCTCCGTGTAGTTC TGGATGCTAAAGGTCAGATGGTGGTTGTTCCACTTCCTCCCGGTG
MT3-MMP	CACTTCCAAGGGTTATCAAGTCATGAGGGTAACCAGGTTGAAGAGTT GTATCCTTGAACACCCAATATTTGTTACCTTTAAAGAACACAAAATTC CCGTCGCTATTTTCATAAACTGCATCGATACTAGGAGGCAAGCCCCG CCAGAAGTAAGTAATTTGCATTGGGTATCCATCCATCACCCTGTTGTT TCTCACTCGCCAAAACCACTGGTCCTTGAAAACAAACATCTCACGAC GAAGAATAGCTAGAGTGTTAAAGTTCCCATCACAGATGTTGGGTTTG GCTCCGGGATAGGAGGGTCTGCCGGTTGGAGGCCGAGGAGGTTTTGG CCTGTCATTTTTCCTTGGGTCAGCCGGAGGAATAGAGCGGTGTGGGG GC
MT4-MMP	CGCCATCCAGCACTTTCCAGTACTCCTGGCCACGGAAGAAGTAGGAG GCACCGTCGGACCAGCGCATGGCGTCGTCCAGCGTGCTGGGGACACC CCTCCACAGGGGGCTCTGGGCGGGGTAGCCGGGGTCCATGTGCCTCG TGTGGTCATCGTAGCGCCAGTACAGCTGGTCCTTAAAGAAATAAGTC CTGTCATTGTGGGCCCA

Table 9.1: List of asRNA sequences

Target gene	Name	Number	Oligo sequence
MT1-MMP	shRNA1	TRCN0000050853	CCGG**GCTGAGATCAAGGCCAATGTT**CTC GAGAACATTGGCCTTGATCTCAGCTTTTG
	shRNA2	TRCN0000050854	CCGG**CGGCCTTCTGTTCCTGATAAA**CTC GAGTTTATCAGGAACAGAAGGCCGTTTTG
	shRNA3	TRCN0000050855	CCGG**CGATGAAGTCTTCACTTACTT**CTC GAGAAGTAAGTGAAGACTTCATCGTTTTG
	shRNA4	TRCN0000050857	CCGG**GCTACAGCAATATGGCTACCT**CTC GAGAGGTAGCCATATTGCTGTAGCTTTTG
	shRNA5	TRCN0000050856	CCGG**GTGGATGGACACGGAGGATTT**CT CGAGAAATTCTCCCTGTCCATCCACTTTTG
VEGFR-1	shRNA1	TRCN0000000631	CCGG**CCCGTCTCTATACCAACCAAA**CTC GAGTTTGGTTGGTATAGAGACGGGTTTTT
	shRNA2	TRCN0000000632	CCGG**CCCGAATCTATCTTTGACAAA**CTC GAGTTTGTCAAAGATAGATTCGGGTTTTT
	shRNA3	TRCN0000000633	CCGG**CGCCGGAAGTTGTATGGTTAA**CTC GAGTTAACCATACAACTTCCGGCGTTTTT
	shRNA4	TRCN0000000634	CCGG**GAGAGACTTAAACTGGGCAAA**CT CGAGTTTGCCCAGTTTAAGTCTCTCTTTTT
	shRNA5	TRCN0000000635	CCGG**CTTGACACTTTGATCCCTGAT**CTC GAGATCAGGGATCAAAGTGTCAAGTTTTT
VEGFR-2	shRNA1	TRCN0000001685	CCGG**GCGGCACGAAATATCCTCTTA**CTC GAGTAAGAGGATATTTCGTGCCGCTTTTT
	shRNA2	TRCN0000001686	CCGG**AGGCTAATACAACTCTTCAAA**CTC GAGTTTGAAGAGTTGTATTAGCCTTTTTT
	shRNA3	TRCN0000001687	CCGG**GTGCTGTTTCTGACTCCTAAT**CTC GAGATTAGGAGTCAGAAACAGCACTTTTT
	shRNA4	TRCN0000001688	CCGG**CTTTACTATTCCCAGCTACAT**CTC GAGATGTAGCTGGGAATAGTAAAGTTTTT
	shRNA5	TRCN0000001689	CCGG**GTGGTCTCTCTGGTTGTGTAT**CTC GAGATACACAACCAGAGAGACCACTTTTT

Table 9.2: List of MISSION® shRNA sequences

The target sequence is shown in bold letters.

10 Appendix C

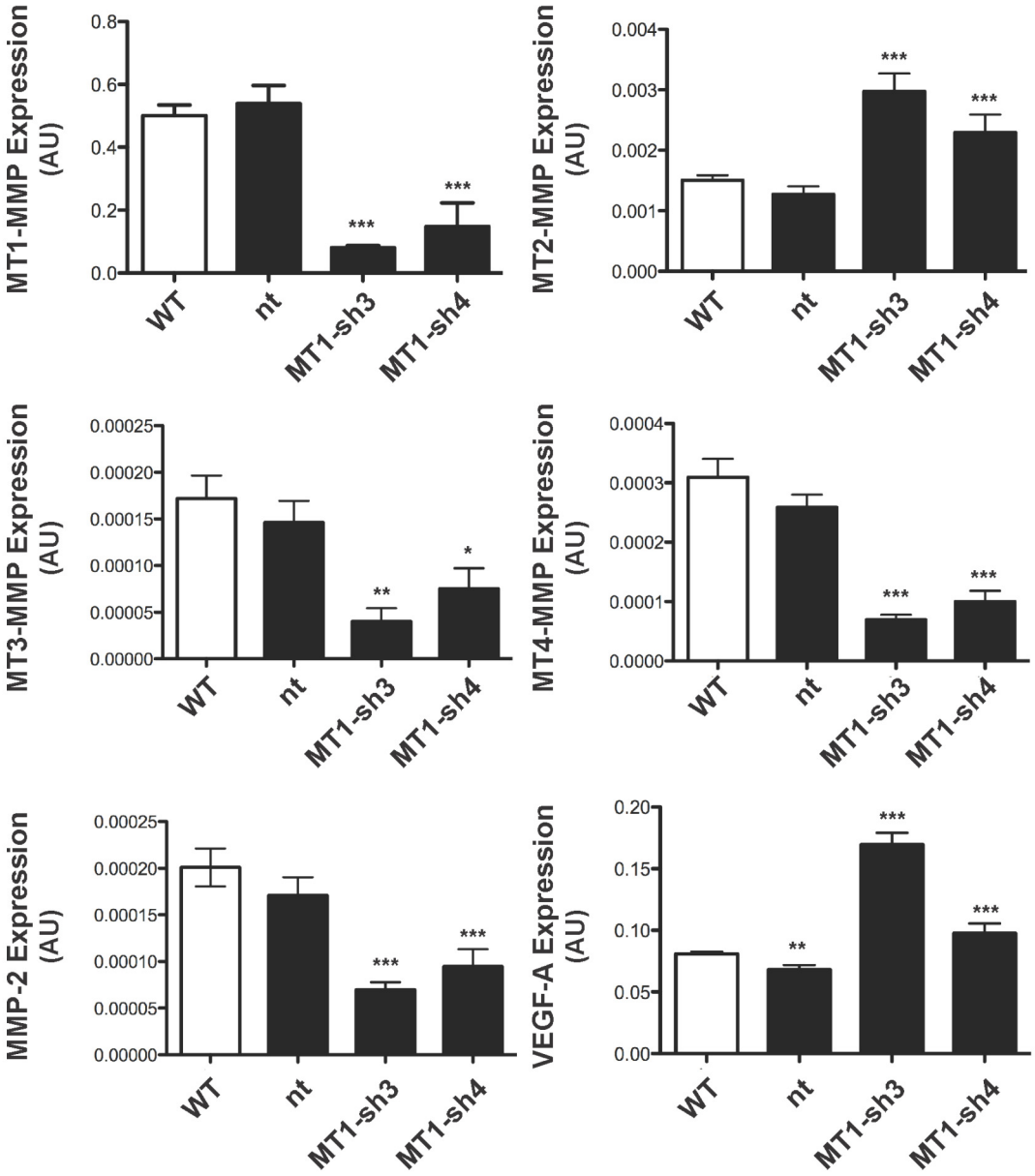

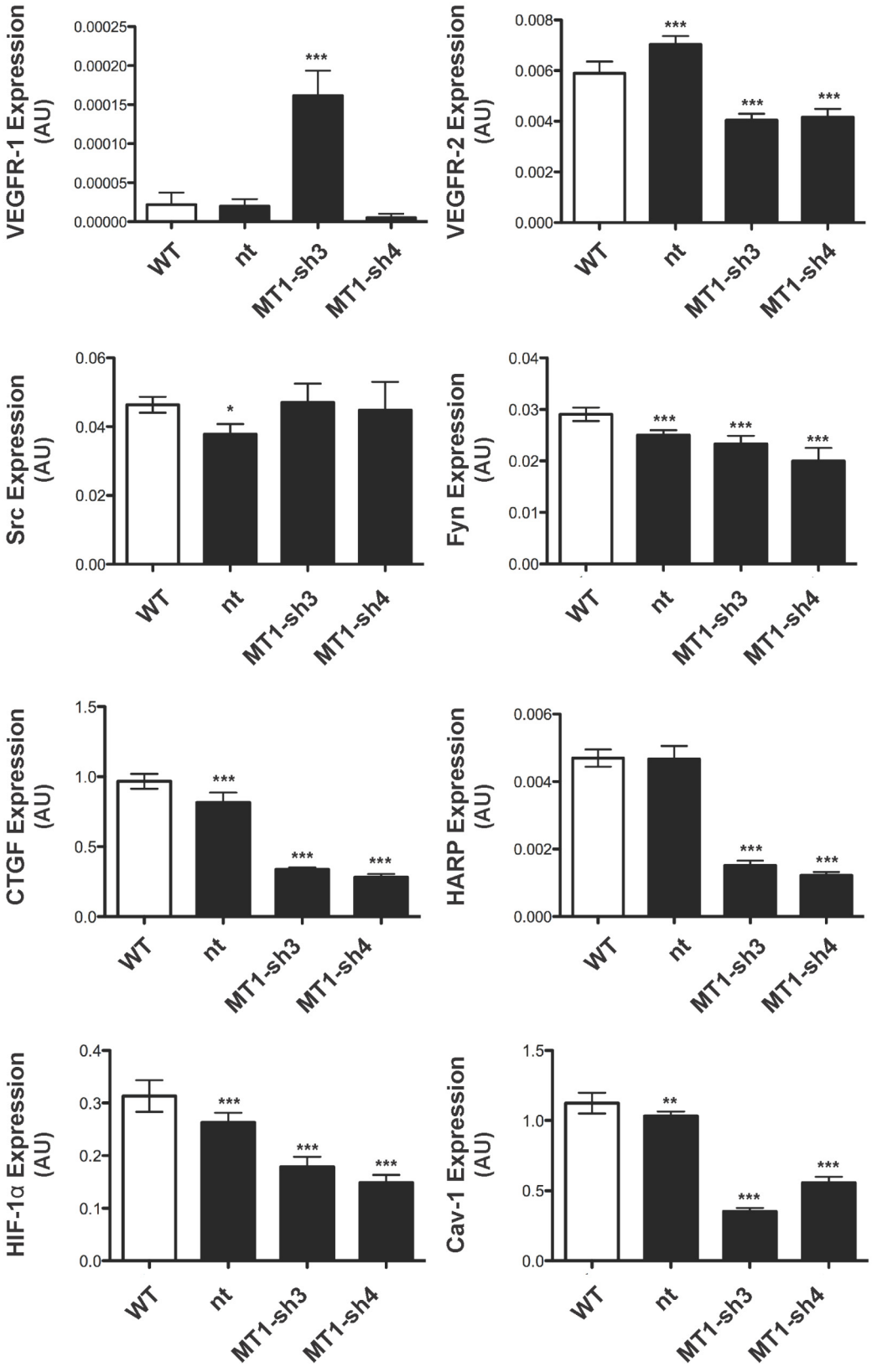

Figure 10.1: Gene expression profile of MDA-MB-231 transduced with MT1-MMP targeting shRNA

Single analysis of data shown in Figure 3.37.

11 Appendix D

Meta-analysis of MT1-MMP, VEGFR-2 and VEGF-A mRNA expression profile in microarray studies derived from the Oncomine™ database comparing breast carcinoma tissues derived from ***(i)*** tumours of different stages, ***(ii)*** tumours of different grading, ***(iii)*** tumours exhibiting different estrogen receptor (ER) status or ***(iv)*** basal or luminal tumours. Data represent the name and details of the studies revealing data sets that are differentially expressed.

Analysis of MT1-MMP expression

Study **Link**	**Class1** **(number)**	**Class2** **(number)**	**Class3** **(number)**	***P*-value** ***t*-test**
Ginestier_Breast	1(4)	2(12)	3(39)	**0.004**
Ivshina_Breast http://www.ncbi.nlm.nih.gov/geo/query/acc.cgi?acc=GSE4922	1(68)	2(126)	3(55)	**0.025**
Miller_Breast	1(67)	2(128)	3(54)	**0.029**
Sotiriou_Breast_3 http://www.ncbi.nlm.nih.gov/geo/query/acc.cgi?acc=GSE2990	1(67)	2(46)	3(59)	**0.031**
Bittner_Breast http://www.ncbi.nlm.nih.gov/geo/query/acc.cgi?acc=GSE2109	1(30)	2(107)	3(141)	0.077
Finak_Breast http://www.ncbi.nlm.nih.gov/geo/query/acc.cgi?acc=GSE9014	1(3)	2(23)	3(27)	0.126
Farmer_Breast http://www.ncbi.nlm.nih.gov/geo/query/acc.cgi?acc=GSE1561	1(22)	2(16)	3(8)	0.134
Sorlie_Breast http://www.ncbi.nlm.nih.gov/geo/query/acc.cgi?acc=GSE3193	1(9)	2(33)	3(33)	0.149
Ma_Breast_3	1(3)	2(39)	3(18)	0.251
Sotiriou_Breast_2 http://www.pnas.org/cgi/content/full/1732912100/DC1	1(16)	2(37)	3(45)	0.278
Hess_Breast http://bioinformatics.mdanderson.org/pubdata.html	1(2)	2(54)	3(77)	0.33
Kreike_Breast http://www.ncbi.nlm.nih.gov/geo/query/acc.cgi?acc=GSE4913	1(10)	2(12)	3(28)	0.41
vantVeer_Breast http://www.rii.com/publications/2002/vantveer.html	1(12)	2(27)	3(78)	0.901

Table 11.1: MT1-MMP expression in breast carcinomas derived from differently graded tumours

Data represent studies in which MT1-MMP was found to be expressed differentially. The name of the study, the n-numbers of each category and the corresponding link are indicated. Significance was calculated using the Student *t*-test. Bold *P*-values indicate $P < 0.05$.

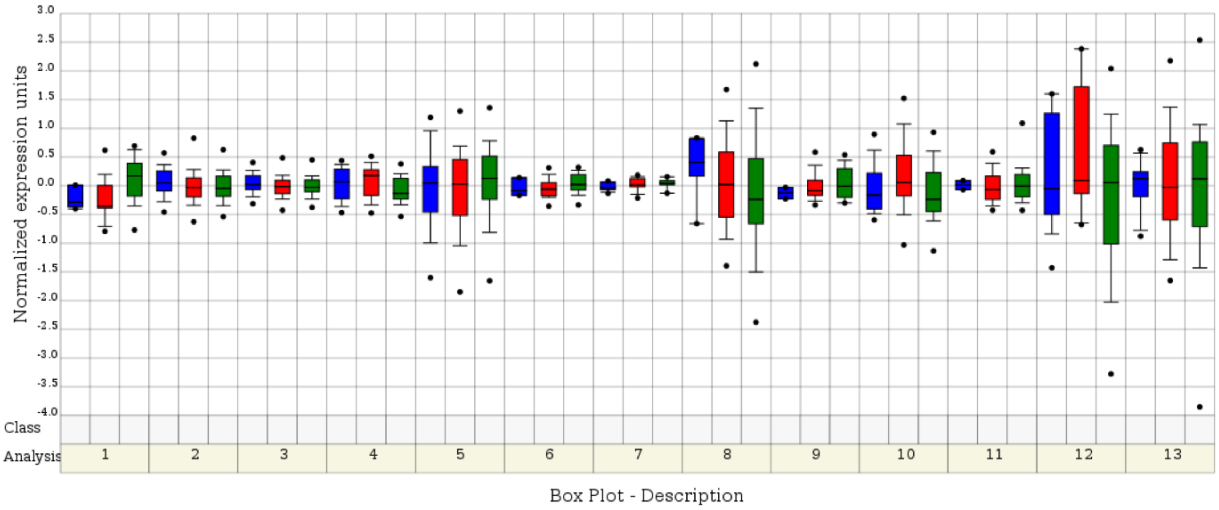

Figure 11.1: MT1-MMP expression in breast carcinomas derived from differently graded tumours

Data represent the box-plots of 13 different studies as listed in Table 11.1 showing category 1 (blue), category 2 (red) and category 3 (green) graded breast carcinomas.

Study Link	Class1 (number)	Class2 (number)	*P*-value *t*-test
Hess_breast http://bioinformatics.mdanderson.org/pubdata.html	N0(40)	N1(62), N2(14), N3(17)	0.056
Sorlie_Breast_2 http://www.ncbi.nlm.nih.gov/geo/query.acc.cgi?acc=GSE4382	N0(25)	N1(35), N2(19)	0.083
Sorlie_Breast http://genome-www5.stanford.edu/cgi-bin/SMD/publication/viewPublication.pl?pub_no=95	N0(23)	N1(34), N2(19)	0.103
Yu_Breast http://www.ncbi.nlm.nih.gov/projects/geo/query/acc.cgi?acc=GSE2294	N0(37)	N1(12), N2(46)	0.119
Sotiriou_Breast_2 http://www.pnas.org/cgi/content/full/1732912100/DC1	N0(46)	N1(52)	0.972

Table 11.2: MT1-MMP expression in breast carcinomas derived from differently staged tumours

Data represent studies in which MT1-MMP was found to be expressed differentially. The name of the study, the n-numbers of each category and the corresponding link are indicated. Significance was calculated using the Student *t*-test. Bold *P*-values indicate $P < 0.05$.

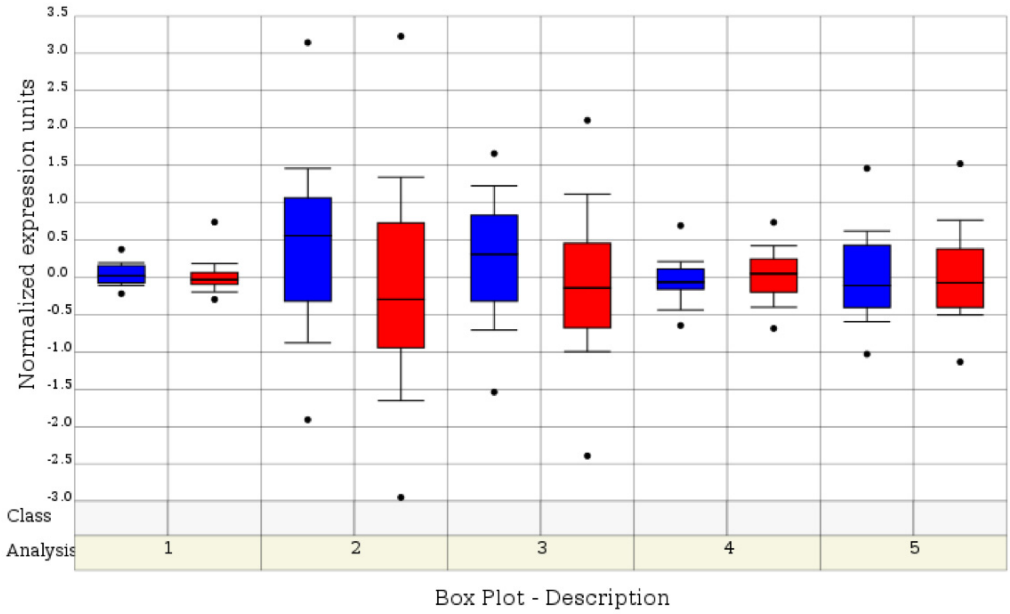

Figure 11.2: MT1-MMP expression in breast carcinomas derived from differently staged tumours

Data represent the box-plots of 5 different studies as listed in Table 11.2 showing stage 1 (blue) or stage 2 (red) classified breast carcinomas.

Name Link	Class1 (number)	Class2 (number)	*P*-value *t*-test
Hess_Breast http://bioinformatics.mdanderson.org/pubdata.html	ER-(51)	ER+(82)	**8.4E-04**
Ginestier_Breast	ER-(28)	ER+(27)	**8.5E-04**
Sotiriou_Breast	ER-(34)	ER+(85)	**0.003**
Sotiriou_Breast_2 http://www.pnas.org/cgi/content/full/1732912100/DC1	ER-(33)	ER+(65)	**0.006**
Minn_Breast_2 http://www.ncbi.nlm.nih.gov/geo/query.acc.cgi?acc=GSE2603	ER-(42)	ER+(57)	**0.01**

Table 11.3: MT1-MMP expression in breast carcinomas derived from tumours with different ER status

Data represent studies in which MT1-MMP was found to be expressed differentially. The name of the study, the n-numbers of each category and the corresponding link are indicated. Significance was calculated using the Student *t*-test. Bold *P*-values indicate $P < 0.05$.

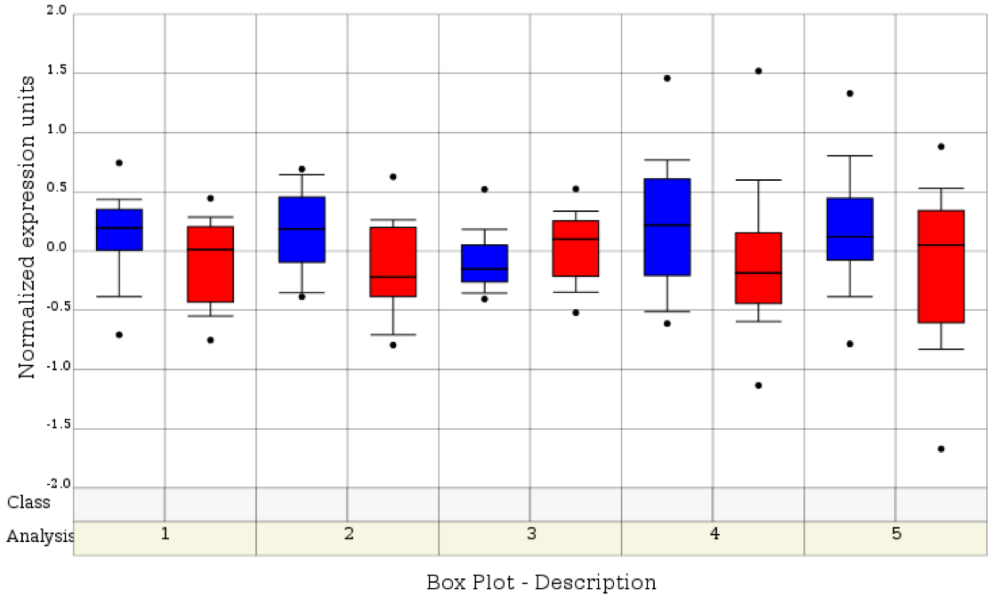

Figure 11.3: MT1-MMP expression in breast carcinomas derived from tumours with different ER status

Data represent the box-plots of 5 different studies as listed in Table 11.3 showing ER- (blue) or ER+ (red) classified breast carcinomas.

Name Link	Class1 (number)	Class2 (number)	*P*-value *t*-test
Farmer_Breast	Apocrine(6) Basal(16)	luminal(27)	**0.023**
http://www.ncbi.nlm.nih.gov/geo/query/acc.cgi?acc=GSE1561			

Table 11.4: MT1-MMP expression in breast carcinomas derived from tumours of different histology

Data represent studies in which MT1-MMP was found to be expressed differentially. The name of the study, the n-numbers of each category and the corresponding link are indicated. Significance was calculated using the Student *t*-test. Bold *P*-values indicate $P < 0.05$.

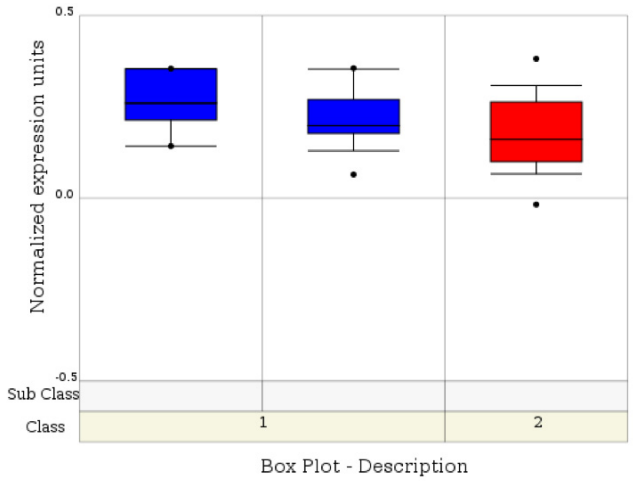

Figure 11.4: MT1-MMP expression in breast carcinomas derived from tumours of different histology

Data represent the box-plots one study as listed in Table 11.4 showing apocrine (blue, left), basal (blue, right) or luminal (red) classified breast carcinomas.

Analysis of VEGF-A expression

Study Link	Class1 (number)	Class2 (number)	Class3 (number)	*P*-value *t*-test
vantVeer_Breast http://www.rii.com/publications/2002/vantveer.html	1(12)	2(27)	3(78)	**3.8E-05**
Ishvina_Breast http://www.ncbi.nlm.nih.gov/geo/query/acc.cgi?acc=GSE4922	1(68)	2(126)	3(55)	**8.2E-05**
Miller_Breast	1(67)	2(128)	3(54)	**9.3E-05**
Bittner_breast http://www.ncbi.nlm.nih.gov/geo/query/acc.cgi?acc=GSE2109	1(30)	2(107)	3(141)	**1.2E-04**
Sotiriou_Breast_3 http://www.ncbi.nlm.nih.gov/geo/query/acc.cgi?acc=GSE2990	1(67)	2(46)	3(59)	**0.001**
Hess_Breast http://bioinformatics.mdanderson.org/pubdata.html	1(2)	2(54)	3(77)	**0.003**
Ginestier_breast	1(4)	2(12)	3(39)	**0.003**
Farmer_Breast http://www.ncbi.nlm.nih.gov/geo/query/acc.cgi?acc=GSE1561	1(22)	2(16)	3(8)	**0.003**
Finak_Breast http://www.ncbi.nlm.nih.gov/geo/query/acc.cgi?acc=GSE9014	1(3)	2(23)	3(27)	**0.04**
Sorlie_Breast http://www.ncbi.nlm.nih.gov/geo/query/acc.cgi?acc=GSE3193	1(9)	2(33)	3(33)	**0.046**
Sotiriou_Breast_2	1(16)	2(37)	3(45)	0.164

http://www.pnas.org/cgi/content/full/1732912100/DC1				
Ma_Breast_3	1(3)	2(39)	3(18)	0.247
Kreike_Breast http://www.ncbi.nlm.nih.gov/geo/query/acc.cgi?acc=GSE4913	1(10)	2(12)	3(28)	0.357

Table 11.5: VEGF-A expression in breast carcinomas derived from differently graded tumours

Data represent studies in which MT1-MMP was found to be expressed differentially. The name of the study, the n-numbers of each category and the corresponding link are indicated. Significance was calculated using the Student *t*-test. Bold *P*-values indicate $P < 0.05$.

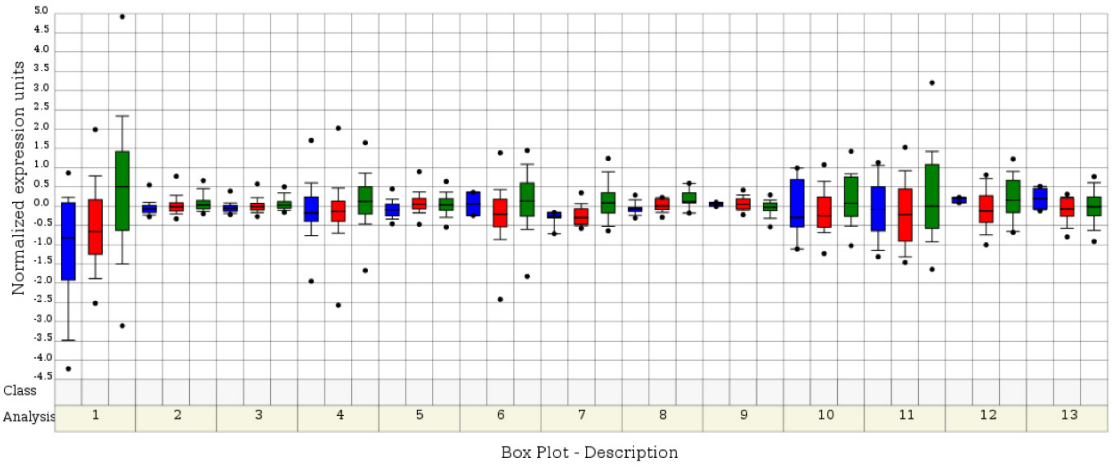

Figure 11.5: VEGF-A expression in breast carcinomas derived from differently graded tumours

Data represent the box-plots of 13 different studies as listed in Table 11.5 showing category 1 (blue), category 2 (red) and category 3 (green) graded breast carcinomas.

Study **Link**	**Class1** **(number)**	**Class2** **(number)**	***P*-value** ***t*-test**
Hess_breast http://bioinformatics.mdanderson.org/pubdata.html	N0(40)	N1(62), N2(14), N3(17)	0.184
Sotiriou_Breast_2 http://www.pnas.org/cgi/content/full/1732912100/DC1	N0(46)	N1(52)	0.343
Sorlie_Breast http://genome-www5.stanford.edu/cgi-bin/SMD/publication/viewPublication.pl?pub_no=95	N0(23)	N1(34), N2(19)	0.582
Yu_Breast_3 http://www.ncbi.nlm.nih.gov/projects/geo/query/acc.cgi?acc=GSE2294	N0(37)	N1(12), N2(46)	0.674
Sorlie_Breast_2 http://www.ncbi.nlm.nih.gov/geo/query.acc.cgi?acc=GSE4382	N0(25)	N1(35), N2(19)	0.699

Table 11.6: VEGF-A expression in breast carcinomas derived from differently staged tumours

Data represent studies in which MT1-MMP was found to be expressed differentially. The name of the study, the n-numbers of each category and the corresponding link are indicated. Significance was calculated using the Student *t*-test. Bold *P*-values indicate $P < 0.05$.

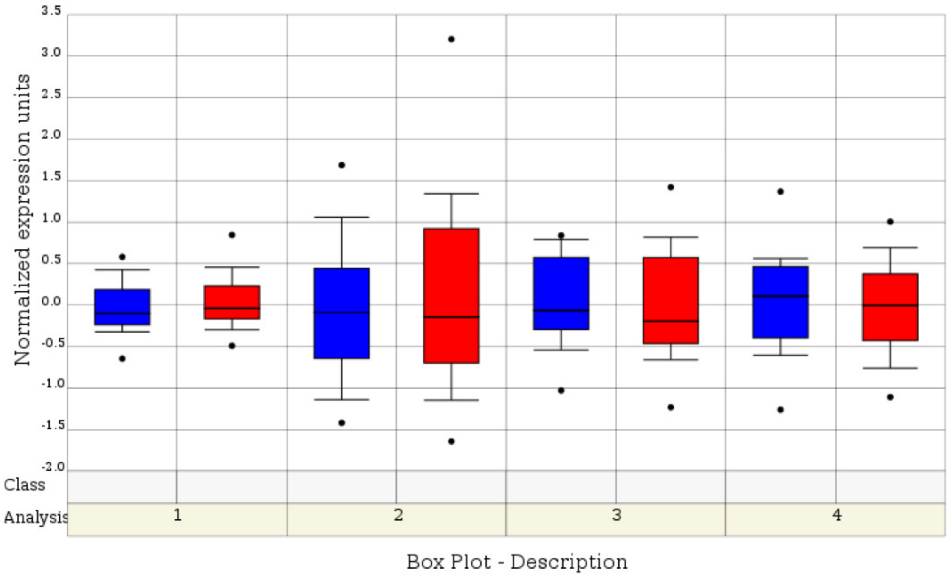

Figure 11.6: VEGF-A expression in breast carcinomas derived from differently staged tumours

Data represent the box-plots of 4 different studies as listed in Table 11.6 showing stage 1 (blue) or stage 2 (red) classified breast carcinomas.

Name Link	Class1 (number)	Class2 (number)	*P*-value *t*-test
Desmedt_Breast http://www.ncbi.nlm.nih.gov/geo/query.acc.cgi?acc=GSE7390	ER-(64)	ER+(134)	**1.1E-07**
Wang_breast http://www.ncbi.nlm.nih.gov/geo/query.acc.cgi?acc=GSE2034	ER-(77)	ER+(209)	**6.6E-07**
Hess_Breast http://bioinformatics.mdanderson.org/pubdata.html	ER-(51)	ER+(82)	**7.3E-07**
Yu_Breast http://www.ncbi.nlm.nih.gov/geo/query.acc.cgi?acc=GSE2294	ER-(39)	ER+(57)	**1.4E-05**
Bittner_breast http://www.ncbi.nlm.nih.gov/geo/query/acc.cgi?acc=GSE2109	ER-	ER+	**3.5E-05**

Table 11.7: MT1-MMP expression in breast carcinomas derived from tumours with different ER status

Data represent studies in which MT1-MMP was found to be expressed differentially. The name of the study, the n-numbers of each category and the corresponding link are indicated. Significance was calculated using the Student *t*-test. Bold *P*-values indicate $P < 0.05$.

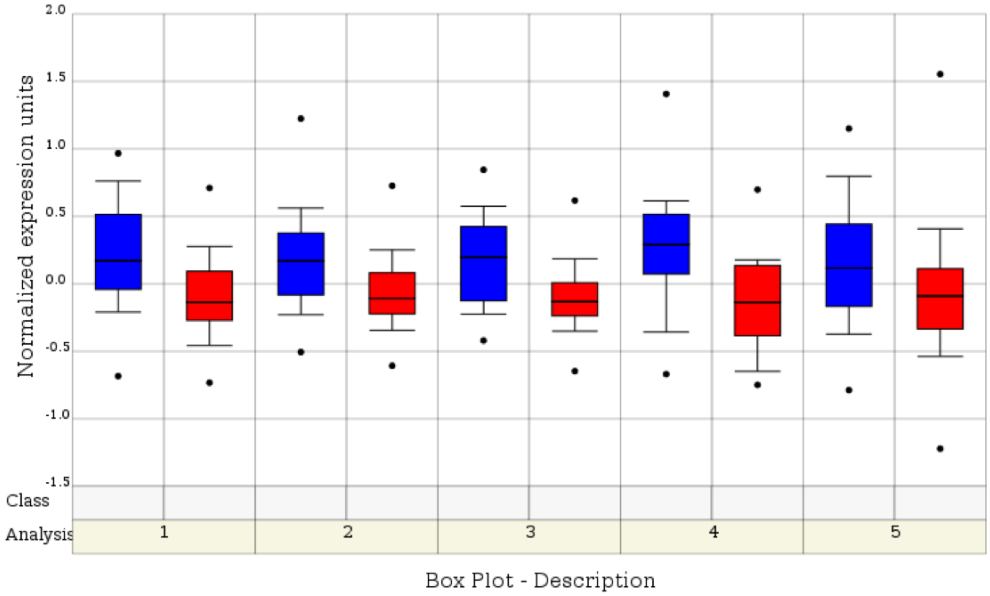

Figure 11.7: VEGF-A expression in breast carcinomas derived from tumours with different ER status

Data represent the box-plots of 5 different studies as listed in Table 11.7 showing ER- (blue) or ER+ (red) classified breast carcinomas.

Name Link	Class1 (number)	Class2 (number)	*P*-value *t*-test
Farmer_Breast	Apocrine (6) Basal (16)	luminal (27)	**1.2E-05**
http://www.ncbi.nlm.nih.gov/geo/query/acc.cgi?acc=GSE1561			

Table 11.8: VEGF-A expression in breast carcinomas derived from tumours of different histology

Data represent studies in which MT1-MMP was found to be expressed differentially. The name of the study, the n-numbers of each category and the corresponding link are indicated. Significance was calculated using the Student *t*-test. Bold *P*-values indicate $P < 0.05$.

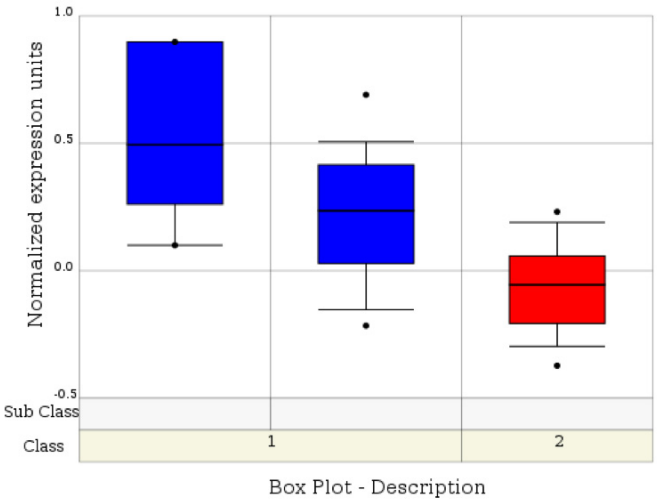

Figure 11.8: VEGF-A expression in breast carcinomas derived from tumours of different histology

Data represent the box-plots of the study as listed in Table 11.8 showing apocrine (blue, left), basal (blue, right) or luminal (red) classified breast carcinomas.

Analysis of VEGFR-2 expression

Study Link	Class1 (number)	Class2 (number)	Class3 (number)	*P*-value *t*-test
Sotiriou_Breast_2 http://www.pnas.org/cgi/content/full/1732912100/DC1	1(16)	2(37)	3(45)	**0.038**
Ginestier_Breast	1(4)	2(12)	3(39)	0.124
Miller_Breast	1(67)	2(128)	3(54)	0.19
Ishvina_Breast http://www.ncbi.nlm.nih.gov/geo/query/acc.cgi?acc=GSE4922	1(68)	2(126)	3(55)	0.227
Sotiriou_Breast_3 http://www.ncbi.nlm.nih.gov/geo/query/acc.cgi?acc=GSE2990	1(67)	2(46)	3(59)	0.366
Sorlie_Breast http://www.ncbi.nlm.nih.gov/geo/query/acc.cgi?acc=GSE3193	1(9)	2(33)	3(33)	0.374
Finak_Breast http://www.ncbi.nlm.nih.gov/geo/query/acc.cgi?acc=GSE9014	1(3)	2(23)	3(27)	0.555
Farmer_Breast http://www.ncbi.nlm.nih.gov/geo/query/acc.cgi?acc=GSE1561	1(22)	2(16)	3(8)	0.668
Hess_Breast http://bioinformatics.mdanderson.org/pubdata.html	1(2)	2(54)	3(77)	0.684
Bittner_Breast http://www.ncbi.nlm.nih.gov/geo/query/acc.cgi?acc=GSE2109	1(30)	2(107)	3(141)	0.701

vantVeer_Breast http://www.rii.com/publications/2002/vantveer.html	1(12)	2(27)	3(78)	0.919
Ma_Breast_3	1(3)	2(39)	3(18)	0.951
Kreike_Breast http://www.ncbi.nlm.nih.gov/geo/query/acc.cgi?acc=GSE4913	1(10)	2(12)	3(28)	0.968

Table 11.9: VEGFR-2 expression in breast carcinomas derived from differently graded tumours

Data represent studies in which MT1-MMP was found to be expressed differentially. The name of the study, the n-numbers of each category and the corresponding link are indicated. Significance was calculated using the Student *t*-test. Bold *P*-values indicate $P < 0.05$.

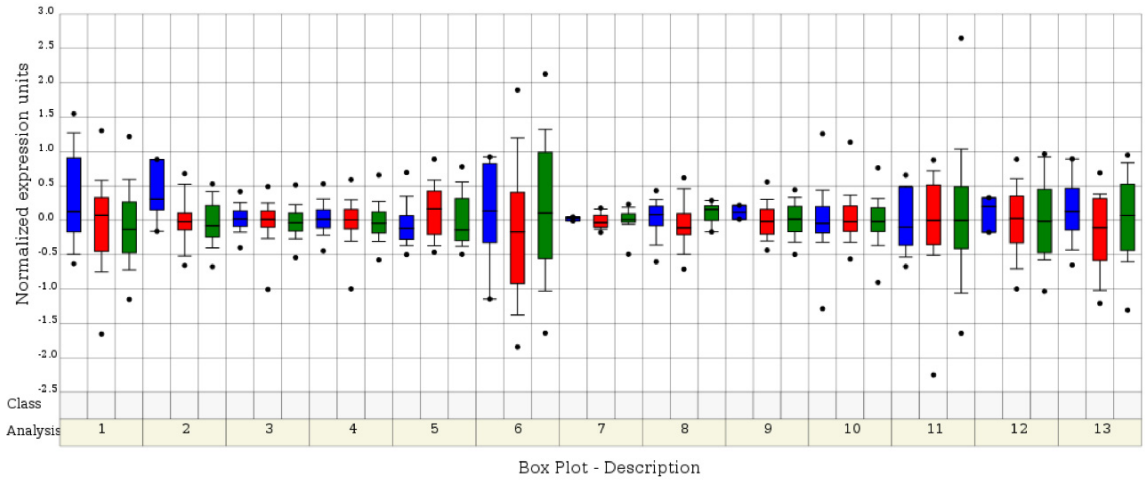

Figure 11.9: VEGFR-2 expression in breast carcinomas derived from differently graded tumours

Data represent the box-plots of 13 different studies as listed in Table 11.9 showing category 1 (blue), category 2 (red) and category 3 (green) graded breast carcinomas.

Name **Link**	**Class1** **(number)**	**Class2** **(number)**	***P*-value** ***t*-test**
Sotiriou_Breast_2 http://www.pnas.org/cgi/content/full/1732912100/DC1	N0(46)	N1(52)	0.078
Yu_Breast http://www.ncbi.nlm.nih.gov/projects/geo/query/acc.cgi?acc=GSE2294	N0(37)	N1(12), N2(46)	0.086
Sorlie_Breast_2 http://www.ncbi.nlm.nih.gov/geo/query.acc.cgi?acc=GSE4382	N0(25)	N1(35), N2(19)	0.126
Sorlie_Breast http://genome-www5.stanford.edu/cgi-bin/SMD/publication/viewPublication.pl?pub_no=95	N0(23)	N1(34), N2(19)	0.233
Hess_breast http://bioinformatics.mdanderson.org/pubdata.html	N0(40)	N1(62), N2(14), N3(17)	0.056

Table 11.10: VEGFR-2 expression in breast carcinomas derived from differently staged tumours

Data represent studies in which MT1-MMP was found to be expressed differentially. The name of the study, the n-numbers of each category and the corresponding link are indicated. Significance was calculated using the Student *t*-test. Bold *P*-values indicate $P < 0.05$.

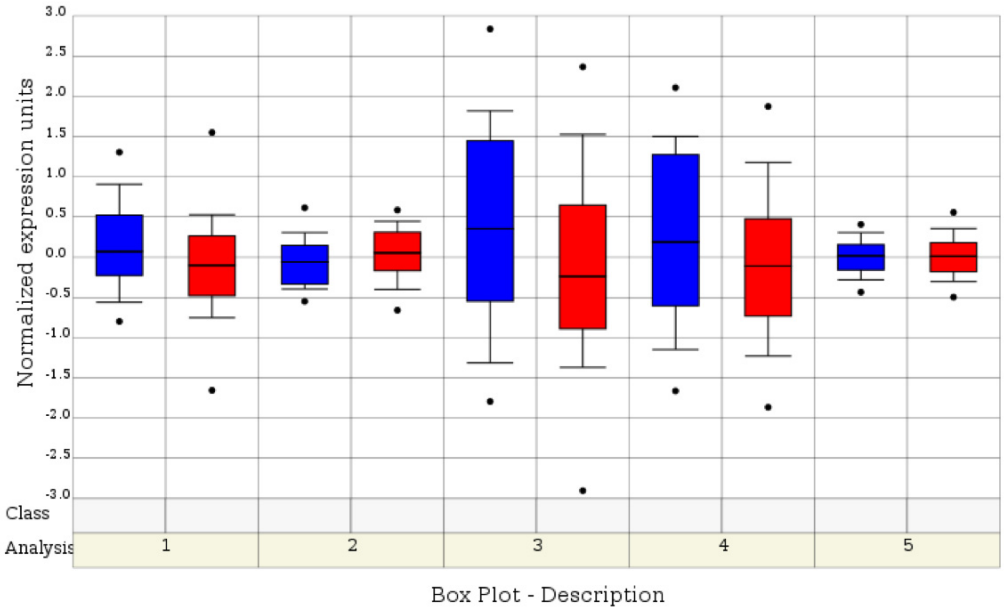

Figure 11.10: VEGFR-2 expression in breast carcinomas derived from differently staged tumours

Data represent the box-plots of 5 different studies as listed in Table 11.10 showing stage 1 (blue) or stage 2 (red) classified breast carcinomas.

Name Link	Class1 (number)	Class2 (number)	*P*-value *t*-test
Hess_Breast http://bioinformatics.mdanderson.org/pubdata.html	ER-(51)	ER+(82)	**0.002**
Wang_breast http://www.ncbi.nlm.nih.gov/geo/query.acc.cgi?acc=GSE2034	ER-(77)	ER+(209)	**0.024**
Sotiriou_Breast_3 http://www.ncbi.nlm.nih.gov/geo/query/acc.cgi?acc=GSE2990	ER-(34)	ER+(85)	**0.026**
Sotiriou_Breast	ER-(33)	ER+(65)	0.095

Table 11.11: VEGFR-2 expression in breast carcinomas derived from tumours with different ER status

Data represent studies in which MT1-MMP was found to be expressed differentially. The name of the study, the n-numbers of each category and the corresponding link are indicated. Significance was calculated using the Student *t*-test. Bold *P*-values indicate $P < 0.05$.

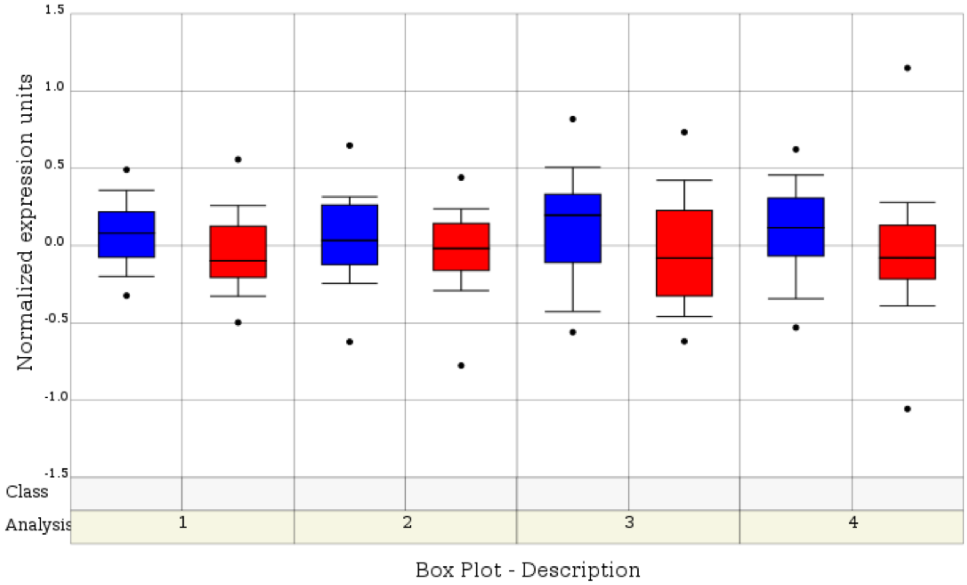

Figure 11.11: VEGFR-2 expression in breast carcinomas derived from tumours with different ER status

Data represent the box-plots of 4 different studies as listed in Table 11.11 showing ER- (blue) or ER+ (red) classified breast carcinomas.

No studies with differential VEGFR-2 expression was found in the category of different histological classifications.

Curriculum vitae

Name Patricia Alice Eisenach
Address
Cambridge Research Institute (CRI)
Robinson Way
Cambridge, CB2 0RE, UK
Tel. +44 (0)1223 404472

Nationality German
Date of birth 12th June 1979
Place of Birth Munich, Germany

Email patricia.eisenach@cancer.org.uk

Education

Since Dec 2005 -	**PhD** at the University of Cambridge (in co-operation with the University of Kiel, Germany), Cambridge Research Institute (CRI), Department of Oncology. Supervisors: Prof. Dr. G. Murphy & Prof. Dr. H. Kalthoff. Project: "Dissecting MT1-MMP induced signalling pathways"
June 2004	**Diplom (M.Sc.)** in Molecular Biology, Zoology and Computer Science; final result: 1.0 (*summa cum laude*).
June 2003 - April 2004	**Diploma-thesis** at the "Universitäts-Klinikum Schleswig-Holstein (UK SH)", Kiel, Germany. Clinic for General and Thoracic Surgery, Division of Molecular Oncology. Supervisor: Prof. Dr. H. Kalthoff. Project: "Verification and validation of new tumour-markers generated by data-mining of gene-expression datasets".
1998 - 2003	Undergraduate studies of biology at the Christian-Albrechts-University of Kiel and the Ludwig-Maximilian-University of Munich, Germany.
2000	**Vordiplom (B.Sc.)**, final result: 1.2.

Publications

Eisenach PA, Roghi C, Fogarasi M, Murphy G, English WR. MT1-MMP regulates VEGF-A expression via a complex with VEGFR-2 independently of proteinase activity. *(submitted)*.

Krubasik D, Eisenach PA, Kunz-Schughart LA, Murphy G, English WR (2008). Granulocyte-macrophage colony stimulating factor induces endothelial capillary formation through induction of membrane-type 1 matrix metalloproteinase expression in vitro. *Int J Cancer* **15**.

Olempska M, Eisenach PA, Ammerpohl O, Ungefrorem H, Fandrich F, Kalthoff H (2007). Detection of tumor stem cell markers in pancreatic carcinoma cell lines. *Hepatobiliary Pancreat Dis Int.* **6**.

Presentations & Abstracts

Eisenach PA, Roghi C, Murphy G, English WR. Disecting the mechanisms of Signal Transduction by MT1-MMP. *Beatson Conference, Glasgow, UK, 5h July – 8th July 2009 (Poster presentation).*

Eisenach PA, Roghi C, Murphy G, English WR. Disecting the mechanisms of Signal Transduction by MT1-MMP. *Models and Mechanisms of Cancer, Hinxton, UK, 8h March – 9stOctober 2009 (Poster presentation).*

Eisenach PA, Roghi C, Murphy G, English WR. Disecting the mechanisms of Signal Transduction by MT1-MMP. *Cancer Degradome Meeting, London,UK, 8h March – 9stOctober 2008 (Poster presentation).*

Eisenach PA, Roghi C, Murphy G, English WR. Disecting the mechanisms of Signal Transduction by MT1-MMP. *Cancer Research UK Cambridge Research Institute International Symposium, Cambridge, UK, 12h March – 13st September 2008 (Poster presentation).*

Eisenach PA, Roghi C, Murphy G, English WR. MT1-MMP induces VEGF-A expression via the PI3 Kinase / Akt pathway. *Cancerdegradome Final Meeting, Krajnska Gora, Slovenia, 30th March – 1st April 2008 (Poster presentation).*

Eisenach PA, Roghi C, Murphy G, English WR. Disecting the mechanisms of Signal Transduction by MT1-MMP. *Cancerdegradome Final Meeting, Krajnska Gora, Slovenia, 30th March – 1st April 2008 (oral presentation).*

Eisenach PA, Roghi C, Murphy G, English WR. MT1-MMP induced signalling pathways. *Internal Seminar Series, Cancer Research UK Cambridge Research Institute, Cambridge, UK, 13th February 2008 (oral presentation).*

Eisenach PA, Schäfer H, Ungefroren H, Fändrich F, Kalthoff H. Identification of putative cancer stem cells in pancreatic adenocarcinoma cell lines. *International Conference on Stem Cells and Cancer, DKFZ in Heidelberg, Germany, 12th - 14th March 2006 (Poster presentation).*

Eisenach, PA, Ungefroren H, Schäfer H, Kalthoff H. Identification and Characterization of Tumour Stem-Cells in Pancreatic Adenocarcinoma Cell Lines. *9. Chirurgische Forschungstage, Frankfurt a.M., Germany, 19th – 21th September 2005 (Oral presentation).*

Scholarships / Awards

August 2009	IPS (International Proteolysis Society) travel-grant to attend IPS meeting in Surfers Paradise, Australia
September 2008	Poster-prize: Cancer Research UK Cambridge Institute International Symposium, Cambridge, UK, 12th-13th September 2008
April 2008-Present	Graduate scholarship, Cancer Research UK
Dec 2005 - Jun 2006	Graduate Scholarship, Studienstiftung des deutschen Volkes (German National Academic Foundation)
2005-present	e-fellows scholarship
2005	Research-scholarship “Dr. Helmut-Robert-Gedächtnis-Stiftung“
2004	Award for the Diploma thesis
2001	DAAD (German Academic Exchange Service) scholarship for internship in Trinidad & Tobago

Acknowledgements

I would like to thank Prof. Gillian Murphy for providing me with an interesting project, her support, her always open door for discussions but also for giving me freedom in research. Especially I would like to thank Prof. Dr. Holger Kalthoff for taking over the supervision of my thesis and his constant support and patience as well as his enthusiasm for science.

I further thank Dr. William English and Dr. Christian Roghi for their supervision, help with technical questions and the correction of this thesis. My work would not have been possible without numerous reagents and cDNA constructs provided by C. Roghi and his ideas especially on the “MT1-MMP ICD release” project.

Thanks to Jason Carroll and especially Kelly Holmes for their help in setting up the ChIP assay and to Virgilio Failla for being a steady source of support in all aspects of microscopy.

Importantly, I thank the whole “Murphy-group”, past and present, for their support - Sarah Morrow for her help and smooth organisation of various lab-related questions, Dr. Marton Fogarasi for his help in doing ELISAs and Dr. Meng-Huee Lee for answering all biochemically questions. Especially, I would like to thank Dr. Anne Leclercq, Dr. Anthea Messent, Helen Gillingham, Pedro Correa-DeSampaio and João Pereira for lots of laughter, lots of coffee, many shared late hours and making the CRI a pleasant place to work.

This work was funded by the *Studienstiftung des deutschen Volkes* and Cancer Research UK. I am very thankful for their support and the unbureaucratic process of setting up the funding.

I thank Stefan Thomsen for coming with me to the UK, his constant support through rough phases and everything else beyond the bench-work.

Finally I would like to thank my family for their support – it was more than I could have ever asked for.

Erklärung

Hiermit versichere ich ausdrücklich, dass ich die vorliegende Arbeit selbständig verfasst und keine anderen als die angegebenen Hilfsmittel und Quellen verwendet habe. Weder vor noch gleichzeitig habe ich andernorts einen Antrag auf Zulassung zur Promotion gestellt oder diese Dissertation vorgelegt. Ich habe mich bisher noch keinem Promotionsverfahren unterzogen.

Kiel, den _____

Patricia A. Eisenach